Evaluating the Ceramide Nanoliposome as a Therapy for Head and Neck Squamous Cell Carcinoma: Circumventing Resistance, Characterizing Death, Utilizing Dual Therapies, and Manipulating Metabolism.

Jeremy Joseph Porter Shaw
Cortland, OH

M.S. Biological & Physical Sciences, University of Virginia, 2016
B.S. Molecular/Cellular Biology (Minor: Chemistry), Kent State University, 2014

A Dissertation presented to the Graduate Faculty of the University of Virginia in Candidacy for the Degree of Doctor of Philosophy

Department of Pathology

University of Virginia
December, 2020

TABLE OF CONTENTS

THESIS ABSTRACT

Head and Neck Squamous Cell Carcinoma (HNSCC) is the seventh most deadly cancer in the world. While traditional therapies are highly morbid, there have been only a few new systemic treatments developed in the last few decades, and these benefit only a small population of patients. The anti-cancer signaling sphingolipid ceramide has shown promise as a therapeutic in many cancer models including preliminary work in HNSCC. The ceramide nanoliposome (CNL) is a nanoscale, therapeutic ceramide-delivery vehicle currently in Phase I clinical trials for treating advanced solid tumors. Thus, the thesis seeks to evaluate the CNL as a potential therapeutic for HNSCC. This is accomplished by exploring methods to circumvent resistance (**Chapter 2**), identify novel markers of non-canonical cell death (**Chapter 3**), utilize synergistic dual therapeutic approaches with previously failed EGFR inhibitors (**Chapter 4**), and manipulate sphingolipid metabolism (**Chapter 5**). These studies elucidate a myriad of signaling pathways as well as specific druggable targets that can be manipulated to enhance therapeutic efficacy of CNL or other ceramide-based therapies for treatment of HNSCC.

ACKNOWLEDGEMENTS

Though my name is the only one on the front of this thesis, it would be a catastrophic misjudgment for any reader to give me all of the credit. To thank everyone adequately would double the size of this thesis, however, so I will attempt to keep this short(ish) and sweet. From Mr. Sean Craigo and Ms. Maureen Bucko in high school, to Dr. Douglas Kline and Dr. Christopher Malcuit at Kent State, to Dr. Justin Lathia at the Cleveland Clinic, these kind and amazing mentors were instrumental in helping me reach the University of Virginia. In fact, if not for Dr. Lathia's advice and support, I likely would not have applied nor been accepted to UVA. Thank you all so much for helping me to get here.

Thank you to Mary Hall and Dr. Janet Cross who made sure I felt welcome by the administration here and never felt alone from the moment I arrived in Charlottesville. I could not be more grateful for the amazing fellow BIMS students as well. To "The Family" Coley McKenna, Laryssa Manigat, Tiffany Wang, and Ellen Mintz, thank you for somehow managing to make the Insanity of our lives so much more enjoyable and always including a guy in the plans. To Luke Oostdyk and Steven Keller, thank you for inviting me in the move to Shamrock and giving me some ridiculous nerf-dart, 1/3rd of a billionaire, heavy exo memories with my bros. To Clint Upchurch and Will Moffat, the Borderlands/Rick-and-Morty nights, crazy late-night conversations, and Shamrocked parties really did help keep me going through some of the later years, and I'm very grateful for those nights with you guys. Although there are too many friends to name from FC Beercelona to GBS, I cannot understate how great it has been to have a great friend and leader in Tori Osinski there with me since day one at the "local Charlottesville restaurant" Qdoba.

Although I can't say for sure, I have to assume the Kester Lab is… atypical. However, I wouldn't trade my experiences in this lab for anything. I've received advice and help from knowledgeable and kind technicians from learning my signature MTS assay technique from

Younhee Choi, to how to hold mice without accidentally throwing them across the room from Alexis Gademsey, to tons of other tips from Jason Smith, Eunji Lee, Brett Moseley, and Susan Walker. To Dr. Tye Deering and Dr. Andrei Khokhlatchev, thank you for your extensive patience and frequent advice as I struggled to even pull off the most basic assays when I first joined the lab. Dr. Todd Fox, thank you for always making time and putting in effort to teach me about the world of sphingolipids, for teaching me how to write (via ~20 rounds of revisions), and never once kicking me out of your office even when you were swamped with other work. To Dr. Mark Kester, as two strong personalities do, we often bumped heads, but at the end of the day I have nothing but gratitude and have learned so much from you including topics outside the realm of experimental science. Thank you for teaching me about intellectual property, management, and how to sell your science. I will always be appreciative of you for being a sincere mentor during times when I questioned my own project and abilities.

And of course, there's "The Kester Boys". To Kelly Drews, thank you for your (or maybe Camille's) patient assistance in so many different assays and for helping me see to understand that there are other ways to do things outside of "my way" (and also for the cookie dough and indelible friendship)! To Logan Patterson, we may have totally different approaches and opinions to most things, but I've never questioned that you would have my back at your own expense if I asked. Thank you for being a good labmate, a great friend, always keeping me laughing, and being my go-to guy if I ever needed to vent (even on your own anniversary! – Sorry Meredith!) And Peeeeedro Pinheiro, I'm so glad you decided to join the Kester Lab. I couldn't count the number of experiments you helped me design, interpret, and even occasionally perform. You've been with me on almost every major trip from our joint podium talk/comedy show in New York, conferences in North Carolina and Texas, our interviews at Stanford, and my first ever trip out of the USA to Portugal when you shared your home with me. Thank you for being such a great tour guide, partner, and friend.

One of the best experiences I've had at UVA was getting to train and mentor undergraduate students from UVA as well as other institutions. Thank you to "Team Juggernaut/Druggernaut", named because, like The Juggernaut from the X-Men, when we hit a wall with our science we just keep going. To those I only mentored for short periods, Tayyeb Dinn, Nicholas Roig, Alexandra Hickman and Sragdhara "Sragi" Khakurel, thank you for your quick immersion in the science and for doing your part to progress this work. To Tara Caste and Tristen Slamowitz, thank you for the long hours which were of tremendous help and for bearing with me in my early stages of being a mentor. To Emily Venner, thank you for all of your time, hard work, and independence, if not for you, the EGFR project would have certainly fallen to the wayside. To Tim Boyer, your growth as a well-rounded scientist has been fantastic to watch and incessant assistance could not be more appreciated. If not for your eager and vital help, the Cell Death chapter would consist of entirely negative data and the Ceramide Metabolism chapter would have only been an interesting thought, thank you for going above and beyond without hesitation. Finally, Patrick Beck aka "Double Hoo", "Patty B", and "lil thicc", your commitment to the lab has been incredible and I am so glad Kelly sent you my way. You single handedly drove the EGFR project making vital discoveries in genes I hadn't even heard of while also leading a capstone team working on making the EGFR project into a real therapeutic that could help patients. Thank you for your constant dedication to the project, your assistance in shaping my mentoring style, and your partnership over the years. To all of the members of Team Juggernaut, I cannot express the pride and gratitude I feel towards all of you and I know you will continue to succeed in all of your respective endeavors.

To my thesis committee (and maybe the only people to ever read past the table of contents), Dr. Janet Cross, Dr. Mark Jameson, Dr. Christopher Moskaluk, Dr. Thurl Harris, and Dr. Robin Felder, thank you so much for your support. I've heard horror stories of many graduate students who were afraid to talk to or meet with their committee. On the contrary, you have all backed me without hesitation and even when disagreeing, I knew you had my best interests at heart. I must

add a second thank you to Dr. Jameson who was always willing to meet me with me and offer me his assistance and advice, and encouraged me to make my thesis a true representation of my work instead of just a passable attempt. A special thank you also to Dr. Cross who has been a remarkable once-in-a-lifetime mix of an advisor, mentor, and friend.

To my family, Matt, Noel, Beckie, Mom, and Grandma, your support has been amazing. Thank you for learning about "Qualifying Exams" and "Private Defenses", for letting me present a PowerPoint of my research to you on our family vacation, and for finally taking the hint to stop asking me when I was graduating. I know none of you like or care about science much, but it means the world to me that you have always believed in me no matter what. Things have not always been easy and our family has gotten a good deal smaller over the past few years, but it has also gotten a little bigger a few Septembers ago. Thank you for never doubting me even when I doubted myself, I love you all so much.

Thank you to Dr. Adrian Halme, Stacey Criswell, Jeremy Gatesman, and Marya Dunlap-Brown for all of their help with the microscopy cores and mouse models. Thank you to Dr. Amy Bouton, Dr. BJ Purow, Dr. Dave Kashatus, Dr. Scott Vandepol and Dr. Timothy Bullock (aka Scotty V and Timmy B) for being faculty that always treated me like an equal but still sought to help me.

Finally, since I absolutely hate leaving people out, thank you to Marty Knauf and Zane Durbin, for starting and maintaining the UVA Club Dodgeball team to let me live out my glory days a few years longer (then I should have). Thank you to all of my amazing friends in the First Harmonics for the great practices, karaoke nights, and concerts. Thank you to everyone who helped make The Oncobusters Relay for Life team such a success! Thank you to my Quarantine Gang #PodGoals: Will, Katie, Meg, and of course "Kitchen Babe" Niki! Thank you to all my volleyball and flag football friends and Kyvory Henderson who was both! Thank you to my great friends from back home, Greg (NFL), Eli, Kyle, Chris, A.J., Ian, Rachael, and Brooke. Thank you to my KSU

Culture Shock friends, Sneha, Aiza, Akansha, Gabe, Alex, Cody, and Anthony. Thank you to the hooligans who won't let me get away, Kurt, Andrew, Justin, and Courtney. Thank you to all of the doctors here at UVA who have fixed my torn meniscus, broken pinky, broken thumb, and ACL…twice. And I can't forget to thank Marla Ferradino, Camille Drews, Breanna Noffsinger, Paige Larkin, Mike Raymond, Riley Hannan, Zollie White, Tucker Lynn, Tom Moutinho, Katie Gorick, Lee Talman, Delaney Fisher, Natasha Sheybani, TK Phung, Katya Sracic, Madison Keller, Lyndsey Myers, Ali and Hunter Harris, Stephanie Melchor, Kate Still, Catherine Lammert, Silas Griffith, Phil Seegren, Taylor Downs, Zach Zwahl, Mouadh Benamar, Grace Cummings, Collin Dube, Justin Elfman, and anyone else I may have missed for their friendship. All of you have helped me retain my sanity and given me the motivation and strength to keep working hard.

Sincerely, thank you all.

This thesis is dedicated to Gordon Shaw and Deryl Porter, my father and grandfather whom I dearly miss. I will always try to make you proud.

CHAPTER ONE: INTRODUCTION TO HEAD AND NECK CANCER AND SPHINGOLIPIDS

CHAPTER ONE: INTRODUCTION TO HEAD AND NECK CANCER AND SPHINGOLIPIDS

HEAD AND NECK SQUAMOUS CELL CARCINOMA:

Head and Neck Squamous Cell Carcinoma (HNSCC) is a cancer which arises from the squamous cells of the oral cavity, tongue, larynx, pharynx, and paranasal sinuses. Although HNSCC is not the only cancer which occurs in these tissues, it makes up 90% of cancers in this region (1); with the other major contributors being adenocarcinomas, sarcomas, and lymphomas (2). Below we will discuss the causes, epidemiology, current treatments, and molecular landscape of HNSCC.

In the search for causative factors of HNSCC, the only major contributors have been smoking and/or drinking or HPV status. Anecdotally, very few cases of cancers of the head and neck were described in Europe before the introduction of tobacco in the 16th century (3, 4). Despite arguments persisting almost a century later, smoking was deemed the cause of tongue cancer in the year 1900 (5). Later studies performed in the United States identified that over 75% of the patients who were diagnosed with HNSCC either smoked cigarettes, drank alcohol, or both (6). While tobacco use in the US has been on the decline for many years (7), unfortunately, usage of e-cigarette products has risen dramatically in recent years (8), being declared an epidemic by the US Surgeon General in 2018 (9). Though these products do not often contain tobacco and are thought to be orders of magnitude less carcinogenic than cigarette smoke (10), a report from the National Academies of Sciences claims “substantial evidence” that some chemicals in e-cigarettes can cause DNA damage and mutagenesis and, thus, could increase cancer risk (11). Though long-term studies into cancer risk of e-cigarettes is warranted, it is possible that even as the use of traditional cigarettes continues to fall, the number of cases of HNSCC may continue to rise. However, even prior to this period of rising e-cigarette usage, decreases in tobacco use in the United States, counter-intuitively, did not decrease the number of HNSCC diagnoses at the same rate (12).

After further research into HNSCC in more recent years it has become apparent that Human

Papilloma Virus (HPV), a virus which infects epithelial cells and is responsible for nearly all cases of cervical cancer (13), has also caused an increase in HNSCC cases (14). This HPV contribution is incredibly tissue site-specific in that while HPV causes the vast majority of HNSCC of the oropharynx, only a small fraction of HNSCC cases in other upper aerodigestive sites have been noted to have associated HPV DNA (15). It is worth noting, however, that HPV+ HNSCC patients have better survival rates (16, 17) than HPV- patients, even leading to dose de-escalation studies in an attempt to relieve the burden of excessive radiotherapy on patients with HPV+ HNSCC (18, 19).

However, for the large majority of patients with HPV-negative HNSCC, classical and targeted therapies for patients are still lacking. Up until the year 2008, the standard of care treatment generally involved some combination of surgery, radiation, and/or cytotoxic chemotherapy. However, while this regimen led to modest increases in progression free survival, 5-year survival, and decreased local/regional relapses, this therapeutic approach caused adverse events in large populations of patients (20, 21). Worse still, for those who develop recurrent and/or metastatic disease that is refractory to treatment with cisplatin-based chemotherapy, the overall response rate to second-line therapy was only 2.6% (22). Following a report published in 2008 showing a moderate increase in survival around 2-3 months, the current standard of care was expanded to also incorporate treatment with the monoclonal antibody, termed "Cetuximab", which inhibited Epidermal Growth Factor Receptor (EGFR) (23). [More information on EGFR as a therapeutic target and the success and failure of EGFR inhibitors in HNSCC will be covered in **Chapter 4.**] Unfortunately, almost a decade later, for patients with advanced disease who develop recurrent/metastatic disease, first-line treatment is often unsuccessful, and second-line options are limited with extremely poor response rates (24).

In order to give patients more successful therapeutic options, multiple studies sought to identify subtypes of HNSCC to gain better understanding of the disease and elucidate potential druggable targets (25). Though the approaches and outcomes of these studies vary slightly, multiple studies agree on four subtypes: atypical, mesenchymal, basal, and classical (26-28). The atypical

subtype is composed primarily of HPV+ cells lacking EGFR amplification, mesenchymal contains many innate immunity alterations and characteristics of epithelial to mesenchymal transition, basal is characterized by stem cell-like signaling cascades, and classical has amplification of EGFR and CCND1 (25). Taken together, the field understands the major altered signaling cascades in HNSCC to be related to: HPV, p53, cell-cycle, epigenetics, oxidative stress, and WNT (28). Using multiple sources as references, (25, 27, 28). I've re-analyzed and consolidated TCGA data to simplify mutations and amplifications/deletions of the major signaling cascades in HNSCC into **Table 1-1**. Overall, it can be appreciated that the most altered genes in HNSCC are: TP53, CDKN2A, PIK3CA, FAT1, CCND1, NOTCH1, KMT2D, and EGFR. However, despite all of these new subtypes of cancer and potentially druggable molecular targets, with the exception of Cetuximab, none have been successfully incorporated into FDA-approved therapies as of yet.

Pathway	Genes	Protein	Type of Gene*	Mutation %	CNA %	MUT + CNA %
Survival and proliferation	TP53	Tumor protein p53 (p53)	Tumor Suppressor	72	1.4	73.4
Cell Cycle	CDKN2A	p16INK4A	Tumor Suppressor	22	32	54
Survival and proliferation	PI3KCA	Catalytic p110a subunit of class 1 PI3Ks	Oncogene	18	21	39
WNT Signaling	FAT1	Protocadherin FAT1	Tumor Suppressor	23	8	31
Cell Cycle	CCND1	Cyclin D1	Oncogene	0.6	25	25.6
WNT Signaling	NOTCH1	Notch Homolog 1, Translocation-Associated	Tumor Suppressor	18	4	22
Epigenetic Regulation	KMT2D (MLL2)	Histone-lysine N-methyltransferase 2D	Tumor Suppressor	16	0.4	16.4
Survival and proliferation	EGFR	Epidermal Growth Factor Receptor	Oncogene	4	11	15
Apoptosis	CASP8	Cysteine-Aspartic Acid Protease 8 (Caspase 8)	Tumor Suppressor	11	2.6	13.6
Epigenetic Regulation	NSD1	Nuclear receptor binding SET Domain Protein 1	Tumor Suppressor	12	0.8	12.8
Oxidative Stress Response	NFE2L2	Nuclear factor erythroid 2-related factor 2 (NRF2)	Tumor Suppressor	5	5	10
WNT Signaling	AJUBA	LIM Domain-Conatining Protein AJUBA	Tumor Suppressor	7	1.2	8.2
Survival and proliferation	PTEN	Phosphatase and Tensin Homolog	Tumor Suppressor	2.8	4	6.8

Table 1-1: Summary of Most Altered Genes in HNSCC (Data Obtained From TCGA Through cBioPortal
**Type of gene is oversimplified to either "Tumor Suppressor" or "Oncogene" in this context to keep nomenclature from Leemans et. al*

Thus, treatment with 5-Flurouracil, Cisplatin (or Carboplatin), and Cetuximab, referred to as the "EXTREME" regimen, has remained the standard of care for recurrent/metastatic disease for approximately a decade despite over 80% patients displaying adverse events and only having minor increases in survival (23). Even with this EXTREME regimen, in 2018 HNSCC remained the seventh most diagnosed and seventh most deadly cancer in the world with over 875,000 diagnoses and over 450,000 deaths (29). Since this time, two immunotherapies Pembrolizumab and

Nivolumab, that block the programmed cell death protein 1 (PD-1) inhibitory receptor, have been approved (30). Briefly explained, multiple cancers including HNSCC express programmed death ligand 1 (PD-L1) which binds PD-1 on T-cells and dampens an effective immune response. These immunomodulatory drugs block PD-1 from binding to PD-L1 which helps maintain an effective T-cell-mediated immune response (31). Unfortunately, these drugs are limited by initial failure to elicit effective immune responses (primary resistance) as well as an eventual decrease of effect (adaptive resistance) in many patients (32). Thus, while Pembrolizumab and Nivolumab have minimal toxicity and can display robust, long-term benefits, they are only effective in 1 out of 10 HNSCC patients (30, 33). Thus, even with three FDA-approved therapies, there remains a desperate need to develop new treatments for HNSCC. One promising avenue for treating HNSCC is utilizing sphingolipid-based therapeutics.

SPHINGOLIPIDS:

Sphingolipids were first identified in 1884 and were named after the Egyptian sphinx due to their riddled and enigmatic nature (34). Unlike many other classes of lipids which are built upon a glycerol backbone, sphingolipids are all synthesized with an 18-carbon sphingosine backbone and have an amide linkage at the second position instead of a carbon-carbon bond. This sphingosine backbone can be altered in three ways: the addition of a fatty acid to its second carbon position (via an amide bond), addition of a phosphate, phosphoethanolamine, phosphocholine, or single/multi-chain sugar residues to its 1-hydroxyl position, or a combination of the above to generate most of the canonical sphingolipid species. The base sphingosine structure, binding sites of additional groups, and types of molecules which can be added of sphingolipids is detailed in **Figure 1-1**. Though the structure of different sphingolipids is somewhat simplistic, keeping true to their mysterious nomenclature, they have vastly different, occasionally opposite, functions.

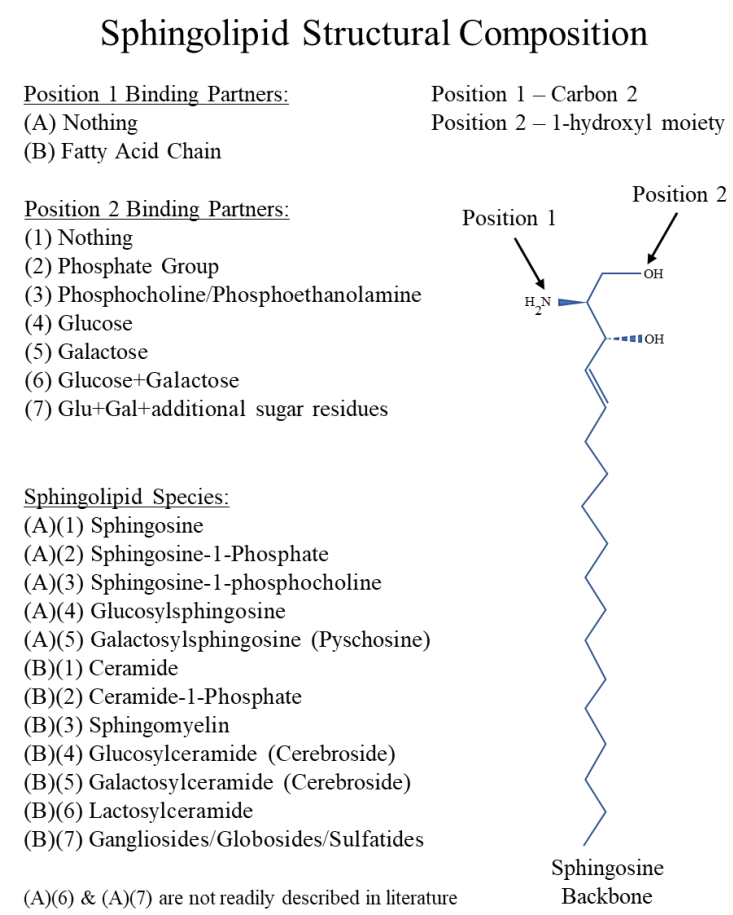

Figure 1-1: Simplified Sphingolipid Structural Composition.
A combination of "Position 1 Binding Partner" (A or B) and "Position 2 Binding Partner" (1-7) can be attached to the Sphingosine Backbone (shown on right) at their designated positions. Names and binding partner combinations are denoted under "Sphingolipid Species"

Although previous work establishes the structural role of sphingolipids in membrane biology (35, 36), sphingolipids have garnered attention as having significant roles in both promoting and inhibiting a myriad of pathologies including diabetes and metabolic disorders (37, 38), atherosclerosis (39) and cardiovascular diseases (40), non-alcoholic fatty liver disease (41) aging and age related diseases (42), neurological disorders (43) and cancer (44). Within the field of cancer alone, different sphingolipid species have vastly different, often opposing roles. While some sphingolipids or sphingolipid mimetics are able to induce cancer cell death and are undergoing clinical trials as treatments for cancer (45), counter-intuitively, others have been shown to promote cancer progression (46, 47), drive inflammation (48), serve as biomarkers (49), correlate with metastasis (50) and promote chemotherapeutic resistance (51-53). Sphingolipid species and sphingolipid mimetics which are currently undergoing clinical trials are shown in **Figure 1-2**, adapted from Shaw/Pinheiro 2018.

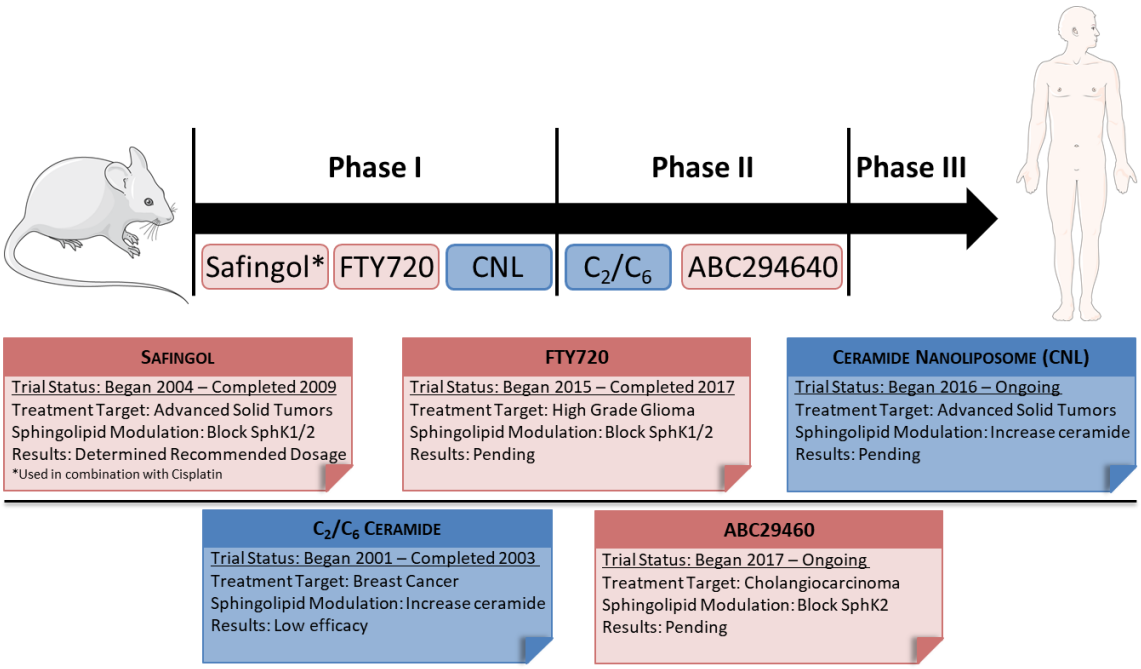

Figure 1-2: Sphingolipids and Sphingolipid Mimetics in Clinical Trials for Cancer
*An outline of the sphingolipid-based therapeutics currently undergoing clinical trials for cancer treatment. Although there are few sphingolipid therapies currently on the clinical track ,many others are showing promise in preclinical models *Last Updated 2018**

Further complicating a simplified functional understand of sphingolipid biology is the presence of numerous families of enzymes which can rapidly mediate the metabolism of one sphingolipid species to another. Similar to the sphingolipids themselves, sphingolipid metabolizing enzymes often have multiple differing isoforms, cellular localization, and signaling pathways. Thus, considering the potential role of these enzymes to metabolize anti-cancer sphingolipid species into pro-cancer sphingolipid species, or vice-versa, inhibitors or inducers of sphingolipid metabolism have also gained attention as potential therapeutics. These inhibitors and inducers of sphingolipid metabolism (both direct or indirect) are summarized in **Figure 1-3** – (taken from Shaw/Pinherio 2018) and discussed in further detail below.

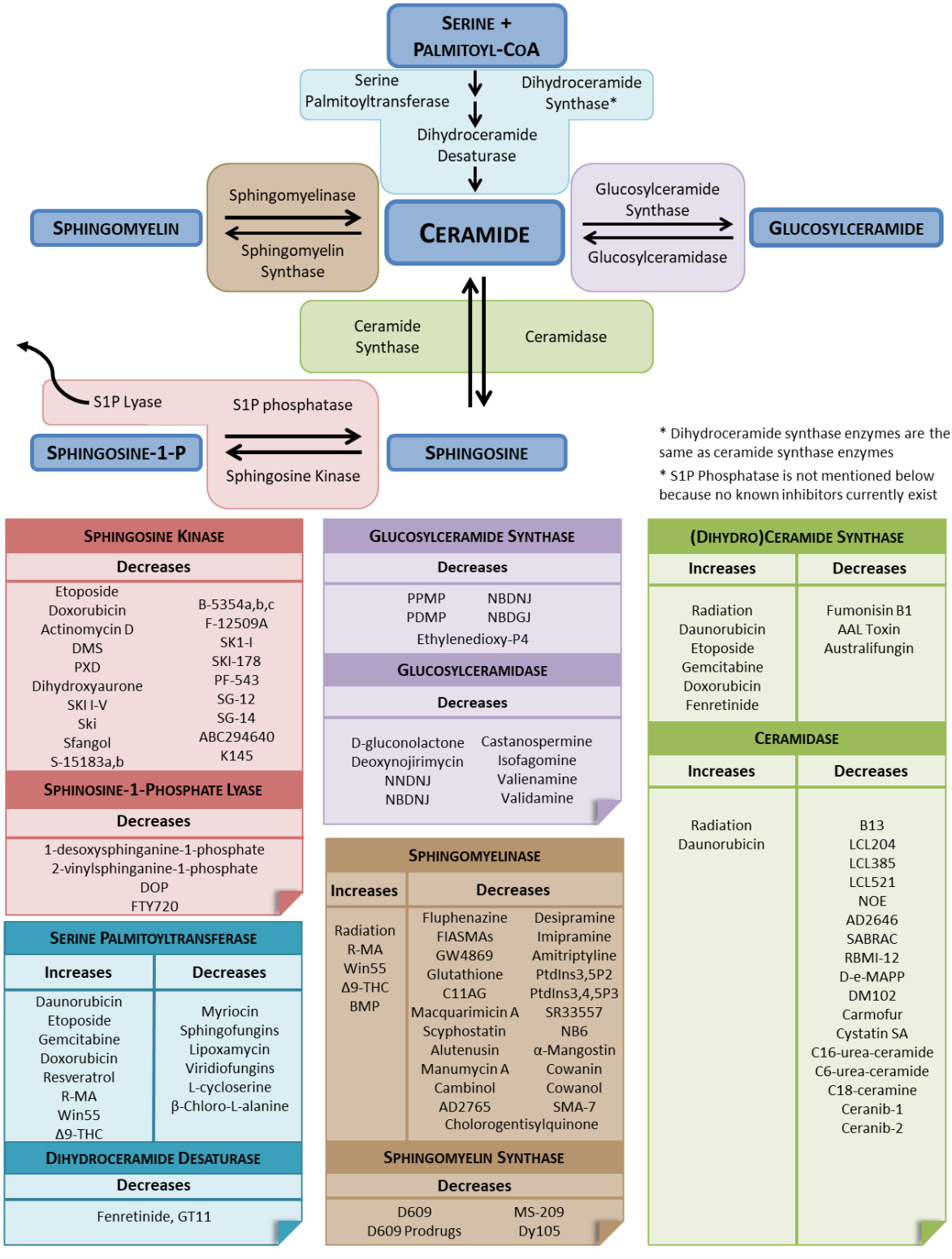

Figure 1-3: Inducers and Inhibitors of Sphingolipid Metabolism
Using ceramide as a central point for understanding sphingolipid metabolism, the above figure outlines the current major sphingolipid species (blue boxes) and the enzymes which metabolize these lipids (multicolored boxes). The current inhibitors for specific enzymes in the pathway are listed below in the color-coded sticky notes.

Considering the above, a complete understanding of sphingolipid biology requires understanding of the individual sphingolipid's numerous signaling cascades, cellular localization, enzymes which metabolize it, as well as those same factors for the sphingolipid species into which it can be metabolized. This must all then be re-evaluated for the specific pathology in which these sphingolipids are being examined. This is further complicated by more recent studies which show the significance of specific structures such as double bonds, chain lengths, and hydroxyl groups of an individual sphingolipid species (54, 55).

In order to build a foundational understanding of this pathway, we, and others, place the sphingolipid ceramide at its center. Ceramide is a somewhat structurally simple sphingolipid composed of a sphingosine backbone with a fatty acid chain attached via an amide linkage at the second carbon position, and is widely considered to be the most anti-cancer sphingolipid species. Anecdotally, it's effectiveness in promoting cancer cell death can be appreciated from numerous studies finding that many chemotherapeutics increase levels of ceramide in cancer cells which lead to cell death (56-58). These chemotherapeutics are listed alongside the previously mentioned inducers and inhibitors of ceramide metabolism in Figure 1-3 taken from Shaw/Pinheiro 2018.

More recent studies in a variety of cancer models have identified the role of ceramide to, among other signaling pathways covered later in this chapter, induce apoptosis (59, 60), differentiation (61, 62), and cell cycle arrest (63, 64) earning it the nickname the "Tumor Suppressor" lipid (65-67). Interestingly, despite early work showing ceramide's role in inducing apoptosis, more recent findings in many cancer models suggest ceramide induces cell death via a non-apoptotic mechanism (68-71)(Chapter 2). Thus, the type of cell death induced by ceramide is an area of active investigation in the sphingolipid field. [My preliminary work in identifying hallmarks of non-canonical cell death in HNSCC is covered in **Chapter 3**].

Despite lacking a comprehensive understanding of the exact type of death induced by ceramide, it is well-accepted that the accumulation of ceramide is a promising approach to prevent cancer growth and survival. Considering this, many groups have sought to increase levels of

ceramide by activating endogenous cellular pathways that generate ceramide, or by exogenously adding ceramide or ceramide analogs. Along the same vein, it can be appreciated that enzymes that metabolize ceramide into other sphingolipids and thus decreas cellular levels of ceramide, are thought to promote cancer cell survival. [More information on the role of ceramide-metabolizing enzymes in ceramide-induced cell death will be covered in **Chapter 5**]. Finally, it is imperative to consider that this system of generation, signaling cascades, and metabolism of ceramide is not static, but rather flowing in a constant state of flux.

Metaphorically, as we described in *Shaw/Pinheiro et. al 2018*, if the cellular "pool" of ceramide becomes too high at any time, the cell will die. In order to fill this pool, pathways which generate ceramide act as "faucets" which can be turned on, or exogenous ceramide/ceramide analogs can be added. On the other hand, pathways which metabolize ceramide and act as "drains" can decrease the ceramide pool. Thus, to appreciate this full pathway, it is necessary to consider ceramide generation (faucets), degradation (drains), overall levels (sink volume), and flux through this system. This process is pictographically shown in Figure 1-4 as taken from Shaw/Pinheiro 2018.

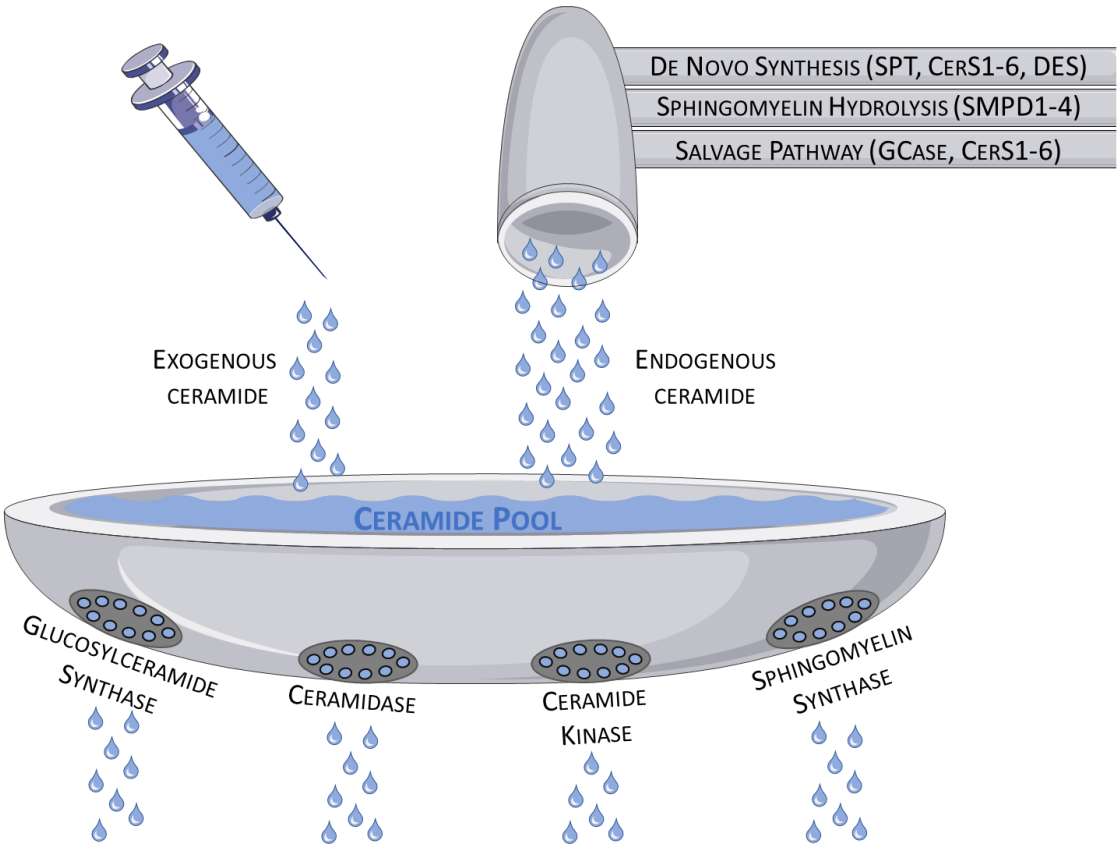

Figure 1-4: The "Flow" of Sphingolipid Metabolism
The accumulation of ceramide can be generated from three main pathways (Sphingomyelin Hydrolysis, de novo synthesis, or salvage pathway) or exogenously added (in the form of short chain ceramides) while the degradation of ceramide is facilitated by 4 main enzymes (SMS, GCS, CDase, and CerK). At a steady state the levels of ceramide are maintained as flux through the system stays fairly constant. However, similarly to increasing flow through the faucet or clogging the drain, increasing the generation of ceramide or preventing its degradation can lead to an accumulation of the lipid which can be toxic to cells.

Exogenous addition of ceramide (depicted as the syringe in the previous figure) has numerous advantages as well as a few disadvantages. Though simplified, in the sink diagram above, there are over 20 different enzymes for ceramide generation and degradation. Thus, adding exogenous ceramide as opposed to stimulating ceramide-generating enzymes eliminates complicating variables such as differing levels, or increased/decreased activity of these upstream enzymes. Moreover, adding exogenous ceramides also allows for consistent, quantifiable, and time-controlled addition of ceramide. Finally, exogenous addition of ceramides affords the opportunity to manipulate these ceramides before addition in order to address the role of different

structures and make them more therapeutically relevant through increasing solubility, stability, or death-inducing potential. Thus, the Kester Lab at the University of Virginia utilizes the addition of exogenous ceramides to eliminate complicating variables, enhance delivery, and improve therapeutic relevance. The disadvantages of exogenous addition of ceramide is that there may be differences between the structure, location, and signaling of exogenous compared to endogenous ceramides and that delivery of these ceramides is often problematic.

In regards to these difficulties in delivery, the hydrophobic nature of ceramide had previously mitigated its use as a therapeutic (72). However, researchers found that decreased fatty acid chain lengths of synthetic, short chain ceramides (2-8 carbons) compared to endogenous normal length ceramides (14-26 carbons) decreased the hydrophobicity and even increased its cytotoxic effect (73). Due to successful *in vitro* studies with short-chain ceramides in cervical cancer (69) and *in vivo* tests in breast cancer (exact chain length undeterminable from source - (74)) these "short chain ceramides" were tested in clinical trials. While they were deemed safe via Phase I trials, when added as a cream to treat breast cancer, they unfortunately failed to show meaningful clinical benefit in Phase II (75). Thus, though short chain ceramides had shown great promise, limitations in delivery prevented them from showing clinical benefit (76).

Attempts to improve the delivery of ceramide have included modification of the ceramide's structure as well as exploration of naturally occurring ceramide derivatives found in other species (76). Though not the primary focus of this thesis, briefly, promising chemical modifications include development of pyridinium-ceramides, uracil-linked ceramides, ceramines, N-substituted sphingosine analogs, serinamides, and 4,6-Diene-ceramide, while natural ceramide derivates include sphingadienes and sphingatrienes from sea cucumbers and ceramide methylaminoethylphosphonates (CMAEPh) from oysters (76).

However, perhaps the greatest improvement to enhancing ceramide delivery without altering the structure came about in 2003, when it was discovered that incorporation of C6 ceramide into liposomal formulations, including nano-sized formulations containing other lipids, could

prevent immune cell uptake, increasing half life and delivery (77-79). Since its development, the C6 ceramide-containing nanoliposome or ceramide nanoliposome (CNL) has shown *in vitro* and/or *in vivo* efficacy in multiple blood cancers such as Acute Myeloid Leukemia (AML)(80, 81), Chronic Lymphocytic Leukemia (CLL) (82, 83), and Natural Killer Large Granulocytic Leukemia (NK-LGL) (84, 85), as well as solid tumor models including melanoma (86), ovarian (87), pancreatic (88), breast (86, 89), colorectal (90, 91) and liver cancers (91-93). Currently, the CNL is being evaluated in Phase I 3x3 dose escalation clinical trials for advanced solid tumors. Preliminary Phase I results showed stable disease in 50% of patients without identification of any dose limiting toxicities with minimal adverse events (NCT 02834611). Thus, the CNL affords the advantages of exogenous ceramide delivery while mitigating difficulties in delivery and providing additional therapeutic relevance.

SPHINGOLIPIDS IN HNSCC

Though this thesis outlines the first use of the CNL in HNSCC, research involving sphingolipids has been previously conducted in the HNSCC field. Though not a comprehensive summary, these research endeavors include studying altered sphingolipid profiles in HNSCC, highlighting sphingolipid enzymes for therapeutic intervention, identifying drugs which induce ceramide levels in HNSCC, and evaluating ceramide or ceramide derivatives directly as a therapeutic.

In regards to the implication of general sphingolipid signaling in HNSCC, multiple studies have elucidated the significance of different sphingolipid species and enzymes. It has been established that sphingolipid profiles in HNSCC compared to normal tissues are altered in both mouse models (94), as well as human tissues (95). Specifically in human cancers, sphingosine kinase 1 (SphK1) is increased in malignant tissues and is associated with shorter patient survival (96, 97). Similarly, higher glucosylceramide synthase (GCS) expression is associated with worse disease-free and overall survival (98). On the other hand, decreases in ceramide synthase 1 (CerS1)

and its lipid product C18 ceramide are correlated with lymphovascular invasion and nodal metastasis (95). Interestingly, the levels of C18 ceramide mentioned above have since been explored as a biomarker in Phase II clinical trials (49).

While the above-mentioned changes represent correlative sphingolipid alterations in HNSCC, two sphingolipid enzymes, CerS1 and glucosylceramide synthase (GCS), as well as their sphingolipid products, C18 ceramide and glucosylceramide, respectively, have been explored for portential therapeutic intervention. Specifically, decreasing levels of C18 ceramide by knocking down the CerS1 enzyme decreases the *in vitro* efficacy of chemotherapeutics (99) and photodynamic therapy (100) in HNSCC while increasing levels of C18 ceramide via overexpression of a mouse homolog of CerS1 have decreased *in vivo* tumor growth by approximately 75% (101). Another sphingolipid class, the glucosylceramides, have shown a somewhat more controversial role in HNSCC. While one report suggests inhibition of Glucosylceramide Synthase (GCS), the enzyme which synthesizes glucosylceramides, enhances efficacy of the chemotherapeutic cisplatin (52), another claims that addition of glucosylceramides via dietary supplementation actually suppresses tumor growth (102).

While perhaps not a direct interrogation of sphingolipid signaling in HNSCC, it is worth noting that drugs that induce ceramide production have also shown promise in treating HNSCC and drugs that alter sphingolipid metabolism may enhance these therapies. Of interest, two chemotherapeutics used to treat HNSCC (103), Cisplatin and 5-Fluorouracil, both increase ceramide levels in other cancer models as well as HNSCC (76, 104-106). Interestingly, in HNSCC models, resistance to cisplatin can be decreased by inhibiting enzymes which metabolize ceramide, GCS (52) or Acid Ceramidase (107), and enhanced by inhibiting an enzyme that generates ceramide, CerS6 (108). Similarly *in vitro* HNSCC studies demonstrate 5-Fluorouracil synergizes with the drug deguelin, that has also been shown to increase cellular levels of ceramide. Taken together these data suggest that increased ceramide generation or prevention of ceramide breakdown correlates with enhanced cell death in HNSCC.

Finally, previous studies have explored short-chain ceramide or ceramide analog signaling in HNSCC. These studies have not only shown the potential for ceramide as a single agent in HNSCC, but have also identified potential combinatorial therpies utilizing Palitaxel (Mehta 2000), PKC412 (109), gemcitabine (110), photodynamic therapy (111), and an ERK inhibitor (PD98059) (112). Furthermore, these results have shown success *in vitro* as well as *in vivo.* These studies laid excellent groundwork and identified key hubs for ceramide's signaling effect including effects on telomerase (113), cell cycle arrest (110), and most importantly, the induction of autophagy (112). [More background and new findings on ceramide's role inducing mitochondrial permeability, autophagy, and mitophagy are covered in **Chapter 2**]. Taken together, there is a large body of evidence suggesting ceramide has numerous roles in preventing HNSCC survival and growth, highlighting its role as a potential therapeutic for this disease.

In summary, HNSCC is the seventh most deadly cancer in the world. While traditional therapies are highly morbid, there have been only a few new systemic treatments developed in the last few decades, and these benefit only a small population of patients. The anti-cancer signaling sphingolipid ceramide has shown promise as a therapeutic in many cancer models including preliminary work in HNSCC. This thesis project evaluates the capacity of the ceramide nanoliposome (CNL) as a potential therapeutic for head and neck squamous cell carcinoma. This is accomplished by exploring methods to circumvent ceramide resistance (**Chapter 2**), identify novel markers of non-canonical cell death (**Chapter 3**), utilize synergistic dual therapeutic approaches with previously failed EGFR inhibitors (**Chapter 4**), and manipulate sphingolipid metabolism (**Chapter 5**). These studies elucidate a myriad of signaling pathways as well as specific druggable targets that can be manipulated to enhance therapeutic efficacy of CNL or other ceramide-based therapies for treatment of HNSCC.

CHAPTER TWO: CERAMIDE AND AUTOPHAGIC/MITOPHAGIC INHIBITION SYNERGIZE IN HNSCC

CHAPTER TWO: CERAMIDE AND AUTOPHAGIC/MITOPHAGIC INHIBITION SYNERGIZE IN HNSCC

PRIMER:

The primary undertaking for this thesis was to first learn and make observations about CNL-induced cell death in HNSCC and then explore and interrogate those observations. This project is featured first in the thesis because of that fundamental nature in first identifying hallmarks of CNL-induced death and then exploring them for functional relevance. Furthermore, in order to adequately present the work, only minor modifications (placement of figures, figure order numbers, etc.) from the final product submitted for publication in Molecular Cancer Therapeutics are presented herein.

Inhibition of Lysosomal Function Mitigates Protective Mitophagy and Augments Ceramide Nanoliposome-Induced Cell Death in Head and Neck Squamous Cell Carcinoma

Jeremy JP Shaw[1], Timothy Boyer[2], Emily Venner[3], Patrick Beck[2], Tristen Slamowitz[2], Tara Caste[2], Alexandra Hickman[2], Michael H Raymond[4], Pedro Costa-Pinheiro[1], Mark J Jameson[6], Todd E. Fox[4], Mark Kester[2,5]

Department of Pathology[1], Department of Biomedical Engineering[2], Department of Biology[3], Neuroscience Graduate Program[4], Department of Pharmacology[5], Department of Otolaryngology - Head and Neck Surgery[6], University of Virginia, Charlottesville, VA.

Running Title: Lysosome Inhibition Enhances Ceramide-Induced Cell Death

Abbreviations:

HNSCC - Head and Neck Squamous Cell Carcinoma, PGF - Primary Gingival Fibroblasts

CNL - Ceramide Nano Liposome, CQ - Chloroquine, MP – Methyl Pyruvate, Baf - Bafilomycin, AMS - Apilimod Mesylate

PARP - Poly ADP Ribose Polymerase, LAMP1 - Lysosomal Associated Protein 1, LC3B - microtubule-associated proteins 1A/1B light chain 3B, BNIP3 - BCL2 and adenovirus E1B 19-kDa-interacting protein 3, LAMP2 - Lysosomal Associated Protein 2, Rab7 - Ras-related protein 7, p62- Nucleoporin p62, PINK1 - PTEN-induced kinase 1

Conflict of Interest: Penn State Research Foundation has licensed Ceramide nanoliposomes to Keystone Nano Inc., State College PA, MK is CMO and co-founder of KeystoneNano.

Abstract

Therapies for Head and Neck Squamous Cell Carcinoma (HNSCC) are, at best, moderately effective, underscoring the need for new therapeutic strategies. Ceramide treatment leads to cell death as a consequence of mitochondrial damage by generating oxidative stress and causing mitochondrial permeability. However, HNSCC cells are able to resist cell death through mitochondria repair via mitophagy. Through the use of the C6-ceramide nanoliposome (CNL) to deliver therapeutic levels of bioactive ceramide, we demonstrate that the effects of CNL are mitigated in drug-resistant HNSCC via an autophagic/mitophagic response. We also demonstrate that inhibitors of lysosomal function, including chloroquine (CQ), significantly augment CNL-induced death in HNSCC cell lines. Mechanistically, the combination of CQ and CNL results in dysfunctional lysosomal processing of damaged mitochondria. We further demonstrate that exogenous addition of Methyl Pyruvate rescues cells from CNL+CQ-dependent cell death by restoring mitochondrial functionality via the reduction of CNL- and CQ-induced generation of reactive oxygen species and mitochondria permeability. Taken together, inhibition of late stage protective autophagy/mitophagy augments the efficacy of CNL through preventing mitochondrial repair. Moreover, the combination of inhibitors of lysosomal function with CNL may provide an efficacious treatment modality for HNSCC.

Keywords:

Sphingolipids, Ceramide, Mitochondria, Autophagy, Cancer, Apoptosis, Drug Therapy, Lipids, Lipid Treatments, Signal Transduction, Transcription

Introduction

Head and Neck Squamous Cell Carcinoma (HNSCC) is a cancer originating from squamous cells, mainly of the larynx, pharynx, and oral cavity. The worldwide incidence and mortality are over 830,000 and 430,000 per year, respectively (29). While traditional surgery and chemoradiotherapy offer patients substantial benefit, these modalities cause serious adverse events and relapse still occurs (114). Until the very recent approval of immune checkpoint inhibitors (30), Cetuximab, an epidermal growth factor receptor (EGFR) inhibitor, was the only targeted therapy approved in combination with chemoradiotherapy for first-line treatment in HNSCC. With cancer recurrence, first line therapy is offers only around a 20-40% 3-year survival rate (115), and second-line therapies offer an even more dismal response (24). Despite attempts to identify subtypes of HNSCC that would be amenable to targeted therapies, these endeavors have proven difficult due to the molecular heterogeneity, late stage of detection, and lack of susceptibility to multiple specific EGFR tyrosine kinase inhibitors (TKIs) (114, 116). Thus, there is an urgent need for new therapeutic approaches.

Sphingolipid metabolites, including ceramide, and the enzymes that regulate their levels are dysregulated in a myriad of pathologies, including cancers (44, 106, 117). Ceramide is well established as a pro-apoptotic lipid. However, ceramide metabolites, including sphingosine-1-phosphate and glucosylceramide, have been shown to be anti-apoptotic and promote drug resistance (44, 106). Previously, C6-ceramide, a synthetic short-chain form of ceramide, has been shown to induce cell cycle arrest and apoptosis in HNSCC *in vitro* (118). In fact, many chemotherapeutic approaches increase levels of ceramide within tumors leading to cell death (44, 105, 106, 119, 120). Our laboratory has engineered a water-soluble, non-toxic delivery platform for C6-ceramide, the ceramide nanoliposome (CNL) (77), that is currently being evaluated in a Phase I human trial for solid tumors (79).

Like many chemotherapeutics, the efficacy of ceramide (or CNL) may be limited by drug resistance mechanisms, including autophagy (121). Autophagy is a cellular recycling process that

sequesters damaged proteins or organelles within an isolation membrane which matures to form an autophagosome. The autophagosome then fuses with an acidified lysosome, a necessary step for degradation and recycling of its cargo (122). Autophagy is frequently dysregulated in cancer and has previously been identified as a mechanism of resistance to cell death (121). However, in the context of ceramide-signaling, it is still unclear if ceramide induces protective autophagy-mediated survival or lethal autophagy-mediated cell death (123). Furthermore, the mechanism and stage at which ceramide induces autophagy appears to be multi-faceted and cell-type dependent (117).

Our laboratory has previously published that inhibitors of microtubules (and possibly autophagosomes), such as vinblastine, augment the efficacy of CNL in solid (91) and non-solid cancers (81, 124). Both ceramide signaling and autophagic inhibition have been independently shown to alter mitochondrial function. Ceramides have previously been shown to induce oxidative stress which can alter mitochondrial function, directly induce pore-formation in mitochondria, and drive mitophagy (124-126). Mitophagy, a subclass of autophagy, is responsible for recycling damaged parts of the mitochondria to promote mitochondrial health and functionality (127). However, how inhibition of autophagic/lysosomal processing affects ceramide-dependent mitochondrial damage and/or mitophagy is undefined.

In the present work, we examine if direct inhibitors of lysosomal function enhance the therapeutic effect of CNL in drug resistant HSNCC by circumventing autophagic resistance. We further evaluated the mechanisms by which inhibitors of late-stage autophagy/mitophagy can augment mitochondrial-dependent CNL-induced cell death. Taken together, this work defines a novel combinatorial therapeutic strategy to enhance the efficacy of CNL in drug-resistant HSNCC.

Materials and Methods:

Cell Culture:

The HNSCC cell lines, Cal27, FaDu, UNC-7, UNC-10, SCC-25, SCC-61, and OSC-19 were obtained from Mark Jameson's Lab (University of Virginia) and grown in DMEM/F-12 media (Thermo Fisher Scientific, Waltham, MA) supplemented with 10% FBS (Gemini Bio Products, West Sacramento, CA) and 1% Antibiotic-Antimycotic (Thermo Fisher Scientific). SCC-61 media was additionally supplemented with 0.5mg/mL hydrocortisone (Millipore Sigma, Burlington, MA). The Primary Gingival Fibroblasts (PCS-201-018 ATCC, Manassas, VA) were grown in Fibroblast Basal Media supplemented with Fibroblast Growth Kit-Low serum (ATCC PCS-201-041) and 1% antibiotic-antimycotic. TrypLE (Thermo Fisher Scientific) was used to passage cells. All cell lines were authenticated via DNA fingerprinting (University of Arizona) of early passage, confirmed mycoplasma via MycoAlert® System (University of Virginia) after thawing, and did not exceed 25 passages.

Inhibitors:

Chloroquine (Thermo Fisher Scientific) and Methyl Pyruvate (Alfa Aesar, Haverhill, MA) were dissolved in water. Working stocks of staurosporine (ApexBio, Houston, TX), Apilimod Mesylate (Millipore Sigma), Bafilomycin, Rapamycin, (LC Laboratories, Woburn, MA) and Torin-1 (Cayman Chemical Company, Ann Arbor, MI) were prepared in DMSO.

Ceramide Nano Liposome (CNL) Formulation:

Ceramide nanoliposomes were a generous gift from KeystoneNano (State College, PA) and manufactured according to published methods (79). Control (ghost) formulations included all liposomal ingredients except C6-ceramide.

MTS Assay:

HNSCC cells were seeded on 96 well plates to achieve a similar confluency. After 24 hours, cells were pre-treated for 4 hours (Rapamycin and Torin 1), 2 hours (MP), or 1 hour (CQ, Baf, AMS) and subsequently treated with CNLs or ghost liposomes at concentrations indicated in the text.

MTS assays were performed according to the manufacturer's instructions (Promega, Madison, WI). Absorbance at 490nm was determined with a Cytation 3 plate reader (Bio Tek, Winooski, VT). After subtracting the background absorbance (no cells), all values were normalized to their intra-plate controls.

Western Blot:

Cells were treated as indicated in the text. RIPA buffer (Alfa Aesar) with protease inhibitor (Thermo Fisher Scientific) and phosphatase inhibitor (Roche, Basel, Switzerland) was used to lyse the cells. Protein concentrations were determined with a BCA protein assay (Pierce, Appleton, WI). 20-30µg of protein was added to a NuPAGE 4-12% Bis-Tris gel (Thermo Fisher Scientific) and ran at 120V for 2 hours and 20 minutes. Transfer to a nitrocellulose membrane (Bio-Rad Laboratories, Hercules, CA) was performed using the Bio-Rad Turbo-Transfer apparatus. Blocking with 5% BSA (Thermo Fisher Scientific) in TBST was done for 1 hour at room temperature and blots were cut before an overnight primary antibody incubation at 4°C. Primary antibodies were, LAMP1 [sc-20011], LAMP2 [sc-18822], SQSTM1 (p62) [sc-28359], GSK-3α/β [sc-7291] (Santa Cruz Biotechnologies, Dallas, TX), Beta Actin [A5441] (Millipore Sigma), LC3B [3868], Beclin-1 [3738], Caspase 3 [9662] (Cell Signaling Technologies, Danvers, MA) and BNIP3 [ab10433], Rab7 [ab137029], PINK1 [ab23707] (Abcam, Cambridge, United Kingdom). Blots were washed 3x5 minutes with TBST. Horseradish peroxidase conjugated secondary antibody against rabbit or mouse (Thermo Fisher Scientific) was then added for 1 hour at room temperature. Three additional five minute washes were performed prior to detection with enhanced chemiluminescence (Prometheus, San Diego, CA) and imaged with a G:Box Chemi XX6 (Syngene, Bangalore, India). If blots were re-probed, a stripping step was performed using Restore Western Blot Stripping Buffer (Thermo Fisher Scientific) according to the manufacturer's instructions. Densitometry of each target was performed using ImageJ software and were normalized: first, to β-actin, then to the vehicle treatment at the respective time-point from the same blot.

Transmission Electron Microscopy (TEM):

Cells were treated as indicated in the text. After treatment, samples were fixed in 4% paraformaldehyde + 2% glutaraldehyde, post-fixed in 4% osmium tetroxide, dehydrated through a gradient of ethanol into propylene oxide, then embedded in the epoxy resin Embed 812. Samples were sectioned at 70nm with a UC7 Ultramicrotome (Leica, Nussloch, Germany), placed on 200 mesh copper grids, and contrast-stained with uranyl acetate and lead citrate. Microscopic analysis was performed using a JEM-1230 TEM microscope (JEOL, Tokyo, Japan) and images captured with a 4K X 4K CCD camera.

Quantitative Real-Time Polymerase Chain Reaction:

Treated cells were washed and RNA extracted using the RNeasy Mini Kit (Qiagen, Hilden, Germany). RNA content was quantified using a Cytation 3 (BioTek Winooski, Vermont). 800-1000ng of RNA was used in the iScript cDNA Synthesis Kit (Bio-Rad Laboratories) to synthesize cDNA. FAM probes (BNIP3-[qHsaCIP0040441], MAP1LC3B-[qHsaCEP0041298], LAMP1-[qHsaCEP0055037], BECN1-[qHsaCIP0030326], PSMB6-[qHsaCEP0052321], B2M-[qHsaCIP0029872]) and iTaq Universal Probes Supermix (Bio-Rad Laboratories) were used and CT values were measured using CFX Connect Real-Time PCR Connection System (Bio-Rad Laboratories). CT values were normalized first to the housekeeping gene control (PSMB6 and/or B2M), and then to their respective timepoint/vehicle controls.

Flow Cytometry Assays:

Cells were treated as indicated in the text. The media containing floating cells and the adherent cells, after trypsinization, were combined. Cells were centrifuged and the supernatant discarded. To assess cell viability, autophagic vacuole presence, and mitochondrial permeability on the resultant cell pellet, Fixable Viability Dye 780 (Thermo Fisher Scientific), CYTO-ID Autophagy detection kit 2.0 (Enzo Biochem, Farmingdale, NY), and BD MitoScreen (JC-1) (BD Biosciences, Franklin Lakes, NJ) dyes, were used respectively, according to the manufacturers' instructions. Samples were measured by the Attune NxT Flow Cytometer (Thermo Fisher Scientific). Forward and side scatter measurements were used to gate for singlets and exclude debris. Single-stain

compensation controls were collected and gates were drawn accordingly.

ROS/Superoxide Assay & ATP Measurement Assay: Cells were treated as described in the text and the ROS/Superoxide Detection Assay Kit (Cell-based) (ab139476) (Abcam) and Luminescent ATP Detection Assay Kit (ab113849) (Abcam) were utilized according to the manufacturer's instructions A Cytation 3 plate reader was used to analyze general ROS (Ex/Em: 490/525nm), Superoxides (Ex/Em: 550-620nm), and ATP (luminescence). Background was subtracted and all results were normalized to the respective vehicle controls.

Statistics:

All statistics were performed on GraphPad Prism 8 (GraphPad Software, San Diego, CA). All experiments were repeated at least three times unless otherwise stated. A one-way ANOVA was performed with Tukey's multiple comparison post-hoc test to determine significance between all groups. The markers *, **, and *** indicate significance of $p < 0.05$, 0.01, and 0.001 respectively. All error bars are standard deviation of the mean. Bliss scores were calculated using SynergyFinder (128)

Results

CNL Induces a Time- and Concentration-Dependent Decrease in Cell Viability

To determine the response of HNSCC cell lines to CNL treatment, seven HNSCC cell lines and non-transformed primary gingival fibroblasts (PGF) were treated with varying concentrations of CNL for 24 hours (Fig. 2-1A). CNL induced a concentration-dependent decrease in cell viability in all cell lines with varying sensitivities. No significant cell death occurred in all cell lines treated with ghost liposomes (Fig. 2-1A). The most resistant cancer cell line, FaDu (81% viable with 25μM CNL) was similar to the non-transformed PGF. In contrast, after 48 hours FaDu cells exhibited a larger reduction in viability compared to PGF (Fig. 2-1B). PGF and FaDu cells were further analyzed for viability dye exlusion measured via flow cytometry (Fig. 2-1C). Confirming the MTS results, PGF cells were more resistant to CNL than FaDu, and only showed significant cell death with 10μM and 25μM CNL after 48 hours. These data support that, though variable, HNSCC cell lines are more sensitive than non-transformed cells to CNL.

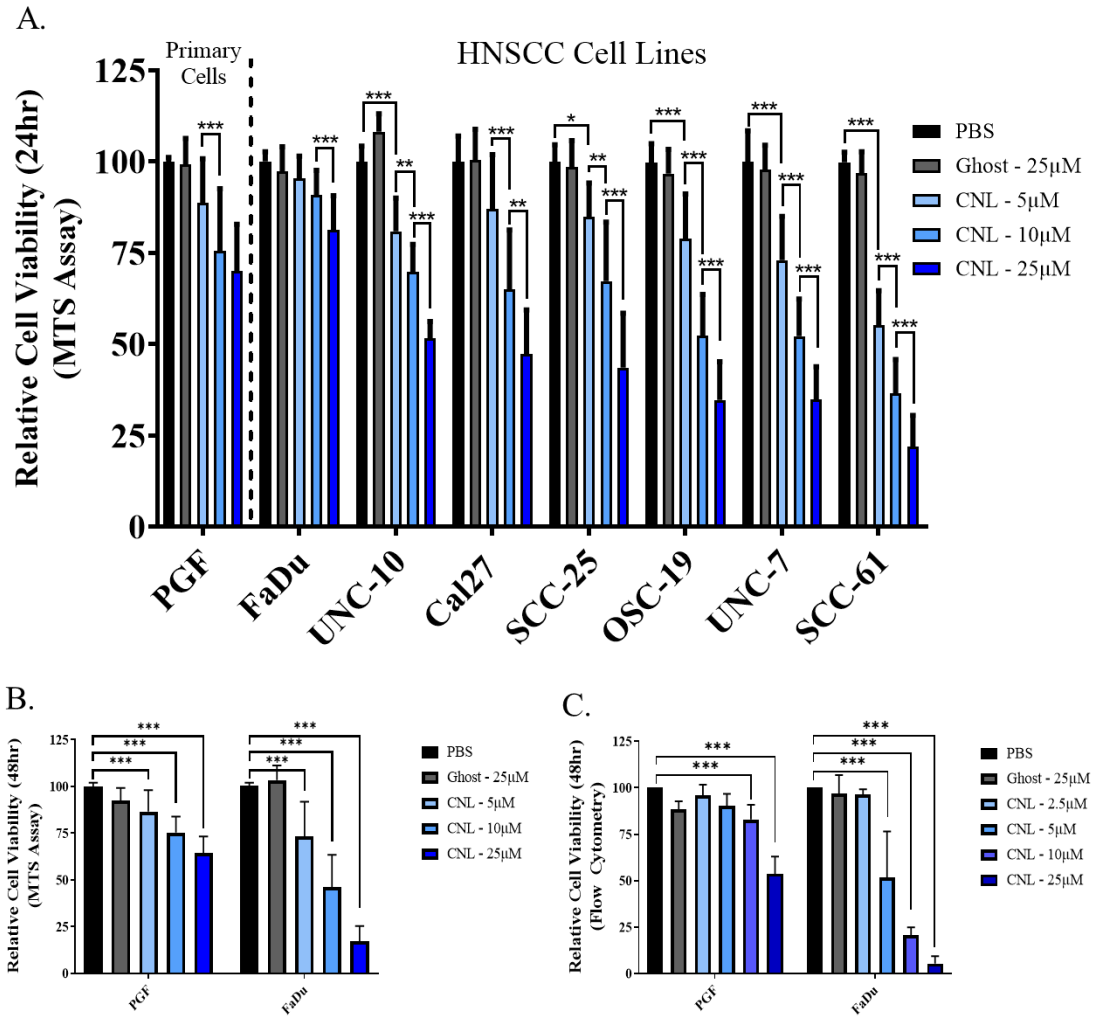

Figure 2-1: CNLs Induce a Time and Concentration-Dependent Decrease in Cell Viability
PGF- Primary Gingival Fibroblasts, HNSCC – Head and Neck Squamous Cell Carcinoma
(A) *A primary gingival fibroblast (PGF) cell line and seven HNSCC cell lines were treated with PBS, Ghost liposomes (25μM) or CNL (5μM, 10μM or 25μM) for 24 hours and cell viability assessed with an MTS assay. Statistical comparisons displayed compare 5μM CNL to 10μM and from 10μM CNL to 25μM CNL -All cell line comparisons to PBS (within a cell line) were at least $P<0.05$ except the following: PGF 5μM, FaDu 5μM, Cal27 5μM* ***(B-C)*** *PGF and FaDu cells were treated with controls (PBS or ghost liposomes) or CNL (2.5μM, 5μM, 10μM, or 25μM CNL) for 48 hours and cell viability was assessed via* ***(B)*** *MTS assay* ***(C)*** *via flow cytometry. The markers *, **, and *** indicate significance of $p < 0.05$, 0.01, and 0.001 respectively, displayed error bars represent standard deviation of the mean, and all experiments were performed with at least three biological replicates.*

CNLs Induce Autophagy but Not Apoptosis

Because FaDu cells require a longer duration of CNL treatment to observe a robust response compared to other HNSCC cell lines, experiments to investigate mechanisms of ceramide resistance are focused on FaDu cells. Caspase-3 and PARP cleavage are indicative of increased caspase-dependent apoptotic cell death and a decrease in commitment to DNA-repair (129). Supporting results from Fig. 1A, western blotting confirmed neither caspase-3 nor PARP protein cleavage occurs in response to CNL within 24 hours in FaDu cells. (Fig. 2-2A). As a positive control, staurosporine treatment resulted in cleavage as early as 6 hours. To further examine the lack of apoptotic markers, TEM imaging was used to identify morphological differences in cells treated with CNL or ghost liposomes after 12 hours (Fig. 2-2B). Further ruling out canonical apoptosis, increased membrane blebbing and apoptotic body formation were not observed. Interestingly, FaDu cells showed a marked increase in the number of autophagosomes after CNL, but not ghost liposome treatment. This suggests that CNL may be triggering an autophagic response.

To evaluate this autophagic response, markers of autophagy were assessed by western blotting (Fig. 2-2C/D). The two forms of the protein encoded by microtubule-associated proteins 1A/1B light chain 3B (*MAP1LC3B* or LC3B) were measured. The cytosolic form of LC3B, LC3B-I, (top-band) can be conjugated with phosphatidylethanolamine generating LC3B-II (lower band), a marker of increased autophagosomes in cells (122). In cells treated with CNL, a 4.6-fold increase of LC3B-II was observed at 24 hours (Figures. 2-2C/D). Moreover, LC3B transcripts also increased (Fig. 2-2E). The adenovirus E1B 19-kDa-interacting protein 3 (BNIP3), which is associated primarily with the mitophagy subclass of autophagy (130), was next assessed. Similar to LC3B-II, a 3.1-fold increase in BNIP3 protein expression was observed at 24 hours (Fig. 2-2C/2D) which was consistent with BNIP3 RNA expression (Fig. 2-2E). While LC3B-II is a marker of autophagosomes, it is not a direct measurement of late autophagy or lysosomal function. Lysosome-associated membrane glycoprotein 1 (LAMP1) is a multi-functional protein located within the

lysosomal membrane (122, 131). In contrast to LC3B-II, a time-dependent 0.56-fold decrease in LAMP1 was seen in cells treated with CNL (Fig. 2-2C/2D). LAMP-1 transcript levels were not changed with CNL treatment (Fig. 2-2E) suggesting the effect of ceramide on LAMP-1 is post-transcriptional. These data demonstrate that CNL alters multiple autophagic/mitophagic targets (LC3B, BNIP3, and LAMP1) through transcriptional, translational, and post-translational mechanisms.

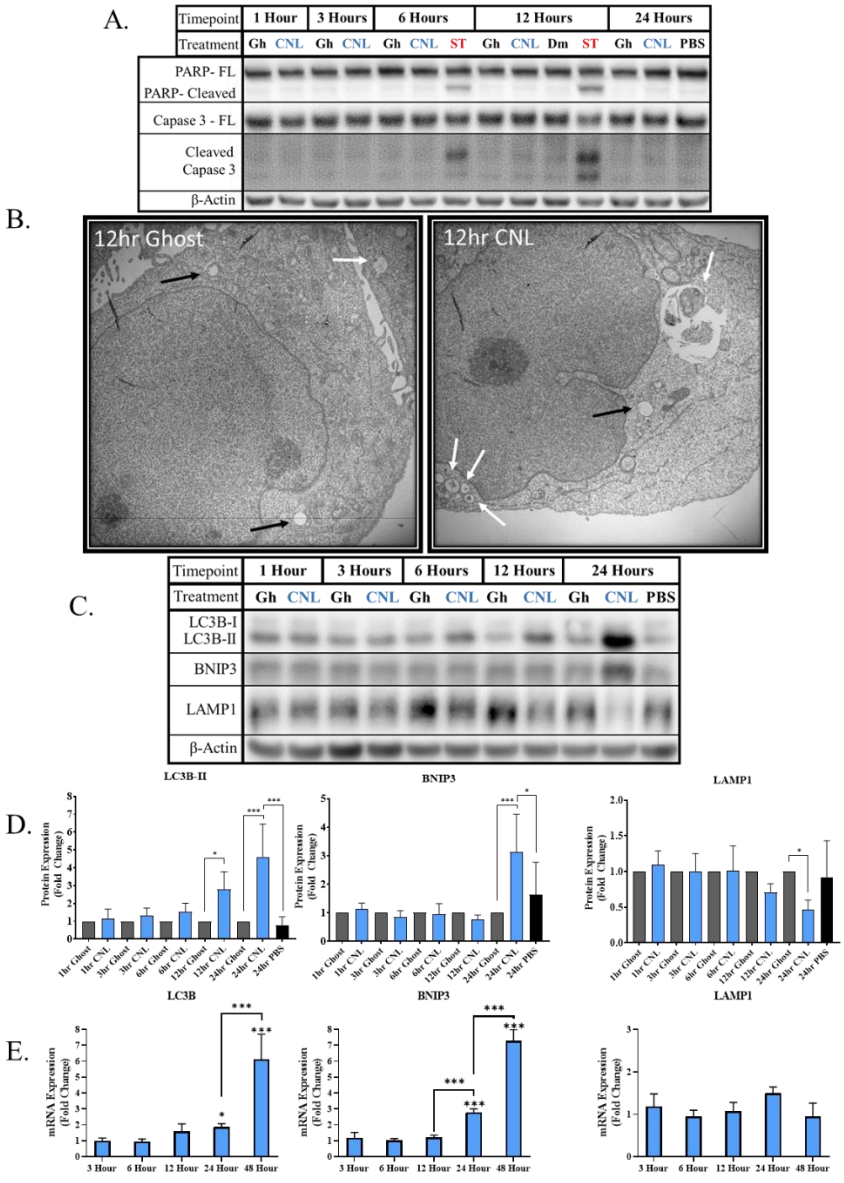

Figure 2-2: CNLs Induce Autophagy but Not Apoptosis

CNL - C, Ghost - Gh, ST - Staurosporine, Dm – DMSO, PARP - Poly ADP Ribose Polymerase, LAMP1 - Lysosomal Associated Protein 1, LC3B - microtubule-associated proteins 1A/1B light chain 3B, BNIP3 - BCL2 and adenovirus E1B 19-kDa-interacting protein 3. ***(A)*** *Western Blot showing FaDu cells treated with 10μM CNL or ghost liposomes for 1, 3, 6, 12, or 24 hours. Additionally, positive control (Staurosporine 500nM) and vehicle (DMSO) were added at 6hr and 12hr timepoints as shown. Apoptotic targets: PARP-Full Length, PARP- Cleaved, Caspase 3 –Full Length, and Cleaved Caspase were measured and compared to a β-Actin loading control.* ***(B)*** *TEM images of FaDu cells treated with 10μM CNL or ghost liposomes for 12 hours. Autophagic vacuoles (white arrows) and empty vacuoles (black arrows) are identified.* ***(C)*** *Western Blot showing FaDu cells treated with 10μM CNL or ghost liposomes for 1, 3, 6, 12, or 24 hours. Autophagic/mitophagic/lysosomal targets (LC3B-I, LC3B-II, BNIP3, and LAMP1) and loading control (β-Actin) were measured.* ***(D)*** *Densitometric analysis of protein targets measured in C normalized first to internal β-Actin loading controls, then to the ghost liposome treatment at each timepoint.* ***(E)*** *RT-qPCR measuring transcript expression levels of LC3B, BNIP3, and LAMP1 after treatment with CNL for 3, 6, 12, 24, or 48 hours normalized first to PSMB6, then to the ghost liposome treatment at each timepoint. The markers *, **, and *** indicate significance of $p < 0.05$, 0.01, and 0.001 respectively, displayed error bars represent standard deviation of the mean, and all experiments were performed with at least three biological replicates.*

Inhibition of Late-Stage Autophagy Synergizes with CNL to Induce Cell Death in Resistant HNSCC

To determine the functional relevance of the CNL-driven autophagic response, early (autophagosome formation and cargo sequestration) and late (autophagosomal maturation and lysosomal fusion) stage autophagy was investigated. Two inducers of early autophagy, Torin1 and Rapamycin, did not alter CNL-mediated cell death at 24 or 48 hours (Supplemental Fig. 2-1). Consistently, inhibitors of early stage autophagy, the PI3K inhibitors 3-methyladenine or wortmannin, did not alter viability in the presence or absence of CNL (data not shown).

In contrast to modulating early stage autophagy, inhibition of late stage autophagy using chloroquine (CQ) significantly augmented CNL-induced cell death in CNL resistant HNSCC cells. Specifically, non-transformed (PGF), ceramide-resistant (FaDu), moderately ceramide-sensitive (UNC-10), and ceramide-sensitive (SCC-61) cells were pre-treated with CQ before CNL treatment and the viability was assessed 24 hours later (Fig. 2-3A-D). In PGF and FaDu cells, CQ had minimal impact on cell viability as a single agent, only decreasing viability at 25μM concentrations (Fig. 2-3A/B). However, CQ dramatically augmented CNL-driven reduction in cell viability at both 24 and 48 hours in FaDu cells, with negligible effects seen in PGF cells (Fig. 2-3A/B). Specifically, at 48 hours, CNL treatment reduced viability of FaDu cells by 22%, whereas CNL with 5μM CQ pretreatment resulted in a 68% decrease in viability. (Fig. 2-3A/B). In FaDu cells, the combinatorial effect of CQ and CNL was highly synergistic with a Bliss score of 26.9 at 48 hours (Fig. 2-3B) Synergism was also observed with UNC-10 cells, where CNL+CQ had a Bliss Score of 16.4 (Fig. 2-3C). In contrast, Bliss score analysis revealed minimal synergy between CQ and CNL in PGF (Fig. 2-3A) and CNL-sensitive SCC-61 cells (Fig. 2-3D). The combinatorial decrease in viability by CNL and CQ treatment in FaDu cells was confirmed via viability dye staining (Fig. 2-3E). Moreover, TEM analysis of CQ and CNL dual-treated FaDu cells revealed a marked increase in the number of autophagic vacuoles compared to either treatment alone (Fig. 2-3F).

To confirm the specificity of synergy between CNL and CQ, FaDu cells were next treated with other inhibitors of late-stage autophagy/lysosomal function, Bafilomycin (Baf) and Apilimod Mesylate (AMS). Baf, which inhibits V-ATPase-dependent acidification and autophagosome-lysosome fusion (132), dramatically sensitized cells to CNL-induced cell death at 24 hours (Fig. 2-3G). Similarly, AMS, an inhibitor of the enzyme PIKfyve shown to prevent fusion of autophagosomes with lysosomes (133), also induced synergistic cell death (Fig. 2-3H). Taken together, these data suggest that late-stage, but not early stage autophagy, is a resistance mechanism to CNL-treatment.

Supplemental Figure 2-1: Inducing Early Stage Autophagy Does Not Alter CNL-Induced Cell Death in HNSCC

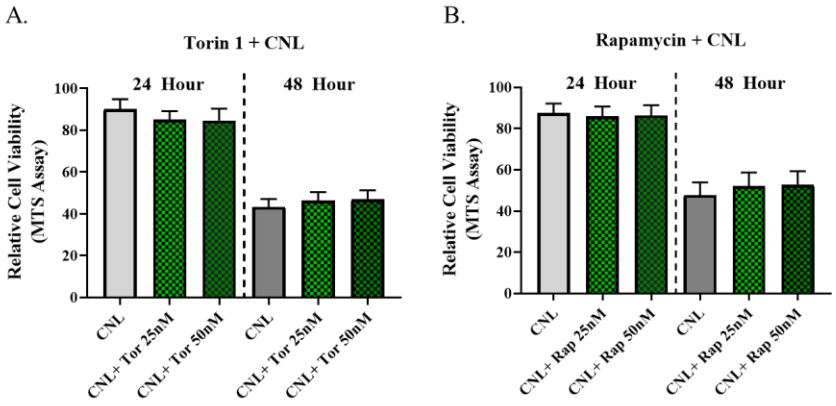

Rap- Rapamycin, Tor - Torin 1,PGF - Primary Gingival Fibroblasts, HNSCC - Head and Neck Squamous Cell Carcinoma

(A-B) *MTS assay assessing cell viability after pre-treatment with* ***(A)*** *Rapamycin (25nM and 50nM) or* ***(B)*** *Torin-1 (25nM and 50nM) or their respective vehicles for 4 hours before being treated with 10μM CNL or equivalent ghost liposomes for 24, 48, and 72 hours. All values are normalized to cells treated with ghost liposomes and vehicle. The markers *, **, and *** indicate significance of $p < 0.05$, 0.01, and 0.001 respectively. The markers *, **, and *** indicate significance of $p < 0.05$, 0.01, and 0.001 respectively, displayed error bars represent standard deviation of the mean, and all experiments were performed with at least three biological replicates.*

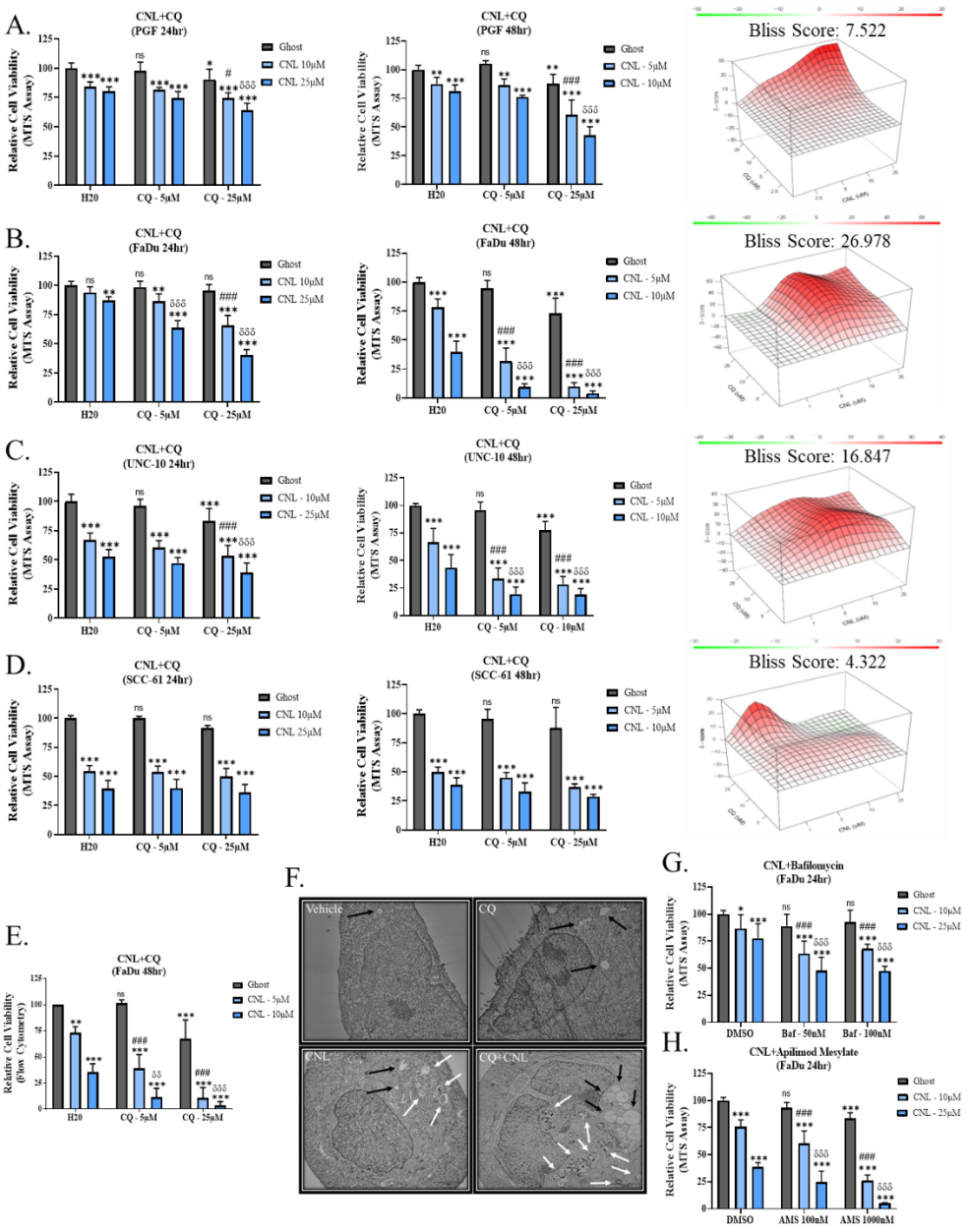

Figure 2-3: Inhibiting Autophagy Synergizes with CNL to Induce Cell Death in HNSCC

CQ – Chloroquine, Baf – Bafilomycin, AMS – Apilimod Mesylate

(A-D) *MTS assay assessing cell viability (24 and 48hr), Bliss synergy score (48hr), and 3D synergy plot (48hr) after CQ pre-treatment (H20, 5μM, 10μM, or 25μM) and CNL treatment (ghost liposomes, 5μM, 10μM, 25μM) in* ***(A)*** *"Non-transformed" PGF cells* ***(B)*** *"Resistant" FaDu* ***(C)*** *"Moderately resistant" UNC-10 cells, and* ***(D)*** *"Sensitive" SCC-61 cells. (E) FaDu cells were pre-treated with CQ (H20, 5μM, or 25μM) then treated with CNL (ghost liposomes, 5μM, 10μM) for 48 hours; cell viability was assessed via flow cytometry.* ***(F)*** *TEM images of FaDu cells treated with 10μM CNL or ghost control and CQ or vehicle for 24 hours. Autophagic vacuoles (white arrows) and empty vacuoles (black arrows) are identified.* ***(G-H)*** *MTS assay assessing cell viability (24hr), after pre-treatment with* ***(G)*** *Bafilomycin (DMSO, 50nM, 100nM) or* ***(H)*** *Apilimod Mesylate (100nM, 1000nM) before CNL treatment (ghost liposomes, 10μM, 25μM). Asterisks (*), pound signs (#), and delta (δ) denote significant differences from the ghost+Ctrl condition, the first concentration of CNL+Ctrl, and the second concentration of CNL+Ctrl respectively. The number of symbols 1, 2, and 3 indicate significance of $p < 0.05$, 0.01, and 0.001 respectively. Each bar represents N≥3 experiments.*

Inhibiting Late-Stage Autophagy Alters Lysosomal-Mediated CNL Signaling

Although late-stage autophagic inhibition sensitized FaDu cells to CNL-induced cell death, the underlying mechanism remained unknown. Thus, the effects of CNL and CQ on autophagy-related targets (LC3B-II, BNIP3, LAMP1, and Rab7) were analyzed to ascertain if these drugs elicit a response that corresponds with the combinatorial treatment (Fig. 2-4A/B). At 24 hours, the combination of CQ and CNL significantly increased LC3B-II levels 5.1-fold, compared to 3.0-fold by CQ and 1.8-fold by CNL alone. Furthermore, BNIP3 levels increased 9.0-fold after CQ+CNL compared to smaller changes from either drug alone. The late-endosome marker Rab7 increased 1.4-fold after CQ+CNL treatment with no changes observed with either compound alone. The protein expression increases of BNIP3 and LC3B were consistent with mRNA measurements (Fig. 4C). In contrast, the CNL-induced reduction of LAMP1 and LAMP2 was unaffected by CQ.

To further confirm the combinatorial effect of CQ and CNL on autophagy, autophagic vacuole formation was measured using Cyto-ID dye incorporation. Autophagic vacuoles increased 2.3-fold by CQ, 1.7-fold by CNL, and 4.5-fold by the combination. (Fig. 2-4D) The combination of rapamycin and CQ was used as a positive control for vacuole presence (Fig. 2-4D). These data are consistent with TEM images (Fig. 2-3F) demonstrating elevation of autophagic vacuoles. Taken together, these data support a buildup of CNL-driven autophagic vacuoles and autophagic/mitophagic proteins after inhibition of lysosomal function by CQ.

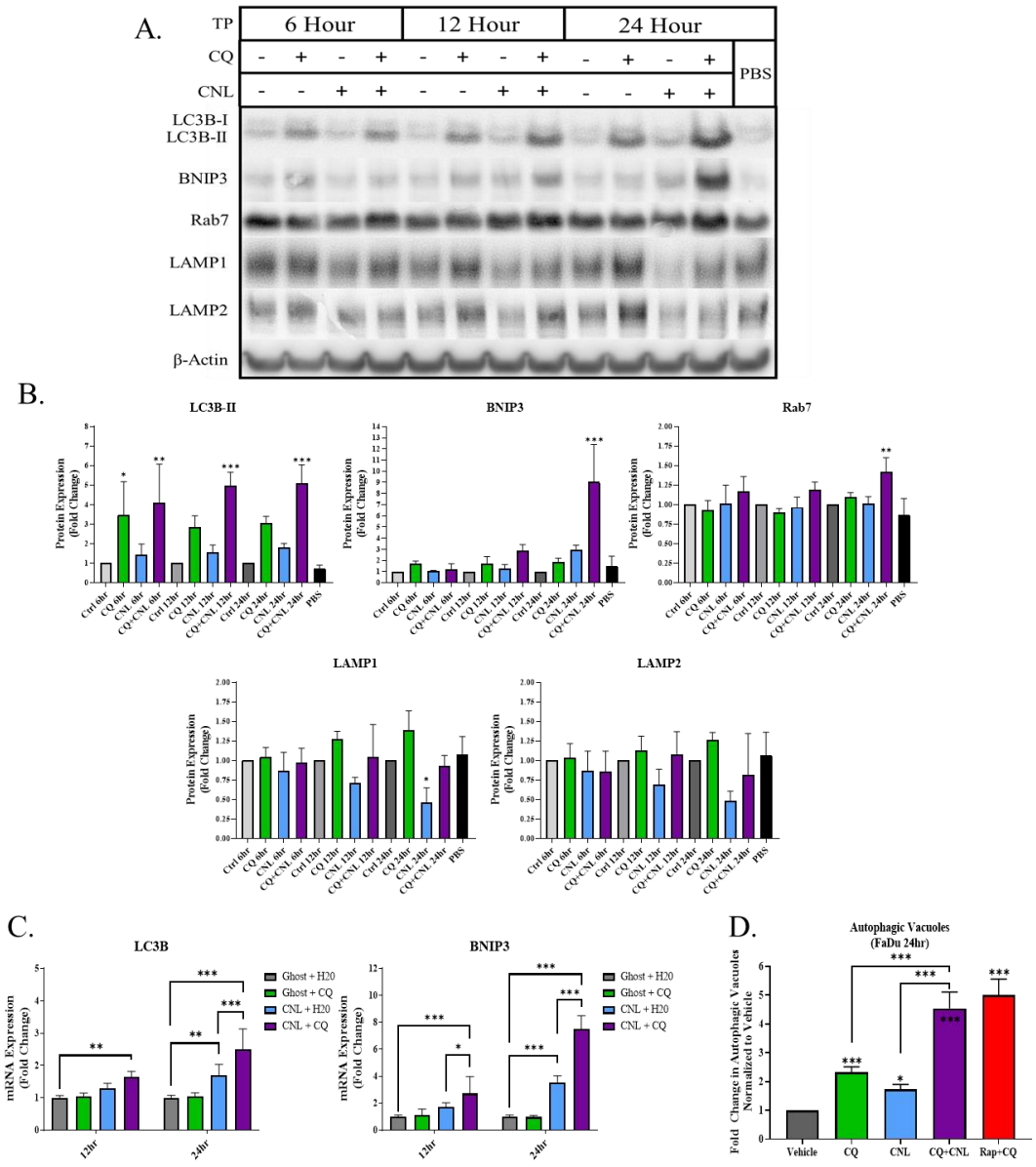

Figure 2-4: Inhibiting Late-Stage Autophagy Alters Lysosomal-Mediated CNL Signaling

CNL - C, Ghost - Gh, CQ - Chloroquine, LC3B - microtubule-associated proteins 1A/1B light chain 3B, BNIP3 - BCL2 and adenovirus E1B 19-kDa-interacting protein 3, LAMP1 - Lysosomal Associated Protein 1, LAMP2 - Lysosomal Associated Protein 2, Rab7 - Ras-related protein 7

(A) *Western Blot showing FaDu cells pre-treated with CQ or H20, then treated with 10μM CNL or ghost liposomes for 6, 12, or 24 hours. Autophagic/mitophagic/lysosomal targets (LC3B-I, LC3B-II, BNIP3, Rab7, LAMP1, and LAMP2) and loading control (β-Actin) were measured.* ***(B)*** *Densitometric analysis of protein targets measured in* ***A*** *normalized first to internal β-Actin loading controls, then to the ghost+Ctrl treatment at each timepoint. Each bar represents N≥3 experiments.* ***(C)*** *RT-qPCR measuring transcript expression levels of LC3B and BNIP3 after treatment with CNL or ghost and CQ or H20 for 12 and 24 hours normalized first to PSMB6, then to the ghost+Ctrl treatment at each timepoint.* ***(D)*** *Flow cytometry measuring the amount of autophagic vacuoles (via Cyto-ID dye incorporation) present in cells treated with CQ, CNL, or their combination. Rapamycin+CQ was used as the included positive control for the assay. The markers *, **, and *** indicate significance of p < 0.05, 0.01, and 0.001 respectively, displayed error bars represent standard deviation of the mean, and all experiments were performed with at least three biological replicates.*

Methyl Pyruvate Partially Rescues from CNL+CQ-driven Autophagic/Mitophagic Response

As ceramide has been shown to stress cells (134) and cells can activate an autophagic response to generate energy under stressful conditions (135), the synergism of CNL and CQ may be attributed to depletion of necessary energy sources. To assess this and circumvent the necessity of a cellular energy-generating response, Methyl Pyruvate (MP) at a concentration consistent with previous studies (82, 134) was used as an exogenous energy source. FaDu cells were pre-treated with MP prior to vehicle, CQ, CNL, or CQ and CNL together and autophagic protein targets were measured by western blotting (Fig. 2-5A/B). MP significantly decreased CNL+CQ-induced LC3B-II protein expression by 47%. Similarly, MP decreased BNIP3 protein levels by 85% after CNL or CQ+CNL treatments. Similar MP protection from CQ+CNL-mediated increases in BNIP3 were also observed at the RNA level (Fig. 2-5C). Other mitophagic proteins, PINK1 and p62, were also significantly increased after CQ+CNL, an effect which was decreased by MP (Fig. 2-5A/B). This expression pattern was also seen with Rab7, a late-endosomal marker, but not the early endosomal marker Rab5. Beclin-1, a driver of autophagy previously shown to be increased by ceramide (136) remained unchanged (Fig. 2-6 A/B). Validating the MP-driven decrease in LC3B-II and BNIP3 proteins, TEM reveals that MP significantly reduced autophagic vacuoles (Fig. 2-5D). In contrast to LC3B-II, BNIP3, p62, PINK1, and Rab7, CNL-induced reductions in LAMP1 and LAMP2 expression were not reversed by MP (Fig. 2-5A/B). Taken together these data show that MP limits CQ+CNL-driven dysregulation of the autophagic and/or mitophagic pathways, but not lysosomal degradation.

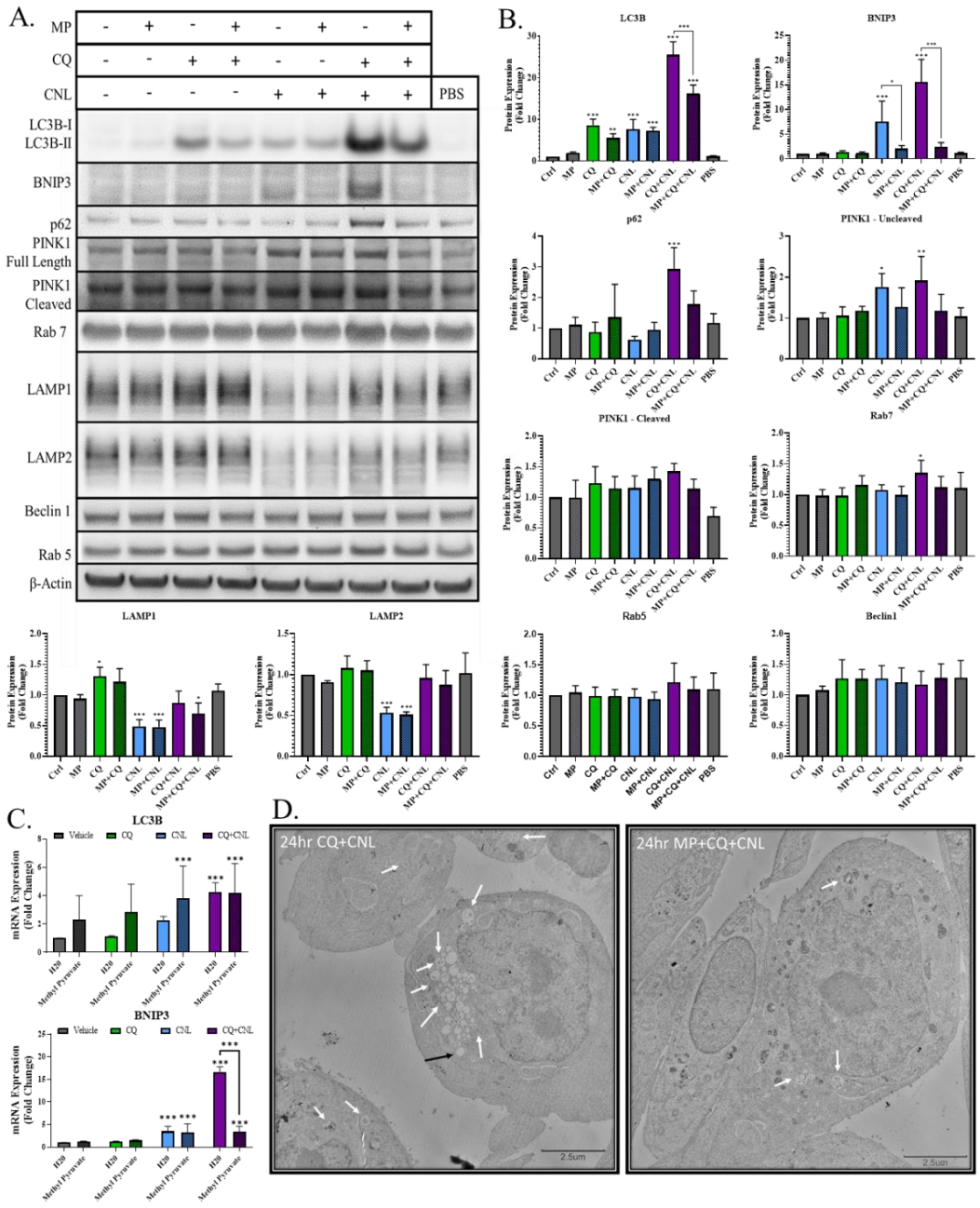

Figure 2-5: Methylpyruvate Partially Rescues from CNL+CQ-driven Autophagic/Mitophagic Response

CNL - C, Ghost - Gh, CQ - Chloroquine, MP – Methyl pyruvate, LC3B - microtubule-associated proteins 1A/1B light chain 3B, BNIP3 - BCL2 and adenovirus E1B 19-kDa-interacting protein 3, p62- Nucleoporin p62, PINK1 - PTEN-induced kinase 1, LAMP1 - Lysosomal Associated Protein 1, LAMP2 - Lysosomal Associated Protein 2, Rab7 - Ras-related protein 7

(A) *Western Blot showing FaDu cells treated with MP or H20, then CQ or H20, then 10μM CNL or ghost liposomes, for 24 hours. Autophagic/mitophagic/lysosomal targets (LC3B-I, LC3B-II, BNIP3, p62, PINK1, Rab7, LAMP1, LAMP2, GSK3A, GSK3β, Beclin 1, and Rab 5) and loading control (β-Actin) were measured.* ***B)*** *Densitometric analysis of protein targets measured in* ***A*** *normalized first to internal β-Actin loading controls, then to the H20+H20+ghost treatment. Each bar represents N≥3 experiments.* ***(C)*** *RT-qPCR measuring transcript expression levels of LC3B and BNIP3 after treatment with MP or H20, then 10μM CQ or H20, then 10μM CNL or ghost liposomes for 24 hours normalized first to PSMB6, then to the H20+H20+ghost treatment at each timepoint.* ***(F)*** *TEM images of FaDu cells treated with 10μM CNL or ghost control and CQ or vehicle for 24 hours. Autophagic vacuoles (white arrows) and empty vacuoles (black arrows) are identified.*

Methyl Pyruvate Rescues from CNL+CQ-driven Oxidative Stress and Mitochondrial Function

As MP reduced the CQ+CNL-driven elevations in mitophagic targets (BNIP3, p62, and PINK1), the effects of MP in the presence or absence of CNL and/or CQ on mitochondrial activity was next determined. Oxidative stress levels were determined through measuring total ROS species (hydrogen peroxide, peroxynitrite, hydroxyl radicals, nitric oxide, and peroxy radical) and superoxide levels. While CQ alone did not alter Reactive Oxygen Species (ROS), CNL and the combination of CQ+CNL increased ROS generation 78% and 190%, respectively (Fig. 2-6A). Additionally, MP did not alter basal levels of ROS, but significantly reduced the CNL and CQ+CNL-induced increases in ROS to the same level as the vehicle group (Fig. 2-6A). While neither CQ nor CNL changed superoxide levels as single agents, MP treatment decreased superoxide levels by 51% compared to the vehicle control (Fig. 2-6B). Strikingly, MP reduced the CQ+CNL superoxide levels from a 71% increase to a 33% decrease compared to basal levels (Fig. 2-6B). Mitochondrial permeability was next measured using a cationic dye that only aggregates in healthy mitochondria with an intact mitochondrial potential (Fig. 2-6C). MP significantly protected FaDu cells from mitochondrial permeability by reducing CNL-induced mitochondrial permeability from 70% to 31% and CQ+CNL from 92% to 31% over basal levels. MP also elevated the CQ + CNL-induced decrease in ATP levels from an 87% decrease to 46% from basal (Fig. 2-6D) further supporting the rescue of mitochondrial function by MP. Finally, MP pretreatment reduced CQ+CNL-induced cell death from 83% to 13% as assessed by viability dye staining (Fig. 2-6E). In summary, MP rescues CNL+CQ-dependent mitochondrial dysfunction, consistent with augmented cellular survival.

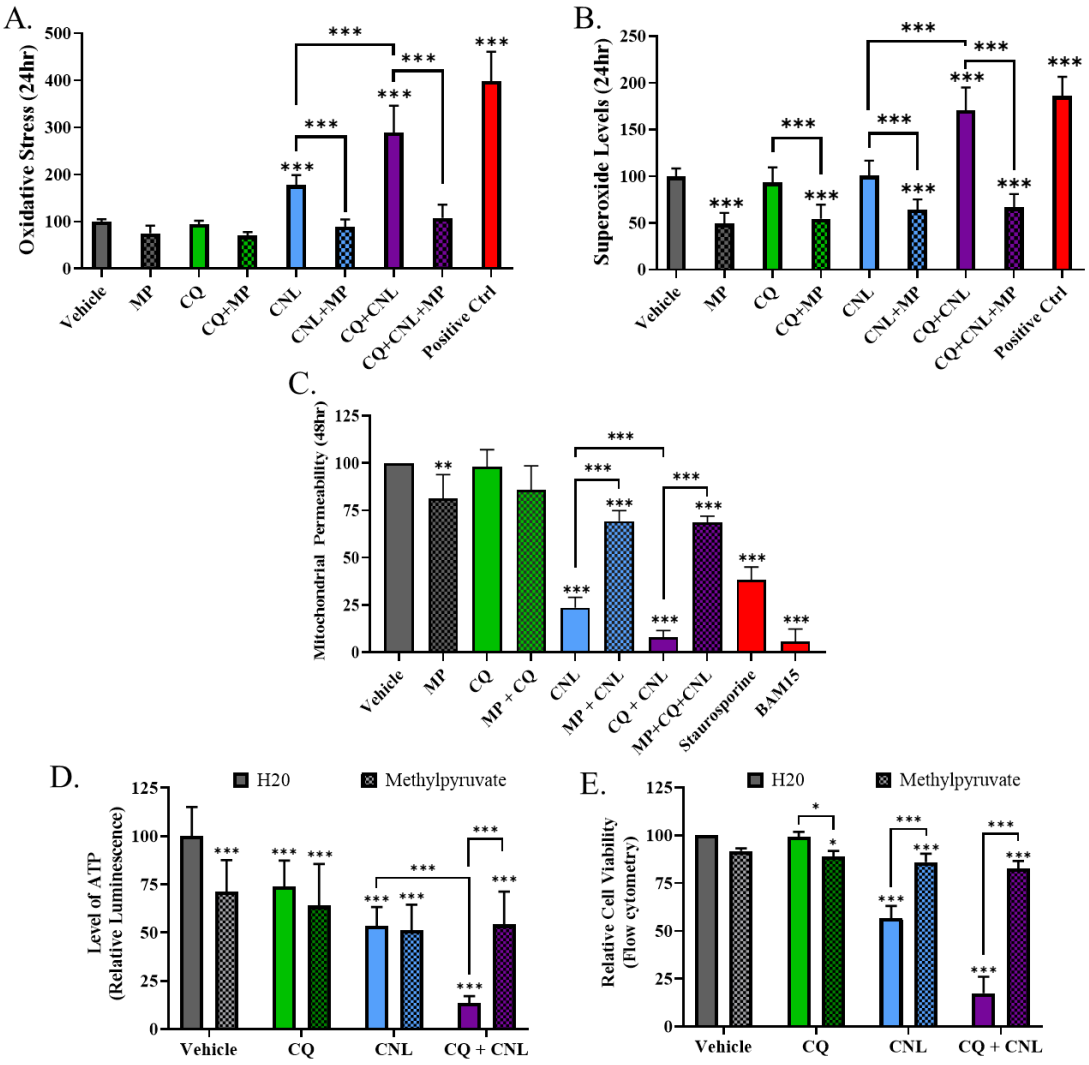

Figure 2-6: Methylpyruvate Rescues from CNL+CQ-driven Oxidative Stress and Mitochondrial Function

CNL - C, Ghost - Gh, CQ - Chloroquine, MP – Methyl pyruvate

(A-B) *FaDu cells were pre-treated with MP or H20, then H20 or 10µM CQ, then 10µM CNL or ghost liposomes for 24 hours and* ***(A)*** *General Oxidative Stress or* ***(B)*** *Superoxide species was measured. Pyocyanin was used as a positive control. (****C-E****) FaDu cells were pre-treated with MP or H20, then H20 or 10µM CQ, then 10µM CNL or ghost liposomes for 48 hours. After this treatment,* ***(C)*** *Mitochondrial permeability,* ***(D)*** *ATP levels, and* ***(E)*** *Cell Viability was assessed. The markers *, **, and *** indicate significance of p < 0.05, 0.01, and 0.001 respectively, displayed error bars represent standard deviation of the mean, and all experiments were performed with at least three biological replicates.*

Discussion

Targeted EGFR inhibition (Cetuximab) and immune checkpoint inhibitors (Nivolumab, Pembrolizumab) are now routinely utilized with conventional therapy for patients with HNSCC. Highlighting the urgent need for new therapies, these inhibitors only increase survival by months and response rates remain very poor (24, 30, 114, 116). C6-ceramide, which has previously been shown to have a large therapeutic window for cancer and augments the efficacy of chemotherapeutic regimens (76, 79, 89, 91, 109, 119), is an attractive therapeutic option for HSNCC. C6-ceramide decreased cell viability in HSNCC cell lines in a concentration and time-dependent manner. Mechanistically, CNL induced mitochondrial damage through the production of oxidative stress and increased mitochondrial permeability. Inhibition of mitophagic repair with late-stage autophagic or lysosomal inhibitors (CQ, BAF, and AMS) synergized with CNL in ceramide-resistant HSNCC cancer cells. To circumvent mitochondria dysfunction, an exogenous energy source, Methyl Pyruvate (MP), rescued CQ+CNL-induced mitochondrial damage and cell death. Taken together, these studies document that targeting the lysosomal portion of mitophagy-mediated repair mechanisms augments CNL-induced cell death.

While the role of ceramide to regulate autophagy is well-documented, the function of autophagy, whether lethal or protective, remains a point of contention (123). Mechanistically, ceramide can increase the expression of autophagic/mitophagic proteins LC3B-II (137), Beclin 1 (136), and BNIP3 (137), and can dissociate autophagy-inhibiting Beclin-1:BCL-2 complexes (138), downregulate nutrient transporters (134, 139), and directly bind LC3B-II to traffic autophagosomes to the mitochondria (126). Consistent with these studies, increased LC3B-II and BNIP3 expression in response to CNL was observed. However, Beclin-1 was not altered, an observation reported by others (124). In a novel observation, ceramide decreased LAMP1 and LAMP2, two proteins which comprise 50% of the lysosomal membrane and promote lysosomal stability, fusion, autophagy, and metastatic potential (122, 131, 140, 141). Further work is needed to determine if ceramide-induced elevation of LC3B-II is a marker of reduced LAMP-dependent

lysosomal breakdown of LC3B-containing autophagosomes.

We and others have previously demonstrated that inhibitors of microtubule assembly, autophagy, and/or lysosomal maturation induce ceramide-dependent "autophagic cell death" in both solid and non-solid tumor models (81, 91, 112, 124, 142, 143). However, we now identify that the synergy between CNL and multiple "autophagy inhibitors" (CQ, Baf, and AMS) occurs at the level of inhibiting lysosome function, explaining why inhibitors of early autophagy fail to synergize in our model and others (91). Of note, some inhibitors of acid ceramidase, a ceramide-metabolizing enzyme, enhance ceramide-induced cell death (144-148). Interestingly, some of these inhibitors also induce rapid destabilization of the lysosome (149) and, thus, may indirectly induce or augment ceramide-dependent cell death by blocking lysosome-mediated protective autophagy/mitophagy. Taken together, there is a great body of direct and indirect evidence that it is specifically lysosomal inhibition, not general autophagic inhibition, which synergizes with ceramide, likely by reducing protective autophagy or mitophagy.

While ceramide promotion of mitochondrial dysfunction, autophagy, and synergism with lysosomal inhibitors have been described previously, the mechanistic links between these findings are still undefined (150, 151). This study may be the first to document that disruption of mitophagy with lysosomal inhibitors exacerbates ceramide-induced mitochondrial damage as evidenced by enhanced ROS production, diminished ATP levels, and decreased membrane permeability. These findings are further supported by CNL+CQ-dependent increases of proteins linked to mitophagy (BNIP3, Rab7, PINK1, and p62). These data support previous findings that ceramide increases BNIP3 expression (137) with this effect exacerbated by lysosomal inhibitors. The role of BNIP3 is controversial in cancer; BNIP3 may be a pro-survival protein, possibly through reducing ROS and inducing autophagy/mitophagy (152, 153) or, in contrast, it may directly induce non-apoptotic cell death (137, 154). Regardless, BNIP3 remains a suitable marker for mitophagy and/or damaged mitochondria (130, 153). Like BNIP3, the canonical late-endosomal protein Rab7 also regulates mitochondrial function, promoting mitophagy and mitochondria-lysosomal contact sites (155).

Ceramide-induced accumulation of PINK1 also suggests mitochondrial damage, as PINK1 drives mitophagy through recruitment of Parkin and subsequent lysosome-driven mitochondrial degradation (156). PINK1 accumulation is further exacerbated by CQ+CNL, suggesting additional mitochondria dysfunction due to limited lysosomal functionality. In contrast, ceramide reduced p62 expression, a finding recently demonstrated by the Cabot Lab (124). Although the necessity of p62 in autophagy, mitophagy, and NRF2-driven ROS clearance are debated, decreases in p62 are consistent with mitochondrial breakdown via autophagy/mitophagy (157). Of interest, CQ co-treatment with ceramide reversed and, in fact, increased protein levels of p62 relative to baseline. Although these observed changes in p62 certainly warrant further causative investigation, we hypothesize that CQ inhibits lysosomal breakdown of damaged mitochondria, preventing ceramide-driven decreases of p62. As we observe altered hallmarks of multiple markers of mitophagy (BNIP3, p62, PINK1, LC3B) after CQ+CNL, further studies are required to elucidate the full signaling cascade and determine which of these targets are effectors of this cell death phenotype. Together, these data indicate that lysosomal inhibitors augment mitochondrial-dependent, ceramide-induced, cell death, likely through inhibition of protective mitophagy.

MP has previously been used to decrease the cytotoxic effects of ceramide. This protection has been attributed to providing an energy source either after ceramide-driven nutrient transporter downregulation (4F2hc, mCAT-1, GLUT-1) (134) and/or reduced glycolysis attributed to a ceramide-induced decrease in glyceraldehyde 3-phosphate dehydrogenase (82). Additionally, MP can rescue from mitochondrial damage induced by SIGMAR1 mutations (158). Consistent with these data, MP limited CQ+CNL-mediated increases in mitophagy-dependent LC3B, BNIP3, Rab7, PINK1, and p62 expression, suggesting that MP may prevent the need for an autophagic or mitophagic response after ceramide administration.

While ceramides induce mitochondrial pore formation, membrane depolarization (125, 150), and mitophagy (126, 142, 151), the role of lysosomal inhibitors to augment or prevent mitochondrial-dependent, ceramide-induced cell death is still somewhat controversial. While prior

studies with the Cabot Lab support CNL-driven mitophagy via co-localization of LC3B-II with LAMP1, the pro-survival/pro-death role of this mitophagy was not explored (124). This current body of work expands those findings to support a "protective" mitophagic phenotype. In contrast to our studies, the Ogretmen group demonstrated that blocking lysosomal acidification with Baf prevented FMS-like receptor tyrosine kinase-3 inhibition-induced cell death, believed to be through C18-ceramide generation in a model of Acute Myeloid Leukemia (142). They demonstrated that a mitochondria-targeted ceramide, C18-Pyr-Cer, induced co-localization of lysosomes and mitochondria and interacted with LC3B-II to drive lethal autophagy/mitophagy. Moreover, they identified a protein, PERMIT, responsible for transporting C18-ceramide to the mitochondria in HNSCC (159). Our data suggests that mitophagy is a controlled compensatory repair mechanism of damaged mitochondria as opposed to a cell death mechanism, and that therapeutic inhibition of autophagic/lysosomal processes contributes to lethal mitophagy in cancer. Discrepancies between the present and previous studies may be due to differences in the therapeutic approach (exogenous CNL addition versus increasing endogenous C18-ceramide through ceramide synthase 1 expression), differences in chain length, trafficking, and metabolism of these ceramides, and potentially type of mitophagy induced. Our studies extend or modify the work of the Ogretmen Lab, suggesting a critical role of lysosomal processing to repair damaged mitochondria. Further studies are needed to elucidate key differences between protective versus lethal mitophagy.

Therapeutically, these studies support that disruption of interconnected autophagic/mitophagic or lysosomal pathways augment the mitochondria-dependent cell death mechanisms induced by ceramide. Of interest, the chemotherapeutic agents commonly used to treat HNSCC, Cisplatin and 5-Fluorouracil (103), both increase ceramide levels in various cancer models, including HPV+ HNSCC (105, 120). Furthermore, inhibiting autophagy with CQ sensitizes HNSCC cells to both Cisplatin and 5-Fluorouracil (105, 160). CNL is currently being evaluated in a phase I monotherapy trial and is well-tolerated. CQ is also well-tolerated and while previously appreciated as an anti-malarial drug, it is now in multiple single agent and combinatorial

trials for cancer (161). Thus, agents like CQ or AMS may potentially be repurposed to improve the efficacy of ceramide-based therapeutics, including CNL, in drug-resistant tumors via blocking mitophagy and exacerbating ceramide-induced mitochondria damage. Taken together, ceramide or ceramide-generating therapeutics in combination with autophagy/lysosome function inhibition may be a viable treatment strategy for HNSCC.

The synergistic effects of CNL+CQ upon mitochondrial dysfunction points to a novel therapeutic intersection between ceramide and lysosomal inhibitors. We further conclude that therapeutic synergy between CNL and CQ is attributed to ceramide–induced mitochondrial stress, which can no longer be mitigated by mitophagy due to inhibition of lysosome function on which mitophagy relies. The promise of enhanced ceramide efficacy by mitigating mitophagy-dependent resistance bodes well for the combination CNL+CQ as a treatment strategy for HNSCC.

Acknowledgements:

The authors would like to thank Stacey Criswell and Adrian Halme from the UVA Microscopy Core.

These studies were supported by the NIH/NCI 2 T32 CA009109 and 1 P01 CA171983. The content is solely the responsibility of the authors and does not necessarily represent the official views of the National Institutes of Health.

CHAPTER THREE: CERAMIDE'S ROLE IN NON-CANONICAL CELL DEATH PATHWAYS IN HNSCC

CHAPTER THREE: CERAMIDE'S ROLE IN NON-CANONICAL CELL DEATH PATHWAYS IN HNSCC

PRIMER:

Though the work covered in Chapter 2 details a specific autophagic/mitophagic mechanism of resistance to ceramide-induced cell death, it does not elucidate the type of cell death induced by CNL. While evidence presented in Figure 2-2A confirm that ceramide does not induce caspase-3 cleavage or PARP cleavage in FaDu cells, these data only suggest that ceramide does not induce caspase-dependent apoptosis in the most-resistant cell line. This chapter will present the work done to characterize the type of cell death induced by ceramide and multiple forms of cell death which are interrogated in this context.

NON-CANONICAL CELL DEATH:

Although many types of cell death are recognized now, even as we approached the start of the 21st century, cell death was categorized as either programmed cell death "apoptosis" or the injury-driven "necrosis" aka necrotic cell death (162, 163). Thus, while understanding of apoptosis continued to progress, anything which was deemed non-apoptotic was categorized into the catch-all black box of unprogrammed cell death or necrosis.

With improved tools, further understanding of signaling cascades, and a multitude of different models, the black box of necrosis has shrunk markedly while the types of programmed cell death have grown tremendously. However, with very few limits placed on the nomenclature or a centralized set of guidelines, the cell death field began to spring up with many types of "osis" often overlapping and making comprehensive summaries difficult (164). Thus, for conciseness, clarity, and to prevent "osis overload", only terms and types of cell death recognized by the Nomenclature Committee on Cell Death will be used.

As beautifully summarized in 2018 by Galluzzi *et. al*, cell death can be separated into

Accidental Cell Death (ACD) or Regulated Cell Death (RCD). ACD is characterized by an overwhelming insult from physical, chemical, or mechanical stress, while RCD relies on molecular mechanisms and signaling cascades which can be regulated. A large portion of RCD is composed of Programmed Cell Death (PCD), an internal, naturally occurring cell death. However, too abundant, prolonged, or uncompensated exposure of certain stimuli which are not intended to induce death, may still kill the cell; this highlights the non-PCD form of RCD (165).

For this thesis, with much assistance from my undergraduate student Tim Boyer, I have summarized and simplified the work in Galluzzi *et al.* in the form of a diagram (**Fig. 3-0**) which organizes the current, recognized forms of cell death as well as in the form of table. To fit in this thesis, the table was split into overall description of cellular death-related processes (**Table 3-1**) and inhibitors and inducers of select types of regulated cell death **(Table 3-2)** which defines key cell death-related terms in the diagram, hallmarks of these death-related pathways, and known inhibitors of these signaling cascades.

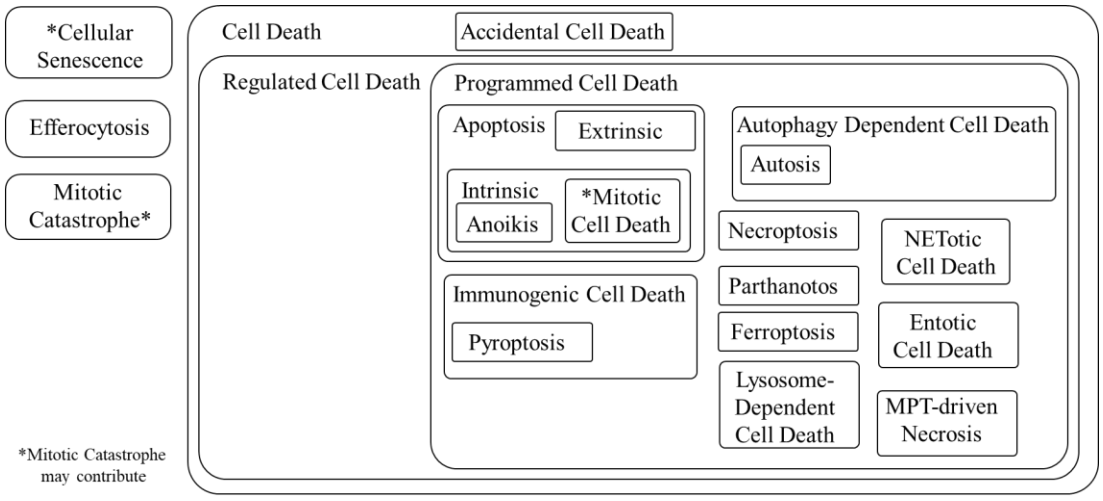

Figure 3-0 Organized Hierarchy of Cell Death Summarized From Galluzzi et. al. 2018

Category	Name	Hallmarks
Cellular Function	Cellular Senescence	
Cellular Function	Mitotic Catastrophe	Multinucleation, Macronucleation, Micronucleation
Not a cell death mechanism, a clearance process	Efferocytosis	Clearance by macrophages after intrinsic apoptosis
Cellular Function	Cell death	Loss of ATP & Redox hemostasis, plasma membrane permeabilization and/or cellular fragmentation
Cell Death	Accidental Cell Death (ACD)	
Cell Death	Regulated Cell Death (RCD)	
RCD	Programmed Cell Death (PCD)	
RCD/PCD	Anoikis	Loss of integrin-dependent anchorage, MOMP
RCD/PCD	Autophagy-dependent cell death	Autophagic Flux independent of other PCD
RCD_Autophagy-dependent Cell Death	Autosis	Autophagy-dependent CD with plasma membrane Na/K+ ATP pump
RCD/PCD	Entotic cell death	RHOA, ROCK1 ROCK2, DIAPH1
RCD/PCD	Extrinsic Apoptosis	CASP8, & CASP3
RCD/PCD	Ferroptosis	GSH, GPX4, xc − , LOX, COX, ACSL4, LPCAT3
RCD/PCD	Immunogenic Cell Death	Various DAMPS (esp. CALR, HMGB1)
RCD/PCD	Intrinsic Apoptosis	MOMP, CyC CASP3
RCD/PCD	Lysosome-dependent cell death	Cathepsins, LMP, maybe MOMP & caspases
RCD/PCD	Mitochondrial permeability transition (MPT)-driven necrosis.	CYPD
RCD-IntrinsicApop/MitoCast	Mitotic Death	RCD driven by Mitotic Catastrophe (often intrinsic apoptosis, Casp2)
RCD/PCD	Necroptosis	RIPK1, RIPK3, MLKL
RCD/PCD	NETotic cell death	ROS-driven, Hematopoetic only
RCD/PCD	Parthanatos	PARP1 hyperactivation, AIF, MIF
RCD/PCD	Pyroptosis	Inflammatory caspase activation - Gasdermin Protein family, IL1B secretion

Table 3-1 Inhibitors and Inducers of Select Types of Regulated Cell Death

Name	Inhibitors	Inducers
Entotic cell death	Y-27632	Androgen Receptor
Extrinsic Apoptosis	Z-VAD-FMK	Staurosporine
Ferroptosis	Ferrostatin-1, Liproxstatin-1, Vitamin E, Coenzyme Q10	RSL3, Erastin, FIN56, Sorafenib, Altretamine
Immunogenic Cell Death	CASP8, CASP3 ????	Chemotherapeutics (anthracyclines, bortezomib)
Intrinsic Apoptosis	Cyclosporin A?, Z-VAD-FMK	Staurosporine
Lysosome-dependent cell death	cystatins and serpins, E64D and Ca-074-Me, pepstatin A	L-leucyl-L-leucine methyl ester, ciprofloxacin, hydroxychloroquine, TRAIL
Mitochondrial permeability transition (MPT)-driven necrosis.	Cyclosporin A, sanglifehrin A, JW47	?
Mitotic Death	?	Casp2
Necroptosis	Necrostatin-1 (RIPK1 inhibitor), Necrosulfonamide (MLKL inhibitor)	TRAIL, B Lapachone, LPS can induce RIPK3
NETotic cell death	Necroptosis inhibitors (Nec-1, NSA)	N/A?
Parthanatos	4-methoxyflavone, 3´,4´-dimethoxyflavone. PARP1 inhibitors: Veliparib, olaparib	RIPK1 & RIPK3 activation (TRAIL, B Lapchone can induce Parp1)
Pyroptosis	Z-VAD-FMK, Y-VAD-FMK, NSA (for Gasdermin D)	LPS, nigericin

Table 3-2 Overall description of cellular death-related processes

This chapter will focus on the following forms of cell death, briefly defined below: Apoptosis, Ferroptosis, Necroptosis, and Pyroptosis.

Apoptosis is a form of cell death with two subtypes (intrinsic and extrinsic) involving a signaling cascade of cysteine-aspartic protease (“caspase” or CASP) proteins that activate widespread, cell death-inducing protease activity. While both extrinsic and intrinsic apoptosis rely on the same downstream signaling cascades (overlapping at Caspase-3 cleavage), their upstream

signaling events differ. For intrinsic apoptosis, a cellular insult induces mitochondrial membrane permeability which causes release of Cytochrome C from the mitochondria. Cytochrome C then binds Apoptotic Protease Activating Factor 1 (APAF-1) and recruits and activates Caspase-9 (generating the "apoptosome") which drives eventual cleavage Caspase-3. For extrinsic apoptosis, an extracellular signaling factor such as tumor necrosis factor alpha (TNF-α) or Fas Ligand (FasL) signal through their "death receptors" (TNFR and FasR, respectively) and form the death-inducing signaling complex (DISC). DISC then cleaves Caspase-8 which can either induce mitochondrial permeability (triggering intrinsic apoptosis) or drive cleavage of Caspase-3 directly. Once Caspase-3, the primary "executioner caspase", is cleaved, it cleaves hundreds of substrates important for cellular survival, eventually leading to cell death (166, 167).

Ferroptosis is a type of cell death involving ROS-driven toxic accumulation of lipid peroxides leading to cell death in an iron-dependent manner (168). The primary cellular pathway for preventing Ferroptosis relies on the metabolite Glutathione which reduces the death-inducing lipid peroxides via activity of the enzyme Glutathione Peroxidase 4 (GPX4). These toxic lipid hydroperoxides can be synthesized by the enzymes lipoxygenase (LOX) and, to a lesser extent, cyclooxygenase (COX), or in the absence of enzymatic activity via autoxidation (169). Additionally, though it is unclear whether directly involved in lipid peroxidation (via Fenton reactions), or in altering the function of LOX enzymes (via iron-binding sites), the depletion of iron is able to inhibit ferroptosis while increased iron promotes it (170).

Necroptosis induces cell death via a signaling cascade involving the receptor-interacting protein kinase (RIPK) family and mixed lineage kinase domain like pseudokinase (MLKL) protein causing pore-formation in the plasma membrane, and potentially organelles (171), resulting in an efflux of cellular components and influx of extracellular components which induce cell death. Mechanistically, RIPK3 is phosphorylated/activated (often by activity of phosphorylated RIPK1) which in turn, phosphorylates MLKL. Once phosphorylated, even if independent of RIPK3 (172), MLKL oligomerizes and translocates to the plasma membrane where it mediates cell permeability

with the extracellular environment, triggering cell death (171).

Discovered in the 21st century (173), pyroptosis is thought to involve the oligomerization of cleaved N-terminal Gasdermin proteins onto the plasma membrane and subsequent rapid permeabilization. Pyroptotic 1-2 nm pores permit the outflow of cellular solutes, and the reduction of cellular osmotic pressure causes cell swelling and lysis. The two most well described pyroptotic pathways are Gasdermin D activation/cleavage via Caspase-1 (canonical pyroptosis), and Gasdermin E activation/cleavage via Caspase-3 (non-canonical pyroptosis). Since non-canonical pyroptosis relies on Caspase-3 activation, it is thought that the interplay of pyroptosis and extrinsic apoptosis may permit cell death switching (165, 174). Non-canonical pyroptotic proteins are also thought to be epigenetically silenced in malignant cells, unless induced by cancer therapeutics (174).

Considering ample data in recent years suggesting ceramide induces non-apoptotic cell death (68, 70, 71)(Chapter 2), published data regarding non-canonical forms of cell death such as necroptosis, ferroptosis, and pyroptosis are strikingly lacking. PubMed searches for “ceramide” and “ferroptosis” or “pyroptosis” gives four and five results, respectively; none with both words in the title. Though “ceramide” and “necroptosis” gives 25 results, very few of these make the assertion that ceramide induces necroptosis. In fact, only one group claims ceramide induces necroptosis, publishing one paper (87) and a review (175) on the subject. However, even in these publications, necroptosis inhibitors fail to rescue from ceramide-induced cell death and an incredibly high concentration of ceramide is used calling into question physiologic induction of necroptosis by ceramide.

Results:

Ceramide and Apoptosis

To adequately interrogate apoptotic pathways, a positive control for apoptotic cell death in HNSCC cell lines was first established. Using staurosporine as a positive control for apoptosis, a concentration-response curve was generated in six different HNSCC cell lines. **(Fig. 3-A1)**. Notably, less than 25% of cells were left alive in all six lines after treatment with 1μM

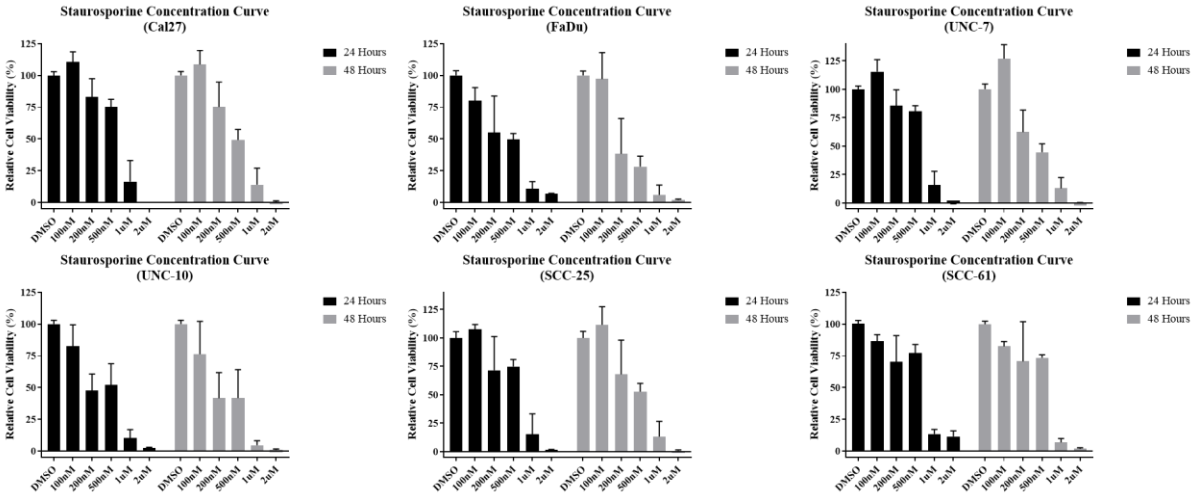

Figure 3-A1 MTS Cell Viability Assay Demonstrating Staurosporine Response Curve in Six HNSCC Cell Lines

staurosporine. To confirm the apoptotic nature of staurosporine-induced cell dearh, staurosporine was added to cells in the presence of the apoptosis inhibitor Z-VAD-FMK (Fig.ure 3-A2). Though the amount of death induced by staurosporine and the amount of rescue via Z-VAD-FMK varied, Z- VAD-FMK rescued from staurosporine-induced cell death in all six HNSCC cell lines at both 24 and 48 hours.

Having now verified the apoptotic inhibition mediated by Z-VAD-FMK, the effect of Z VAD-FMK on CNL-induced cell death was tested. Cells pre-treated with Z-VAD-FMK showed no rescue from CNL-induced cell death at either 24 or 48 hours in any of the cell lines tested. **(Fig. 3-A3)**. Further ruling out caspase-dependent apoptosis as the mechanism of CNL-induced cell

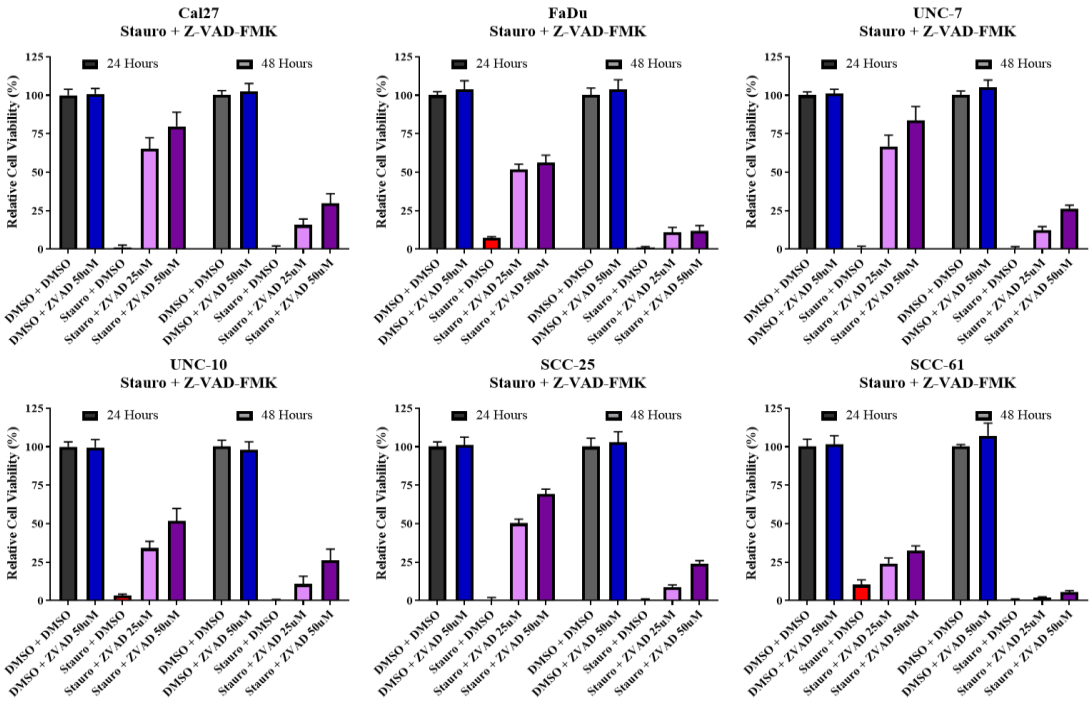

Figure 3-A2 MTS Cell Viability Assay Demonstrating Z-VAD-FMK Mediated Rescue From Staurosporine-Induced Cell Death in Six HNSCC Cell Lines

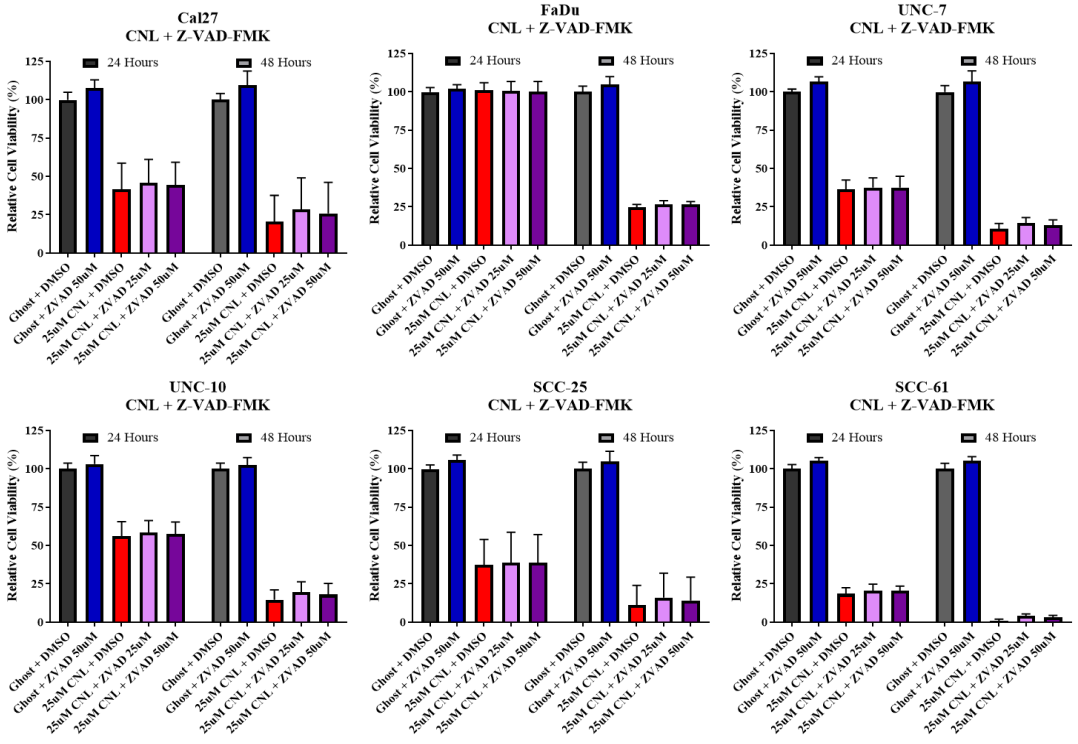

Figure 3-A3 MTS Cell Viability Assay Demonstrating A Lack of Z-VAD-FMK Mediated Rescue From CNL-Induced Cell Death in Six HNSCC Cell Lines

death, CNL showed no caspase activity in either the most resistant (FaDu) or most sensitive (SCC-

61) cell lines, while staurosporine again induced a large increase in caspase 3/7 activity **(Fig. 3-A4)**.

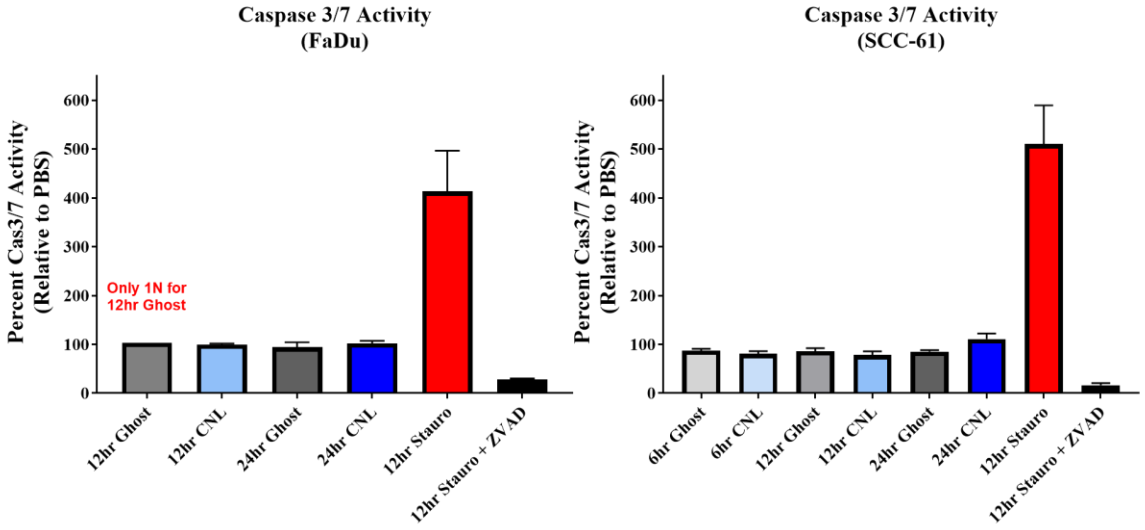

Figure 3-A4 Caspase 3/7 Activity Assay Demonstrating A Lack Caspase Activity From CNL-Induced Cell Death in the Most Resistant and Most Sensitive HNSCC Cell Lines

Although data in Chapter 2, showed no appreciable markers of apoptosis activation in the more-resistant FaDu HNSCC cells (Figure 2-2A), this could have been an artifact of using the most resistant cell line. Using the SCC-61, the most sensitive HNSCC cell line tested, negligible Caspase-3 activation is again demonstrated, however, minor PARP cleavage is noted (**Fig. 3-A5**). Taken together, these data establish ceramide causes little to no induction of caspase-3/7 activity or caspase-3 cleavage, and cannot be rescued by inhibiting caspase-dependent apoptosis.

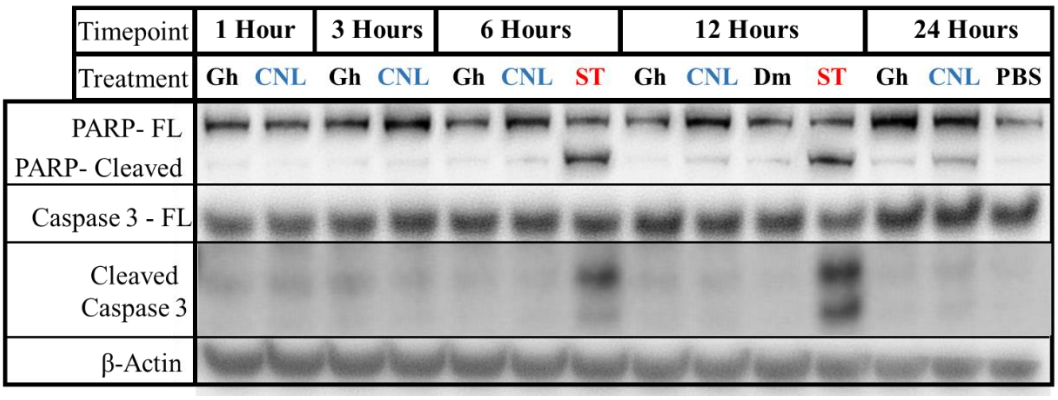

Figure 3-A5 Western Blot Demonstrating A Lack Caspase 3 Cleavage and Minor PARP Cleavage in Response to CNL in the SCC-61 Cell Line.

Although the above data effectively establish minimal if any involvement of caspase-dependent apoptosis in CNL-induced cell death, some claims suggest CNL initiates caspase-independent apoptosis (176). In line with this hypothesis, previous reports identify that the flip of phosphatidyl serine (PS) from the inner leaflet to the outer leaflet of the plasma membrane, a hallmark of apoptosis, can occur independently of caspase cleavage (177). Further confounding interpretation, some reports claim PS flipping may occur in non-apoptotic cell death as well (178). Annexin V is a well-established stain which binds to PS after being flipped to the outer leaflet. However, a caveat with Annexin V staining is that if the cell has died and become permeable, annexin V can enter and stain internal PS giving a false positive. To mitigate this effect, it is important to carefully control the timepoints used in experiments and include a cell death dye to know if the Annexin V staining has occurred in cells with intact plasma membranes. In short, a cell "single positive" for Annexin V is characterized as "early apoptosis" while a cell "double positive" for both annexin V and a cell death dye is referred to as "late apoptosis/necrosis" since one cannot determine which dye stained the cell first. Taking into consideration these parameters, to effectively rule out caspase-independent apoptosis after treating cells with CNL, Ghost liposomes, or staurosporine, cells were stained with annexin V and a cell death dye before being analyzed via flow cytometry **(Fig. 3-A6)**.

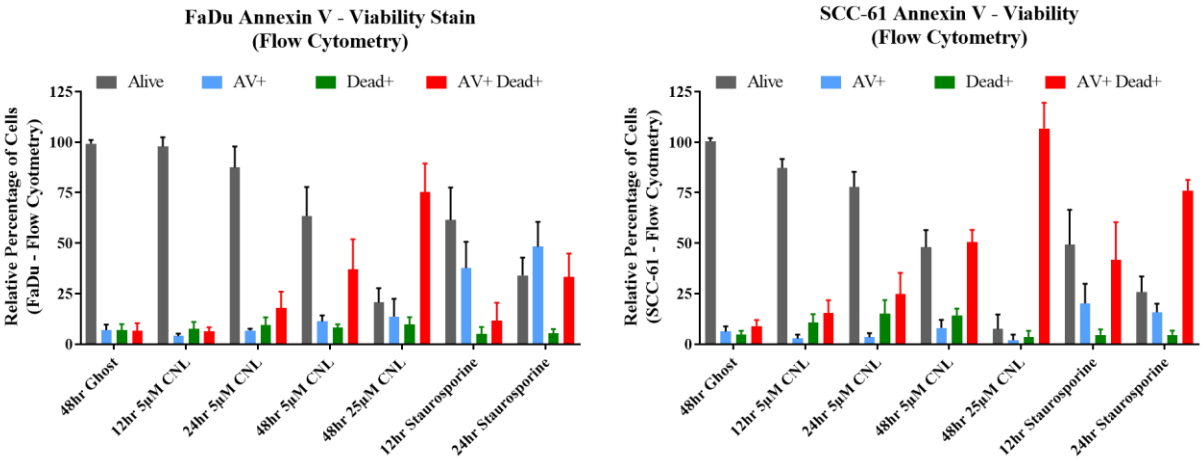

Figure 3-A6 Flow Cytometry Measuring Annexin V Staining and Cell Death Staining in Response to CNL and Staurosporine in the FaDu and SCC-61 Cell Lines.

Again, while both FaDu and SCC-61 cells showed marked increases in the single positive annexin V stain after staurosporine treatment at 12 and 24 hours, CNL was far less effective at inducing Annexin V single-positivity at 12, 24, or 48 hours despite inducing far more cell death. To confirm specificity of staining and further rule-out caspase independent apoptosis, the above flow protocol was used with cells pretreated with Z-VAD-FMK before treatment with

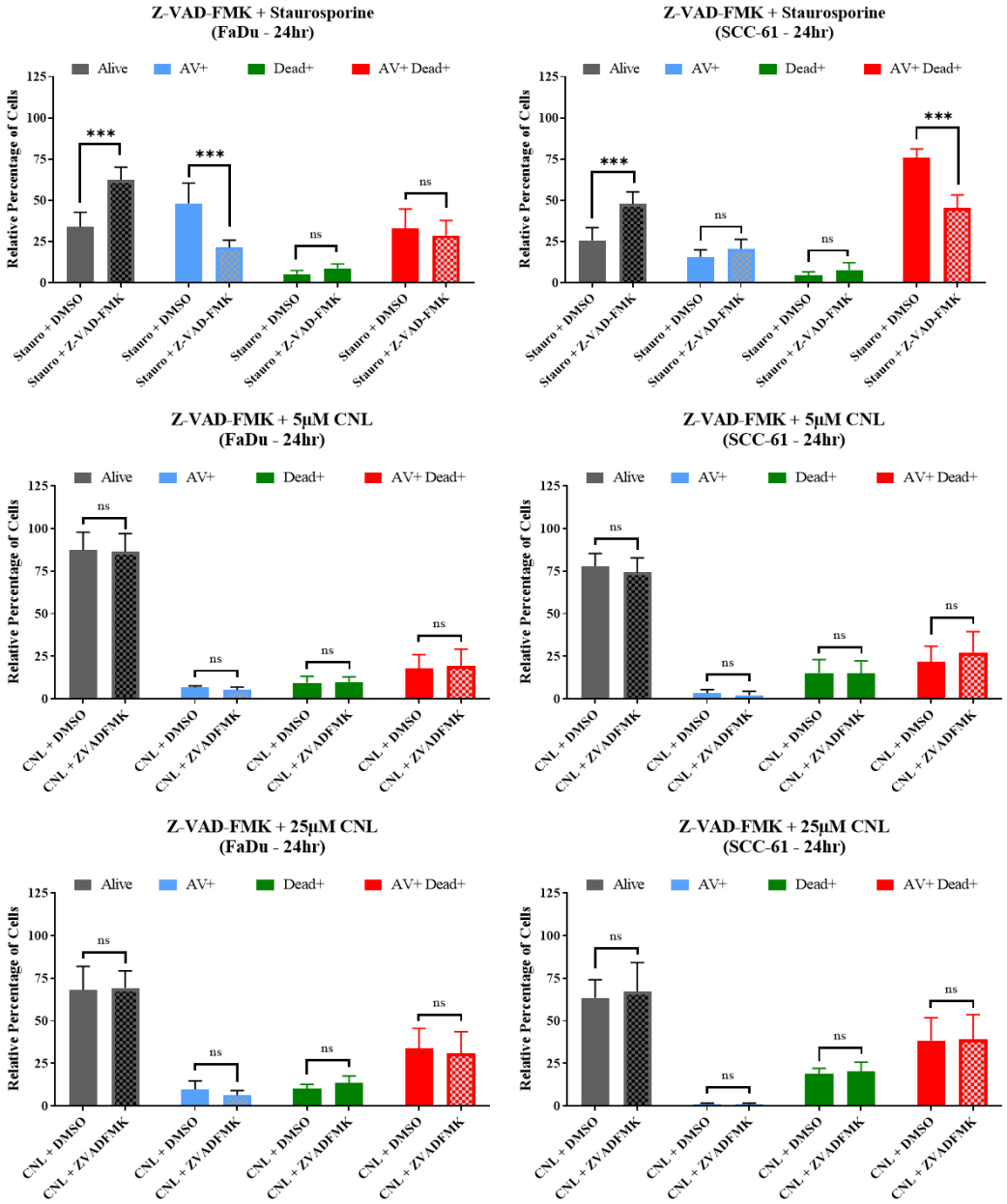

Figure 3-A7 Flow Cytometry Measuring Annexin V Staining and Cell Death of FaDu and SCC-61 Cells Pre-Treated with Z-VAD-FMK before Staurosporine or CNL Treatment

staurosporine or CNL (**Fig. 3-A7).**

Again, after treatment with staurosporine, Z-VAD-FMK was able to rescue the amount of total living cells (grey bars) in both FaDu and SCC-61 cells while decreasing the population of annexin V single stain in FaDu cells and annexin V + cell death double stain in SCC-61 cells. However, Z-VAD-FMK was again unable to significantly alter CNL-induced cell death, annexin V single stain or annexin V + cell death double stain in either cell line. These results strongly indicate that CNL does not induce Caspase-dependent or likely -independent apoptosis in HNSCC.

Ceramide and Ferroptosis

Similarly to the above apoptotic studies, a positive control for ferroptosis was first established. While the ferroptotic positive control Erastin was unable to induce cell death **(Figure 3-F1)**, RSL3 was able to induce a concentration-dependent cell death **(Figure 3-F2)**.

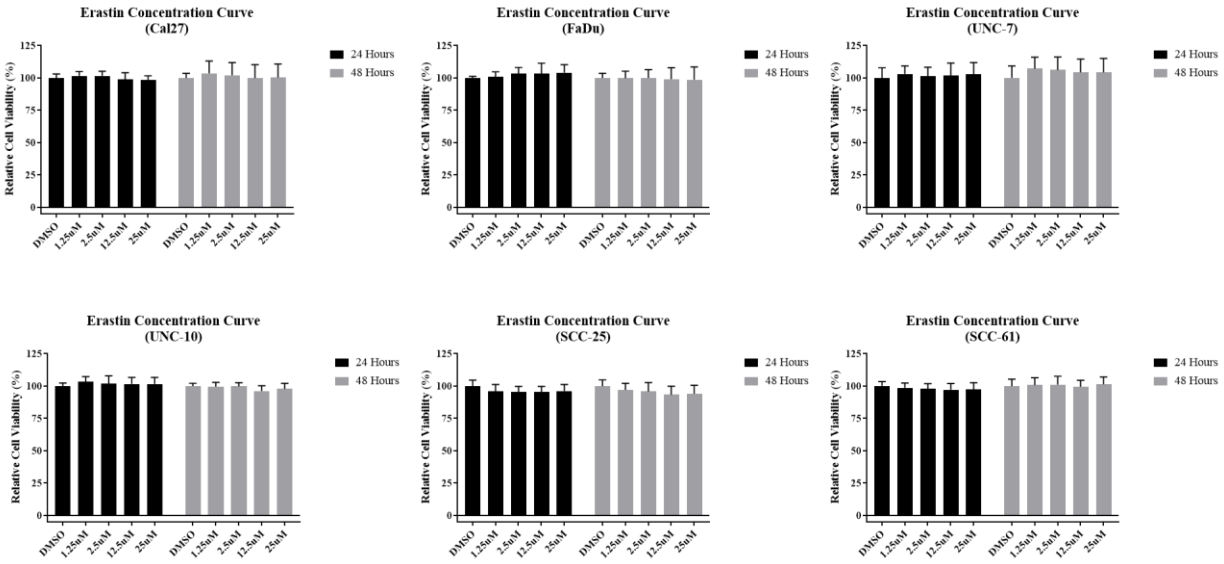

Figure 3-F1 MTS Cell Viability Assay Demonstrating A Lack of Erastin Response Curve in Six HNSCC Cell Lines

Although RSL3 was able to induce cell death in all six HNSCC cell lines tested, there was a highly-variable amount of cell death induced with some cell lines exhibiting <25% cell viability after 500nM RSL3 (Cal27 &=and UNC-7) while other cell lines were >80% viable after 5µM RSL3

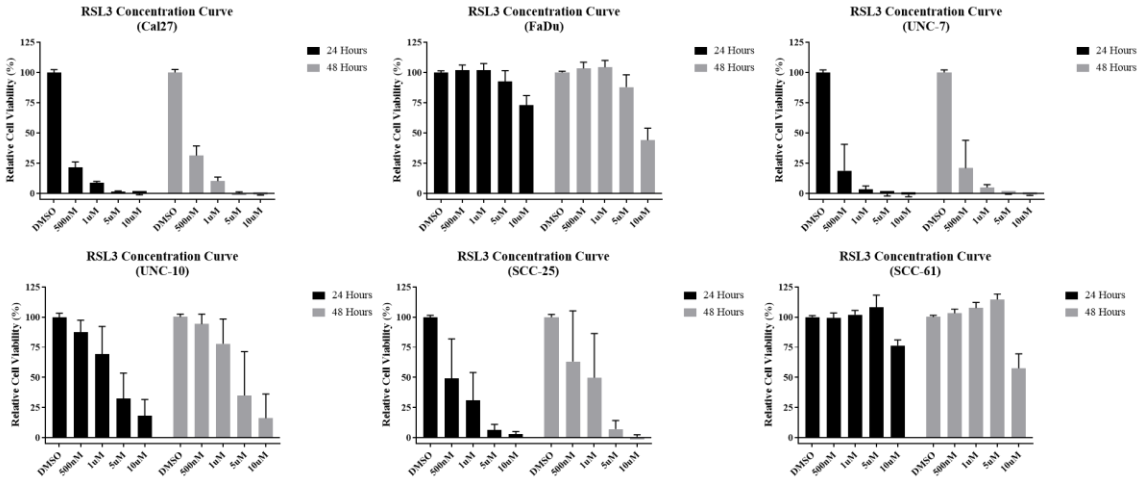

Figure 3-F2 MTS Cell Viability Assay Demonstrating RSL3 Response Curve in Six HNSCC Cell Lines

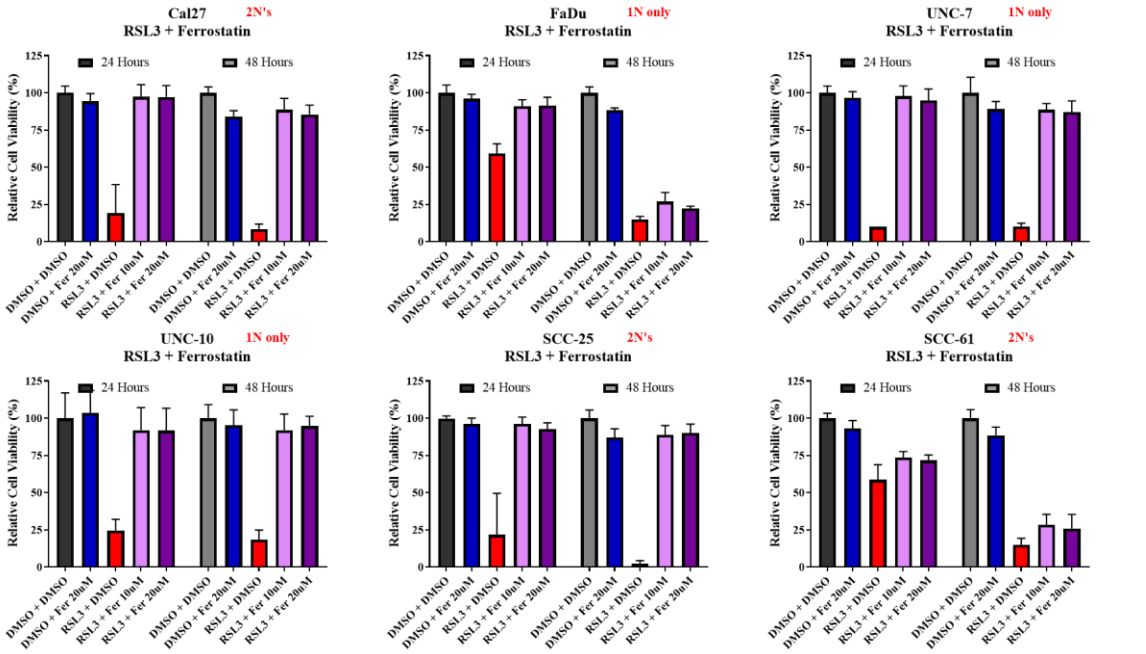

Figure 3-F3 MTS Cell Viability Assay Demonstrating Ferrostatin-1 Mediated Rescue From RSL3-Induced Cell Death in Six HNSCC Cell Lines

(FaDu and SCC-61).

To ensure the cell death was indeed ferroptotic, cells were pre-treated with the ferroptosis inhibitor, ferrostatin-1, before treatment with RSL3 **(Figure 3-F3)**. The preliminary data in all six cell lines showed a robust rescue from RSL3-induced cell death. These data suggest the success of both the positive control and inhibitor of ferroptosis. However, similar to the apoptotic inhibitor Z-

VAD-FMK, pre-treatment with Ferrostatin-1 was unable to rescue from CNL-induced cell death in any of the six HNSCC cell lines tested **(Figure 3-F4)**.

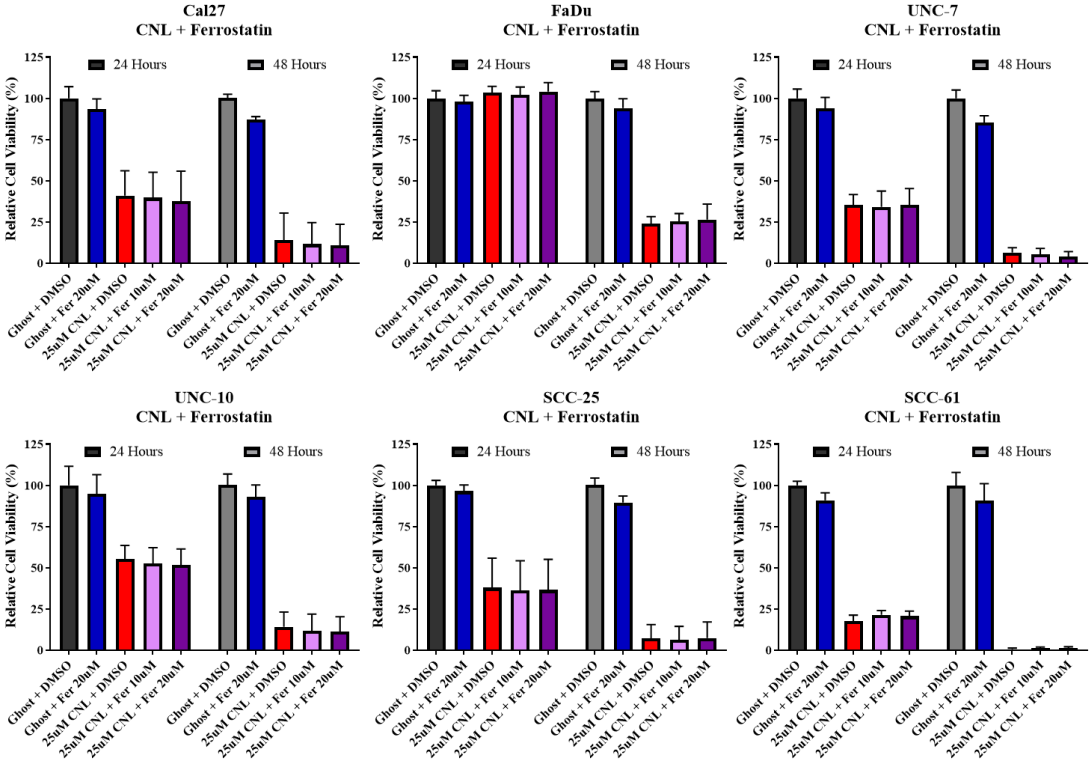

Figure 3-F4 MTS Cell Viability Assay Demonstrating Ferrostatin-1 Mediated Rescue From RSL3-Induced Cell Death in Six HNSCC Cell Lines

Ceramide and Necroptosis

Unlike the apoptotic and ferroptotic positive controls, single-agent necroptosis positive controls are not as widely recognized or available. Despite what its name might suggest and multiple published reports suggesting its efficacy as a single-agent positive control for necroptosis (179, 180), tumor necrosis factor alpha (TNF-α) did not induce any form of cell death in any of the six HNSCC cell lines tested (**Fig. 3-N1)**.

An alternative approach, however, suggested using staurosporine in the presence of Z-VAD-FMK. In theory, this would negate the apoptotic effects of staurosporine and thus, the remaining cell death would be “necroptotic”. After establishing that the combination of staurosporine + Z-VAD-FMK induced cell death in HNSCC cell lines (data not shown), it was

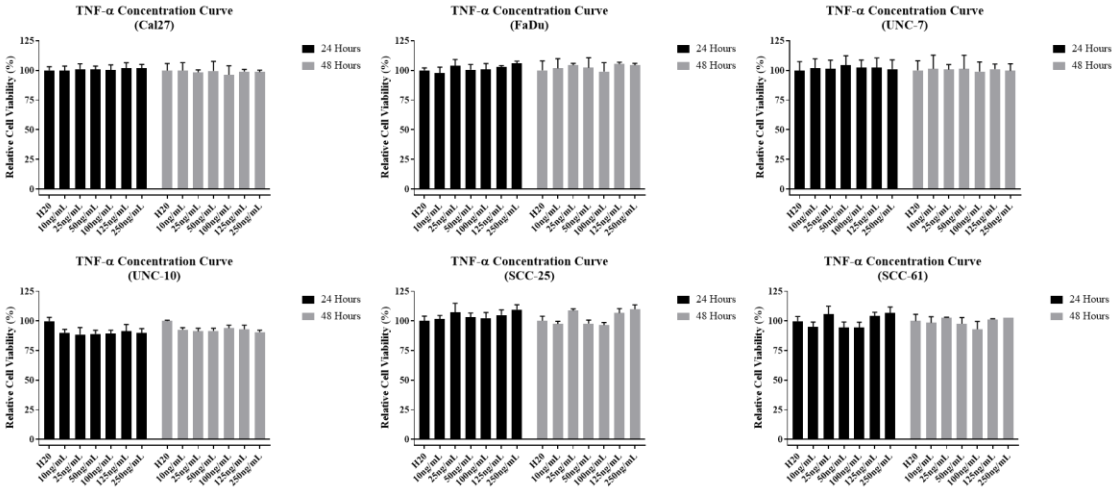

Figure 3-N1 MTS Cell Viability Assay Demonstration a Lack of Cell Death Induced by TNF-α in Six HNSCC Cell Lines

necessary to determine if inhibitors of necroptosis could inhibit this cell death. Thus, Necrostatin-1 (Nec-1) and Necrosulfonamide (NSA), two inhibitors of necroptosis thought to block RIPK1 and MLKL activity, respectively, were obtained. Cells were pre-treated with Nec-1 and NSA before being treated with staurosporine + Z-VAD-FMK to determine if the cell death induced could be rescued by inhibition of necroptosis **(Fig. 3-N2 and 3-N3)**. However, with a potential exception of one inhibitor in one cell line (Nec-1 in SCC-61 cells at 48 hours), neither Nec-1 nor NSA inhibited staurosporine + Z-VAD-FMK-induced cell death.

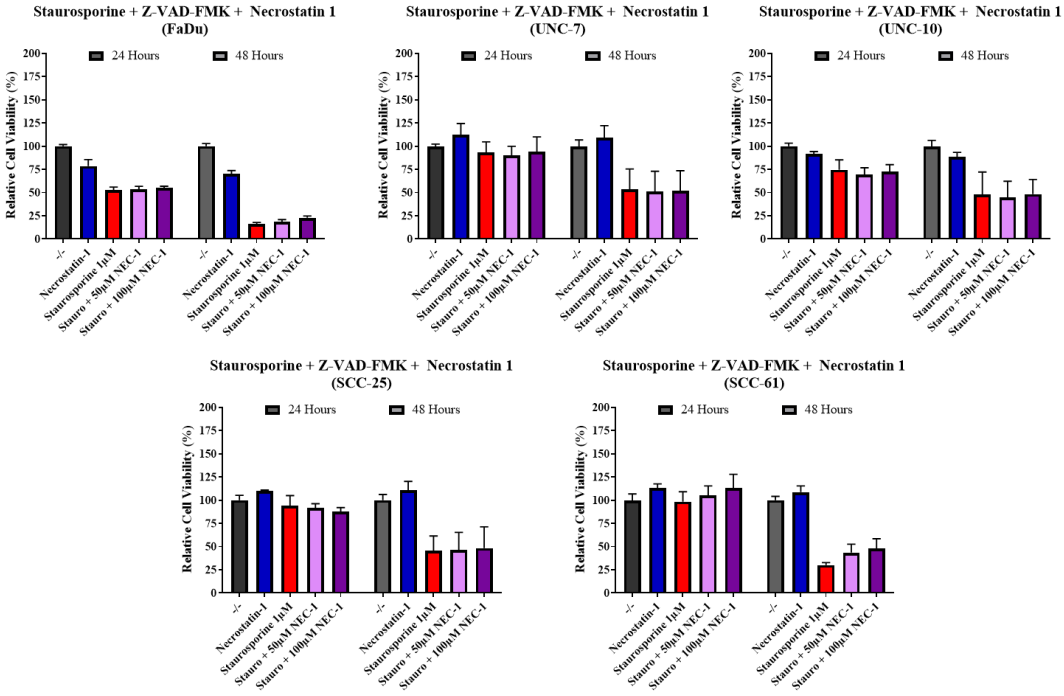

Figure 3-N2 MTS Cell Viability Assay Demonstrating a Lack of Necrostatin-1 Mediated Rescue From Staurosporine + Z-VAD-FMK-Induced Cell Death in Six HNSCC Cell Lines

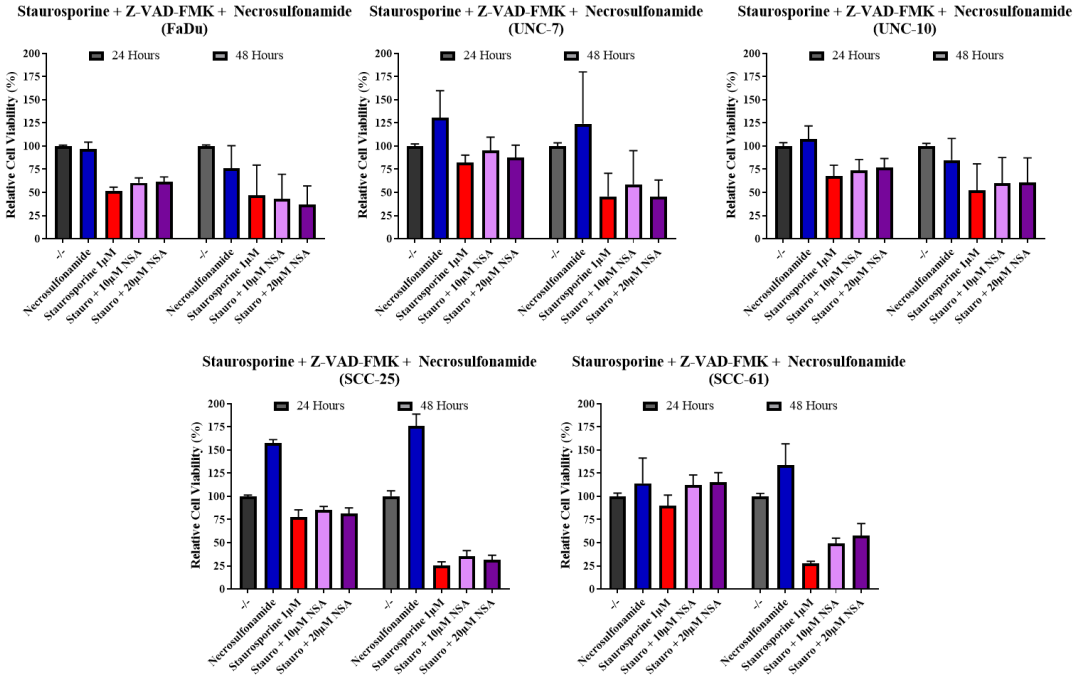

Figure 3-N3 MTS Cell Viability Assay Demonstrating a Lack of Necrosulfonamide-Mediated Rescue From Staurosporine + Z-VAD-FMK-Induced Cell Death in Six HNSCC Cell Lines

Though a successful positive control was lacking to verify the inhibitors were working, if CNL was inducing necroptotic cell death and either Nec-1 or NSA was able to inhibit this death,

that would give strong evidence that CNL was inducing necroptosis. Thus, cells were pre-treated with Nec-1 or NSA before being treated with CNL **(Fig. 3-N4 - 3-N7).** Similar to treatment with staurosporine + Z-VAD-FMK, Nec-1 did not rescue from CNL in any cell line except perhaps the SCC-61 cells **(Fig. 3-N4)**. NSA appeared to reduce CNL-induced cell death in UNC-7, SCC-25,

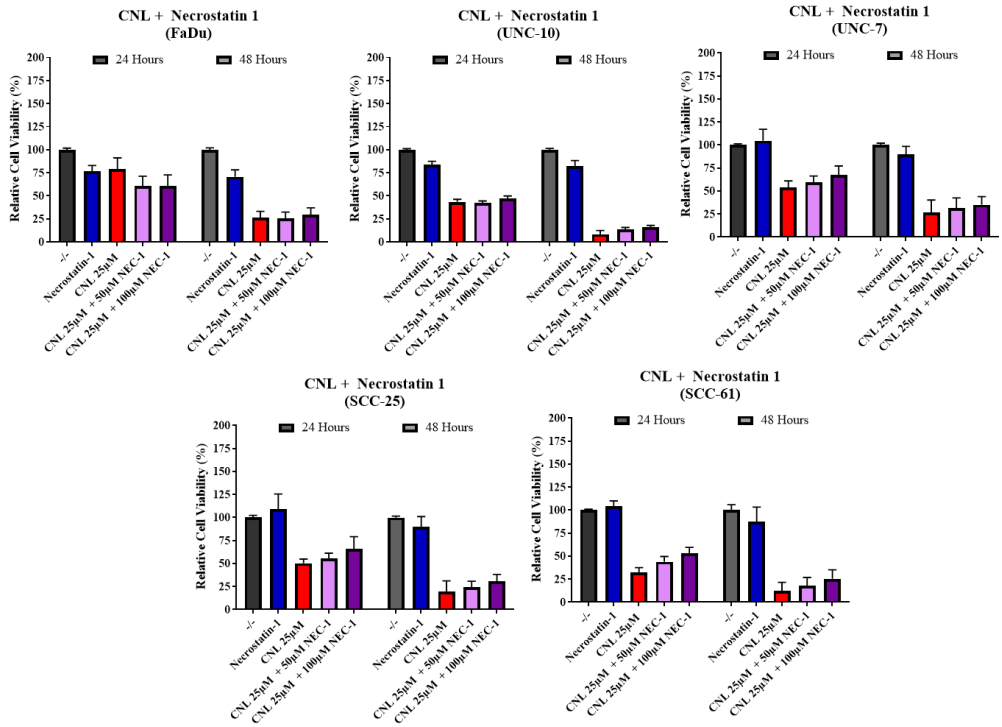

Figure 3-N4 MTS Cell Viability Assay Demonstrating a Lack of Necrostatin-1-Mediated Rescue From CNL-Induced Cell Death in Six HNSCC Cell Lines

and SCC-61 cells, however, NSA treatment alone increases cell viability by 15-48% over baseline **(Fig. 3-N5)**. Thus, NSA is likely inhibiting basal cell death and not CNL-induced cell death.

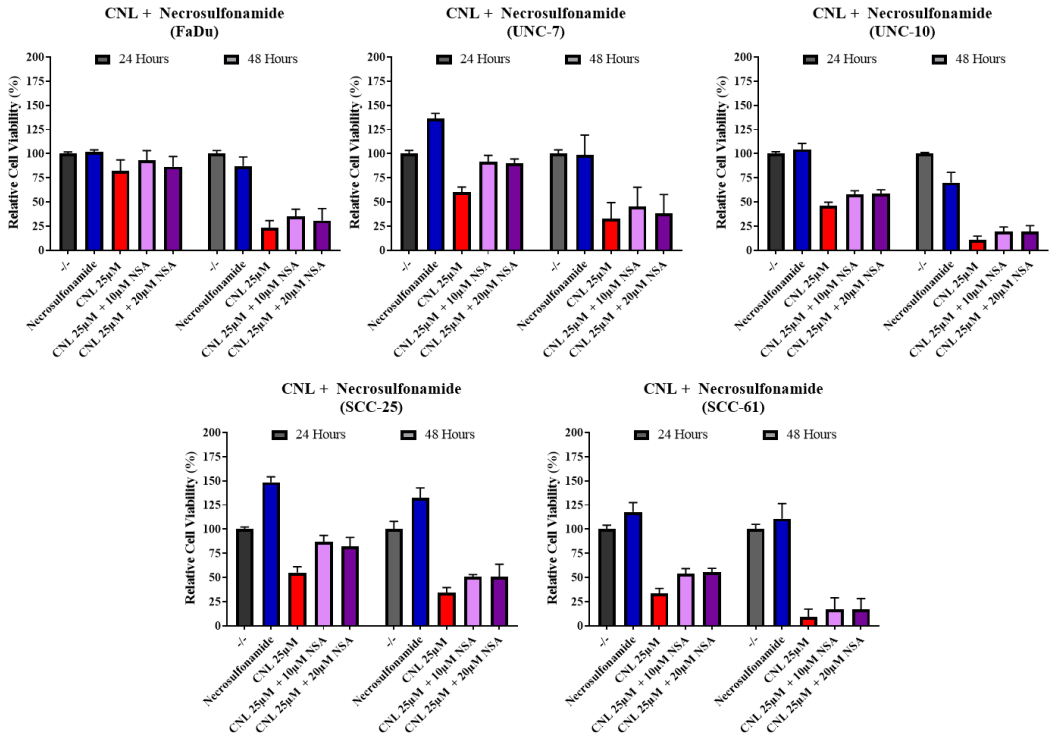

Figure 3-N5 MTS Cell Viability Assay Demonstrating a Lack of Necrosulfonamide-Mediated Rescue From CNL-Induced Cell Death in Six HNSCC Cell Lines

However, while basal cell death did not increase in FaDu cells, there did appear to be a slight rescue at 48 hours. A follow-up experiment using a lower concentration of CNL and NSA in FaDu cells confirmed NSA was able to rescue from CNL-induced

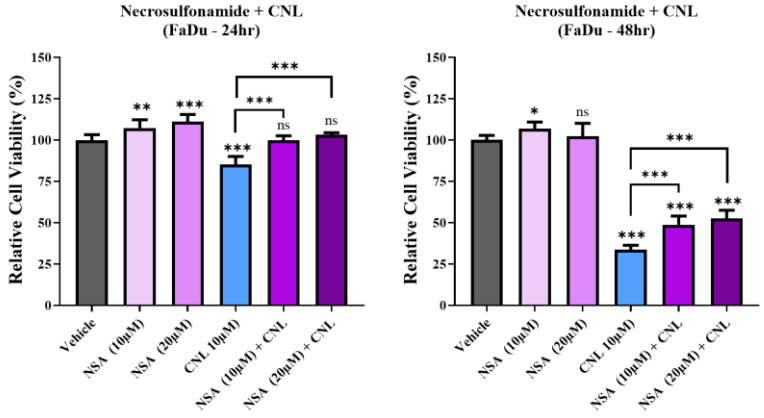

Figure 3-N6 MTS Cell Viability Assay Demonstrating a Lack of Necrosulfonamide-Mediated Rescue From CNL-Induced Cell Death in FaDu cells

cell death at 48 hours without decreasing basal death **(Fig. 3-N6).** However, though an interesting observation that Nec-1 and NSA may rescue SCC-61 and FaDu cells, respectively, neither Nec-1 nor NSA was able to drive a robust, specific inhibition of CNL-induced cell death across multiple cell lines.

Though necroptosis inhibitors do not rescue from CNL-induced cell death, it is possible that either inhibitors themselves are not working (we cannot conclude otherwise without a positive control) or that the CNL is still inducing hallmarks of necroptosis which are not inhibited Nec-1 or NSA. As mentioned above, the primary proteins involved in the necroptotic signaling pathway are RIPK1, RPIK3, and MLKL. However, MLKL can be activated independently of RIPK1 and RIPK3. Thus in order to measure the most downstream target in the necroptotic signaling pathway, after treatment with CNL, phosphorylated and total MLKL were measured via western blot as a preliminary experiment **(Fig. 3-N7)**. Strikingly, though an increase in phosphorylated or total

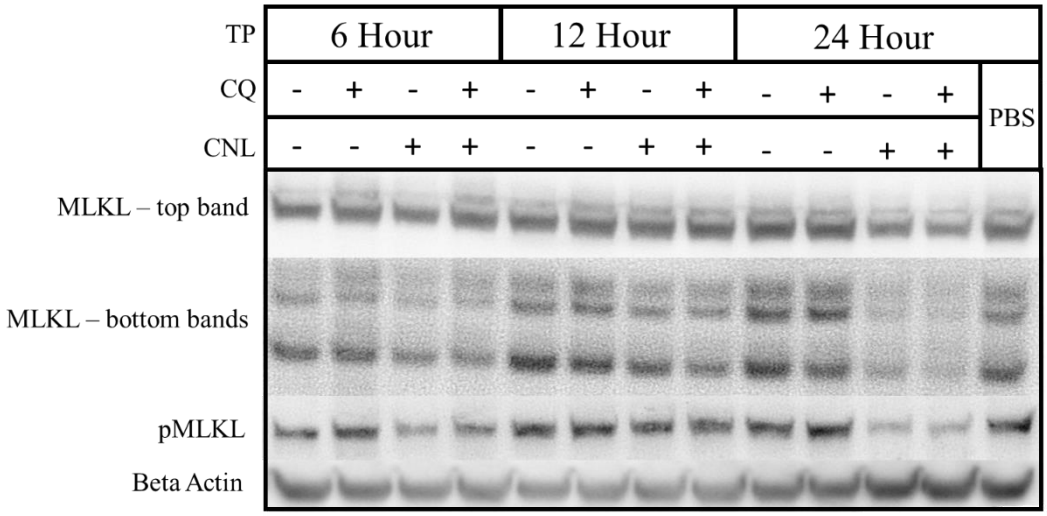

Figure 3-N7 Western Blot Demonstrating a CNL-Mediated Decrease in Total and Phosphorylated MLKL Protein Levels

MLKL protein was expected, the exact opposite phenotype emerged. Though repetition is necessary for this experiment, it appears that CNL is capable of decreasing phosphorylated and total MLKL protein expression as early as 6 hours, an effect which may be exacerbated by the addition of CQ. Though a decrease in phosphorylated MLKL levels is observed, this could simply be due to decreased total MLKL protein by CNL. The banding below and above (only in non-reducing gels – data not shown) the full-length protein, is an interesting observation. However, a literature review reveals that the primary method of activation of MLKL is phosphorylation and does not discuss a cleavage event (181, 182), thus, the smaller bands are likely non-specific. While the larger bands could potentially show oligomerization as previously published (87), these results

require further validation before speculating.

Ceramide and Pyroptosis

Similar to necroptosis, positive controls for pyroptosis are not as widely published and often rely on treatment with LPS which can activate many different signaling cascades (Yang 2015). In regards to pyroptotic inhibitors, the caspase-1 inhibitor Z-YVAD-FMK (henceforth referred to as YVAD to prevent confusion with than the pan-caspase inhibitor Z-VAD-FMK used above) has been identified as a specific inhibitor of caspase-1-dependent pyroptosis. Though, Z-VAD-FMK should have activity against caspase-1, and earlier experiments identified Z-VAD-FMK did not rescue from CNL, there was reason to believe YVAD would also be unable to protect from CNL as well. However, to ensure effective blocking of caspase 1 and caspase 11, the two primary caspases involved in pyroptosis, cells were pre-treated with YVAD in the presence or absence of Z-VAD-FMK before treatment with CNL and cell viability assessment **(Fig. 3-P1)**. However, neither YVAD, Z-VAD-FMK, nor their combination were able to rescue from CNL-induced cell death.

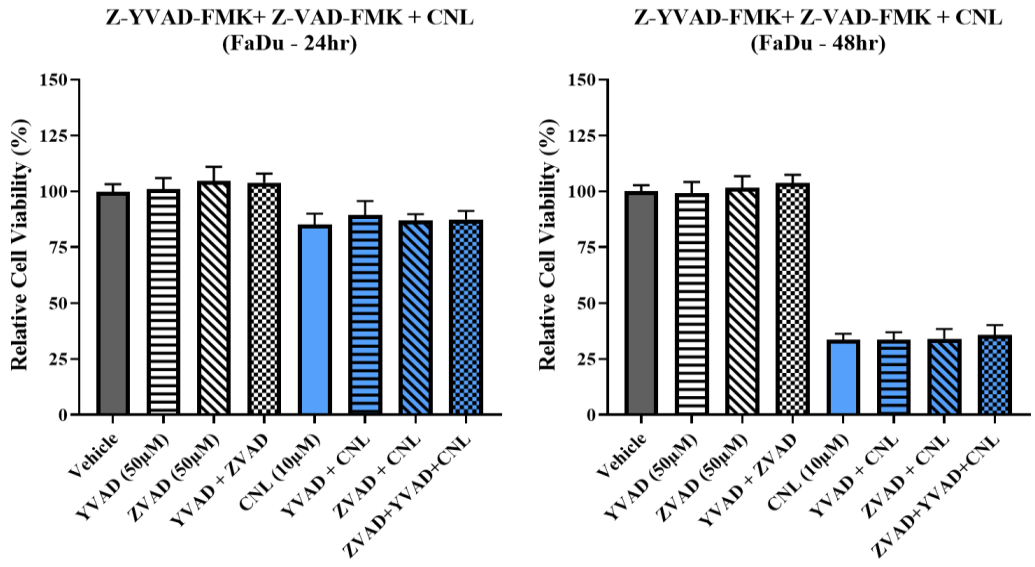

Figure 3-P1 MTS Cell Viability Assay Demonstrating a Lack of Rescue From CNL-Induced Cell Death Mediated by Z-YVAD-FMK, Z-VAD-FMK, or Their Combination

Despite the lack of rescue, in order to more specifically interrogate the pyroptotic pathway,

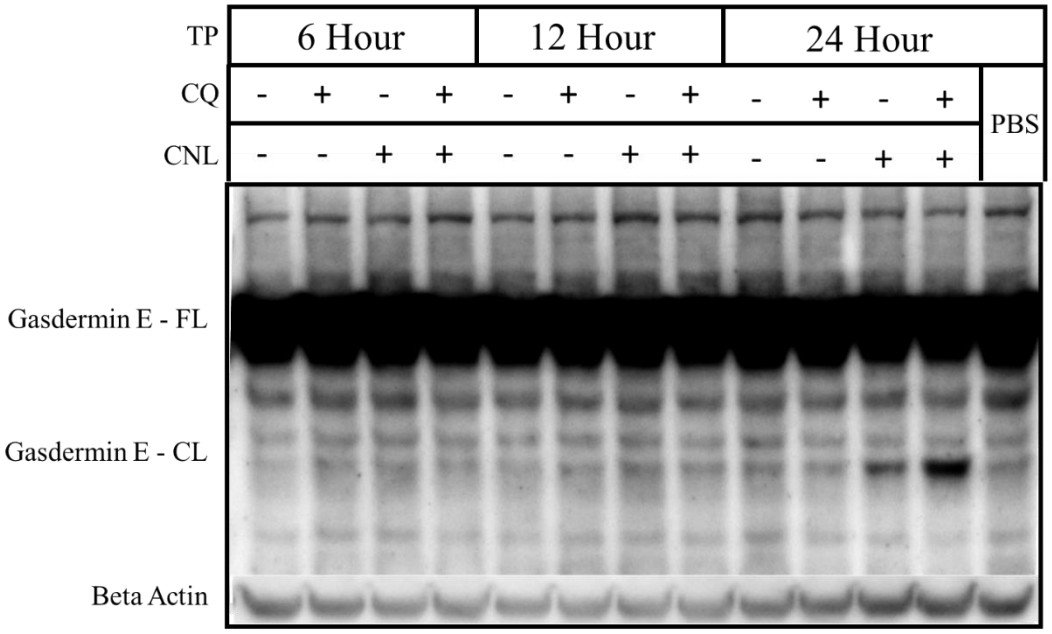

Figure 3-P2 Western Blot Demonstrating a CNL-Mediated Cleavage of Gasdermin E Protein

Gasdermin E was analyzed. As mentioned above, Gasdermin E proteins can be activated via cleavage and can lead to pyroptotic cell death. Thus, after treatment with CNL (with or without CQ), Gasdermin E protein was measured via western blot **(Fig. 3-P2)**. Strikingly, in both biological replicates performed in the FaDu cells, there was markedly increased Gasdermin E cleavage after CNL treatment for 24 hours. Furthermore, the amount of cleavage observed was increased further with CQ treatment.

The finding above when viewed in the context of the available literature brought about an interesting conundrum. CNL can cause Gasdermin E cleavage, and Gasdermin E cleavage leads to cell death. Furthermore, literature claims Gasdermin E cleavage is mediated by caspase 3 activity. However, we establish that inhibiting Caspase 3-does not inhibit CNL-mediated cell death in Figure 3-A3. Thus, either CNL is activating Gasdermin E via a caspase-3 independent mechanism or cleaved Gasdermin E protein is unable to induce cell death in this context. The first hypothesis was tested directly by measuring Gasdermin E cleavage in cells treated with staurosporine, CNL, or CQ+CNL in the presence or absence of Z-VAD-FMK **(Figure 3-P3)**.

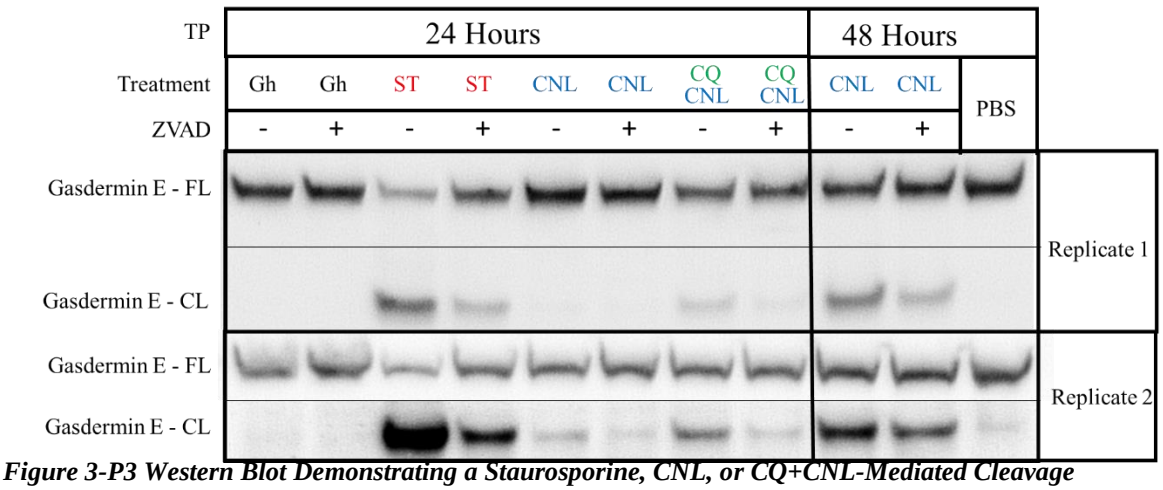

Figure 3-P3 Western Blot Demonstrating a Staurosporine, CNL, or CQ+CNL-Mediated Cleavage of Gasdermin E Protein and Inhibition Via Z-VAD-FMK in FaDu Cells

In two biological replicates (both shown) the positive control staurosporine caused Gasdermin E cleavage and Z-VAD-FMK reduced this cleavage. Furthermore, 24 hours of CNL alone induced Gasdermin E cleavage in one of the two replicates, while 48 hours of CNL alone and 24 hours of CQ+CNL induced cleavage in both replicates. However, all of the above CNL and CQ+CNL-induced Gasdermin E cleavage observed was reduced by Z-VAD-FMK treatment. An almost identical finding of CNL-driven Gasdermin E was observed in two biological replicates

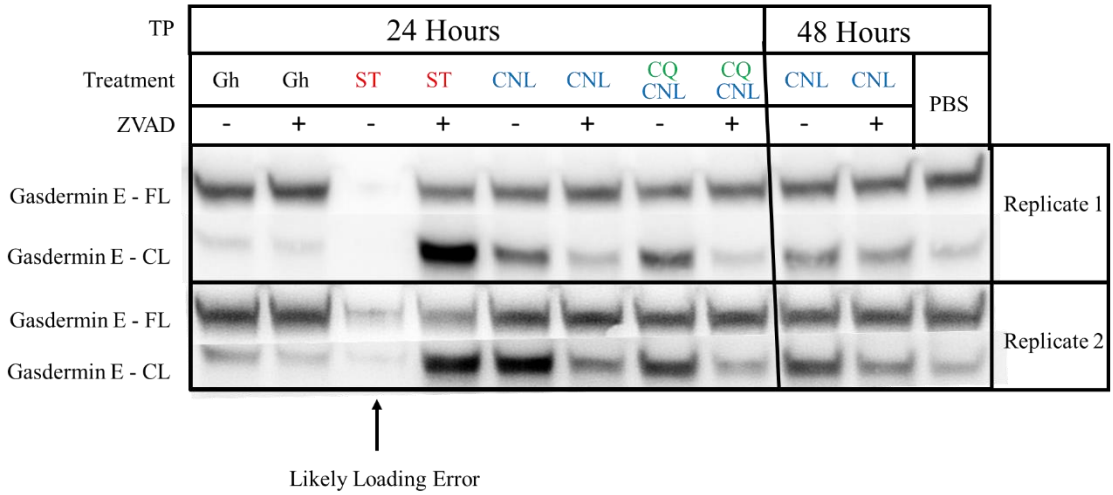

Figure 3-P4 Western Blot Demonstrating a Staurosporine, CNL, or CQ+CNL-Mediated Cleavage of Gasdermin E Protein and Inhibition Via Z-VAD-FMK in SCC-61 Cells

using SCC-61 cells **(Fig. 3-P4).** This observation suggests Gasdermin E is a by-product, not an effector of cell death after CNL treatment. Technical caveats of this experiment include unsuccessful Beta Actin loading controls (due to an overused primary antibody), too great of cell

death to use the 48hr CQ+CNL protein, unsuccessful blotting for Caspase-1 in SCC-61 cells and a likely loading error in the positive control for SCC-61 cells.

Additional Considerations

Although these findings lack the rigor for inclusion above, in one biological replicate of FaDu cells, Caspase-1 cleavage, an effector of pyroptosis, was observed in response to both staurosporine and CNL after 48hours **(Fig. 3-X1)**. If this outcome is reproducible, it suggests a potential upstream activation of a pyroptotic pathway which may lead to Gasdermin protein cleavage. Secondly, treatment of SCC-61 cells with CNL caused a decrease in full length protein and a subsequent increase in a larger band approximately twice the size of Gasdermin D, a second pyroptotic-death inducing protein. **(Figure 3-X2)**. We hypothesize this change may be the formation of a dimer of the protein which

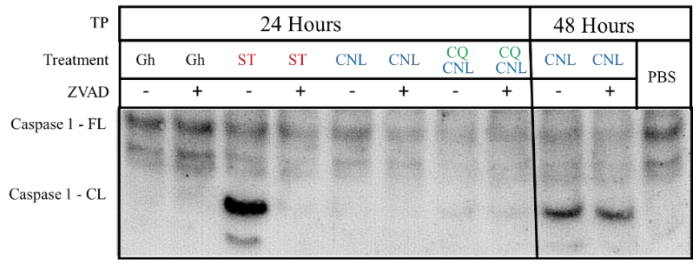

Figure 3-X1 Western Blot Demonstrating a Staurosporine, CNL, or CQ+CNL-Mediated Cleavage of Caspase-1 Protein and Inhibition Via Z-VAD-FMK in SCC-61 Cells

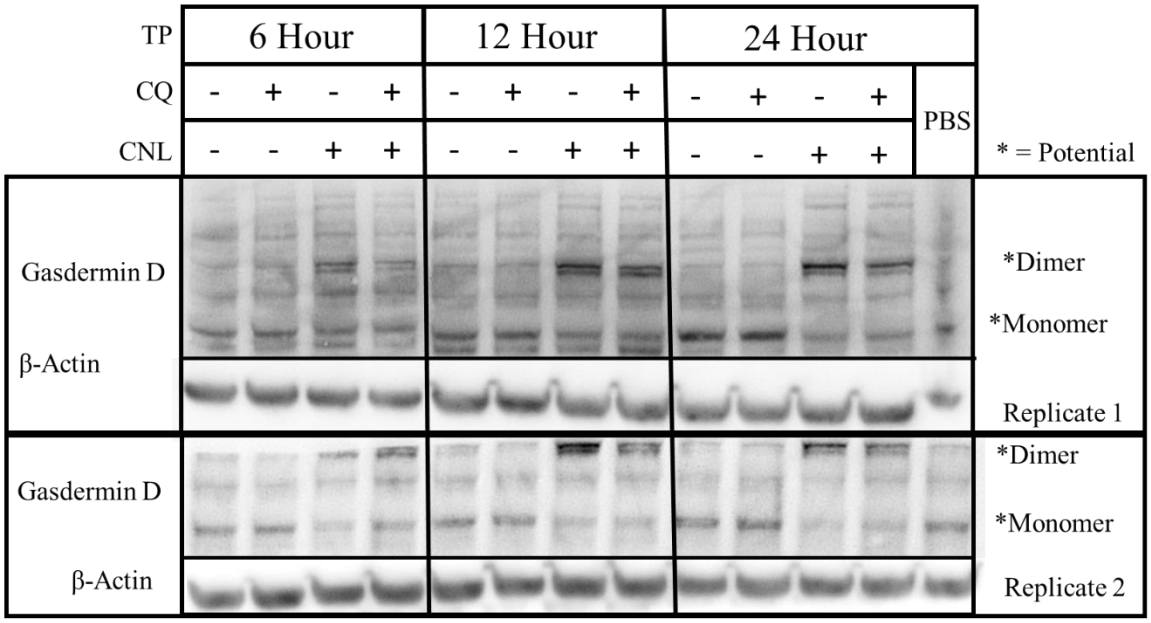

Figure 3-X2 Western Blot Demonstrating a CNL or CQ+CNL-Mediated Potential Dimer Formation of Gasdermin D Protein

may be involved in forming the pores that induce cell death. However, despite at least two of the three biological replicates supporting this finding, the later experiments testing Z-VAD-FMK inhibition did not have successful Gasdermin D staining (data not shown). Furthermore, this same phenotype was not seen in FaDu cells (data not shown). Thus, this finding appears dubius currently.

In an an attempt to further evaluate the role of oligomerization, an additional experiment was performed with the necroptosis inhibitor NSA using reducing vs non-reducing gels (with and without 2-mercaptoethanol, respectively). **(Fig. 3-X3)**. In this experiment, treatment with NSA decreased Gasdermin E cleavage and apparent Gasdermin E dimer formation. The proposed Gasdermin E dimer band was present only in non-reducing lanes, and, relative to the non-reduced lanes, reduced lanes had more full length Gasdermin E, likely due to the comigration of the reduced dimers.

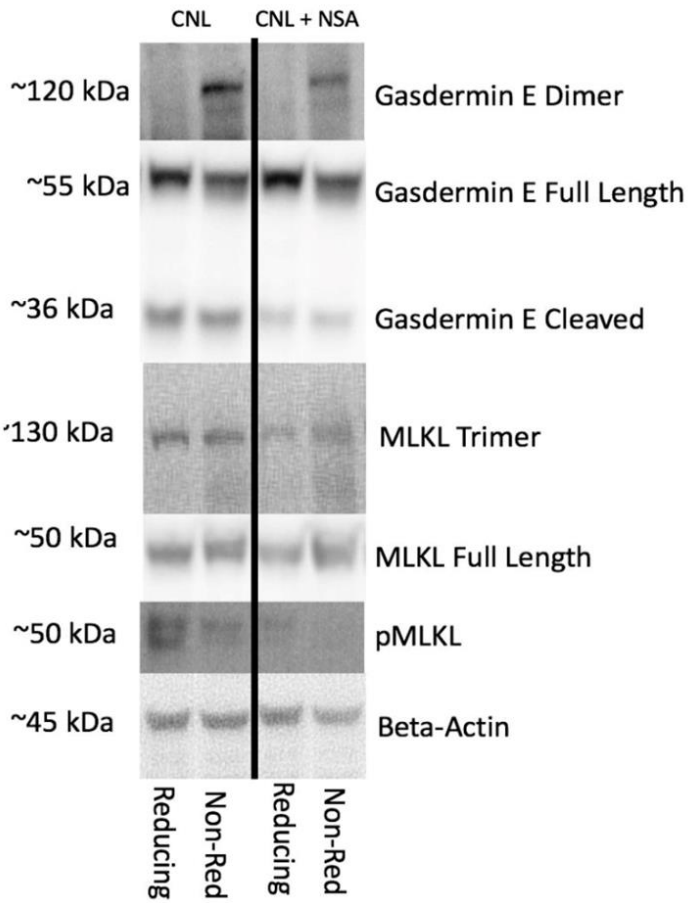

Figure 3-X3 Western Blot Demonstrating a CNL or CNL + NSA Mediated Potential Dime, Phosphorylation, or Cleavage Products of Gasdermin E or MLKL Protein in Reducing or Non-Reducing Gels

Discussion:

Taken as a whole, this work effectively rules out caspase-dependent apoptosis and strongly argue against caspase-independent apoptosis as the mode of CNL-induced cell death in the HNSCC cell lines tested. This was confirmed via multiple cell viability assays, caspase 3/7 activity assays, western blots measuring caspase-3 cleavage, annexin V measurements, and a lack of protection from a pan-caspase inhibitor (Z-VAD-FMK) across multiple assays mentioned above. After identifying one ineffective positive control (Erastin) and one successful positive control (RSL3) for ferroptosis, an interesting wide variety of resistance to RSL3 was observed across the six HNSCC cell lines, suggesting potential resistance mechanisms against ferroptotic cell death in HNSCC. Despite this differential susceptibility to ferroptosis, however, the ferroptosis inhibitor Ferrostatin-1 was unable to inhibit CNL-induced cell death, suggesting an alternative mode of cell death. Exploration into necroptosis revealed a lack of rescue by the necroptosis inhibitor Nec-1 in all cell lines except potentially SCC-61. However, while another necroptosis inhibitor (NSA) did prevent CNL-induced cell death, it was most likely an artifact of preventing basal cell death in all lines which showed increased viability except FaDu. Furthermore, we report for the first time a novel, CNL-induced decrease in MLKL total protein which also manifests as a decrease in phosphorylated MLKL levels. Finally, explorations into pyroptosis reveal a novel increase in Gasdermin E cleavage after CNL treatment, an effect seen in multiple cell lines which can be exacerbated by pre-treatment with CQ and decreased by treatment with Z-VAD-FMK. Unfortunately, knockdown of Gasdermin E or Gasdermin E did not decrease CNL-induced cell death (data not shown). As an additional novel finding, the necroptosis inhibitor NSA, which was the only inhibitor that rescued FaDu cells from CNL-induced cell death, was capable of reducing CNL-induced cleavage of Gasdermin E.

Though the NSA-driven rescue of FaDu cells and potential Nec-1 rescue of SCC-61 cells is certainly interesting, we sought to identify a ubiquitous and unifying form of cell death induced by the CNL in HNSCC cells *in vitro*. While these two findings do not accomplish that goal, from a ceramide-signaling and ceramide-sensitivity perspective, these findings are certainly of interest

and warrant further exploration. Furthermore, the novel, robust and repeatable induction of Gasdermin E cleavage, though not an effector in this model, could be of great significance to the fields of immunology or infectious disease where pyroptosis is emerging as a prominent form of cell death (183).

Though this work identifies multiple novel discoveries of altered signaling pathways mediated by ceramide, neither pharmacological nor molecular inhibition of these pathways has proven capable of rescuing from CNL-induced cell death. As such, we have hesitated to call these ceramide-induced signaling cascades the "effectors" of cell death. Of note, the cell death field almost unanimously acknowledges the interplay of multiple cell death signaling cascades occurring simultaneously (165, 174). If this is the case in our model, inhibition of one particular signaling cascade may be inadequate to rescue from death and our discoveries may in fact be "effectors" which are simply non-necessary as single signaling cascades to lead to cell death. If, in fact, multiple cell death pathways were being activated by ceramide, this would occur via either compensatory (blocking one pathway causes a cell death "switch" to occur) or parallel (multiple death pathways being activated at once) pathways.

Personally, I reject the compensatory hypothesis in our model. I assert that if a molecular cell death was being induced which then switched to a second form of cell death, a decrease in overall cell death or a delay in death would occu upon inhibition of the first mechanism. Metaphorically, if three people were to work together to mow a lawn, the fastest mower would finish the job first. If that mower broke down, certainly the other two could try and cut the rest of the lawn, however, this would certainly happen at a slower rate. Similiarly, though multiple cell death pathways may be occurring simultaneously, if one were to be inhibited, a slight delay or alteration in amount of cell death would certainly have been observed. A delay in cell death was not observed in any of our experiments.

However, the present data does not disprove the "parallel death" pathway. If pyroptosis, necroptosis and other forms of cell death are all activated and pursuing cell death via different yet

parallel pathways, then inhibiting any one of them would be unable to prevent the other forms of cell death from killing. Using the analogy presented above, if three different people were mowing three different lawns, stopping one or even two of the mowers would not prevent a lawn from being completely mowed.

The above work successfully, though somewhat preliminarily, explores multiple forms of cell death including apoptosis, necroptosis, ferroptosis, and pyroptosis. A deeper exploration into these mechanisms may reveal more information, though. Perhaps most relevant to this work are observations that the ESCRT-III family of proteins has been shown to mitigate both necroptotic and pyroptotic forms of cell death. Thus, if pharmacological or molecular inhibition of ESCRT-III signaling enhances CNL-induced cell death, then further exploration into both pyroptosis and necroptosis becomes vital.

Furthermore, even by more strict definitions of cell death types, there are many more forms of cell death which remain uninterrogated in the context of ceramide. I believe the next types of cell death which warrant exploration are parthantos and, more importantly, lysosome-dependent cell death. Parthanatos, a PARP-mediated form of cell death, is suggested due to the induction of PARP cleavage observed in the SCC-61 cells (Fig. 3-A5). Though lysosome-dependent cell death normally relies on caspase activation which was not observed (Fig. 2-2B and 3-A5), there are caspase-independent forms. Considering the data in Chapter 2 discovering CNL-induced damage to the lysosome, this mode of death could certainly be occurring.

Overall, these findings lay the foundation for future work. However, without the ability to rescue from any of the forms of cell death seen above, it is difficult to move past novel correlations into novel causations. Thus, further exploration of the “parallel pathways” hypothesis, inhibiting ESCRT-III signaling, and exploring lysosome-mediated cell death, may help bring this story to a meaningful conclusion.

CHAPTER 4: CERAMIDE SYNERGIZES WITH EPIDERMAL GROWTH FACTOR INHIBITION IN HNSCC

CHAPTER 4: CERAMIDE SYNERGIZES WITH EPIDERMAL GROWTH FACTOR INHIBITION IN HNSCC

PRIMER:

After the deep dive exploring HNSCC resistance mechanisms to CNL and CNL-induced mechanisms of cell death, a more therapeutic approach was taken. Explained in much further detail below, ceramide has shown great efficacy previously in sensitizing a variety of cancer types to anti-cancer agents. With this in mind, we sought to find combinatorial therapies which may lead to synergy in treating HNSCC.

Abstract:

Despite being the seventh deadliest cancer worldwide and over 75% of patients experiencing adverse effects from the current standard of care, Head and Neck Squamous Cell Carcinoma (HNSCC) lags far behind other cancers in the development of effective, targeted therapeutic strategies. Currently, targeting the overexpressed Epidermal Growth Factor Receptor (EGFR) with the monoclonal antibody Cetuximab is the only non-immunological targeted therapy that has shown moderate benefit. Interestingly, two other EGFR inhibitors that target the tyrosine kinase domain, Gefitinib and Erlotinib, failed to benefit HNSCC patients despite efficacy in other cancers. Utilizing the ceramide nanoliposome (CNL) as a therapeutic delivery vehicle for the pro-death sphingolipid ceramide, we explore the therapeutic potential of ceramide in combination with EGFR tyrosine kinase inhibition in HNSCC. We discover a novel synergy between ceramide and both Gefitinib and Erlotinib to induce cell death in a variety of HNSCC cell lines. Strikingly, we report a novel finding that cells increase levels of Early Growth Response 1 (EGR-1) as a compensatory response to ceramide treatment, an effect exacerbated by inhibiting EGFR with Gefitinib. Furthermore, we report that molecular knockdown of EGR-1 further enhances cell death in response to ceramide with or without Gefitinib. Taken together, these data highlight a novel therapeutic approach of combining ceramide with EGFR tyrosine kinase inhibitors as a potential treatment for HNSCC and identifies a circumventable mechanism of resistance.

Introduction:

Head and Neck Squamous Cell Carcinoma (HNSCC) refers to cancers arising from squamous cells mainly in the oral cavity, pharynx, and larynx and affects over 875,000 patients worldwide making it the seventh most common cancer in the world (29). The current standard of care includes a combination of surgical resection, radiation and/or cytotoxic chemotherapy; these treatments lead to adverse effects in over 75% of patients and can be cosmetically and functionally devastating. However, despite decades of attempts to identify targeted therapies, one of the only druggable targets proven efficacious for treatment of HNSCC has been the Epidermal Growth

Factor Receptor (EGFR). EGFR signals through a large number of pro-survival signaling cascades in a variety of cancers (184), is associated with worse prognosis (185, 186), and is overexpressed in 40-80% of HNSCC (187, 188), making it a viable therapeutic target. Canonical EGFR signaling requires ligand binding, which causes dimerization and subsequent activating autophosphorylation of two EGFR monomeric proteins. Once activated via this auto-phosphorylation, EGFR can elicit it's signaling cascade by phosphorylating downstream targets through its tyrosine kinase domain (184).

A monoclonal antibody that inhibits EGFR signaling, Cetuximab, is the only targeted therapy approved for primary treatment of HNSCC. Unfortunately, Cetuximab adds only a few months' survival benefit (23), cannot be given to many patients (189), and has numerous mechanisms of resistance (190, 191). While Cetuximab blocks EGFR signaling through prevention of ligand binding and dimerization (192), other inhibitors, Gefitinib and Erlotinib, block EGFR autophosphorylation and downstream tyrosine kinase activity (193, 194). However, despite sharing the same target as Cetuximab and their success in treating other cancers with aberrant EGFR signaling (195, 196), they failed to show clinical benefit in HNSCC (197-199). Thus, we sought to explore combinatorial treatments which might be able to synergize with EGFR tyrosine kinase inhibitors (TKIs) for potential therapeutic options for patients with HNSCC.

Ceramide is a bioactive, signaling sphingolipid which has previously shown promise as a treatment in HNSCC *in vitro* and *in vivo* as a monotherapy (110, 118)(Chapter 2). Furthermore, ceramide has been shown to synergize with a variety of other drugs in multiple different cancer models (86, 88, 91, 200). Utilizing the ceramide nanoliposome (CNL) as a therapeutic delivery vehicle encapsulating a synthetic, cell-permeable form of ceramide, C6-ceramide, we sought to explore if ceramide was able to enhance the efficacy of EGFR TKIs in inducing cell death in HNSCC.

Though EGFR has numerous signaling cascades which promote cell survival, inhibition of these signals is often not enough to induce cell death as a monotherapy, suggesting compensatory

mechanisms (201, 202). One key downstream target of EGFR, Early Growth Response-1 (EGR-1), has dual roles in both enhancing as well as mitigating cell death.

In the present work we explore the capacity of ceramide to synergize with EGFR TKIs Gefitinib and Erlotinib in inducing cell death in HNSCC. We then explore downstream pathways of EGFR and ceramide signaling to determine which signaling cascades are altered with these combinations. Finally, we perform molecular knockdowns of specific genes increased by the drug combination to determine the role of these genes in protecting from or promoting cell death in HNSCC. Taken together, this work lays the foundation for combinatorial therapies using failed EGFR inhibitors and ceramide-based therapeutics and identifies specific signaling cascades which may further enhance these therapies.

Materials and Methods:

Cell Culture:

The HNSCC cell lines, Cal27, FaDu, UNC-7, UNC-10, SCC-9, SCC-25, SCC-61, and OSC-19 were obtained from Mark Jameson's Lab (University of Virginia) and grown in DMEM/F-12 media (Thermo Fisher Scientific, Waltham, MA) supplemented with 10% FBS (Gemini Bio Products, West Sacramento, CA) and 1% Antibiotic-Antimycotic (Thermo Fisher Scientific). SCC-9 and SCC-61 media was additionally supplemented with 0.5mg/mL hydrocortisone (Millipore Sigma, Burlington, MA). The Primary Gingival Fibroblasts (PCS-201-018 ATCC, Manassas, VA) were grown in Fibroblast Basal Media supplemented with Fibroblast Growth Kit-Low serum (ATCC PCS-201-041) and 1% antibiotic-antimycotic. TrypLE (Thermo Fisher Scientific) was used to passage cells. All cell lines were authenticated via DNA fingerprinting (University of Arizona) of early passage, confirmed mycoplasma via MycoAlert® System (University of Virginia) after thawing, and did not exceed 25 passages.

Inhibitors:

Working stocks of Gefitinib, Erlotinib (Selleck Chemicals, Houston, TX), and staurosporine (ApexBio, Houston, TX) were prepared in DMSO.

Ceramide Nano Liposome (CNL) Formulation:

Ceramide nanoliposomes were a generous gift from KeystoneNano (State College, PA) and manufactured according to published methods (77). Control (ghost) formulations included all liposomal ingredients except C6-ceramide.

Short-Interfering RNA Knockdown:

An appropriate number of cells were plated at a similar confluence to collect enough material for each respective assay. A transfection mix was made in serum free media (Thermo Fisher Scientific), by combining the MISSION transfection reagent (Millipore Sigma) with 40nM of one of three different constructs of siRNA against EGFR (SASI_Hs01_00215449, SASI_Hs01_00215450, SASI_Hs01_00215451) or EGR-1 (SASI_Hs01_00232227,

SASI_Hs01_00232228, and SASI_Hs01_00232229) (Millipore Sigma) according to the manufacturers' instructions. Twenty-four hours after plating, media was changed, and this transfection mix was added to cells. Approximately 20-22 hours later, media was replaced and cells were treated as indicated in the text.

MTS Assay:

HNSCC cells were seeded on 96 well plates to achieve a similar confluency. After 24 hours, cells were pre-treated for 1 hour with either Erlotinib or Gefitinib and subsequently treated with CNLs or ghost liposomes at concentrations indicated in the text. MTS assays were performed according to the manufacturer's instructions (Promega, Madison, WI). Absorbance at 490nm was determined with a Cytation 3 plate reader (Bio Tek, Winooski, VT). After subtracting the background absorbance (no cells), all values were normalized to their intra-plate controls.

Western Blot:

Cells were treated as indicated in the text. RIPA buffer (Alfa Aesar) with protease inhibitor (Thermo Fisher Scientific) and phosphatase inhibitor (Roche, Basel, Switzerland) was used to lyse the cells. Protein concentrations were determined with a BCA protein assay (Pierce, Appleton, WI). 18-28µg of protein was added to a NuPAGE 4-12% Bis-Tris gel (Thermo Fisher Scientific) and ran at 120V for 2 hours and 20 minutes. Transfer to a nitrocellulose membrane (Bio-Rad Laboratories, Hercules, CA) was performed using the Bio-Rad Turbo-Transfer apparatus. Blocking with 5% BSA (Thermo Fisher Scientific) in TBST was done for 1 hour at room temperature and blots were cut before an overnight primary antibody incubation at 4°C. Primary antibodies were, p-AKT [4058], AKT [4691], Caspase 3 [9662], EGR-1 [4153], PARP [9532], p-EGFR [2234], and GADD45a [4632] (Cell Signaling Technologies, Danvers, MA), EGFR [sc-373746], p-ERK1/2 [sc-7383], and ERK1/2 [sc-514302] (Santa Cruz Biotechnologies, Dallas, TX), CyclinD1 [MA5-16356] (Thermo Fisher Scientific), and Beta Actin [A5441] (Millipore Sigma). Blots were washed 3x5 minutes with TBST. Horseradish peroxidase conjugated secondary antibody against rabbit or mouse (Thermo Fisher Scientific) was then added for 1 hour at room temperature. Three additional

five minute washes were performed prior to detection with enhanced chemiluminescence (Prometheus, San Diego, CA) and imaged with a G:Box Chemi XX6 (Syngene, Bangalore, India). If blots were re-probed, a stripping step was performed using Restore Western Blot Stripping Buffer (Thermo Fisher Scientific) according to the manufacturer's instructions. Densitometry of each target was performed using ImageJ software and were normalized: first, to β-actin, then to the vehicle treatment at the respective time-point from the same blot.

Quantitative Real-Time Polymerase Chain Reaction:

Treated cells were washed and RNA extracted using the RNeasy Mini Kit (Qiagen, Hilden, Germany). RNA content was quantified using a Cytation 3 (BioTek Winooski, Vermont). 800-1000ng of RNA was used in the iScript cDNA Synthesis Kit (Bio-Rad Laboratories) to synthesize cDNA. FAM probes (PSMB6-[qHsaCEP0052321], EGFR-[qHsaCEP0052595], EGR-1-[qHsaCEP0039196], GADD45a-[qHsaCEP0039165]) and iTaq Universal Probes Supermix (Bio-Rad Laboratories) were used and CT values were measured using CFX Connect Real-Time PCR Connection System (Bio-Rad Laboratories). CT values were normalized first to the housekeeping gene control (PSMB6), and then to their respective timepoint/vehicle controls.

Flow Cytometry Assays:

Cells were treated as indicated in the text. The media containing floating cells and the adherent cells, after trypsinization, were combined. Cells were centrifuged and the supernatant discarded. To assess cell viability, on the resultant cell pellet, Fixable Viability Dye 780 (Thermo Fisher Scientific), was used according to the manufacturers' instructions. Samples were measured by the Attune Nxt Flow Cytometer (Thermo Fisher Scientific). Forward and side scatter measurements were used to gate for singlets and exclude debris. Single-stain compensation controls were collected and gates were drawn accordingly.

Statistics:

All statistics were performed on GraphPad Prism 8 (GraphPad Software, San Diego, CA). All experiments were repeated at least three times unless otherwise stated. A one-way ANOVA was

performed with Tukey's multiple comparison post-hoc test to determine significance between all groups. The markers *, **, and *** indicate significance of $p < 0.05$, 0.01, and 0.001 respectively. All error bars are standard deviation of the mean. Bliss scores were calculated using SynergyFinder (Ianevski 2017).

Results

CNL and EGFR Inhibitors Induce Synergistic Cell Death in HNSCC

To determine HNSCC sensitivity to Gefitinib and Erlotinib as well as the potential of CNL to enhance this sensitivity, cells were treated with Gefitinib and Erlotinib in the presence or absence of CNL and cell viability was assessed in eight HNSCC cell lines as well as non-transformed PGF cells for 24 and 48 hours. In the absence of ceramide, nearly all HNSCC cell lines and PGF cells demonstrated resistance to both EGFR inhibitors at both time points. In four representative cell lines (FaDu, UNC-7, UNC-10, and SCC-25), Gefitinib alone only showed concentration- and time-dependent responses in one cell line (UNC-10) **(Fig. 4-1A-D)** while Erlotinib alone failed to reduce cell viability by more than 42% at either time point **(Fig. 4-2A-D)** even at greater-than-physiological concentrations.

However, despite the lackluster response of HNSCC cell lines to Gefitinib or Erlotinib alone, combinations of CNL with either EGFR inhibitor demonstrated synergistic cell death in almost all HNSCC cell lines**.** Specifically, after 48 hours UNC-7 cells exhibited -1% and 11% decreased viability after 10μM Gefitinib and 5μM CNL, respectively, while the combination led to a striking 77% decrease in cell viability **(Fig. 4-1A).** Similar decreases in cell viability after combined treatment (Gefitinib, CNL, CNL+Gefitinib) were observed in SCC-25 (0%, 5%, 64%), FaDu (18%, 30%, 87%), and UNC-10 (38%, 27%, 87%) cel llines (**Fig. 4-1B-D**)**.** Interestingly, at these same concentrations, preliminary expreiments in non-transformed PGF cells showed far less synergy and an overall increased resistance to this combination, with viability decreases of only 2%, 13%, and 23% after 10μM Gefitinib, 5μM CNL, and the combination, respectively (**Fig. 4-1E**). Bliss Synergy scores were calculated in all four cell HNSCC lines at the 48 hour timepoint (**Fig. 4-1F).** This HNSCC-specific increase in cell death after Gefitinib + CNL was also confirmed via flow cytometry at 48 hours in both UNC-7 and SCC-25 cell lines (**Fig 4-1G/H).** In both lines, at both concentrations of CNL (5μM and 10μM), greater-than-additive cell death was observed when Gefitinib and CNL were combined compared to the sum of death induced from either drug

alone. CNL also enhanced Erlotinib-driven decreases in cell viability, strangely, the combination was not as efficacious as Gefitinib + CNL **(Fig. 4-2A-D).**

Bliss synergy analysis was conducted to quantify the magnitude of synergy in each HNSCC cell line and PGF cells. For all HNSCC cell lines treated with CNL + Gefitinib, and all but one HNSCC cell line treated with CNL + Erlotinib, synergy was identified with scores ranging from 7.26 to 29.27 for Gefitinib + CNL and -9.91 to 8.17 for Erlotinib + CNL **(Fig. 4-1F & Fig. 4-2E).** Taken together, these data highlight a synergism between CNL and EGFR inhibitors to decrease cell viability in HNSCC cell lines. This synergy is stronger with Gefitinib + CNL than Erlotinib + CNL, and is far more synergistic in HNSCC compared to non-transformed cells. .

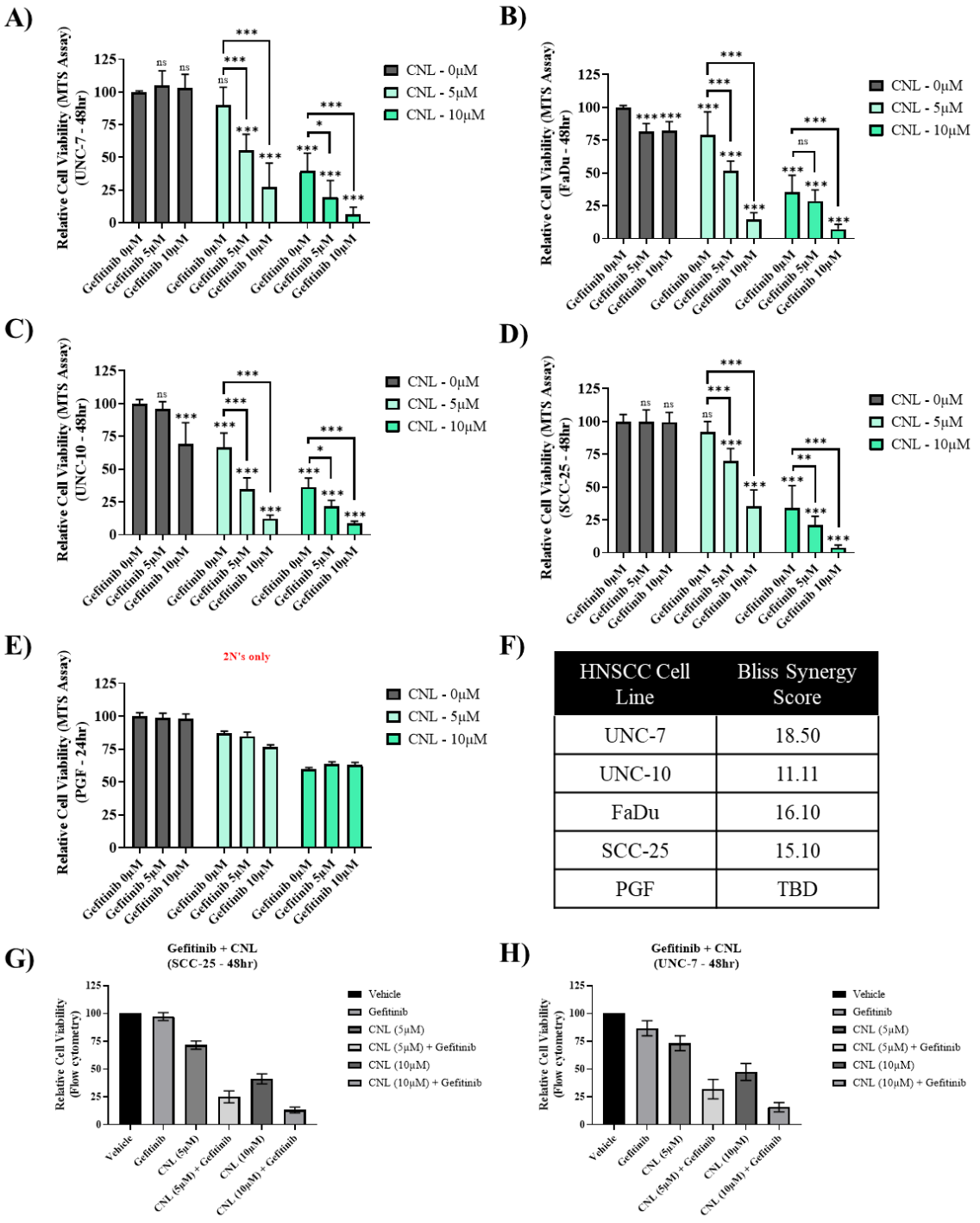

HNSCC Cell Line	Bliss Synergy Score
UNC-7	18.50
UNC-10	11.11
FaDu	16.10
SCC-25	15.10
PGF	TBD

Figure 4-1: HNSCC cell viability in response to treatment with Gefitinib and CNL

*(**A-E**) The response of four HNSCC cell lines and PGF at 48 hours post Gefitinib + CNL treatment measured via MTS assay. **(F)** F displays the Bliss Synergy scores calculated for each cell line. **(G-H)** The response of two HNSCC cell lines to Gefitinib + CNL (5μM and 10μM treatment) at 48 hours as measured via flow cytometry.*

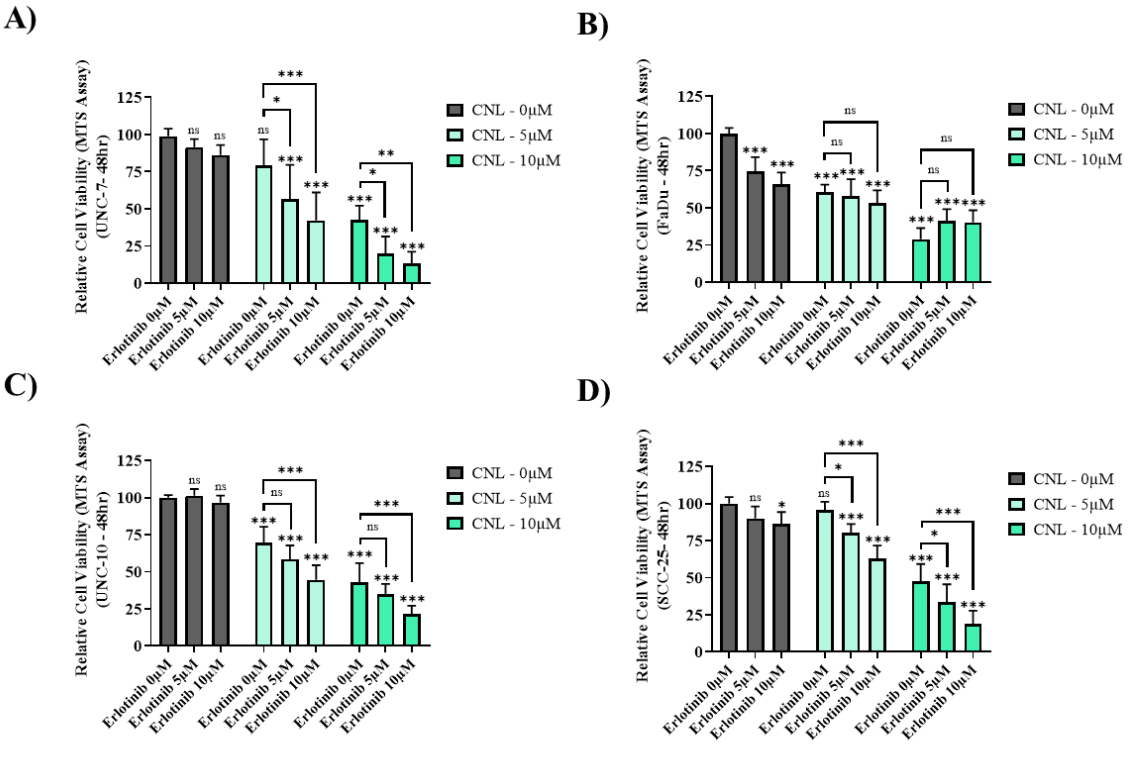

E)

HNSCC Cell Line	Bliss Synergy Score
UNC-7	10.45
UNC-10	10.13
FaDu	-9.91
SCC-25	6.05
PGF	TBD

Figure 4-2: HNSCC cell viability in response to treatment with Erlotinib and CNL
(A-D) *The response of four HNSCC cell lines at 48 hours post Erlotinib + CNL treatment measured via MTS assay.* ***(E)*** *displays the Bliss Synergy scores calculated for each cell line.*

CNL and Gefitinib Increase Levels of EGR-1 in HNSCC

To elucidate the mechanism underlying CNL + Gefitinib synergy, expression/activation changes in targets measuring EGFR-signaling (EGFR, ERK1/2, AKT, EGR-1) were measured. In preliminary experiments, after 24 hours, Gefitinib reduced EGFR phosphorylation 25-fold as a single agent and 3.13-fold in combination with CNL, confirming the successful inhibition of EGFR **(Fig. 4-3A)**.

Interestingly, Early Growth Response-1 (EGR-1), an EGFR downstream target, markedly increased 12.86-fold after Gefitinib + CNL treatment despite only 2.47-fold and 8.52-fold increases with Gefitinib and CNL treatment as single agents, respectively **(Fig. 4-3A)** in preliminary experiments**.** A similar increase was also seen at the RNA level **(Fig. 4-3B).** Notably, the increases in EGR-1 gene expression and protein level were not accompanied by increases in ERK1/2 activation **(Fig 4-3A)**. Collectively, these data demonstrate both mRNA-level and protein-level increases in EGR-1 following treatment with Gefitinib and CNL.

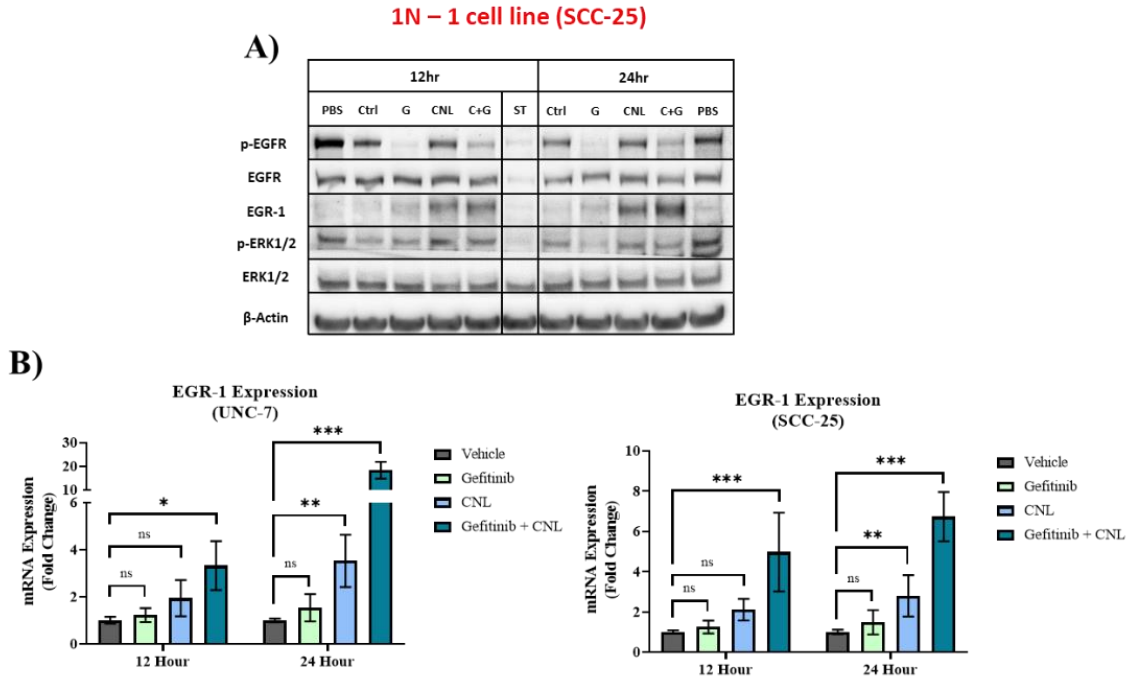

Figure 4-3: CNL + Gefitinib Increases EGR-1 Expression

(A) *Western Blot of SCC-25 cells treated with 10μM Gefintib + 10μM CNL at 12 and 24 hours.* ***(B)*** *RT-qPCR of UNC-7 and SCC-25 cells treated with 25μM Gefitinib and/or 2.5μM CNL at 12 or 24 hours.*

EGR-1 is Sufficient to Decrease CNL + Gefitinib Induced Cell Death in HNSCC

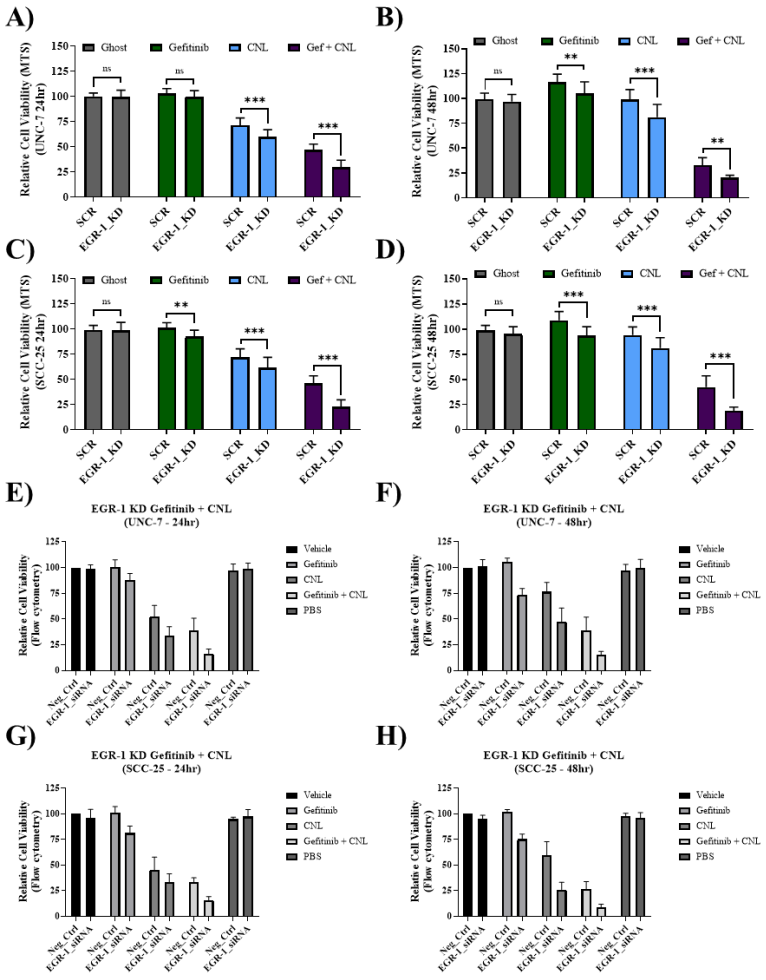

Figure 4-4: EGR-1 is Sufficient to Reduce CNL + Gefitinib Induced Cell Death

(A-D) *MTS Cell Viability assay of UNC-7* ***(A,B)*** *and SCC-25* ***(C,D)*** *cells treated with 10μM Gefitinib and/or 10μM CNL at 24 hours and 10μM Gefitinib and/or 5μM CNL at 48 hours with or without EGR-1 knockdown.* ***(E-H)*** *Flow cytometry measurement of cell death after UNC-7* ***(E,F)*** *and SCC-25* ***(G,H)*** *cells treated with 10μM Gefitinib and/or 5μM CNL at 24 and 48 hours with or without EGR-1 knockdown.*

Considering the role of EGR-1 in both cell death and cell survival processes, preliminary EGR-1 siRNA knockdowns were performed to determine the function of EGR-1 in the context of Gefitinib and CNL-induced cell death. Preliminary expreiments utilizing treatment with anti-EGR-1 siRNA reduced EGR-1 mRNA expression by ~60% (data not shown) for up to 72-hours in both cell lines relative to a scramble siRNA control. After 24 hours of anti-EGR-1 or scramble siRNA knockdown, UNC-7 and SCC-25 cells were treated with Gefitinib with or without CNL and cell viability was measured 24 and 48 hours later **(Fig. 4-4A-D)**. EGR-1 knockdown was sufficient to enhance Gefitinib + CNL cell death in both cell lines. Specifically, at the 24-hour timepoint, EGR-1 knockdown reduced the viability of cells treated with Gefitinib + CNL by 16% (47% to 31%) in UNC-7 cells and 19% (46% to 27%) in SCC-25 cells compared to scramble siRNA **(Fig. 4-4A,C)**. At 48 hours post-treatment, the viability of Gefitinib + CNL -treated UNC-7 and SCC-25 cells was reduced by 12%

and 19%, respectively, relative to their scramble controls **(Fig. 4-4B,D)**. Notably, knockdown of EGR-1 had a significant effect on cells treated with CNL alone, reducing cell viability from 108% to 82% in UNC-7 and 101% to 82% in SCC-25's at 48 hours. Conversely, treatment with Gefitinib alone in conjunction with EGR-1 knockdown experienced a small, decrease in viability at 48 hours in both cell lines. To further validate this EGR-1 dependent effect, Gefitinib + CNL induced death was measured in both UNC-7 and SCC-25 cell lines at 24 and 48 hours via flow cytometry **(Fig. 4-4E-H).** Again, EGR-1 was able to enhance the cell death induced by the combination of Gefitinib + CNL. The increase in Gefitinib + CNL-induced cell death following siRNA knockdown of EGR-1 provides evidence that EGR-1 fulfills a pro-survival function for HNSCC in response to treatment with Gefitinib and CNL.

CNL and Gefitinib Induce Minor PARP Cleavage and Decrease Cyclin D1 in HNSCC

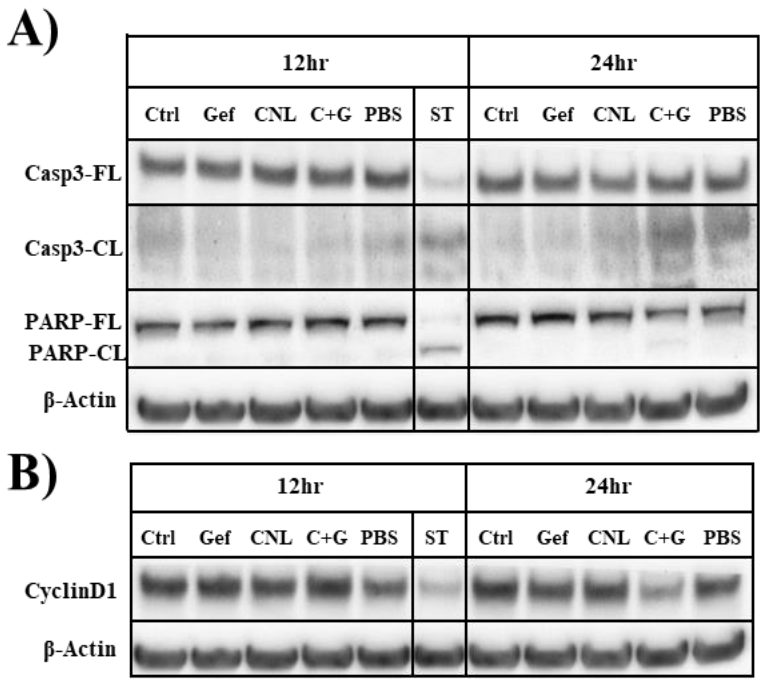

Figure 4-5 Gefitinib + CNL Induced Changes in Cell Death and Cell Cycle Targets

*Western Blot measuring protein changes in **(A)** cell death and **(B)** cell cycle proteins in SCC-25 cells treated with PBS, DMSO/Ghost control (Ctrl), 10μM Gefitinib (Gef), 10μM CNL (CNL), or 10μM Gefitinib + 10μM CNL (C+G). FL = Full Length, CL = Cleaved*

As part of the effort to elucidate the mechanism behind CNL + Gefitinib synergistic cell death, expression/activation changes in mediators of cell death (PARP, Caspase3) and cell cycle (GADD45, CyclinD1) were measured. In preliminary experiments, despite functional cleavage of both PARP and Caspase-3 with the positive control (staurosporine) after 24 hours, Gefitinib and CNL co-treatment resulted in a 24.3-fold increase in cleaved PARP, but failed to induce Caspase-3 cleavage **(Fig. 4-4A).** Alterations in cell cycle proteins were also identified as the combination of Gefitinib and CNL induced a time-dependent decrease in CyclinD1 protein levels, demonstrating 12- and 24-hour decreases of 1.49-fold and 2.33-fold, respectively. Taken together, these data suggest the combination of CNL and Gefitinib alters levels of cell death (PARP) and cell cycle (decreasing CyclinD1), protein-level signaling events.

Discussion

This manuscript identifies and describes a novel cancer-specific synergy between the EGFR inhibitors (Gefitinib and Erlotinib) and ceramide in HNSCC. The robustness of this synergy is determined by utilizing multiple inhibitors, multiple cell lines, and multiple timepoints. In

addition to expected changes in EGFR and pEGFR levels after Gefitinib treatment, ceramide alone or ceramide in combination with Gefitinib increases EGR-1 mRNA and protein levels, a novel finding. Interestingly, molecular knockdown of EGR-1 was sufficient to sensitize two HNSCC cell lines to both ceramide- and ceramide + Gefitinib-induced cell death highlighting the pro-survival role of EGR-1 after ceramide treatment. Preliminary data further suggests, Gefitinib and ceramide treatment may lead to cell cycle arrest (via decreasing Cyclin D1) as well as a decreased DNA damage response (via increased PARP-1 cleavage).

While this manuscript describes the first ceramide-driven increase in EGR-1, as well as establishes the sufficiency of EGR-1 to partially protect HNSCC from cell death, the mechanism of both of these observations remains mostly unknown. In regards to how ceramide increases levels of EGR-1, most research identifies ERK1/2 signaling as the primary driver of EGR-1 levels (203); however, preliminary experiments suggest that ceramide causes EGR-1 increases independent of ERK1/2 (Fig. 4-3A) in this model. Considering ceramide has been shown to induce cellular stress (204), and EGR-1 can be activated by cellular stress signals (205), ceramide-induced cellular stress may drive increases in EGR-1 levels. In regards to how EGR-1 protects HNSCC from cell death, it is known that EGR-1 can promote pro-survival signaling cascades via altering transcription of downstream pro-survival genes such as TGFb1, FN, p21, FAK (206), IGF-2, PDGFA/B, VEGFA (50), PTEN (207) , and p53 (208). Thus, increases in transcription of these genes may promote HNSCC survival in response to ceramide.

Though this manuscript describes a compensatory mechanism of resistance to Gefitinib + CNL treatment, and downstream alterations of the cell cycle and cell death proteins, the full scope of the mechanism of synergy has yet to be elucidated. One possible area for future exploration is to measure other key downstream EGFR signaling pathways which may be a locus of overlap between Gefitinib treatment and ceramide treatment. Of note, phosphorylation of two proteins downstream of EGFR, AKT and STAT3, have previously been identified as resistance mechanisms to Gefitinib treatment in other cancer models (209, 210). Interestingly, ceramide has been shown

to cause dephosphorylation of multiple pro-survival proteins downstream of EGFR including both AKT (211, 212) and STAT3 (83) in other cancer models. Thus, studies investigating STAT3 and AKT signaling after Gefitinib + ceramide treatment may provide additional understanding of their synergistic effects.

The synergism between EGFR inhibition and ceramide could also be at the level of ceramide metabolism. It has been previously reported that ceramide's metabolism into other sphingolipid species can mediate its induction of cell death (44). Thus, considering the lysosome is a primary location of ceramide metabolism (213) and EGFR inhibitors can disrupt endosome trafficking to the lysosome (194), it is possible that the deviation from homeostatic lysosomal processing of ceramide can enhance its capacity to induce cell death. Alternatively, various small molecule inhibitors can increase expression or activity of ceramide synthases (214-216), which in turn, can increase levels of toxic forms of ceramide which lead to cell death in HNSCC (110). Thus, if Gefitinib is able to increase activity of these ceramide synthase enzymes, this would not only increase endogenous levels of ceramide, but may lead to an alternative metabolism of exogenous ceramide (via the CNL) into more pro-death ceramide species. This double-hit of increased endogenous ceramide levels as well as increased metabolism of the CNL could induce greater-than-additive cell death. Additionally, ceramide and ceramide metabolites are vital to the formation of functional lipid-enriched domains (217), which can alter location and signaling properties of EGFR as well as responses to Gefitinib (218). Thus, differential ceramide metabolism may lead to alteration in these lipid-enriched domains which may, in turn, alter EGFR dimerization, stability, signaling cascades, and response to Gefitinib.

The increased capacity of Gefitinib compared to Erlotinib in inducing synergistic cell death with ceramide is a curious observation (Fig. 4-1, Fig. 4-2). While Gefitinib and Erlotinib are both competitive inhibitors of EGFR's intracellular ATP-binding domain (219), if not due to an off-target effect, a possible explanation for varying efficacies could stem from differing binding specificities between inhibitors (220). Mutations to residues within the ATP binding pocket can be

specifically favorable for Gefitinib to promote tighter binding than Erlotinib, likely stemming from the difference in molecular structure of the inhibitors (219). Though major EGFR mutations are minimally expressed in HNSCC (221), if HNSCC fosters these small, specific EGFR mutations (221), binding kinetics could alter the magnitude of synergy of EGFR competitive inhibitors in combination with ceramide.

Though these data focus primarily on EGFR inhibitors which work by inhibiting the receptor tyrosine kinase domain, the monoclonal antibody which blocks the ligand binding site of EGFR, Cetuximab, is the only approved molecular therapy for primary treatment of HNSCC. While preliminary work (data not shown) in our lab did not identify *in vitro* synergy of CNL and Cetuximab in HNSCC cell lines, this is not unexpected as many reports agree that Cetuximab is ineffective *in vitro* (222). Thus, CNL and Cetuximab may still demonstrate therapeutic relevance for *in vivo* models of HNSCC.

Overall, this manuscript identifies a novel synergy between a clinically relevant ceramide delivery vehicle and EGFR TKIs in treating HNSCC. Furthermore, novel increases in EGR-1 at both the mRNA and protein levels driven by ceramide as well as ceramide + gefitinib are identified and determined to be a novel protective mechanism from ceramide-induced cell death which may be of therapeutic relevance. Interestingly, these studies also highlight the role of EGR-1 to further enhance cell cycle arrest and/or DNA-damage responses driven by ceramide. Taken together, these data provide a detailed roadmap of ceramide signaling in HNSCC and provide evidence for breathing new life into safe, yet ineffective, EGFR inhibitors for a synergistic treatment with CNL.

CHAPTER FIVE: INHIBITION OF GLUCOSYLCERAMIDE SYNTHASE MITIGATES CERAMIDE-INDUCED CELL DEATH

CHAPTER FIVE: INHIBITION OF GLUCOSYLCERAMIDE SYNTHASE MITIGATES CERAMIDE-INDUCED CELL DEATH:

PRIMER:

After exploring mechanisms of resistance to CNL, the type of cell death induced by CNL, and potential combinatorial therapies with CNL, a switch of focus was warranted to take a more biochemical and global, yet still therapeutic, approach of study. As covered in more detail in the Chapter 1 Sphingolipid Intro and below, ceramide can be metabolized into four other sphingolipid species. These species can have differing structure, localization, and can activate entirely different signaling cascades. Thus, by using inhibitors of different ceramide metabolizing enzymes, one can potentially increase the half-life of unmetabolized ceramide as well as alter its metabolism to the most anti-cancer ceramide metabolites – making it a more effective therapeutic. The work below seeks to determine which ceramide metabolites are pro-survival and which are pro-death to build the foundation for therapeutic alteration of ceramide metabolism.

Abstract:

Bioactive signaling lipids in the sphingolipid family have roles ranging from promoting cancer progression and resistance to inducing cancer cell death. Thus, manipulation of these different sphingolipids and sphingolipid-metabolizing enzymes represents a crucial point of therapeutic intervention for cancer. Because ceramide has been identified as the primary pro-death sphingolipid in a variety of cancer models, ceramide's metabolism into other pro-survival sphingolipids represents a key area of focus to improve sphingolipid-based therapies. Using the ceramide nanoliposome (CNL), a therapeutically relevant delivery vehicle encapsulating a synthetic, cell-permeable C6-Ceramide, the role of ceramide-metabolizing enzymes on ceramide signaling and cell deathvwas explored in head and neck squamous cell carcinoma (HNSCC). It was

determined that inhibition of the "pro-survival" enzyme Glucosylceramide Synthase (GCS) inhibits ceramide-induced cell death in a time and concentration-dependent manner.

Introduction:

Sphingolipids are a class of lipids comprised of a sphingosine backbone involved in numerous signaling cascades (223). Although originally identified as having a role in membrane biology (35), sphingolipids have garnered attention as having roles both promoting and inhibiting a myriad of pathologies including diabetes (37), atherosclerosis (39, 41), neurodegenerative disorders (43), and cancer (44). Studies in a variety of cancer models have identified the role of the sphingolipid ceramide to induce cell death (45, 119). Thus, decreasing the amount of the pro-death sphingolipid ceramide via metabolism into other sphingolipid species is described as a survival mechanism in a variety of cancers. However, while studies into the effects of these enzymes on cancer-intrinsic properties have been previously explored, the effect of the enzymes on altering ceramide-induced cell death signaling require further investigation.

Ceramide can be primarily metabolized into four different sphingolipids via four different families of enzymes; one family breaks down ceramide while the others generate larger sphingolipid products (224). Enzymes in the ceramidase family are responsible for breakdown of ceramide by cleaving the fatty acid chain at the amide bond generating the sphingolipid sphingosine. The generation of larger sphingolipid products from ceramide is achieved via the conjugation of an additional compound (phosphocholine/phosphoethanolamine, phosphate, or glucose) on carbon-1 position of the sphingosine near the polar head group. The addition of phosphoethanolamine and/or phosphocholine via the Sphingomyelin Synthase enzyme family generates Sphingomyelin, the addition of a phosphate group by the Ceramide Kinase enzyme generates Ceramide-1-Phosphate, and the addition of a glucose by the Glucosylceramide Synthase (GCS) enzyme generates Glucosylceramide. While each of these four sphingolipid products generated via ceramide metabolism have unique cellular localization, signaling cascades, and

enzymes which can further mediate their metabolism, the enzymes which generate them are all viewed as pro-survival species due to their role in decreasing levels of the cytotoxic ceramide.

One of the most well-described, pro-survival metabolism pathways for ceramide is the addition of glucose onto ceramide, mediated by GCS, generating glucosylceramide. Not only has GCS been shown to decrease the cell-death effects of ceramide (85, 225), it also promotes resistance to chemotherapeutics (51, 52, 226), promotes metastasis (227), and is correlated with decreased patient survival (98). However, glucosylceramide can be further metabolized into "higher-order" glycosphingolipids. First, a lactose group can be added via the B4GALT5 or B4GALT6 enzyme generating lactosylceramide. Lactosylceramide can then be acted on via a multitude of enzymes which can conjugate a variety of additional sugar residues to multiple locations on the glycosylated chain generating cerebrosides, sulfatides, globosides, and gangliosides. These higher-order sphingolipids have vastly varying roles including increasing drug resistance (88, 228, 229) in some instances through multidrug resistance gene 1 (MDR1) expression (230), increasing (231, 232) and decreasing (233) (234) markers of metastasis, and inducing mitochondrial permeability-driven apoptosis (235, 236). Considering this, GCS and B4GALT5/6 are not only enzymes which can decrease ceramide levels, but also two necessary gatekeepers mediating the generation of a myriad of functional, higher-order sphingolipids. Thus, while the role of GCS in signaling cascades (227) has been well studied, its role in altering ceramide's generation of higher-order sphingolipids and these consequences on cell death remain poorly understood.

Using the ceramide nanoliposome as a therapeutic delivery vehicle for short-chain C6 ceramide, we show that pharmacological inhibition (Ibiglustat or PPMP) of GCS strikingly prevents C6-ceramide induced cell death in multiple HNSCC cell lines. Future steps include the following: Mechanistically, we seek to determine if inhibiting GCS in the presence of C6-ceramide prevents its metabolism into not only glucosylceramide, but also into higher order sphingolipids such as globosides, gangliosides, or sulfatides. We will then seek to determine if inhibition of GCS also decreases major hallmarks of ceramide-driven signaling cascades involving autophagy,

mitophagy, DNA damage response, and drug efflux pumps. Finally, we seek to molecularly knockdown the enzyme responsible for synthesis into the most abundant higher-order sphingolipid identified above to determine if, similar to knockdown of GCS, this is also able to rescue from ceramide-mediated cell death. Taken together, we seek to further validate this novel role of GCS to promote ceramide-induced cell death in HNSCC.

Materials and Methods:

Cell Culture

The HNSCC cell lines, Cal27, FaDu, UNC-7, UNC-10, SCC-9, SCC-25, SCC-61, and OSC-19 were generously provided by the Mark Jameson Lab (University of Virginia). All cell lines were grown and maintained in DMEM/F-12 media (Thermo Fisher Scientific, Waltham, MA) supplemented with 10% FBS (Gemini Bio Products, West Sacramento, CA) and 1% Antibiotic-Antimycotic (Thermo Fisher Scientific). Media for the SCC-61 cells was additionally supplemented with 0.5mg/mL hydrocortisone (Millipore Sigma, Burlington, MA). The Primary Gingival Fibroblasts (PCS-201-018 ATCC, Manassas, VA) were grown in Fibroblast Basal Media supplemented with Fibroblast Growth Kit-Low serum (ATCC PCS-201-041) and 1% antibiotic-antimycotic. TrypLE (Thermo Fisher) was used to detach and passage adherent cells. All cell lines were authenticated via DNA fingerprinting (University of Arizona) of early passage, confirmed mycoplasma via MycoAlert® System (University of Virginia) after thawing, and did not exceed 25 passages.

Inhibitors:

Ibiglustat (MedChem Express) and 1-phenyl-2-palmitoylamino-3-morpholino-1-propanol (PPMP) (Millipore Sigma) were dissolved in DMSO. Fumonisin B_1 (FB_1) (Cayman Chemical Company) was dissolved in methanol.

Ceramide Nano Liposome (CNL) Formulation:

90nM-sized ceramide nanoliposomes were a generous gift from KeystoneNano (State College, PA) and were manufactured according to published methods (79) under GMP conditions. Control (ghost) formulations included all liposomal ingredients, at the same ratio as CNL, except for the omission of the bioactive C6-ceramide.

MTS Assay:

HNSCC cells were seeded on 96 well plates to achieve a similar confluency. After 24 hours, cells were pre-treated with drug (Ibiglustat, PPMP, or FB1) for one hour and subsequently treated with CNLs or ghost liposomes at concentrations indicated in the text. Assays utilizing [3-(4,5-dimethylthiazol-2-yl)-5-(3-carboxymethoxyphenyl)-2-(4-sulfophenyl)-2H-tetrazolium, inner salt (MTS) reagent (Promega, Madison/WI) and phenazine methosulfate (PMS) reagent (Millipore Sigma) were performed according to the manufacturer's instructions (Promega, Madison, WI). Absorbance at 490nm was determined with a Cytation 3 plate reader (Bio Tek, Winooski, VT). After subtracting the background absorbance (no cells), all values were normalized to their intra-plate controls.

Flow Cytometry Assays:

A total of 29,000 cells were plated in 24-well plates and allowed to adhere at 37 C overnight before being treated with Ibiglustat (5μM), CNL (10, 25μM) or the combination (Ibiglustat 5μM + CNL 10μM, Ibiglustat 5μM + CNL 25μM). For the combined treatment, Ibiglustat was treated 50-70 minutes before CNL. To be able to be compared with the combined conditions, treatments of Ibiglusat and CNL alone were used in combination with Ghost and DMSO in water, respectively. After 24 or 48 hours of incubation, media with floating cells were collected and adherent cells were lifted with TrypLE. This mixture was centrifuged and the supernatant aspirated. Fixable Viability

Dye 780 (Thermo Fisher Scientific) was used to assess cell viability and the appropriate controls were performed and used based on the manufacturers' instructions. The samples were measured by the Attune Nxt Flow Cytometer (Thermo Fisher Scientific). Forward and side scatter measurements were used to gate for singlets and exclude debris. Following this, single-stain compensation controls were collected and gates were drawn accordingly.

Sphingolipidomic Mass Spectrometry:

A total of 321,000 cells were plated on 60.8cm^2 dishes and allowed to adhere overnight. Cells were treated with GCS inhibitors and C6-ceramide as indicated in the text, briefly washed with 1X PBS, then frozen at -80°C. Cells were then lysed with 0.1X PBS, scraped, and protein content was determined using a BCA protein assay (Pierce, Appleton/WI). An equivalent amount of 150ug's of protein was used and lipids were extracted as previously described (237) before being analyzed via electrospray ionization tandem mass spectrometry.

Generation of Knockdown Cell Lines:

Four plasmids containing short hairpin RNA segments against GCS, an mCherry tag, and a puromycin resistance gene were obtained from Genecopia (Rockville, MD). HEK-293 cells were plated in 6 well plates at ~25% confluence, and 24 hours later, plasmids for VSV, a lentiviral backbone, and the shRNA against GCS were mixed with PEI and added to HEK cells. The following day the media was replaced, that new media containing virus was collected 24 hours later and frozen at -80°C to kill any lifted HEK cells. After plating 100,000 UNC-7 and SCC-9 cells in 6-well plates, cells were treated with polybrene for 6 hours before the virus was thawed and added to cells. Forty-eight hours later, puromycin was added and maintained until all cells with empty vector plasmids had died.

Western Blot:

A total of 321,000 cells were plated on 60.8cm^2 dishes and allowed to adhere overnight. Cells were treated with GCS inhibitors and C6-ceramide as indicated in the text. RIPA buffer (Alfa Aesar) with protease inhibitor (Thermo Fisher Scientific) and phosphatase inhibitor (Roche, Basel/Switzerland) was used to lyse the cells. Protein concentrations were determined with a BCA protein assay (Pierce, Appleton/WI) using BSA to construct a standard curve. 20-30µg of protein was added to a NuPAGE 4-12% Bis-Tris gel (Thermo Fisher Scientific) and ran at 120V for 2 hours and 15 minutes. Transfer to a nitrocellulose membrane (Bio-Rad Laboratories, Hercules, CA) was performed using the Bio-Rad Turbo-Transfer apparatus. Five percent BSA (Thermo Fisher Scientific) in TBST was used to block the membrane for one hour at room temperature before an overnight primary antibody incubation at 4°C. The following antibodies were used: LAMP1 [sc-20011], SQSTM1 (p62) [sc-28359] (Santa Cruz Biotechnologies, Dallas/TX) Beta Actin [A5441] (Millipore Sigma), LC3B [3868], Caspase 3 [9662] (Cell Signaling Technologies, Danvers/MA) and BNIP3 [ab10433], PINK1 [ab23707] (Abcam, Cambridge/United Kingdom, MDR-1 [Product #](Headquarters) and others were used. Blots were washed 3x5minutes with TBST. A secondary antibody against rabbit or mouse containing a horseradish peroxidase tag (Thermo Fisher Scientific) was then added to the membrane and allowed to shake for one hour at room temperature. Three additional five minute washes were performed prior to membrane chemiluminescence using peroxide and luminol solutions (Prometheus, San Diego, CA) at a 1:1 ratio and imaging with a G:Box Chemi XX6 (Syngene, Bangalore, India). Densitometry of each target was performed using ImageJ software and underwent two normalization steps. First, the density value of each protein target for each well was normalized to its respective density value of the loading control, β-actin. Those values were then normalized to the value of the vehicle treatment at the respective time-point control.

Quantitative Real-Time Polymerase Chain Reaction:

A total of 29,000 cells were plated in 24-well plates and allowed to adhere at 37°C overnight before

being treated with GCS inhibitors and C6-ceramide as indicated in the text. Cells were then washed and RNA was extracted using the RNeasy Mini Kit (Qiagen, Hilden, Germany). RNA content was quantified using a Cytation 3 (BioTek Winooski, Vermont), then 800-1000ng of RNA was used in the iScript cDNA Synthesis Kit (Bio-Rad Laboratories) to synthesize cDNA. FAM probes (BNIP3-[qHsaCIP0040441], MAP1LC3B-[qHsaCEP0041298], LAMP1-[qHsaCEP0055037], PSMB6-[qHsaCEP0052321], B2M-[qHsaCIP0029872]) and iTaq Universal Probes Supermix (Bio-Rad Laboratories) were used and CT values were measured using CFX Connect Real-Time PCR Connection System (Bio-Rad Laboratories). CT values were normalized first to the housekeeping gene control (PSMB6 and/or B2M), and then to their respective timepoint/vehicle control.

Results:

Inhibition of glucosylceramide, but not ceramide synthase, inhibits CNL-induced cell death

To determine which ceramide-metabolizing enzymes might mediate ceramide-induced cell death in HNSCC, pharmacological inhibition of GCS and the ceramide synthases was performed in the presence or absence of ceramide. As single agents, the CNL showed a time- and concentration-dependent decrease in cell viability while the GCS inhibitor, Ibiglustat, did not alter

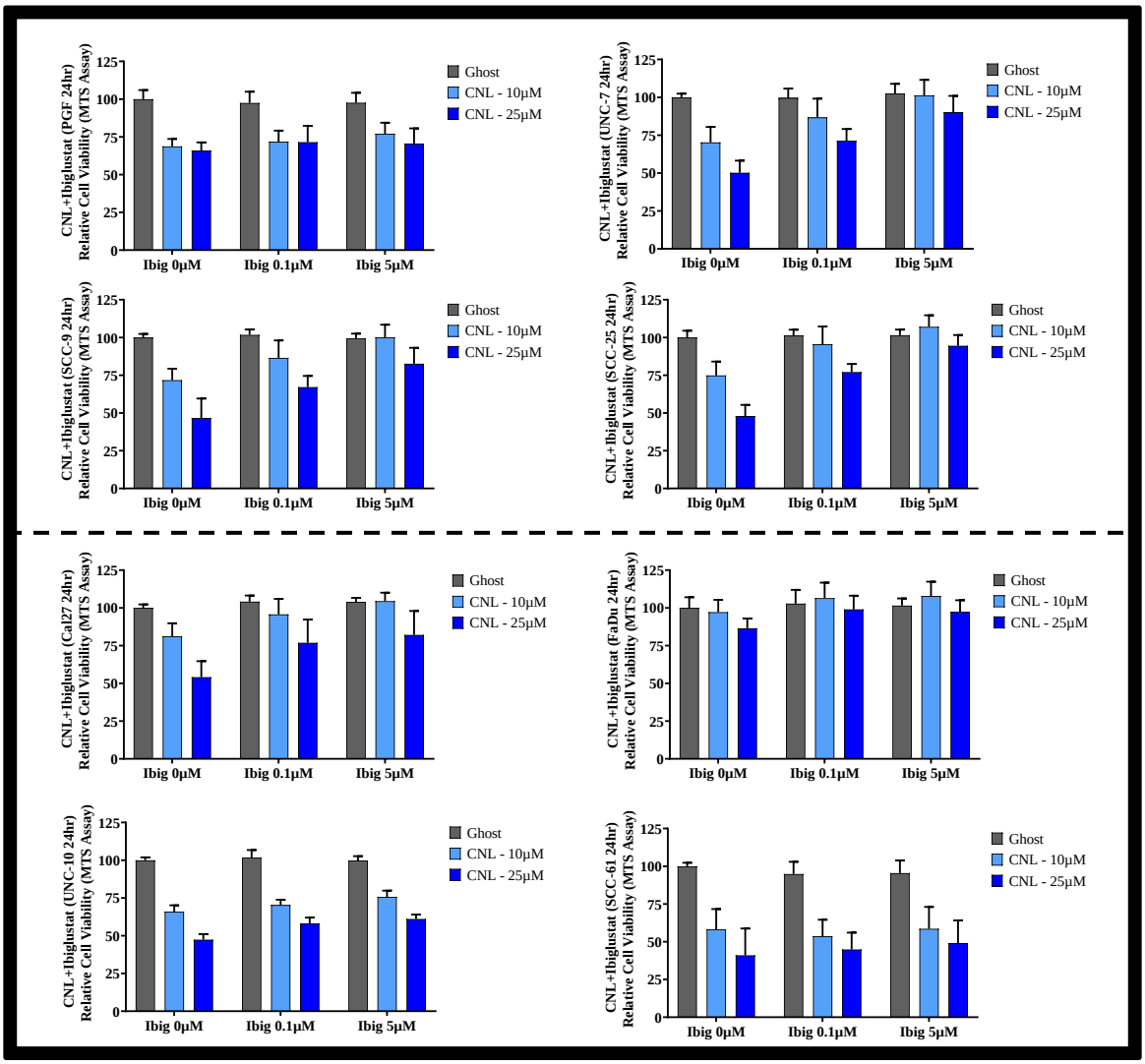

Figure 5-1: Pre-Treatment with Ibiglustat Prevents CNL-Induced Cell Death in Seven HNSCC Cell Lines (24hr)

One non-transformed cell line (PGF) and seven HNSCC cell lines were treated with Ibiglustat (DMSO, 0.1μM, 5μM) and one hour later with CNL (ghost liposomes, 10μM & 25μM). Cell viability was assessed using an MTS assay 24 hours later.

cell viability **(Fig. 5-1)**. Strikingly, however, Ibiglustat reduced CNL-induced cell death in a time- and concentration- dependent manner at both 24 and 48 hours in nearly every HNSCC cell line. In the UNC-7, SCC-9, and SCC-25 cell lines at 24 hours, 25µM CNL decreased cell viability by 50%, 53%, and 52% respectively; however, treatment with both 5µM Ibiglustat and 25µM CNL only reduced cell viability by 10%, 17%, and 6%, displaying a protection of 40, 36, and 46%. After 48 hours, this effect was exacerbated reducing 25µM CNL-induced cell death from 76% to 9%, 83% to 27%, and 85% to 11% in UNC-7, SCC-9, and SCC-25 cell lines, respectively **(Fig. 5-2)**. On the contrary, Ibiglustat did not prevent CNL-induced cell death in non-cancerous Primary Gingival Fibroblast cells at 24 **(Fig. 5-1)** or 48 hours after treatment **(Fig. 5-2).**

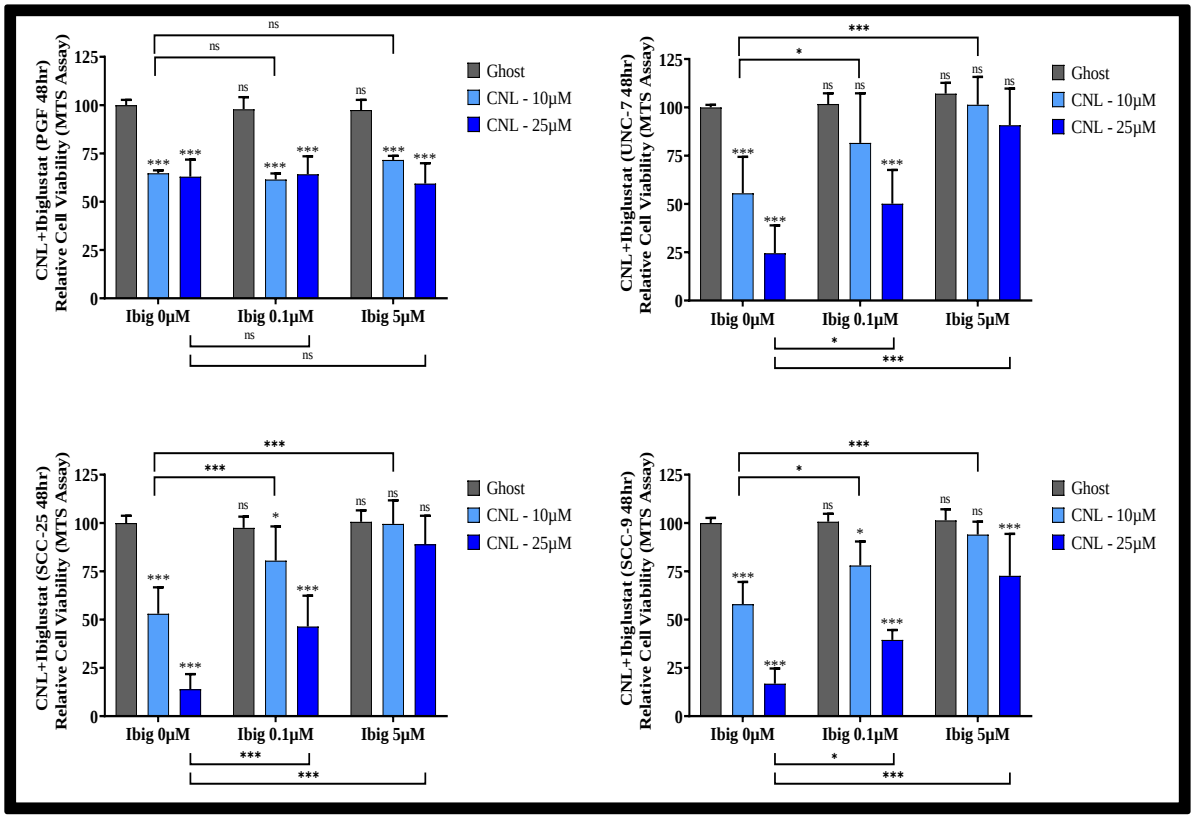

Figure 5-2:Pre-Treatment with Ibiglustat Reduces CNL-Induced Cell Death in Select Lines (48hr)

*Three HNSCC cell lines and one non-transformed cell line (PGF) were treated as described in Figure 5-1 with MTS viability assessed 48 hours later. The markers *, **, and *** indicate significance of $p < 0.05$, 0.01, and 0.001, respectively, displayed error bars represent standard deviation of the mean, and all experiments were performed with at least three biological replicates.*

To more directly assess the role of Ibiglustat to rescue from CNL-induced cell death, flow cytometry was performed. By 48 hours, 5µM Ibiglustat significantly rescued from 25µM CNL reducing cell death from 80% to 27%, 87% to 25%, and 93% to 40%, in UNC-7, SCC-9, SCC-25 cells, respectively. **(Fig. 5-3).** However, Ibiglustat did not rescue PGF cells from CNL-induced cell death **(Fig. 5-3).** Taken together, this data suggests that inhibition of GCS is able to protect HNSCC cell lines, but not non-transformed lines from CNL-induced cell death.

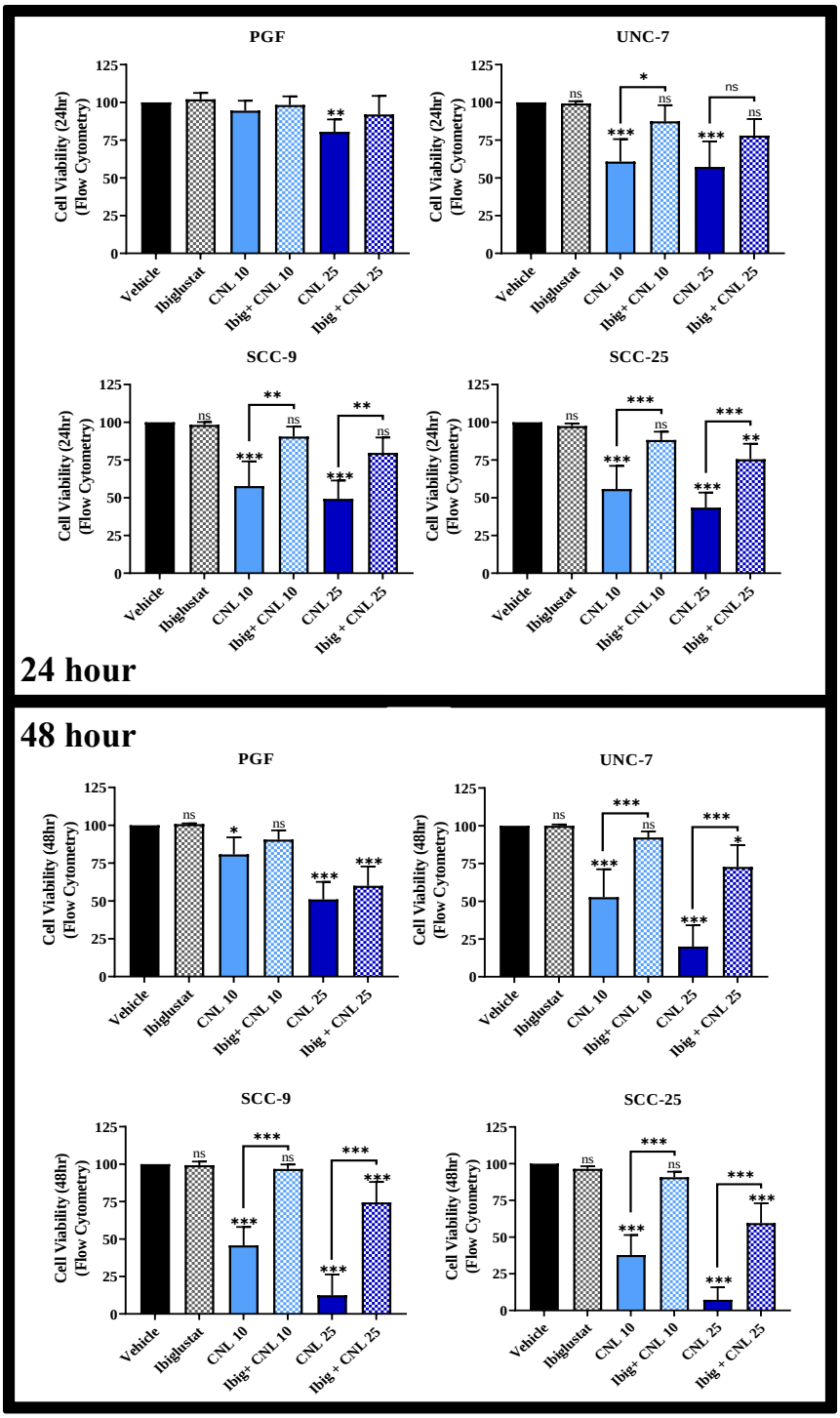

Figure 5-3: Ibiglustat Protects From CNL-Induced Cell Death via Flow Cytometry

Cell death was determined using flow cytometry (24 & 48hrs) with PGFs and three HNSCC cell lines with pretreatment (DMSO, Ibiglustat 5µM) and treatment of CNL (Ghost, 10µM, 20µM)

Further evaluation of the role of GCS on CNL-induced cell death was accomplished using the well-studied GCS inhibitor, 1-phenyl-2-palmitoylamino-3-morpholino-1-propanol (PPMP) Interestingly, PPMP's protectivity was strongly concentration-dependent. At a lower concentration which did not alter cell death in PGF cells, 5μM PPMP significantly mitigated CNL-induced cell death in UNC-7, SCC-9, and SCC-25 cells at 24 hours reducing cell death from 51% to 38%, 48% to 33%, and 49%, to 33% **(Fig. 5-4)** However, at a higher concentration, 20μM PPMP greatly

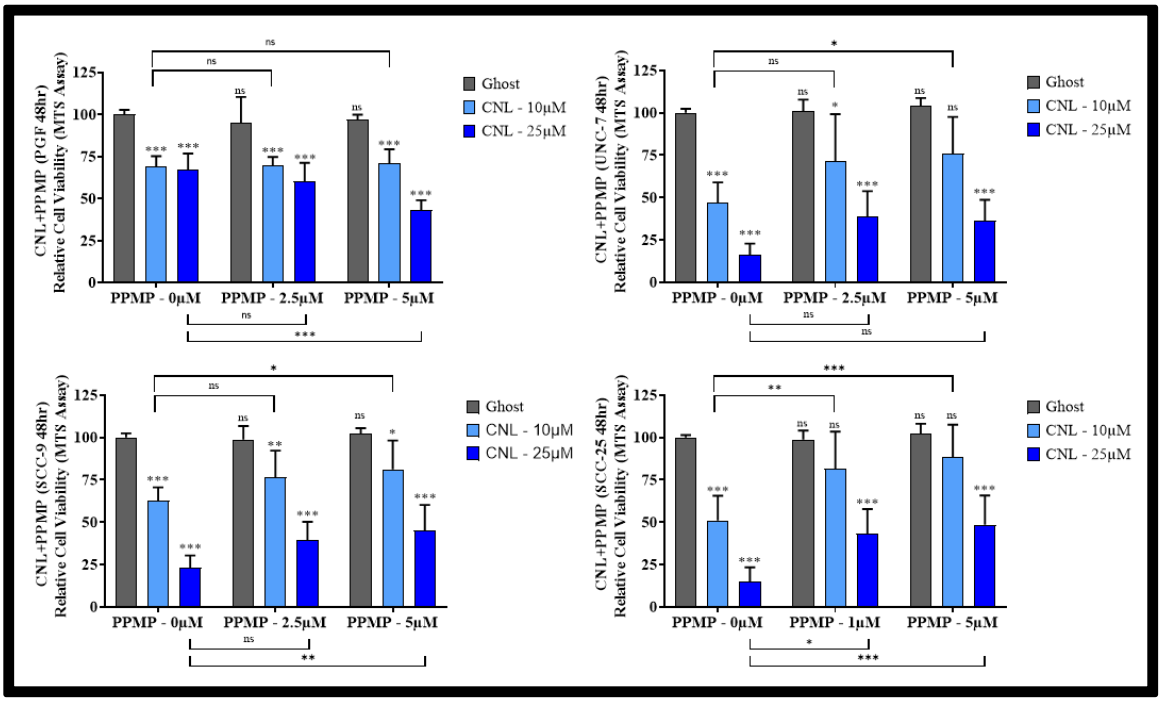

Figure 5-4: Pre-Treatment with Low Concentrations of PPMP Prevents CNL-Induced Cell Death in Select Lines (48hr)
MTS assay (24hrs) using one PGF cell line and three selected HNSCC cell lines, treated with CNL (ghost liposomes, 10μM & 25μM) following pretreatment of PPMP at low concentrations (H20, 2.5μM, 5uM)

augmented CNL-induced cell death, increasing cell death from 51% to 84% in UNC-7, 48% to 81% in SCC-9, and 49% to 88% in SCC-25 **(Fig. 5-5).** This high concentration was cytotoxic to non-transformed cells, though, inducing 80% death in PGFs at 24 hours. Unlike both inhibitors of GCS, Fumonisin B1 (FB1), an inhibitor of Ceramide Synthases (CerS) did not reduce cell viability alone or in the presences of CNL in UNC-7, SCC-9, SCC-25 or PGF cells. (Data not Shown).

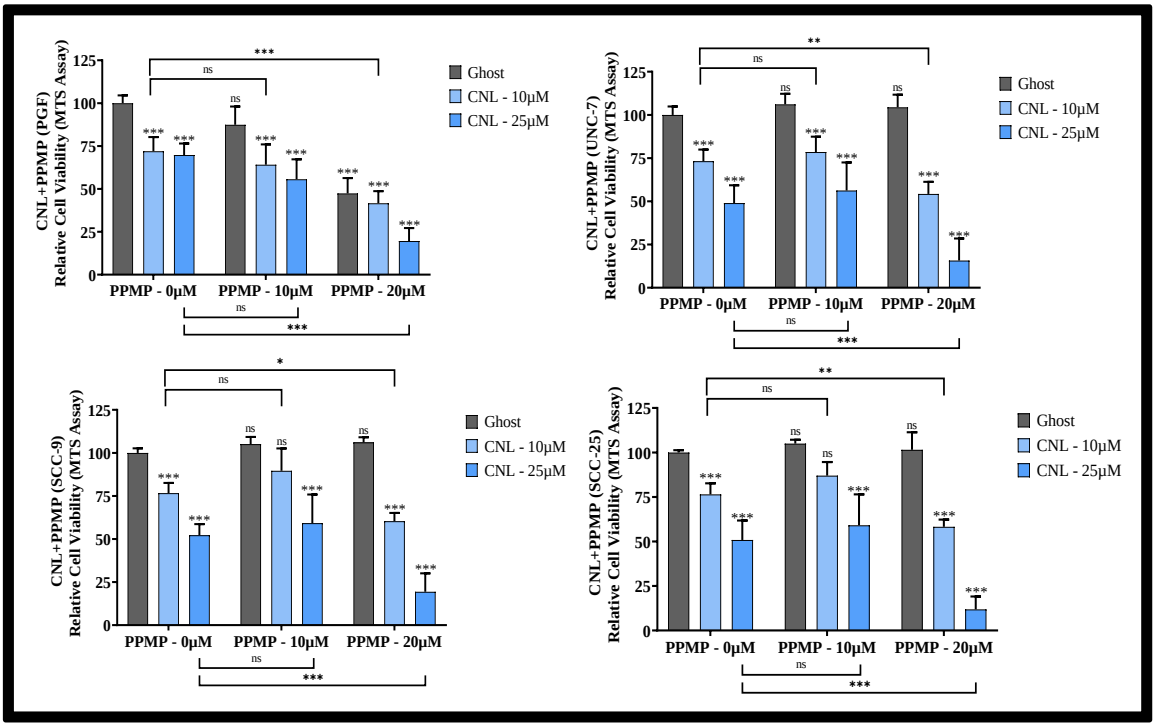

Figure 5-5: Pre-Treatment with High Concentrations of PPMP Synergizes with CNL-Induced Cell Death in Select Lines (48hr)

MTS assay (24hrs) using one PGF cell line and three selected HNSCC cell lines, treated with CNL (ghost liposomes, 10μM & 25μM) following pretreatment of PPMP at low concentrations (H20, 2.5μM, 5μM)

Discussion:

The above data highlights an entirely novel observation that Ibiglustat elicits a strong, concentration- and time-dependent protection from CNL induced cell death. Though Ibiglustat is not very well explored, experiments run by a colleague in the lab (Logan Patterson) have confirmed the specificity of this drug *in vitro*. Furthermore, we believe the drug is, in fact, targeting GCS due to a similar rescue seen at lower concentrations with the widely-published GCS inhibitor, PPMP in Figure 5-4. Of the 45+ drugs tested in lab over the past six years, Ibiglustat been the most potent drug to rescue from CNL. Thus, even with the low likelihood this drug is eliciting a non-specific protection, the mechanism by which Ibiglustat is working warrants further study.

At first glance, our data appears to be in stark contrast to the dogmatic role of GCS as pro-survival. However, we do not make the claim that GCS is pro-death. If the enzyme has a pro-death effect, inhibition of it with Ibiglustat would lead to less death than the no-treatment control, an effect we do not observe (Figure 5-1). Rather, our data suggest that GCS has a role in enhancing ceramide-induced cell death, but not basal cell death.

Additionally, it is important to consider GCS is not only a protein with its own functions, but also a bottleneck of the sphingolipid metabolic pathway, leading to the generation of higher-order sphingolipids with many discrete functions. It is possible that GCS is simply the gatekeeper from which pro-survival and pro-death glycolipids can be synthesized. Thus, more GCS activity may not inherently be pro-cancer. When paired with increased activity of other sphingolipid enzymes which lead to survival, or decreased activity of sphingolipid enzymes which lead to death, GCS may consequently play a larger role towards sphingolipid metabolism.

Considering the above, it is likely Ibiglustat is either preventing ceramide metabolism into a pro-death higher-order glycosphingolipid, increasing ceramide metabolism into a more pro-survival, non-glycosylated lipid, or inhibiting a downstream pro-death signaling event from ceramide. While an argument could be made for pro-survival roles of certain lipid metabolites (46), there is ample evidence linking higher-order glycosphingolipid gangliosides to cell death. For

example, GD3, a ganglioside derivative downstream of GCS, has been shown to induce mitochondrial permeability (235), a result seen with ceramide treatment alone. While there are many higher-order sphingolipids synthesized by the product of GCS, we hypothesize Ibiglustat pre-treatment protects from CNL-driven build up of a specific glycosphingolipid species which induces cell death.

Anecdotally, while a wealth of literature exists regarding GCS in promoting negative outcomes in patients (51, 98), very little information in the cancer field exists about Glucocerebrosidase, the enzyme which removes the glucose group from glucosylceramide, thus generating ceramide. If this glycosylation was indeed the key step in the reaction, one would expect that Glucocerebrosidase would have been identified as a prognostic indicator for better response in patients, but this is not the case.

Perhaps the most interesting observation from this study is that Ibiglustat's rescue from CNL is cancer-specific. Although we have previously reported that PGF cells were more resistant than HNSCC cells to CNL-induced cell death (Chapter 2), the observation that GCS inhibition only rescues HNSCC cells and not normal cells is striking. This observation is made all the more strange considering transformed-cell viabilities become greater than those of non-transformed cells after both cell lines are pre-treated with Ibiglustat before CNL. We hypothesize that since transformed cells have upregulated metabolism in order drive increased proliferation, migration, and growth (238), they may be more sensitive to changes in sphingolipid-related enzymes than non-transformed cells.

Taken together, these data highlight a strong, novel, and counter-intuitive role for GCS in inducing cell death in a cancer-specific context. We highlight important considerations for these studies and outline the key experiments to continue this work.

Future Directions:

1. Use mass spectrometry to measure differences in sphingolipid metabolism after CNL with or without Ibiglustat.

This experiment would allow us to determine not only how the CNL is metabolized in different HNSCC cell lines, but also how Ibiglustat is able to mediate this metabolism. The differences between these two groups as well as a no treatment group would allow us to view which sphingolipid species correlate with basal sphingolipid levels vs. sphingolipid profile which leads to death vs. a sphingolipid profile which rescues from the aforementioned death. Specific lipids which correlate with either survival or death could then be directly added to confirm their effects in the absence of C6 ceramide.

2. Confirm Ibiglustat specificity with a molecular knockdown of GCS.

Utilizing stable knockdown cell lines, we could confirm the effects of Ibiglustat's rescue are specific to the inhibition of GCS. Knockdown validation would be accomplished via measuring RNA levels, protein levels, and activity of the assay (as determined via mass spec measuring reactants and products). Following validation, cell viability assays (MTS and flow cytometry) as well as mass spectrometry (as mentioned in #1) could be performed to confirm all results from Ibiglustat.

3. Determine the role of delivery and chain length of ceramide on Ibiglustat-mediated protection

In order to understand if this finding has relevance to therapeutics which induce endogenous ceramide levels (as opposed to just exogenous ceramide addition), we could determine if the Ibiglustat-mediated protection is applicable to all ceramide species, or only C6 ceramide. Thus, different chain lengths of ceramide, both synthetic (C2 and C6) as well as endogenous (C14, C16, C18, C24, C24:1), would be delivered to cells in a non-liposomal formulation and cell death will be measured in the presence or absence of Ibiglustat.

4. Confirm the specificity of the inhibitors

It is necessary to establish the efficacy and concentration-dependence of PPMP, FB1, and Ibiglustat

at the level of lipid metabolism as well as the off-target effects of PPMP that alter its impact from protective at low concentrations to synergistically cell death-promoting at high concentrations.

Additional, Lower Priority Experimental Ideas.

Though it becomes difficult to plan too much further in the absence of these results, protein and mRNA analysis after CNL + Ibiglustat should evaluate changes in mitophagy proteins identified in Chapter 2 (LC3B-II, BNIP3, LAMP1/2) as well as some specific targets of higher order glycosphingolipids (MDR1, VEGF-2, etc.) (234). Utilizing a isotopically labeled C6 ceramide would also allow for additional specificity identifying the individual lipid species generated from the metabolism of C6 ceramide.

CHAPTER 6: MAJOR CONCLUSIONS, DISCUSSIONS, AND TAKE HOME MESSAGES

CHAPTER 6: MAJOR CONCLUSIONS, DISCUSSIONS, AND TAKE HOME MESSAGES

Although most of the individual projects have been discussed at length in their representative sections, here I detail a brief summary of the most noteworthy findings, therapeutic relevance, and an overarching summary of themes detailed in this thesis.

Overall Novel Findings:

In Chapter 2, ceramide-induced LAMP1 and LAMP2 protein decreases were observed for the first time. Although enhancement of ceramide's effect with autophagic inhibition has been shown before, we not only demonstrate that this occurs primarily in more resistant cells, but also identify that inhibition of the PIKfyve enzyme (using the drug Apilimod mesylate) is also capable of synergizing. We further identify that in the context of HNSCC, that ceramide-induced mitophagy is protective, a statement controversial in the ceramide field. Finally, we identify that Methylpyruvate is able to rescue from CNL- and CQ+CNL-stimulated increases in ROS and decreases in cell viability.

In Chapter 3, after exhaustingly ruling out caspase-dependent apoptosis, we report the first known evidence against a ferroptotic mechanism for cell death mediated by CNL. Furthermore, despite previous reports suggesting ceramide causes oligomerization of necroptotic protein MLKL, we demonstrate that ceramide counter-intuitively decreases total and phosphorylated levels of the necroptosis protein MLKL. Furthermore, although a universal rescue across all HNSCC cell lines via Nec-1 or NSA was not identified, Nec-1 and NSA were able to rescue from CNL-induced cell death in SCC-61 and FaDu cells, respectively. Most interestingly was the identification of a robust increase in Gasdermin E cleavage, a pyroptotic effector protein, mediated by CNL. This cleavage could be enhanced by pre-treatment with CQ and inhibited by Z-VAD-FMK.

In Chapter 4, we identify for the first time a novel synergy between ceramide combined with two different EGFR inhibitors (Gefitinib and Erlotinib). Though the extent of synergy varies, a greater-than-additive effect was observed across all of the HNSCC cell lines tested and decreased synergy was observed in primary gingival fibroblasts, suggesting a potential cancer-specific effect.

Furthermore, for the first time we identify Early Growth Response 1 (EGR-1) as greatly increased transcriptionally and translationally after CNL and Gefitinib+CNL-induced cell death. Furthermore, EGR-1 knockdown is sufficient to enhance CNL- and Gefitinib+CNL-induced cell death highlighting the importance of this novel ceramide-induced compensatory mechanism.

Finally, in Chapter 5, we discover a novel and entirely counter-intuitive rescue from CNL-induced cell death via treatment with a Glucosylceramide Synthase (GCS) inhibitor named Ibiglustat. This rescue, though varying in magnitude, occurs in all of the HNSCC cell lines tested, but not in the non-transformed PGF cells. Furthermore, we identify this effect occurs using a commonplace inhibitor of GCS (PPMP) but only at the lower concentrations, suggesting an off-target effect when used in excess.

Therapeutic Relevance:

My main goal for my graduate work was to identify and drive findings which could lead to therapies that could reduce patient suffering from HNSCC, a task I approached at least tangentially in all of my projects. Although use of the CNL, the most clinically relevant ceramide delivery vehicle, inherently gives all of the work more translational relevance, I detail below the major findings which I believe may contribute to future therapies.

In Chapter 2, I addressed the therapeutic potential of using CNL plus Chloroquine (CQ) as a potential treatment for HNSCC. Although inhibition of autophagy using CQ to amplify the effects of ceramide has been addressed previously (112), some recent publications suggest that autophagy/mitophagy is actually the mechanism by which ceramide kills as opposed to a protective mechanism (126). Considering this, my work more specifically identifies the mechanism by which ceramide and autophagic inhibition synergize, at least in HNSCC, highlighting other opportunities for drug intervention. Specifically, I believe ceramide's therapeutic effect can be augmented by inhibiting lysosome function, (Lys05, pepstatin A, E64d, leupeptin) (239) mitophagy (mdivi-1) (240), or even ROS antioxidant pathways including inhibitors of superoxide dismutase, catalase, and glutathione peroxidase (241).

Additionally, I also show for the first time that using Apilimod Mesylate, a PIKfyve inhibitor which has passed phase I and II clinical trials, induces even less death as a single agent and synergizes with ceramide potentially even more effectively than CQ. An incredibly broad PubMed search of "Apilimod cancer" yields only seven results, 6 of which are from 2017 or later, highlighting the novelty of this finding. Although not mentioned in the text of Chapter 2, this synergy may occur due to ceramide's inhibition of AKT, a suggested requirement for Apilimod mesylate's toxicity (242).

In Chapter 3, I identify novel hallmarks of ceramide-induced cell death including cleavage of Gasdermin D and Gasdermin E as well as alterations in MLKL protein levels. Although these findings do not immediately lend themselves to therapeutic development, they have the potential to increase ceramide's death-inducing effects. In short, if ceramide is capable of inducing death via a cancer-specific pyroptotic signaling cascade resulting in Gasdermin E cleavage, a drug which targets a protein capable of inhibiting Gasdermin E may specifically enhance ceramide-induced cell death. Thus, as the cell death field progresses, these findings may identify non-apoptotic opportunities for synergistic induction of cell death.

Chapter 4 likely has the findings of greatest clinical significance. Not only are Gefitinib and Erlotinib both drugs which are FDA-approved for other cancers, but they appear to have widespread efficacy and synergy in multiple cell lines. Although the very minimal work done using the other EGFR inhibitor, the monoclonal antibody Cetuximab, failed to show meaningful effect *in vitro*, this does not mean it lacks clinical relevance. In fact, it is well documented that Cetuximab's *in vitro* effects are far less efficacious than Gefitinib and Erlotinib, but displays far more success *in vivo*. Thus, I believe all three of the aforementioned EGFR inhibitors should be tested with CNL *in vivo*.

Also in Chapter 4, it was established that Early Growth Response 1 (EGR-1) could mitigate CNL-induced cell death. Though no inhibitors of EGR-1 are currently available, one publication shows that treatment with an adenylate-cyclase activator (Forskolin) or the combination of an

agonist of PKA (cAMP analogues 8-CPT-2'-O-Me-cAMP ([CPT]) and an agonist of EPAC (N^6-Benzoyl-cAMP (BNZ) can inhibit EGR-1 in vascular smooth muscle cells (243). Since the mechanism of the aforementioned inhibitors is partially mediated through inhibition of Rac-1, the Rac-1 inhibitor CAS 1177865-17-6 may also be of therapeutic relevance to CNL-based treatments.

Similar to Chapter 3, Chapter 5's therapeutic relevance may also accrue with time. As more specific inhibitors of ceramide metabolism are generated, the breakdown of ceramide can be better directed to increase its therapeutic effect. Most importantly, however, is that directly contrary to the widespread belief in the field, our findings suggest inhibition of Glucosylceramide Synthase (GCS) actually prevents ceramide from being as effective of a therapy in HNSCC. Although due to time limitations we were unable to determine which specific higher-order sphingolipid species were responsible for the GCS-driven cell death, I believe this lipid or these lipids will be paramount to fully understanding and enhancing ceramide's full signaling effects.

Overarching Summary – Lysosome, Sweet Home

Outside of the generalization of "trying to increase the efficacy of CNL in HNSCC" it is difficult to connect all of these different projects in a single summary. However, if there is indeed an underlying message in all of these projects, I believe it points to one specific organelle which is greatly underappreciated in the ceramide field, the lysosome.

Before considering our results, if one contextualizes the implications of mutated sphingolipid genes, the connection to the lysosome becomes increasingly evident. The term "sphingolipidoses" refers to a series of lipid storage disorders caused by mutations in particular sphingolipid genes: Gaucher's Disease, Farber's Disease, Fabry's Disease, Krabbe's Disease, Neimann-Pick Disease, Sandhoff-Jatzkewitz's Disease, GM1 gangliosidosis, and metachromatic leukodystrophy (244). However, despite the fact that these different diseases occur from mutations in many different sphingolipid genes, every single one of the sphingolipidoses are classified as "lysosomal storage disease" (LSD). LSDs were aptly named because mutations in the genes which

cause them cause an increase in the size and or number of lysosomes (245). Thus, considering the number of different mutations in sphingolipid enzymes which can causes LSDs, specifically sphingolipidoses, it strongly suggests that the relationship with overall sphingolipid metabolism and the acidic organelle is vital.

In Chapter 2, the decrease in both LAMP1 and LAMP2 proteins, an effect which has remarkably never been reported previously, implicates a ceramide-driven signaling decrease in some of the most abundant and integral lysosomal proteins. This strongly suggests that ceramide alone is able to disrupt lysosomal function, perhaps via inducing lysosomal permeabilization directly (246) or conversion into sphingosine which can act as a Lysosometrophic agent (121). Even if ceramide does not directly cause lysosome degradation, however, decreased levels of LAMP2 can strongly downregulate chaperone mediated autophagy which relies on lysosome function (247). Also in Chapter 2, the lysosome represents the primary switch point in the autophagic pathway between "autophagy inhibitors" which do not synergize (Rapamycin and Torin1) and the ones that do (Bafilomycin, CQ, and AMS). These data suggest that a double hit on the lysosome (ceramide decreasing lysosomal proteins and CQ decreasing lysosomal acidification of the remaining intact lysosomes) may be a primary method of synergistically inducing cell death in HNSCC cells.

In Chapter 3, we identify that there are multiple mechanisms of cell death which center around the lysosome. Specifically, breakdown of the lysosome leads to release of the cathepsin proteins which can induce cell death. Although these cathepsins can induce apoptosis, this is not the only mechanism by which they can elicit their effect and may lead to caspase-independent cell death (248). The EGFR inhibitor which synergizes with CNL, Gefitinib, actually inhibits lysosome acidification which can manifest in impaired degradation of proteins (249). Thus, the synergy between these two drugs may also involve lysosomal inhibition in addition to the signaling pathways identified in the chapter.

Finally, the subcellular localization of some ceramide metabolizing enzymes is so vital, it

is in their nomenclature – Acid Ceramidase and Acid Sphingomyelinase. Thus, degradation of the lysosome would manifest in not just a decrease in efficacy of certain sphingolipid metabolizing enzymes, due to removing them from their ideal enzymatic conditions, but would also change the metabolism of the ceramide species and the subcellular localization of the species themselves. To elaborate, if the ceramide species is not broken down into sphingosine via acid ceramidase in the lysosome, it could instead be converted into glucosyleramide in the golgi or sphingomyelin at the plasma membrane. Considering ceramide can directly lead to cell death when in the mitochondria, but sphingomyelin on the plasma membrane is considered highly non-toxic, both the species and subcellular localization of ceramide are can have a major impact on sphingolipid signaling.

Final Take Home Message

Although all of my work in this thesis was performed in HNSCC, I do not believe these findings to be limited to this cancer type. It is true cancer types across different tissues can vary wildly in both genotypic and phenotypic characteristics, but a benefit of doing this work in so many different cell lines in such a heterogenous cancer is that I believe them to be widely applicable to other fields. Furthermore, if ceramide and the CNL are unsuccessful in clinical trials, it is important to realize this work still has merit- I believe a lot of these findings can be easily translatable for any of the drugs or chemotherapeutics which are capable on inducing endogenous ceramide generation.

While this body of work fails to solidify ceramide as the panacea for HNSCC, I believe it can be a very successful springboard for others who wish to continue this work into the fields of ceramide in autophagy/mitophagy, cell death, EGFR inhibition, or ceramide metabolism in HNSCC… and I wish them the best of luck! -J$

APPENDIX

APPENDIX

APPENDIX A1: HYPOXIA – THE RED HERRING

During the course of the project covered in Chapter 1 involving ceramide's effect on autophagy and mitophagy as well as the CNL's synergy with Chloroquine, a series of experiments were conducted interrogating a possible involvement of hypoxia in ceramide signaling. Below is the rationale for this study, a brief background of hypoxia, results, and conclusions.

Hypoxia background:

Oxygen molecules are essential for the completion of mitochondrial respiration and consequently affect energy-driven cellular activity, permitting functioning on multiple structural levels (250). In fact, lack of oxygen on a cellular level often leads to "necrotic" cell death as mentioned in Chapter 2 (251). On a tissue level, lack of oxygen getting to the heart results in a myocardial infarct, or "heart attack" (252), while lack of oxygen getting to the brain results in a stroke (253). Considering the detrimental effects which result from lack of oxygen, it is unsurprising that a cellular mechanism which allows a rapid, widespread response exists.

In response to a low-oxygen, or hypoxic, environment, cells activate mechanisms which either lead to cell death or promote cellular survival as well as the generation of new blood vessels which can increase oxygen delivery (254, 255). Although these responses are numerous and involve many different pathways, they are primarily controlled by the hypoxia induced factor (HIF) family of proteins: Hif1a, Hif2a, Hif3a, and Hif1b. Canonical regulation of HIF family signaling pathways and the cellular hypoxic response has been well characterized (256). Briefly, under normoxic conditions, Hif-1a & Hif-2a are actively degraded via von Hippel-Lindeau (VHL)-driven ubiquitination. However, under hypoxic conditions, a conformational change in VHL prevents the degradation of Hif-1a or Hif-2a allowing these proteins to dimerize with Hif-1b, translocate to the nucleus, potentially bind activating or inhibitory co-factors, bind to HIF-responsive elements, and activate over 100 downstream targets which serve to respond to hypoxic conditions (257, 258).

These transcribed genes can regulate angiogenesis, the process of growing new blood vessels, cellular metabolism, cell death, cell survival, and many other processes.

However, complexities and alternatives in dogmatic HIF-driven hypoxia signaling have recently begun to be appreciated. At a cellular level, multiple studies have shown that hypoxic responses can vary between cell types (259, 260). Furthermore, molecular differences in hypoxic signaling deviate from canonical HIF-signaling as well branching off of findings of hypoxia signaling in the absence of active HIF-1A and/or HIF-1B signaling (261, 262). These differences include alternative activation of hypoxia signaling driven by growth factors such as PI3k (263, 264), cell cycle genes CDK1 & CDK2 (265, 266), MDM-2 (267), and HSP-90 (268), as well as differential translation mechanisms utilized in hypoxic conditions (269, 270).

Thus, although HIF family/hypoxia signaling cascades are intricate and highly regulated, a final step in this process is the transcription of genes which mediate a cellular hypoxic response. A review by Benita *et. al* describes genes regulated by HIF family/hypoxia signaling which include VEGF-A, an angiogenic gene, BNIP3 & BNIP3L, cell death genes, and ANKRD37, a novel hypoxic gene with unknown function (255).

Rationale:

After measuring ceramide-driven increases in BNIP3 at both the RNA and protein level, an effect greatly enhanced with CQ treatment in FaDu cells, (Chapter 1 – Figure 4), I sought to explore how ceramide was leading to these increases. Some previous work surmises that ceramide-driven BNIP3 increases are directly mediated by FOXO3 (271). However, after tracing back the source mentioned, I discovered this stated causation was misattributed correlation. While FOXO3A could indeed increase levels of BNIP3 in skeletal muscle *in vivo*, there was no mention of ceramide in the cited material (272). Upon additional searching, it is true that ceramide addition did, weakly and unconvincingly, decrease phosphorylation of FOXO3A and increase activation of "FOXO3A target genes" (GABARAP, GABARAPL1, BNIP3, BNIP3L, BIM, & PUMA). However, this study

never performs a rescue of this effect (273). Thus, these genes could have been activated via a myriad of mechanisms and not necessarily due to FOXO3A activation. Considering the above, we agree with a recent review claiming that ceramide does indeed cause transcription of BNIP3, however, this effect may be due to FOXO3A activation or other mechanisms (117).

Outside the realm of ceramide literature, while BNIP3 can be regulated by FOXO3A, Retinoblastoma (274), NFkB (275), Thymidine Phosphorylase (276), or even S100A4 (277) most articles attribute BNIP3 increases in response to hypoxia signaling (152). Not only are there multiple potential hypoxia response elements (HREs) in the BNIP3 promoter (278), but there are also many studies and reviews directly showing hypoxia-induced activation of BNIP3 (130, 279-281) with one publication even showing it to be the most transcriptionally increased gene product under hypoxic conditions (262).

Upon further investigation, I discovered many other connections between hypoxia and the signaling process I was describing with ceramide and CQ signaling. Specifically, hypoxia can stress cells and cause mitochondrial depolarization, ROS accumulation (282), and induction of autophagy and mitophagy (152, 283). Meanwhile, ceramide has been shown to "stress" cells and can even "starve" cells despite ample available nutrients (284). Considering the above, I hypothesized that if ceramide was able to activate a hypoxic stress phenotype, this would explain nearly all of the subsequent phenotypes: expression increases of BNIP3 and NIX, aka BNIP3L, mitochondrial depolarization, ROS generation, and autophagic/mitophagic repair. Additionally, discovering a ceramide-driven hypoxia signaling cascade (which could potentially be enhanced by CQ treatment) would be a massive, novel discovery to the ceramide field.

Results and Conclusions:

Correlating Hypoxia Signaling in CNL-Induced Cell Death

To explore the lowest-hanging fruit of hypoxia signaling and draw a correlation to transcription factors which may be driving BNIP3, I performed RT-qPCR on a small number of genes which were downstream of FOXO3A, NFkB, or hypoxia signaling, including BCL-2 as a "BCL-2 family member" control. To get a binary "Yes or No" result, I treated cells with either CQ + CNL (Treated) or neither drug (Mock) for 24 hours (**Figure H1**).

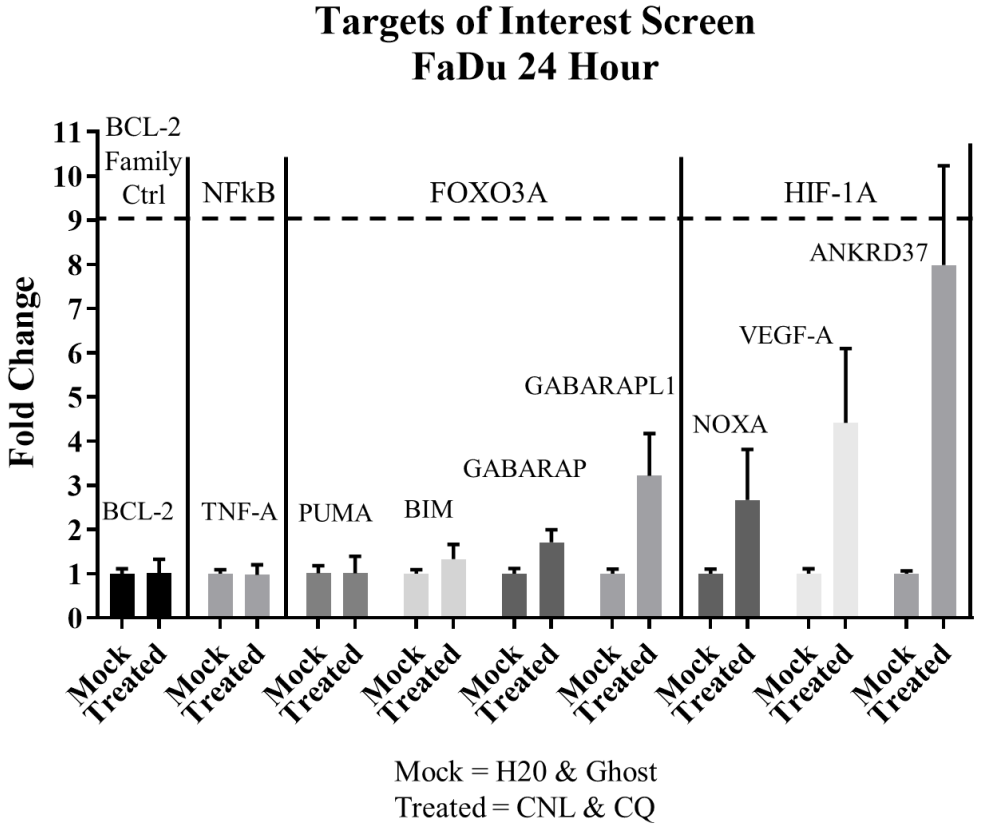

Figure H-1: CQ+CNL – BNIP3-Related Transcript Screen

Strikingly, while BCL-2 and the NFKb transcription factor (TNF-A) both showed no change, there were increases in some (GABARAP and GABARAPL1) but not other (PUMA and BIM) FOXO3A target genes. However, all three hypoxia-induced genes (PMAIP1, VEGF-A, ANKRD37) showed drastic increases in response to CQ+CNL treatment. These data suggest a

correlation between CQ+CNL signaling and a hypoxia gene expression response.

A follow up experiment measuring the hypoxia genes (BNIP3L, ANKRD37, and VEGF-A) transcription in FaDu cells followed a nearly identical pattern to BNIP3 mRNA increases after CQ, CNL, and their greater-than-additive combination published in Chapter 1 (**Figure H2-A**). However, the SCC-61 cells (cells more sensitive to CNL in which CQ does not greatly enhance death), appear to show a greater increase in hypoxia gene transcription after CNL alone; an effect which is not exacerbated to the same extent by CQ pre-treatment (**Figure H2-B**). Thus, in both resistant (FaDu) and sensitive (SCC-61) cell lines expression of these hypoxic signaling genes correlate with cell death (or lack thereof) after

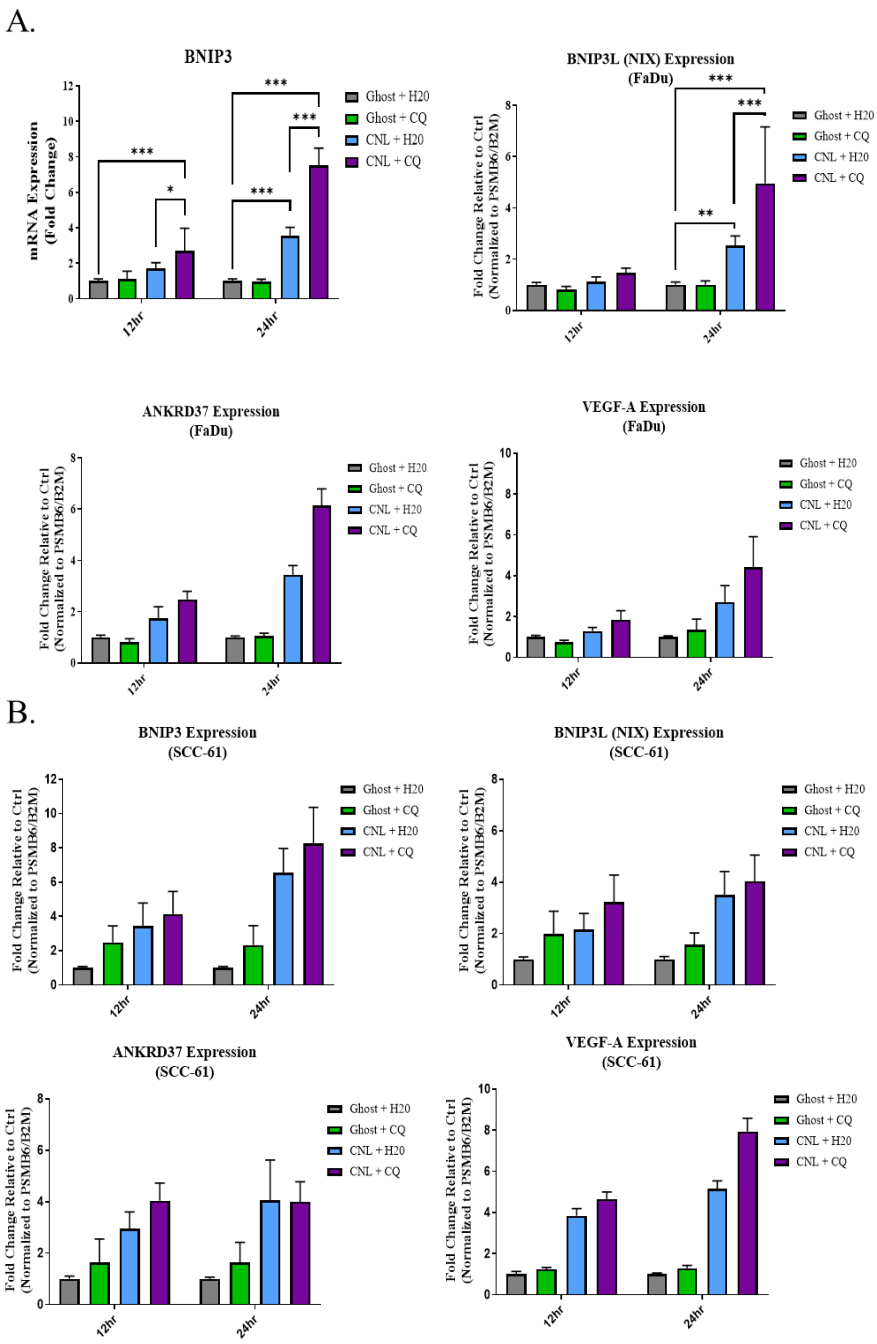

Figure H-2: CQ+CNL Expression of Hypoxia Genes – FaDu and SCC-61 Cells

treatment with CQ, CNL, and their combination. Of note, the FOXO3A target gene (GABARAPL1) did also increase in both cell lines, suggesting FOXO3A signaling may be playing a role (**Figure H3**). However, since GABARAPL1 is associated with an autophagic response (285), and autophagy is induced by ceramide treatment, this could simply be an expression increase independent of FOXO3A signaling.

Additionally, HIF-1A expression did not increase after these treatments, suggesting a non-

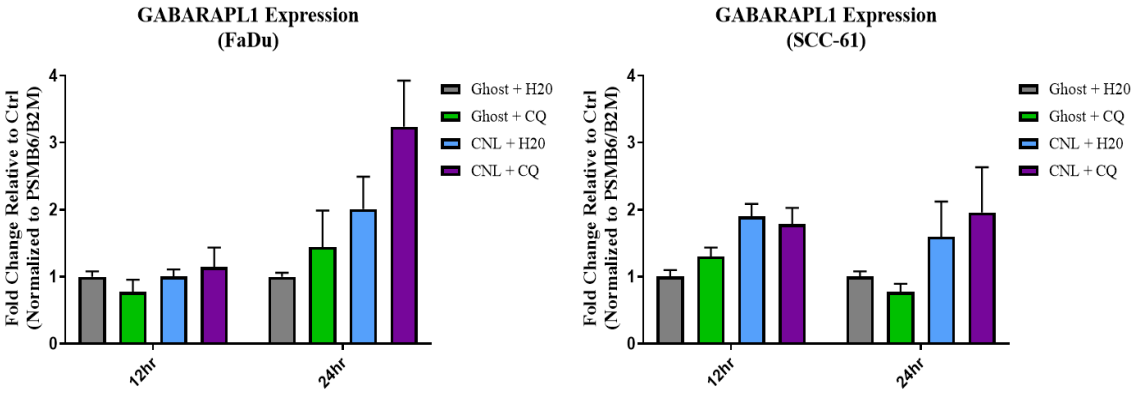

Figure H-3: CQ+CNL Expression of GABARAPL1 (a FOXO3A Target Gene)

expression-level change in hypoxia signaling, as expected (**Figure H4**).

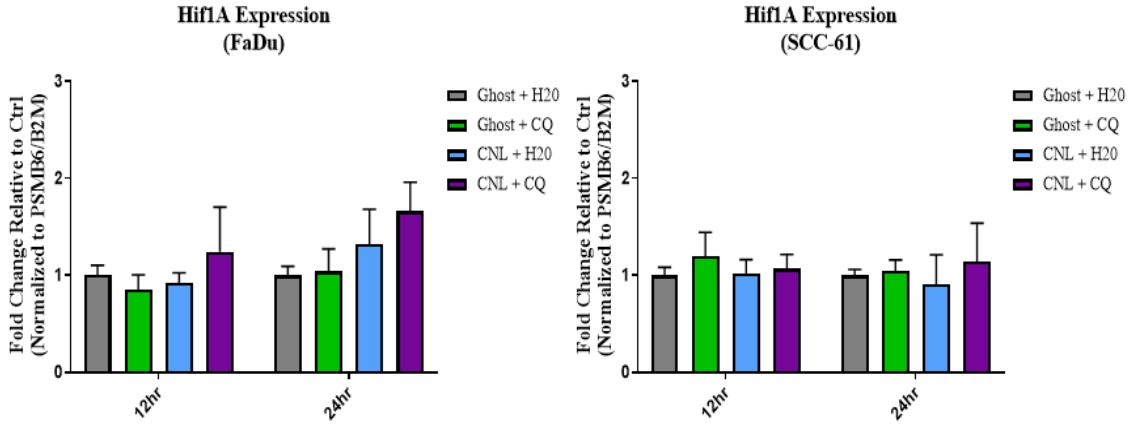

Figure H-4: CQ+CNL Expression of Hif1A

Perhaps the most striking, however, is that pre-treatment with MP (which partially protects FaDu cells from CQ+CNL-induced cell death) reduced the expression of multiple CQ+CNL-driven hypoxia genes (BNIP3L, ANKRD37, and perhaps NOXA) in FaDu cells to nearly the same extent

as it did BNIP3 in Chapter 2 (**Figure H5**).

Though the RNA data was striking, attempts to measure protein-level changes in Hif1A,

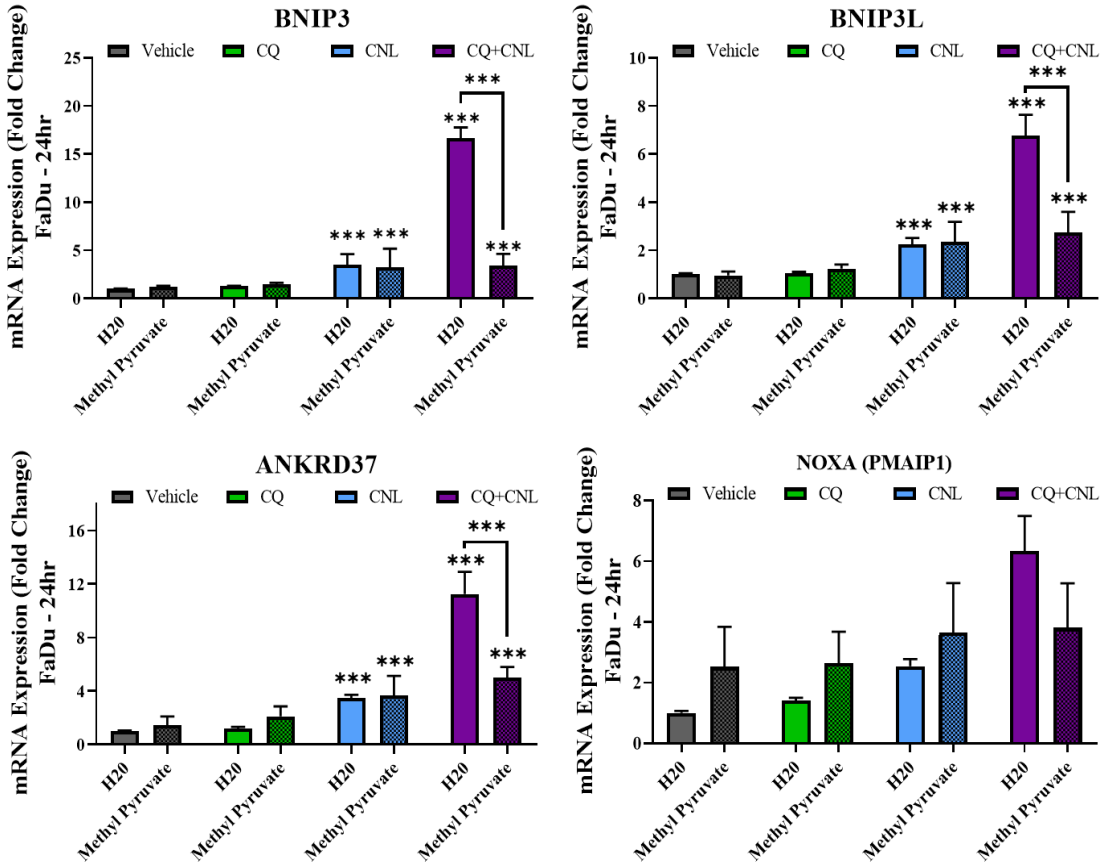

Figure H-5: MP+CQ+CNL Expression of Hypoxia Genes

Hif1B, or Hif2A proved difficult. Though changes in band size were not observed for Hif1A, Hif1B, or Hif2A, after CQ+CNL treatment, even with positive controls for hypoxia (CoCl2 or <3% O2 incubation), changes were not evident and specific band determination was difficult (data not shown). A similar difficulty occurred for measuring VEGF or ANKRD37 proteins, transcriptional targets of these Hif-family proteins.

Effects of Pharmacological Inhibitors of Hypoxia Signaling on CNL-Induced Cell Death and Transcription

Since protein-level data supporting the hypothesis that CNL was affecting hypoxia signaling was not generated, alternative methods of measuring hypoxia signaling were employed. Though not as well characterized, changes in hypoxia signaling can occur in the absence of increased HIF family protein expression. Specifically, changes in dimerization, cofactor interaction/binding, nuclear localization, or DNA binding could still alter hypoxia-driven signaling upstream of the measured transcriptional increase in ANKRD37 and VEGF-A. Thus, in an attempt to determine the role, if any, of hypoxia signaling in CNL and CQ+CNL-driven death, I utilized three inhibitors of hypoxia signaling. Acriflavine which blocks Hif1A or Hif2A from dimerizing with Hif1B (286), Chetomin, which blocks a co-activator, p300, from binding (287), and Echinomycin which blocks HIF-1 binding to DNA (288). Preliminary results using these three inhibitors demonstrated that while Chetomin and echinomycin did not show meaningful effect, Acriflavine showed a trend towards a rescue from CNL-induced cell death in FaDu cells but not SCC-61 cells (**Figure H6**). Further analysis confirmed a time-and concentration dependent rescue

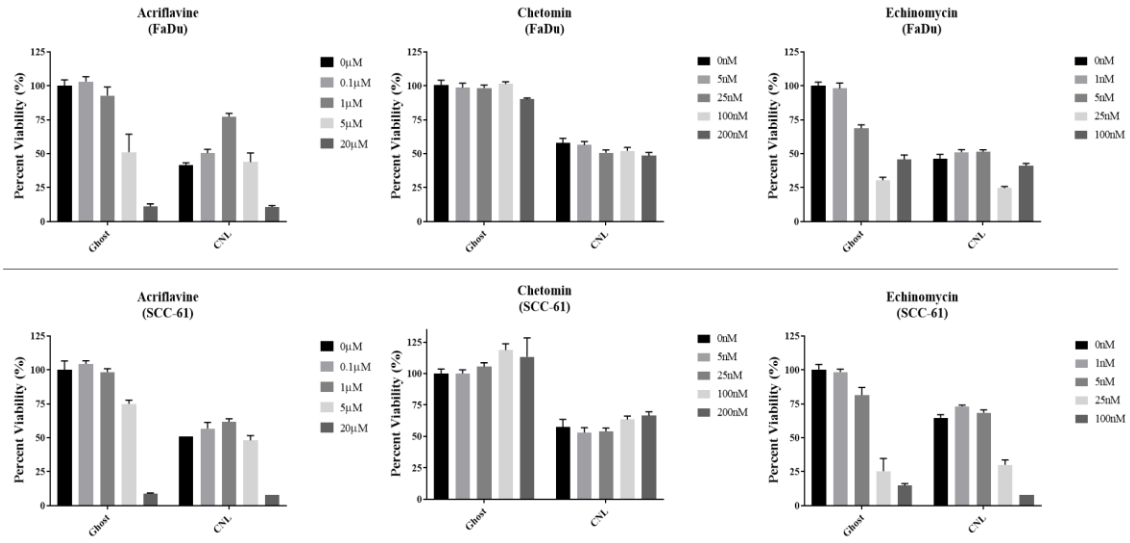

Figure H-6: Effect of Hypoxia Inhibitors on CNL-Induced Cell Death – Preliminary Data

in FaDu cells, but not in SCC-61 cells (**Figure H7**).

In FaDu cells after 48 hours, 1µM Acriflavine alone decreased viability by 34% and 10µM CNL alone decreased viability by 69%, strikingly, their combination only decreased viability by 48% demonstrating a rescue of >20% from CNL alone.

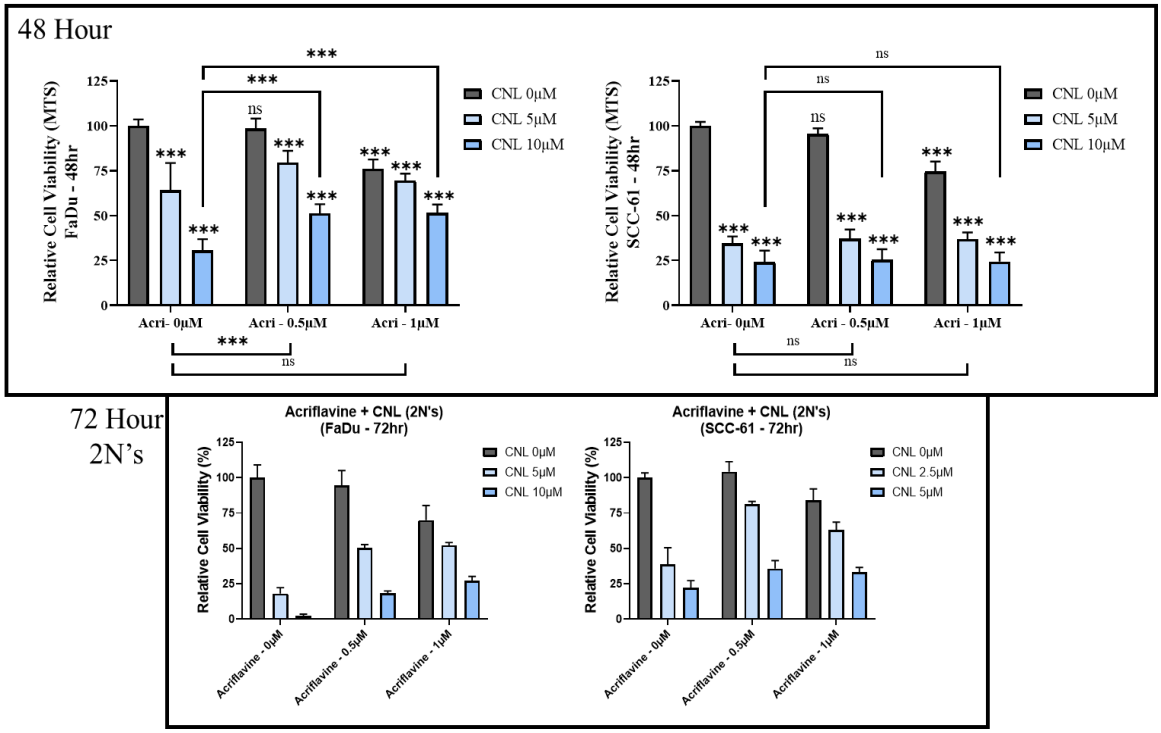

Figure H-7: Effect of Acriflavine on CNL-Induced Cell Death - Select Concentrations

Furthermore, Acriflavine was not only able to rescue FaDu cells from CNL alone, but also CQ+CNL as determined via MTS assay (**Figure H8-A**).

While the synergistic combination (10µM CQ + 10µM CNL) reduced cell viability by 50%, pre-treatment with 0.5µM Acriflavine mitigated this effect to only reduce viability by 35%, a 15% rescue. In the SCC-61 cells, this rescue by Acriflavine was not observed after CNL or CQ+CNL. The rescue of FaDu cells was confirmed via flow cytometry where Acriflavine reduced CNL-induced death from 43% to 31% and reduced CQ+CNL-induced death from 83% to 48% (**Figure H8-B**). Taken together this data suggests that Acriflavine is able to partially protect from both

CNL- and CQ+CNL-induced cell death in FaDu cells, but is unable to rescue SCC-61 cells.

Though an interesting rescue, only one of three hypoxia inhibitors demonstrating a rescue suggests an off-target effect. Thus, to test if Acriflavine was indeed inhibiting CNL-induced

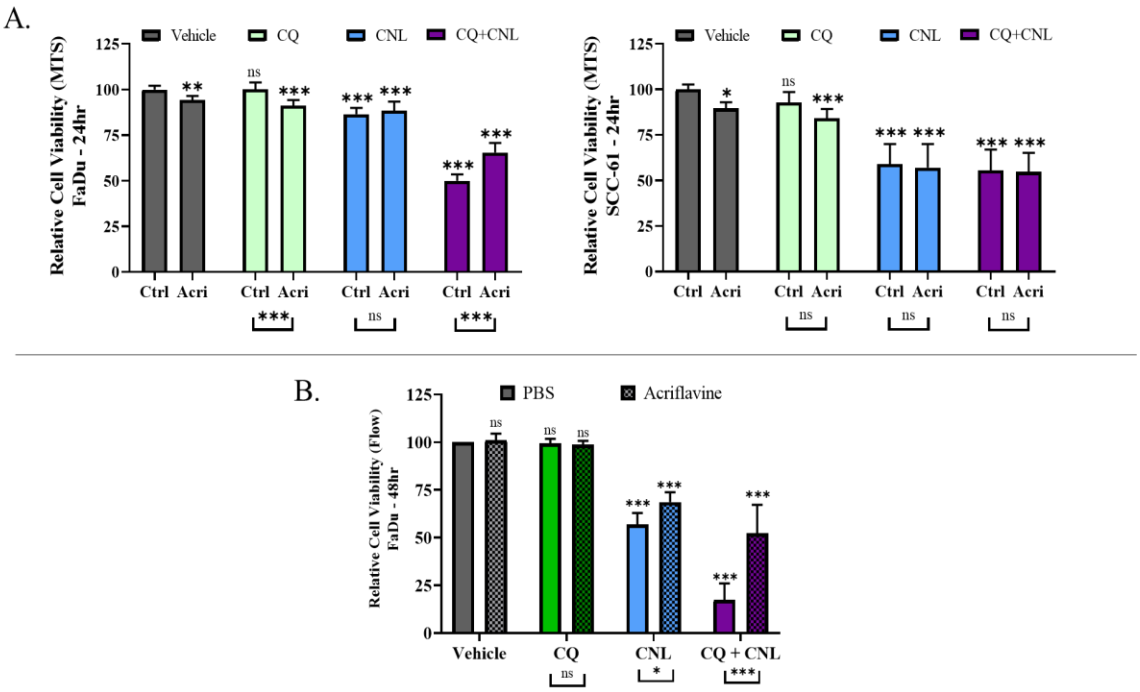

Figure H-8: Acriflavine's Effect on CQ+CNL-Induced Cell Death – Select Concentrations

hypoxia signaling, cells were treated with Acriflavine in the presence or absence of CNL. In preliminary experiments, while pre-treatment with Acriflavine did not decrease hypoxic genes as a single agent, it did partially reduce CNL-driven increase in 4/5 hypoxic targets (ANKRD37, BNIP3, BNIP3L, and VEGF-A, not NOXA), but only at the 24hr timepoint (**Figure H9**).

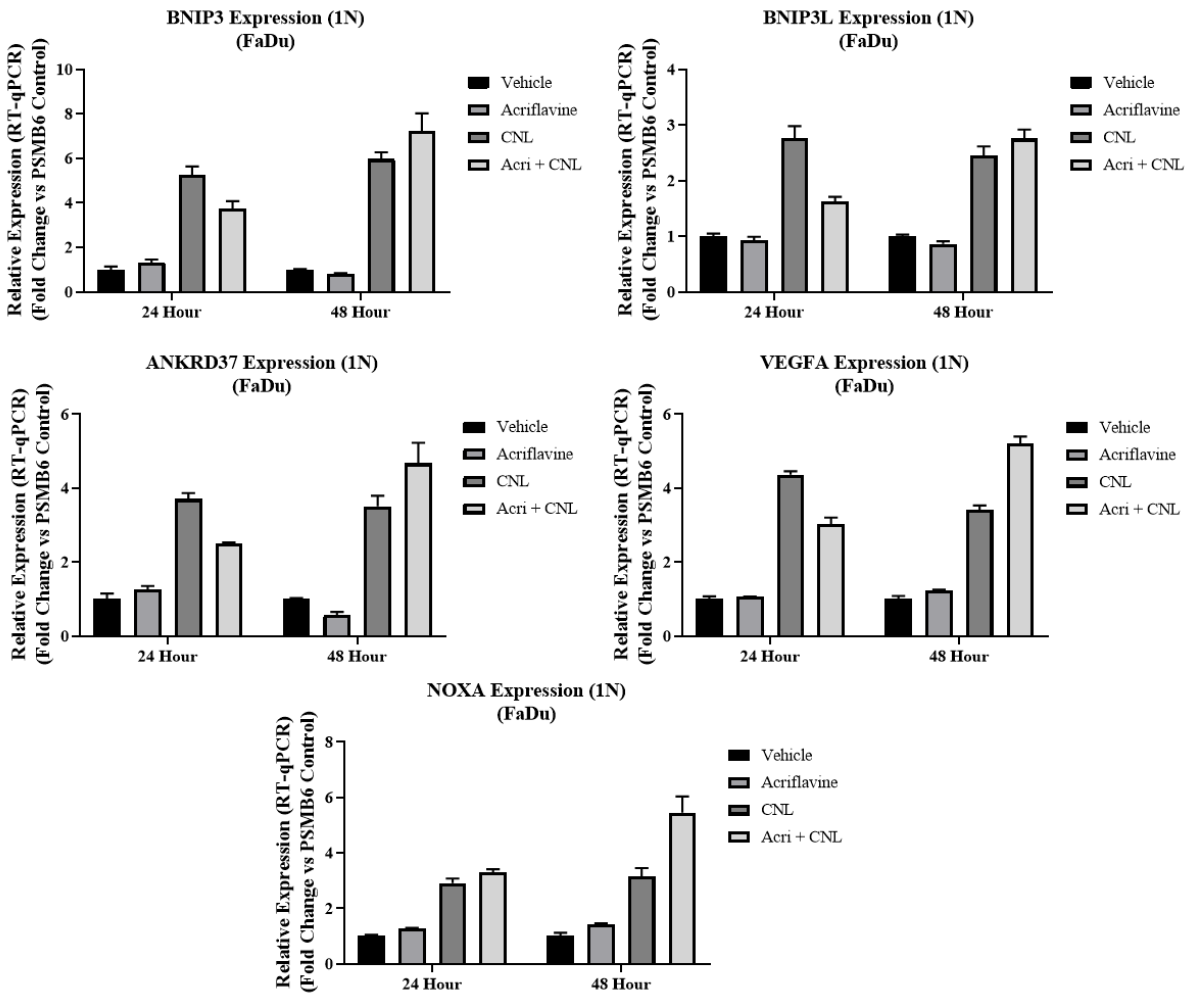

Figure H-9: Acriflavine's Effect on CNL-Induced Hypoxia Transcripts

Further preliminary experiments suggested Acriflavine was also able to decrease CQ+CNL's expression of 3/4 hypoxia genes (ANKRD37, BNIP3, and BNIP3L, not NOXA) (**Figure H10**).

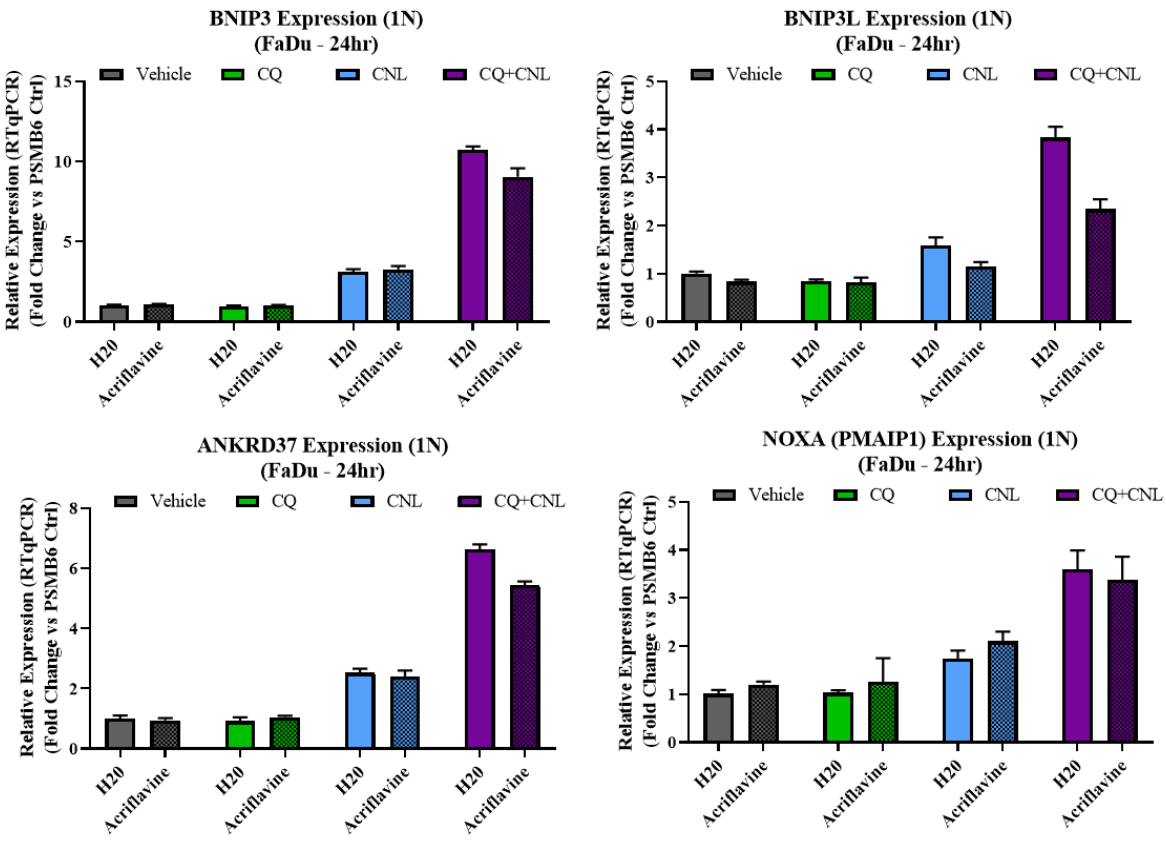

Figure H-10: Acriflavine's Effect on CQ+CNL-Induced Hypoxia Transcripts

However, despite all of the above data suggesting Acriflavine was successful in inhibiting CNL and CQ+CNL-driven death and increases in hypoxia signaling, preliminary data suggested Acriflavine failed to block transcription of hypoxia gene targets induced by the positive-control for hypoxia, <3% O2 or CoCl2 treatment for 24 hours (**Figure H11**). Furthermore, similar to western blots measuring total Hif family protein members, co-localization experiments were also plagued by a lack of effective

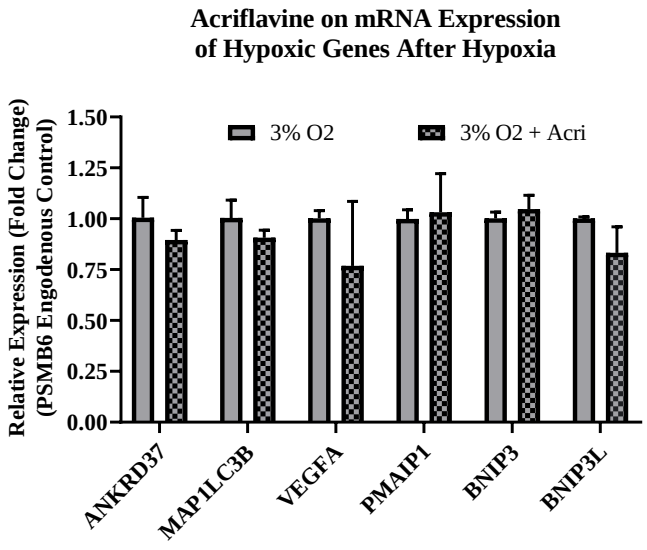

Figure H-11: Acriflavine's Effect on Hypoxia Transcripts After Hypoxic Treatment

differences seen by positive controls (data not shown).

Conclusions:

In order to interpret this data, a brief recall of data from Figure 3 and 4 of Chapter 1 is necessary. In short, FaDu cells were the most resistant to CNL at 24 hours while SCC-61 cells showed the greatest decrease in viability, however, while treatment with autophagy/lysosome inhibitor CQ synergistically enhanced CNL-induced cell death in the resistant FaDu cells, it had minimal effect on the already-sensitive SCC-61 cells. Additionally, transcription of BNIP3 in FaDu cells correlated with cell death induced by MP, CQ, CNL, and every combination of those drugs.

Strikingly, mRNA expression of ANKRD37, follows the same pattern as expression of BNIP3 after treatment with MP, CQ, CNL and their combinations. This result suggests that ANKRD37 and BNIP3 are regulated by the same transcriptional machinery and/or that ANKRD37 is associated with mitophagic signaling. If the former, it is the first evidence for ceramide and ceramide in combination with CQ to activate hypoxic signaling. If the latter, I believe it identifies a novel function for the ANKRD37 protein.

These data suggest that the "Hif inhibitor" Acriflavine partially protects from decreases in cell viability and partially prevents increases in BNIP3/ANKRD37 expression after CNL alone and CQ+CNL treatment. Most interestingly, using concentrations of Acriflavine which kill cells as a single agent, protects them from CQ+CNL-induced cell death. This observation highlights an interesting interaction between pathways which drive CNL-induced cell death and which Acriflavine can inhibit. One possibility is that CNL signals through a more-lethal pathway which can be overridden by a less-lethal but more penetrant signaling cascade. Alternatively, if Acriflavine is preventing cell cycle progression, that could inhibit mitotic-dependent death signaling by ceramide.

I recognize that hypoxia signaling is often beneficial to cancer and the cancer microenvironment (289), in fact, I see that inhibiting hypoxia signaling via high concentrations of Acriflavine is able to directly induce cell death (Figure H7). On the other hand, there is also a large

body of literature showing hypoxia signaling can induce cell death. It is possible ceramide may be partially signaling through these pathways to induce cell death in HNSCC cell lines. Although I do not see changes in HIF family transcript or protein levels, nor nuclear translocation in preliminary experiments, there are numerous alternatives by which ceramide can accomplish this signaling event. As an example, ceramide has been previously shown to decrease levels of GSK3B (290) and that GSK3B can inhibit Hif1a's transcription of downstream targets (291), this inhibition of an inhibitor could lead to increased hypoxia signaling. Though hypoxia signaling activates 81 genes as a "core response" to hypoxia (255), well over 100 (254) downstream genes can be activated in this cascade with cell-type specific changes (292). As such, focusing on hypoxia activated genes such as NOXA, BNIP3, BNIP3L, PP7, mdm2, NPM, or p21 or even hypoxia induced DNA damage (293) could be a novel and underappreciated mechanism of CNL-induced cell death.

However, though these findings are certainly interesting, in the absence of effective positive controls for either western blots showing protein-level increases or confocal microscopy showing translocation to the nucleus, ceramide-driven changes in Hif family members cannot be ruled in or out. Additionally, the failure of other Hif inhibitors, Chetomin or Echinomycin, to rescue from CNL-induced cell death as well as Acriflavine's inability to block canonical hypoxia transcripts in preliminary experiments brings into question the off-target nature of Acriflavine's effect. Furthermore, though the rescue from CQ+CNL is validated via multiple assays and multiple time points, the magnitude of rescue after CNL alone is highly variable and on occasion does not reach statistical significance for unknown reason.

Remaining Questions:

<u>If Acriflavine is, in fact, having an off-target effect, what is the mechanism by which it is reducing ceramide-driven transcripts and rescuing from CNL and CQ+CNL-induced cell death?</u> Although few papers on Acriflavine have been published, one report claims it can increase levels of LC3B (294). However, even if this were the case, other inhibitors which should increase levels

of LC3B (Rapamycin and Torin-1) failed to rescue from CNL-induced cell death (Supplemental Figure 2-1). Though not reported, perhaps Acriflavine is preventing cell cycle progression. This would explain not only the decreased viability after Acriflavine alone, but also provide a senescence-based protection from CNL.

To what extent is ceramide driving hypoxia signaling? Considering both BNIP3 and ANKRD37 are well-recognized targets of hypoxia signaling and follow the same pattern of expression after treatment with MP, CQ, CNL, and all of the combinations, the most likely explanation is that ceramide is activating both of these genes through a hypoxic signaling event. However, if this is not the case, how is ceramide increasing ANKRD37 expression?

Is this effect dependent on the chain length or method of synthesis of ceramide? While all of these data utilize exogenously delivered C6 ceramide, will other synthetic (C2) or physiological (C14-C24:1) chain lengths of ceramide have the same effect? Furthermore, will generation of intracellular ceramides cause a different response than ceramides adding exogenously to cells?

Final Thoughts:

Though these data are novel and certainly interesting, too many missing variables and the large possibility of either an off-target effect or a non-causative correlation led to the exclusion of this data from the first manuscript in Chapter 2. However, I believe there is still valuable information to be gleaned from this data and questions which should be asked and answered to elucidate the potential relationship between ceramide signaling and hypoxia which could prove vital to furthering understanding of the sphingolipid field. Additionally, although I performed multiple experiments trying to validate studies confirming the role of BNIP3 to drive hypoxia-induced protective autophagy (281), death (295, 296), or both (297) these studies lack the rigor and non-correlative data to warrant publication.

APPENDIX A2: DYSREGULATION OF LIPID METABOLISM IN MULTIPLE SCLEROSIS

Though all of my experimental research involves sphingolipids in cancer, I have come across what I believe to be the foundation for vital research involving sphingolipids in multiple sclerosis. Below I detail my findings and proposed experiments in the form of a pseudo F31 grant submission.

Abstract

Multiple Sclerosis (MS) has long been characterized as an auto-immune disease which targets myelin and myelin-producing cells in the CNS. Recently, however, an alternative hypothesis has arisen; that the primary cause of the disease is a dysfunction in the myelin itself which then activates an auto-immune response. Multiple studies measuring single nucleotide polymorphisms across over 30,000 MS patients identifies the single most associated gene to be Galacto-cerebrosidase (GALC) gene. Although the function of GALC has not been explored in the context of MS, it has been previously well-characterized in Krabbe's Disease, a disease caused by mutations in GALC which leads to degradation of the myelin sheath. The protein product of the GALC gene is the GALC enzyme, a key regulator of sphingolipid metabolism vital for normal myelin makeup and cell survival. Specifically, GALC directly metabolizes the main lipid class which makes up the myelin sheath (galactocerebrosides), decreases levels of a myelin-toxic lipid (psychosine), increases levels of pro-survival lipids structurally similar to current MS therapeutics (S1P), and is in the same pathway as a lipid which strengthens the myelin sheath and modulates auto-immune antibody functions (sphingomyelin). However, despite all of this evidence, this role of GALC on sphingolipids in MS remains completely unexplored. This study seeks to close this gap in understanding by elucidating the sphingolipid profile of MS, and identifying targets for therapeutic intervention to restore functional sphingolipid composition of the myelin.

Background and Significance

Multiple Sclerosis (MS) is defined as an autoimmune disorder with destruction of the axonal myelin sheath in the central nervous system. The prevailing "outside-in" hypothesis, supported by both genetic (298) and environmental (299) evidence, suggests an underlying autoimmune disorder leads to myelin destruction. However, a more-recent, "inside-out" hypothesis suggests that the primary defect occurs in the myelin of the central nervous system which then, in turn, activates the auto-immune response (300, 301).

Multiple separate genetic screens looking at single-nucleotide polymorphisms in over 30,000 combined adult (302) (303) and pediatric MS patients (304) identified the galactosyl-cerebrosidase (GALC) gene of the sphingolipid family to have the strongest association of any gene, including immunological genes, to MS (305). The protein product of the GALC gene is an enzyme that, in addition to other roles, is directly responsible for successful catabolism of galactocerebrosides, the primary lipid class which makes up the myelin sheath (306, 307). Indeed, mouse models which have deficient synthesis of galactocerebrosides produce myelin with an altered lipid profile, reduced insulating capacity, and increased rates of demyelination (307, 308). Although only recently recognized and poorly explored in MS, the role of GALC has been well-characterized in Krabbe's Disease (309), a disease caused by inactivating mutations in the GALC gene, which, similar to MS, also results in the destruction and de-myelination of axons (310). Taken together, this discovery highlights a highly prevalent mutation in an enzyme directly responsible for multiple aspects of normal myelin sheath maintenance (309) in MS.

At the level of lipid metabolism and signaling, GALC mutations may be having a dual-negative effect via inducing a robust increase in the GALC substrate galactosyl-sphingosine or psychosine (311) and a concomitant decrease in its product sphingosine. On one hand, psychosine signaling has been shown to be toxic in the central nervous system, especially to oligodendrocytes (311) via a multitude of cell-death signaling pathways (312). Alternatively, decreased sphingosine may lead to decreased sphingosine-1-phosphate (S1P). Though S1P is involved in many signaling

cascades, it is widely-considered pro-growth/survival (46). Thus, a mutation in the normal protective role of GALC to decrease toxic sphingosine and increase pro-survival S1P levels could lead to demyelination and axonal demise.

Further cementing the importance of S1P in MS, is the observation that three current therapies modulating S1P or its receptors are currently FDA-approved for relapse-remitting MS with multiple others currently progressing through clinical trials as summarized in **Table A-A1-1**.

Compound	Drug Name	Target	Disease	Clinical Trials	Phase	As of 04/2020
Fingolimod	Gilenya	S1PR modulator, S1PR1 functional antagonist	RRMS	-	-	FDA Approved
Siponimod (BAF312)	Mayzent	S1PR1 and S1PR5 modulator	RRMS	-	-	FDA Approved
Ozanimod (RPC1063)	Zeposia	S1PR1 and S1PR5 agonist	RRMS	NCT02294058 (SUNBEAM) & NCT02047734 (RADIENCE)	III	FDA Approved (3/2020)
Ponesimod (ACT-128800)	N/A	S1PR1 agonist	RRMS	NCT02907177 (POINT) & NCT02425644 (OPTIMUM)	III	Completed Phase III
Amiselimod (MT-1303)	N/A	S1PR1 modulator	RRMS	NCT01742052	II	Completed Phase II
GSK2018682	N/A	S1PR1 agonist	RRMS	NCT01466322	I	Suspended in 2011
Ceralifimod (ONO-4641)	N/A	S1PR1 and S1PR5 agonist	Multiple sclerosis	NCT01226745	??	Abandoned
Laquinimod	Nerventra	S1PR1	RRMS	NCT00509145 (ALLEGRO) & NCT00605215 (BRAVO)	III	Completed Phase III (Approved in Russia)

Table A-A1-1 Sphingosine 1 Phosphate Receptors Targeted Drugs Tested in Multiple Sclerosis

Although previous literature suggests these drugs elicit their effect by preventing lymphocyte egress, thus halting the invasion and destruction of myelin, a recent study in Krabbe's disease has shown one of these drugs can protect from psychosine-induced demyelination independent of an immune response (313).

Though not a direct product, GALC is also in the same sphingolipid metabolizing pathway which leads to production of sphingomyelin. Not only is sphingomyelin directly related to strengthening the myelin sheath (306), it can also be targeted by and mediate the response of autoimmune antibodies in EAE models of MS (314).

Taken together, GALC is the single-most-mutated gene in MS, directly metabolizes the main lipid class which makes up the myelin sheath (galactocerebrosides), decreases levels of a myelin-toxic lipid (psychosine), increases levels of pro-survival lipids currently used as MS therapeutics (S1P), and is in the same pathway as a lipid which strengthens the myelin sheath and modulates auto-immune antibody functions (sphingomyelin). However, despite all of this evidence, this role of GALC on sphingolipids in MS remains completely unexplored. A Pubmed search of > "sphingolipid" "multiple sclerosis" "galc" < yielded one, unrelated result (315). Thus, this multi-

functional, frequently altered pathway warrants further investigation and may represent a key area for therapeutic intervention in MS.

Specific Aims:

Our goal is to understand the role of GALC on the sphingolipid profile and function of oligodendrocytes. The "Inside-Out" hypothesis has recently gained momentum, but lacks a corresponding model to accompany it as well as a strong hypothesis which unifies the multiple modes of disease progression: initial insult, lymphocyte migration, and relapse. The following research has the potential to provide significant advances in the field of MS by providing an effective, new model, discovering novel initiating steps of the disease, and identifying new drug targets for sphingolipid-mediating therapeutics.

Although serum lipid levels have been analyzed previously (Cendrowski 1968), methods have improved significantly and the actual lipid composition of neural cells, namely oligodendrocytes, remains largely unknown. Furthermore, the recent finding in MS patients of the lipid-metabolism mutated GALC gene has only been explored in Krabbe's disease. Considering the consumption of lipids can have large effects on the disability and death of patients with MS (Swank 1988) and the role lipids play in myelin sheath integrity, lipid biology could be paramount in understanding MS and improving prognosis. This study seeks to discover a necessary and novel missing piece to the puzzle: the effects of dysregulation of lipid metabolism on the primary cells involved in multiple sclerosis. This lab's previous work on sphingolipid signaling as well as access to in-house core facilities to perform lipidomic assays allow for rapid-discovery of such novel lipid profiles of MS.

Specific Aim 1

Determine lipid composition of oligodendrocytes from primary MS samples.

Patient samples will be obtained, and the oligodendrocytes will be sorted using FLOW cytometry.

These cells with then have their lipid profiles (composition of lipids) analyzed using lipidomic mass spectroscopy.

- Are GALC-related sphingolipids altered in these brains? Specifically, is there a buildup of galactosylceramides and psychosine and depleted sphingosine, S1P, and sphingomyelin?

-Will different variants of the disease, Relapsing Remitting MS, Primary Progressive MS, Secondary Progressive MS, & Progressive Relapsing MS have similar profiles?

Specific Aim 2

Determine the consequences of GALC KO in oligodendrocyte cell lines.

Two established oligodendrocyte cell lines will be grown and the GALC genes will be knocked out using Crispr/Cas9. These cells will then have their morphology, cell viability, myelin production, lipid profiles, and immunogenicity analyzed over time compared to the WT controls.

-Will the cell's ability to differentiate to produce effective myelin be affected immediately or only over the long term?

-Will this KO replicate the sphingolipid profile seen from primary patient analysis? Will it shift the sphingosine/psychosine ratio towards the latter?

-Will the cell produce more immunogenic compounds? Damps, pamps, etc.?

Specific Aim 3

Determine in vivo effects of a conditional GALC knock out in oligodendrocytes.

Using an oligodendrocyte-specific promoter, the GALC gene will be specifically knocked out and a YFP gene will be knocked-into oligodendrocytes of mice with a stimulated immune system. The YFP+ cells will then be tested for myelin integrity, lipidomic profile by mass spectrometry, as well as co-localization with immune cells compared with YFP- cells.

-Will the unaffected oligodendrocytes (YFP-) differ in lipid profile from the GALC KO (YFP+) cells?

-Will the immune cells specifically target the cells lacking GALC (YFP+)?

Potential pitfalls of the above experiments are that the first two exclude the major immune component of MS. However, our interest is in discovering the underlying cause or primary insult of MS; for this purpose, these experiments are both sufficient. Another pitfall is that the immune system in the mouse model may not be activated through immune-stimulatory drugs. If this is the case, specific antigens against myelin such as may be used to incite the immune response such as spinal cord homogenate (SCH), Myelin Basic Protein (MBP), or Myelin Oligodendrocyte Glycoprotein (MOG).

Conclusions and Major Takeaways

There is a major relationship between Krabbe's Disease and Multiple Sclerosis which seems unappreciated by much of the field. Perhaps this is because up until recently, the sphingolipid field which is familiar with Krabbe's Disease did not have a genetic link to MS. Three separate groups analyzing tens of thousands of MS patients all identified SNPs in the GALC gene to have the single strongest correlation with MS. However, this finding is frequently brushed over in these papers and work has yet to be done to explore the effect of groundbreaking finding on sphingolipids. Considering GALCs ability to directly and indirectly alter levels of four sphingolipids heavily involved in myelin sheath function (galactosylceramide, psychosine, sphingosine-1-phosphate, and sphingomyelin) GALC's relevance should come as no surprise and there is ample evidence to suggest causation.

In addition, there are other tangential aspects I did not explore for brevity's sake in the above grant application. Notably, that antibodies against GALC and myelin oligodendrocyte glycoprotein (MOG) protein were the only two that led to antibody-based degradation of a key protein for myelin function, myelin basic protein (MBP), in human myelin (316). This study noted that even antibodies against MBP itself did not drive this same degradation. While anti-MOG

responses are known to be involved in multiple demyelinating diseases (acute disseminated encephalomyelitis [ADEM] and neuromyelitis optica spectrum disorders [NMOSD]) (317) and are often misattributed to MS (318), this GALC finding was striking. Retrospectively, if these antibodies were inhibiting the function of GALC, this could explain the primary degradation of myelin in a human model simply by the presence of antibody binding, similar to phenotypes caused by non-functional GALC in Krabbe's disease. Perhaps in patients without SNPs in GALC, or even in patients with these SNPs, there is a yet-unmeasured auto-immune antibody against GALC driving this phenotype. Finally, it is possible that the accumulation of abnormal glycosylated lipids, a result of deficient GALC activity, leads to alteration of the normal glycosylation of the MOG protein which may affect its function.

Of note, this grant was written in Spring 2015 and adapted in Spring 2020. While some of the correlations and initial studies I've discovered have been identified in the literature since this point, none adequately analyze the sphingolipid component of the role of GALC in MS. Sphingolipids have phenotypic roles in cancer, metabolic diseases, neurodegenerative diseases, and more. At worst, accurately studying these lipids in MS will identify an oddly strong correlation to a passenger-type SNP found when studying 30,000 patients. At best, this gene may identify a novel subtype of MS, give credence to the "inside out" hypothesis, identify a new model for MS (which is currently very lacking due to off-target effects of the EAE mouse model), and could lead to identification of new, druggable targets. Although unable to complete this work myself, I hope to gift this to someone in the MS field who can adapt it and utilize the resources in the Kester Lab to perform these studies.

APPENDIX A3: GOING GREEN – SPHINGOLIPIDS AND CANNABINOIDS:

Rationale

When working on the book chapter "Novel Sphingolipid-Based Cancer Therapeutics in the Personalized Medicine Era" (119), I was originally tasked with writing an in-depth review of the history of cannabinoid signaling as it pertained to sphingolipid signaling. Although I was able to accomplish this, it ended up "on the cutting room floor" for the final product. However, considering the strong relationship between sphingolipids and cannabinoid signaling as well as the potential for cannabinoids to be used as cancer therapeutics in the future, this body of work seemed a relevant, though semi-tangential, addition to a thesis primary focused on sphingolipid-based therapeutics in cancer.

Summary of Cannabinoids and Sphingolipids Literature (1998-2018)

By the beginning of 2018, thirty states have legalized the use of medicinal marijuana (http://www.governing.com/gov-data/state-marijuana-laws-map-medical-recreational.html), making it an exciting and evolving therapeutic opportunity. Major signaling molecules such as Tetrahydrocannabinol (THC) that were isolated from the *Cannabis satival* plant were termed phytocannabinoids. Phytocannabinoids along with the endocannabinoids which are produced naturally by animals, and synthetic, manufactured cannabinoids make up the three major classes of cannabinoids. These cannabinoids have demonstrated potential therapeutic benefit or growth inhibition in gliomas, neuroblastomas, leukemias/lymphomas, prostate, breast, lung, skin, and pancreatic cancer as far back as 1975; this was reviewed previously by Sarfaraz *et al.* and Javid *et al.* (319) (320).

However, it was in the year 1998 when two papers by *Sanchez et al.* first reported the relationship between sphingolipids and cannabinoids (321, 322). In the first, they showed that within 15 minutes THC caused an increase in ceramide levels through sphingomyelin hydrolysis in primary cultures of rat astrocytes. Furthermore, the authors demonstrated that ceramide

accumulation was prevented using SR 141716 to block CB_1, one of the two major cannabinoid receptors (CB_1 and CB_2) (321). In their second paper which explored THC-driven apoptosis in C6 glioma cells, they again reported a short-term increase in ceramide levels driven by sphingomyelin hydrolysis. A major finding of this paper though, was that THC treatment induced death of glioma cells after 5 days of treatment; counter-intuitively, this apoptotic cell death and increase in ceramide levels was not mitigated by CB_1 inhibition (322). Although this suggested an alternative pathway by which THC may be affecting sphingolipid levels, it was later shown that both blockade of CB_1 and CB_2 simultaneously or inhibition of *de novo* ceramide synthase, did prevent apoptosis in C6 glioma cells (323, 324). These differential cannabinoid signaling processes were summarized as "short-term", non-toxic increases in ceramide via sphingomyelin hydrolysis compared to "long-term", death-inducing *de novo* ceramide synthesis in glioma cells (325).

In the following years, work in astrocytes elucidated that the short-term, THC-dependent ceramide increase drove THC's ketogenic effect mainly through carnitine palmitoyltransferase 1 (326). Additionally, it was demonstrated that the long-term, cytotoxic ceramide accumulation from THC treatment caused partially ERK-dependent apoptosis *in vitro* in C6 glioma cells (323). Moreover, studies in glioma cells elucidated a CB_1-dependent ER-stress response, mediated by stress regulated protein p8, was responsible for THC-induced cell death in glioma (327).

Ceramides have also been implicated in the therapeutic effect of cannabinoids on other major cancer types as well. In prostate cancer cells, the apoptotic/necrotic effect of Anandamide, an endogenous cannabinoid, was potentiated by the ceramidase inhibitor NOE and partially rescued by FB1 (328). In another cancer model, using cannabinoids targeting CB_2 (and to a lesser extent CB_1) increased ceramide levels and induced apoptosis in colon cancer cells. These effects could be ablated by siRNA knockdown of TNF-alpha, FB1 treatment, or inhibition of either cannabinoid receptor (329). Additionally, R(+)-methanandamide (R-MA), a stable, endocannabinoid analog, and the synthetic cannabinoid Win-55,212-2 (Win55), induced cell death in mantle cell lymphoma (MCL) while leaving B cells unaffected. The authors report that the p38 activation and

mitochondrial depolarization responsible for this cancer-specific effect could be prevented by inhibiting ceramide synthase (330). Further work in MCL showed that R-MA increased levels of specific ceramide species (C16, C18, C24, and C24:1) through the *de novo* pathway, and that CerS3 and CerS6 expression was also increased by both R-MA and Win55. Notably, blocking ceramide metabolism into S1P or GCS also increased the cytotoxic effect of R-MA (331). Recently, in *in vitro* and *in vivo* models of Multiple Myeloma, Win55 induced a large signaling cascade resulting in increases in serine palmitoyl transferase protein levels and apoptosis through cleavage of PARP as well as multiple caspase proteins. Although this cell death could be rescued by a pan-caspase inhibitor, surprisingly, FB1 was able to partially rescue the increase in SPT protein levels (332).

For twenty years, the growing body of evidence suggests the relationship between sphingolipids and cannabinoids may not just be a correlation, on the contrary, alterations of sphingolipids may be necessary for multiple cannabinoid-induced effects. As the potential applications for medicinal marijuana continue to spread, we can be blunt and say research to understand its implications for cancer grow ever more necessary. With a large number of unexplored cancer models affected by cannabinoids and an even larger number of unexplored cannabinoid derivatives, it is likely the greatest promise for novel understanding and joint therapies involving cannabinoids and sphingolipids lie ahead.

LIST OF FIGURES

LIST OF FIGURES

CHAPTER 1:

CHAPTER 2:

CHAPTER 3:

CHAPTER 4:

CHAPTER 5:

APPENDIX:

REFERENCES

REFERENCES

1. Curado MP, Hashibe M. Recent changes in the epidemiology of head and neck cancer. Curr Opin Oncol. 2009;21(3):194-200.
2. Schiff BA. Overview of Head and Neck Tumors 2019 [Available from: https://www.merckmanuals.com/professional/ear,-nose,-and-throat-disorders/tumors-of-the-head-and-neck/overview-of-head-and-neck-tumors.]
3. Nelson WR. In search of the first head and neck surgeon. Am J Surg. 1987;154(4):342-6.
4. Folz BJ, Silver CE, Rinaldo A, Fagan JJ, Pratt LW, Weir N, et al. An outline of the history of head and neck oncology. Oral Oncol. 2008;44(1):2-9.
5. Henry Trentham Butlin WGS. Diseases of the Tongue1900.
6. Hashibe M, Brennan P, Benhamou S, Castellsague X, Chen C, Curado MP, et al. Alcohol drinking in never users of tobacco, cigarette smoking in never drinkers, and the risk of head and neck cancer: pooled analysis in the International Head and Neck Cancer Epidemiology Consortium. J Natl Cancer Inst. 2007;99(10):777-89.
7. Jethwa AR, Khariwala SS. Tobacco-related carcinogenesis in head and neck cancer. Cancer Metastasis Rev. 2017;36(3):411-23.
8. Miech R, Johnston L, O'Malley PM, Bachman JG, Patrick ME. Adolescent Vaping and Nicotine Use in 2017-2018 - U.S. National Estimates. N Engl J Med. 2019;380(2):192-3.
9. Farzal Z, Perry MF, Yarbrough WG, Kimple AJ. The Adolescent Vaping Epidemic in the United States-How It Happened and Where We Go From Here. JAMA Otolaryngol Head Neck Surg. 2019.
10. Stephens WE. Comparing the cancer potencies of emissions from vapourised nicotine products including e-cigarettes with those of tobacco smoke. Tob Control. 2017.
11. National Academies of Sciences E, and Medicine; Health and Medicine Division; Board on Population Health and Public Health Practice; Committee on the Review of the Health Effects of Electronic Nicotine Delivery Systems. . Public Health Consequences of E-Cigarettes. David L. Eaton LYK, and Kathleen Stratton, editor: National Academies Press; 2018.
12. Sturgis EM, Cinciripini PM. Trends in head and neck cancer incidence in relation to smoking prevalence: an emerging epidemic of human papillomavirus-associated cancers? Cancer. 2007;110(7):1429-35.
13. Berman TA, Schiller JT. Human papillomavirus in cervical cancer and oropharyngeal cancer: One cause, two diseases. Cancer. 2017;123(12):2219-29.
14. Chaturvedi AK, Anderson WF, Lortet-Tieulent J, Curado MP, Ferlay J, Franceschi S, et al. Worldwide trends in incidence rates for oral cavity and oropharyngeal cancers. J Clin Oncol. 2013;31(36):4550-9.
15. Mehanna H, Beech T, Nicholson T, El-Hariry I, McConkey C, Paleri V, et al. Prevalence of human papillomavirus in oropharyngeal and nonoropharyngeal head and neck cancer--systematic review and meta-analysis of trends by time and region. Head Neck. 2013;35(5):747-55.
16. Chaturvedi AK, Engels EA, Pfeiffer RM, Hernandez BY, Xiao W, Kim E, et al. Human papillomavirus and rising oropharyngeal cancer incidence in the United States. J Clin Oncol. 2011;29(32):4294-301.
17. Wookey VB, Appiah AK, Kallam A, Ernani V, Smith LM, Ganti AK. HPV Status and Survival in Non-Oropharyngeal Squamous Cell Carcinoma of the Head and Neck. Anticancer Res. 2019;39(4):1907-14.
18. Moore KA, 2nd, Mehta V. The Growing Epidemic of HPV-Positive Oropharyngeal Carcinoma: A Clinical Review for Primary Care Providers. J Am Board Fam Med. 2015;28(4):498-503.
19. Gabani P, Lin AJ, Barnes J, Oppelt P, Adkins DR, Rich JT, et al. Radiation therapy dose de-escalation compared to standard dose radiation therapy in definitive treatment of HPV-positive oropharyngeal squamous cell carcinoma. Radiother Oncol. 2019;134:81-8.

20. Cooper JS, Pajak TF, Forastiere AA, Jacobs J, Campbell BH, Saxman SB, et al. Postoperative concurrent radiotherapy and chemotherapy for high-risk squamous-cell carcinoma of the head and neck. N Engl J Med. 2004;350(19):1937-44.
21. Bernier J, Domenge C, Ozsahin M, Matuszewska K, Lefebvre JL, Greiner RH, et al. Postoperative irradiation with or without concomitant chemotherapy for locally advanced head and neck cancer. N Engl J Med. 2004;350(19):1945-52.
22. Leon X, Hitt R, Constenla M, Rocca A, Stupp R, Kovacs AF, et al. A retrospective analysis of the outcome of patients with recurrent and/or metastatic squamous cell carcinoma of the head and neck refractory to a platinum-based chemotherapy. Clin Oncol (R Coll Radiol). 2005;17(6):418-24.
23. Vermorken JB, Mesia R, Rivera F, Remenar E, Kawecki A, Rottey S, et al. Platinum-based chemotherapy plus cetuximab in head and neck cancer. N Engl J Med. 2008;359(11):1116-27.
24. Siano M, Infante G, Resteghini C, Cau MC, Alfieri S, Bergamini C, et al. Outcome of recurrent and metastatic head and neck squamous cell cancer patients after first line platinum and cetuximab therapy. Oral Oncol. 2017;69:33-7.
25. Walter V, Yin X, Wilkerson MD, Cabanski CR, Zhao N, Du Y, et al. Molecular subtypes in head and neck cancer exhibit distinct patterns of chromosomal gain and loss of canonical cancer genes. PLoS One. 2013;8(2):e56823.
26. Cancer Genome Atlas N. Comprehensive genomic characterization of head and neck squamous cell carcinomas. Nature. 2015;517(7536):576-82.
27. Cho J, Johnson DE, Grandis JR. Therapeutic Implications of the Genetic Landscape of Head and Neck Cancer. Semin Radiat Oncol. 2018;28(1):2-11.
28. Leemans CR, Snijders PJF, Brakenhoff RH. The molecular landscape of head and neck cancer. Nat Rev Cancer. 2018;18(5):269-82.
29. Bray F, Ferlay J, Soerjomataram I, Siegel RL, Torre LA, Jemal A. Global cancer statistics 2018: GLOBOCAN estimates of incidence and mortality worldwide for 36 cancers in 185 countries. CA Cancer J Clin. 2018;68(6):394-424.
30. Sim F, Leidner R, Bell RB. Immunotherapy for Head and Neck Cancer. Hematol Oncol Clin North Am. 2019;33(2):301-21.
31. Pardoll DM. The blockade of immune checkpoints in cancer immunotherapy. Nat Rev Cancer. 2012;12(4):252-64.
32. Nowicki TS, Hu-Lieskovan S, Ribas A. Mechanisms of Resistance to PD-1 and PD-L1 Blockade. Cancer J. 2018;24(1):47-53.
33. Bauml JM, Aggarwal C, Cohen RB. Immunotherapy for head and neck cancer: where are we now and where are we going? Ann Transl Med. 2019;7(Suppl 3):S75.
34. Thudichum JLW. A Treatise on the Chemical Constitution of the Brain: based throughout upon Original Researches. Aids to Physiological Chemistry. 1884.
35. Rao RP, Acharya JK. Sphingolipids and membrane biology as determined from genetic models. Prostaglandins Other Lipid Mediat. 2008;85(1-2):1-16.
36. Lahiri S, Futerman AH. The metabolism and function of sphingolipids and glycosphingolipids. Cell Mol Life Sci. 2007;64(17):2270-84.
37. Russo SB, Ross JS, Cowart LA. Sphingolipids in obesity, type 2 diabetes, and metabolic disease. Handb Exp Pharmacol. 2013(216):373-401.
38. Meikle PJ, Summers SA. Sphingolipids and phospholipids in insulin resistance and related metabolic disorders. Nat Rev Endocrinol. 2017;13(2):79-91.
39. Bismuth J, Lin P, Yao Q, Chen C. Ceramide: a common pathway for atherosclerosis? Atherosclerosis. 2008;196(2):497-504.
40. Alessenko AV, Lebedev capital A CTEC, Kurochkin IN. [The role of sphingolipids in cardiovascular pathologies]. Biomed Khim. 2018;64(6):487-95.
41. Kasumov T, Li L, Li M, Gulshan K, Kirwan JP, Liu X, et al. Ceramide as a mediator of non-alcoholic Fatty liver disease and associated atherosclerosis. PLoS One. 2015;10(5):e0126910.

42. Trayssac M, Hannun YA, Obeid LM. Role of sphingolipids in senescence: implication in aging and age-related diseases. J Clin Invest. 2018;128(7):2702-12.
43. Lin G, Wang L, Marcogliese PC, Bellen HJ. Sphingolipids in the Pathogenesis of Parkinson's Disease and Parkinsonism. Trends Endocrinol Metab. 2019;30(2):106-17.
44. Ogretmen B. Sphingolipid metabolism in cancer signalling and therapy. Nat Rev Cancer. 2018;18(1):33-50.
45. Liu J, Beckman BS, Foroozesh M. A review of ceramide analogs as potential anticancer agents. Future Med Chem. 2013;5(12):1405-21.
46. Nagahashi M, Abe M, Sakimura K, Takabe K, Wakai T. The role of sphingosine-1-phosphate in inflammation and cancer progression. Cancer Sci. 2018;109(12):3671-8.
47. Pyne NJ, Pyne S. Sphingosine 1-phosphate and cancer. Nat Rev Cancer. 2010;10(7):489-503.
48. Kunkel GT, Maceyka M, Milstien S, Spiegel S. Targeting the sphingosine-1-phosphate axis in cancer, inflammation and beyond. Nat Rev Drug Discov. 2013;12(9):688-702.
49. Saddoughi SA, Garrett-Mayer E, Chaudhary U, O'Brien PE, Afrin LB, Day TA, et al. Results of a phase II trial of gemcitabine plus doxorubicin in patients with recurrent head and neck cancers: serum C(1)(8)-ceramide as a novel biomarker for monitoring response. Clin Cancer Res. 2011;17(18):6097-105.
50. Liu YY, Patwardhan GA, Xie P, Gu X, Giuliano AE, Cabot MC. Glucosylceramide synthase, a factor in modulating drug resistance, is overexpressed in metastatic breast carcinoma. Int J Oncol. 2011;39(2):425-31.
51. Liu YY, Han TY, Giuliano AE, Cabot MC. Ceramide glycosylation potentiates cellular multidrug resistance. FASEB J. 2001;15(3):719-30.
52. Roh JL, Kim EH, Park JY, Kim JW. Inhibition of Glucosylceramide Synthase Sensitizes Head and Neck Cancer to Cisplatin. Mol Cancer Ther. 2015;14(8):1907-15.
53. Gouaze-Andersson V, Cabot MC. Glycosphingolipids and drug resistance. Biochim Biophys Acta. 2006;1758(12):2096-103.
54. Grosch S, Schiffmann S, Geisslinger G. Chain length-specific properties of ceramides. Prog Lipid Res. 2012;51(1):50-62.
55. Maula T, Al Sazzad MA, Slotte JP. Influence of Hydroxylation, Chain Length, and Chain Unsaturation on Bilayer Properties of Ceramides. Biophys J. 2015;109(8):1639-51.
56. Bose R, Verheij M, Haimovitz-Friedman A, Scotto K, Fuks Z, Kolesnick R. Ceramide synthase mediates daunorubicin-induced apoptosis: an alternative mechanism for generating death signals. Cell. 1995;82(3):405-14.
57. Hannun YA. Functions of ceramide in coordinating cellular responses to stress. Science. 1996;274(5294):1855-9.
58. Nganga R, Oleinik N, Ogretmen B. Mechanisms of Ceramide-Dependent Cancer Cell Death. Adv Cancer Res. 2018;140:1-25.
59. Haimovitz-Friedman A, Kolesnick RN, Fuks Z. Ceramide signaling in apoptosis. Br Med Bull. 1997;53(3):539-53.
60. Mullen TD, Obeid LM. Ceramide and apoptosis: exploring the enigmatic connections between sphingolipid metabolism and programmed cell death. Anticancer Agents Med Chem. 2012;12(4):340-63.
61. Xu F, Yang CC, Gomillion C, Burg KJ. Effect of ceramide on mesenchymal stem cell differentiation toward adipocytes. Appl Biochem Biotechnol. 2010;160(1):197-212.
62. Wang G, Spassieva SD, Bieberich E. Ceramide and S1P Signaling in Embryonic Stem Cell Differentiation. Methods Mol Biol. 2018;1697:153-71.
63. Venable ME, Lee JY, Smyth MJ, Bielawska A, Obeid LM. Role of ceramide in cellular senescence. J Biol Chem. 1995;270(51):30701-8.
64. Dbaibo GS, Pushkareva MY, Jayadev S, Schwarz JK, Horowitz JM, Obeid LM, et al. Retinoblastoma gene product as a downstream target for a ceramide-dependent pathway of growth

arrest. Proc Natl Acad Sci U S A. 1995;92(5):1347-51.
65. Hannun YA. Sphingolipid second messengers: tumor suppressor lipids. Adv Exp Med Biol. 1997;400A:305-12.
66. Hannun YA, Luberto C. Ceramide in the eukaryotic stress response. Trends Cell Biol. 2000;10(2):73-80.
67. Galadari S, Rahman A, Pallichankandy S, Thayyullathil F. Tumor suppressive functions of ceramide: evidence and mechanisms. Apoptosis. 2015;20(5):689-711.
68. Mengubas K, Riordan FA, Bravery CA, Lewin J, Owens DL, Mehta AB, et al. Ceramide-induced killing of normal and malignant human lymphocytes is by a non-apoptotic mechanism. Oncogene. 1999;18(15):2499-506.
69. Lopez-Marure R, Gutierrez G, Mendoza C, Ventura JL, Sanchez L, Reyes Maldonado E, et al. Ceramide promotes the death of human cervical tumor cells in the absence of biochemical and morphological markers of apoptosis. Biochem Biophys Res Commun. 2002;293(3):1028-36.
70. Mochizuki T, Asai A, Saito N, Tanaka S, Katagiri H, Asano T, et al. Akt protein kinase inhibits non-apoptotic programmed cell death induced by ceramide. J Biol Chem. 2002;277(4):2790-7.
71. Kim WH, Choi CH, Kang SK, Kwon CH, Kim YK. Ceramide induces non-apoptotic cell death in human glioma cells. Neurochem Res. 2005;30(8):969-79.
72. Suhrland C, Truman JP, Obeid LM, Sitharaman B. Delivery of long chain C16 and C24 ceramide in HeLa cells using oxidized graphene nanoribbons. J Biomed Mater Res B Appl Biomater. 2020;108(3):1141-56.
73. Shabbits JA, Mayer LD. Intracellular delivery of ceramide lipids via liposomes enhances apoptosis in vitro. Biochim Biophys Acta. 2003;1612(1):98-106.
74. Maru M, Haraguchi M, Higashi H, Kato S, Kurimura T, Naiki M, et al. Anti-tumor activity of ceramides and glycosphingolipids in a murine tumor system. Int J Cancer. 1993;53(4):645-50.
75. Jatoi A, Suman VJ, Schaefer P, Block M, Loprinzi C, Roche P, et al. A phase II study of topical ceramides for cutaneous breast cancer. Breast Cancer Res Treat. 2003;80(1):99-104.
76. Barth BM, Cabot MC, Kester M. Ceramide-based therapeutics for the treatment of cancer. Anticancer Agents Med Chem. 2011;11(9):911-9.
77. Stover T, Kester M. Liposomal delivery enhances short-chain ceramide-induced apoptosis of breast cancer cells. J Pharmacol Exp Ther. 2003;307(2):468-75.
78. Shabbits JA, Mayer LD. High ceramide content liposomes with in vivo antitumor activity. Anticancer Res. 2003;23(5A):3663-9.
79. Kester M, Bassler J, Fox TE, Carter CJ, Davidson JA, Parette MR. Preclinical development of a C6-ceramide NanoLiposome, a novel sphingolipid therapeutic. Biol Chem. 2015;396(6-7):737-47.
80. McGill CM, Brown TJ, Fisher LN, Gustafson SJ, Dunlap KL, Beck AJ, et al. Combinatorial Efficacy of Quercitin and Nanoliposomal Ceramide for Acute Myeloid Leukemia. Int J Biopharm Sci. 2018;1(1).
81. Barth BM, Wang W, Toran PT, Fox TE, Annageldiyev C, Ondrasik RM, et al. Sphingolipid metabolism determines the therapeutic efficacy of nanoliposomal ceramide in acute myeloid leukemia. Blood Adv. 2019;3(17):2598-603.
82. Ryland LK, Doshi UA, Shanmugavelandy SS, Fox TE, Aliaga C, Broeg K, et al. C6-ceramide nanoliposomes target the Warburg effect in chronic lymphocytic leukemia. PLoS One. 2013;8(12):e84648.
83. Doshi UA, Shaw J, Fox TE, Claxton DF, Loughran TP, Kester M. STAT3 mediates C6-ceramide-induced cell death in chronic lymphocytic leukemia. Signal Transduct Target Ther. 2017;2:17051.
84. Liu X, Ryland L, Yang J, Liao A, Aliaga C, Watts R, et al. Targeting of survivin by nanoliposomal ceramide induces complete remission in a rat model of NK-LGL leukemia. Blood. 2010;116(20):4192-201.

85. Watters RJ, Fox TE, Tan SF, Shanmugavelandy S, Choby JE, Broeg K, et al. Targeting glucosylceramide synthase synergizes with C6-ceramide nanoliposomes to induce apoptosis in natural killer cell leukemia. Leuk Lymphoma. 2013;54(6):1288-96.
86. Tran MA, Smith CD, Kester M, Robertson GP. Combining nanoliposomal ceramide with sorafenib synergistically inhibits melanoma and breast cancer cell survival to decrease tumor development. Clin Cancer Res. 2008;14(11):3571-81.
87. Zhang X, Kitatani K, Toyoshima M, Ishibashi M, Usui T, Minato J, et al. Ceramide Nanoliposomes as a MLKL-Dependent, Necroptosis-Inducing, Chemotherapeutic Reagent in Ovarian Cancer. Mol Cancer Ther. 2018;17(1):50-9.
88. Jiang Y, DiVittore NA, Kaiser JM, Shanmugavelandy SS, Fritz JL, Heakal Y, et al. Combinatorial therapies improve the therapeutic efficacy of nanoliposomal ceramide for pancreatic cancer. Cancer Biol Ther. 2011;12(7):574-85.
89. Stover TC, Sharma A, Robertson GP, Kester M. Systemic delivery of liposomal short-chain ceramide limits solid tumor growth in murine models of breast adenocarcinoma. Clin Cancer Res. 2005;11(9):3465-74.
90. Morad SA, Madigan JP, Levin JC, Abdelmageed N, Karimi R, Rosenberg DW, et al. Tamoxifen magnifies therapeutic impact of ceramide in human colorectal cancer cells independent of p53. Biochem Pharmacol. 2013;85(8):1057-65.
91. Adiseshaiah PP, Clogston JD, McLeland CB, Rodriguez J, Potter TM, Neun BW, et al. Synergistic combination therapy with nanoliposomal C6-ceramide and vinblastine is associated with autophagy dysfunction in hepatocarcinoma and colorectal cancer models. Cancer Lett. 2013;337(2):254-65.
92. Li G, Liu D, Kimchi ET, Kaifi JT, Qi X, Manjunath Y, et al. Nanoliposome C6-Ceramide Increases the Anti-tumor Immune Response and Slows Growth of Liver Tumors in Mice. Gastroenterology. 2018;154(4):1024-36 e9.
93. Tagaram HR, Divittore NA, Barth BM, Kaiser JM, Avella D, Kimchi ET, et al. Nanoliposomal ceramide prevents in vivo growth of hepatocellular carcinoma. Gut. 2011;60(5):695-701.
94. Bai A, Liu X, Bielawski J, Hannun YA. Bioactive sphingolipid profile in a xenograft mouse model of head and neck squamous cell carcinoma. PLoS One. 2019;14(4):e0215770.
95. Karahatay S, Thomas K, Koybasi S, Senkal CE, Elojeimy S, Liu X, et al. Clinical relevance of ceramide metabolism in the pathogenesis of human head and neck squamous cell carcinoma (HNSCC): attenuation of C(18)-ceramide in HNSCC tumors correlates with lymphovascular invasion and nodal metastasis. Cancer Lett. 2007;256(1):101-11.
96. Facchinetti MM, Gandini NA, Fermento ME, Sterin-Speziale NB, Ji Y, Patel V, et al. The expression of sphingosine kinase-1 in head and neck carcinoma. Cells Tissues Organs. 2010;192(5):314-24.
97. Zhou Y, Han Y, Zhang Z, Shi Z, Zhou L, Liu X, et al. MicroRNA-124 upregulation inhibits proliferation and invasion of osteosarcoma cells by targeting sphingosine kinase 1. Hum Cell. 2017;30(1):30-40.
98. Kim JW, Park Y, Roh JL, Cho KJ, Choi SH, Nam SY, et al. Prognostic value of glucosylceramide synthase and P-glycoprotein expression in oral cavity cancer. Int J Clin Oncol. 2016;21(5):883-9.
99. Senkal CE, Ponnusamy S, Rossi MJ, Bialewski J, Sinha D, Jiang JC, et al. Role of human longevity assurance gene 1 and C18-ceramide in chemotherapy-induced cell death in human head and neck squamous cell carcinomas. Mol Cancer Ther. 2007;6(2):712-22.
100. Separovic D, Breen P, Joseph N, Bielawski J, Pierce JS, E VANB, et al. siRNA-mediated down-regulation of ceramide synthase 1 leads to apoptotic resistance in human head and neck squamous carcinoma cells after photodynamic therapy. Anticancer Res. 2012;32(7):2479-85.
101. Koybasi S, Senkal CE, Sundararaj K, Spassieva S, Bielawski J, Osta W, et al. Defects in cell growth regulation by C18:0-ceramide and longevity assurance gene 1 in human head and neck

squamous cell carcinomas. J Biol Chem. 2004;279(43):44311-9.
102. Yazama H, Kitatani K, Fujiwara K, Kato M, Hashimoto-Nishimura M, Kawamoto K, et al. Dietary glucosylceramides suppress tumor growth in a mouse xenograft model of head and neck squamous cell carcinoma by the inhibition of angiogenesis through an increase in ceramide. Int J Clin Oncol. 2015;20(3):438-46.
103. Sindhu SK, Bauman JE. Current Concepts in Chemotherapy for Head and Neck Cancer. Oral Maxillofac Surg Clin North Am. 2019;31(1):145-54.
104. Noda S, Yoshimura S, Sawada M, Naganawa T, Iwama T, Nakashima S, et al. Role of ceramide during cisplatin-induced apoptosis in C6 glioma cells. J Neurooncol. 2001;52(1):11-21.
105. Brachtendorf S, Wanger RA, Birod K, Thomas D, Trautmann S, Wegner MS, et al. Chemosensitivity of human colon cancer cells is influenced by a p53-dependent enhancement of ceramide synthase 5 and induction of autophagy. Biochim Biophys Acta Mol Cell Biol Lipids. 2018;1863(10):1214-27.
106. Truman JP, Garcia-Barros M, Obeid LM, Hannun YA. Evolving concepts in cancer therapy through targeting sphingolipid metabolism. Biochim Biophys Acta. 2014;1841(8):1174-88.
107. Roh JL, Park JY, Kim EH, Jang HJ. Targeting acid ceramidase sensitises head and neck cancer to cisplatin. Eur J Cancer. 2016;52:163-72.
108. Li S, Wu Y, Ding Y, Yu M, Ai Z. CerS6 regulates cisplatin resistance in oral squamous cell carcinoma by altering mitochondrial fission and autophagy. J Cell Physiol. 2018;233(12):9416-25.
109. Zhu Y, Wang C, Zhou Y, Ma N, Zhou J. C6 ceramide motivates the anticancer sensibility induced by PKC412 in preclinical head and neck squamous cell carcinoma models. J Cell Physiol. 2018;233(12):9437-46.
110. Senkal CE, Ponnusamy S, Rossi MJ, Sundararaj K, Szulc Z, Bielawski J, et al. Potent antitumor activity of a novel cationic pyridinium-ceramide alone or in combination with gemcitabine against human head and neck squamous cell carcinomas in vitro and in vivo. J Pharmacol Exp Ther. 2006;317(3):1188-99.
111. Boppana NB, Stochaj U, Kodiha M, Bielawska A, Bielawski J, Pierce JS, et al. C6-pyridinium ceramide sensitizes SCC17B human head and neck squamous cell carcinoma cells to photodynamic therapy. J Photochem Photobiol B. 2015;143:163-8.
112. Zhu W, Wang X, Zhou Y, Wang H. C2-ceramide induces cell death and protective autophagy in head and neck squamous cell carcinoma cells. Int J Mol Sci. 2014;15(2):3336-55.
113. Rossi MJ, Sundararaj K, Koybasi S, Phillips MS, Szulc ZM, Bielawska A, et al. Inhibition of growth and telomerase activity by novel cationic ceramide analogs with high solubility in human head and neck squamous cell carcinoma cells. Otolaryngol Head Neck Surg. 2005;132(1):55-62.
114. Cramer JD, Burtness B, Le QT, Ferris RL. The changing therapeutic landscape of head and neck cancer. Nat Rev Clin Oncol. 2019;16(11):669-83.
115. Dougherty MI, Dougherty W, Kain JJ, Hughley BB, Shonka DC, Jr., Fedder KL, et al. Non-HPV-Related Head and Neck Squamous Cell Carcinoma in a Young Patient Cohort. Ear Nose Throat J. 2020:145561320935839.
116. Lee YS, Johnson DE, Grandis JR. An update: emerging drugs to treat squamous cell carcinomas of the head and neck. Expert Opin Emerg Drugs. 2018;23(4):283-99.
117. Morad SA, Cabot MC. Ceramide-orchestrated signalling in cancer cells. Nat Rev Cancer. 2013;13(1):51-65.
118. Wooten LG, Ogretmen B. Sp1/Sp3-dependent regulation of human telomerase reverse transcriptase promoter activity by the bioactive sphingolipid ceramide. J Biol Chem. 2005;280(32):28867-76.
119. Shaw J, Costa-Pinheiro P, Patterson L, Drews K, Spiegel S, Kester M. Novel Sphingolipid-Based Cancer Therapeutics in the Personalized Medicine Era. Adv Cancer Res. 2018;140:327-66.
120. Thomas RJ, Oleinik N, Panneer Selvam S, Vaena SG, Dany M, Nganga RN, et al. HPV/E7

induces chemotherapy-mediated tumor suppression by ceramide-dependent mitophagy. EMBO Mol Med. 2017;9(8):1030-51.
121. Galluzzi L, Pietrocola F, Bravo-San Pedro JM, Amaravadi RK, Baehrecke EH, Cecconi F, et al. Autophagy in malignant transformation and cancer progression. EMBO J. 2015;34(7):856-80.
122. Glick D, Barth S, Macleod KF. Autophagy: cellular and molecular mechanisms. J Pathol. 2010;221(1):3-12.
123. Jiang W, Ogretmen B. Autophagy paradox and ceramide. Biochim Biophys Acta. 2014;1841(5):783-92.
124. Morad SAF, MacDougall MR, Abdelmageed N, Kao LP, Feith DJ, Tan SF, et al. Pivotal role of mitophagy in response of acute myelogenous leukemia to a ceramide-tamoxifen-containing drug regimen. Exp Cell Res. 2019;381(2):256-64.
125. Siskind LJ. Mitochondrial ceramide and the induction of apoptosis. J Bioenerg Biomembr. 2005;37(3):143-53.
126. Sentelle RD, Senkal CE, Jiang W, Ponnusamy S, Gencer S, Selvam SP, et al. Ceramide targets autophagosomes to mitochondria and induces lethal mitophagy. Nat Chem Biol. 2012;8(10):831-8.
127. Yoo SM, Jung YK. A Molecular Approach to Mitophagy and Mitochondrial Dynamics. Mol Cells. 2018;41(1):18-26.
128. Ianevski A, He L, Aittokallio T, Tang J. SynergyFinder: a web application for analyzing drug combination dose-response matrix data. Bioinformatics. 2017;33(15):2413-5.
129. Morris G, Walker AJ, Berk M, Maes M, Puri BK. Cell Death Pathways: a Novel Therapeutic Approach for Neuroscientists. Mol Neurobiol. 2018;55(7):5767-86.
130. Zhang J, Ney PA. Role of BNIP3 and NIX in cell death, autophagy, and mitophagy. Cell Death Differ. 2009;16(7):939-46.
131. Eskelinen EL. Roles of LAMP-1 and LAMP-2 in lysosome biogenesis and autophagy. Mol Aspects Med. 2006;27(5-6):495-502.
132. Mauvezin C, Neufeld TP. Bafilomycin A1 disrupts autophagic flux by inhibiting both V-ATPase-dependent acidification and Ca-P60A/SERCA-dependent autophagosome-lysosome fusion. Autophagy. 2015;11(8):1437-8.
133. Hessvik NP, Overbye A, Brech A, Torgersen ML, Jakobsen IS, Sandvig K, et al. PIKfyve inhibition increases exosome release and induces secretory autophagy. Cell Mol Life Sci. 2016;73(24):4717-37.
134. Guenther GG, Peralta ER, Rosales KR, Wong SY, Siskind LJ, Edinger AL. Ceramide starves cells to death by downregulating nutrient transporter proteins. Proc Natl Acad Sci U S A. 2008;105(45):17402-7.
135. He L, Zhang J, Zhao J, Ma N, Kim SW, Qiao S, et al. Autophagy: The Last Defense against Cellular Nutritional Stress. Adv Nutr. 2018;9(4):493-504.
136. Scarlatti F, Bauvy C, Ventruti A, Sala G, Cluzeaud F, Vandewalle A, et al. Ceramide-mediated macroautophagy involves inhibition of protein kinase B and up-regulation of beclin 1. J Biol Chem. 2004;279(18):18384-91.
137. Daido S, Kanzawa T, Yamamoto A, Takeuchi H, Kondo Y, Kondo S. Pivotal role of the cell death factor BNIP3 in ceramide-induced autophagic cell death in malignant glioma cells. Cancer Res. 2004;64(12):4286-93.
138. Pattingre S, Bauvy C, Carpentier S, Levade T, Levine B, Codogno P. Role of JNK1-dependent Bcl-2 phosphorylation in ceramide-induced macroautophagy. J Biol Chem. 2009;284(5):2719-28.
139. Hyde R, Hajduch E, Powell DJ, Taylor PM, Hundal HS. Ceramide down-regulates System A amino acid transport and protein synthesis in rat skeletal muscle cells. FASEB J. 2005;19(3):461-3.
140. Huynh KK, Eskelinen EL, Scott CC, Malevanets A, Saftig P, Grinstein S. LAMP proteins

are required for fusion of lysosomes with phagosomes. EMBO J. 2007;26(2):313-24.
141. Agarwal AK, Gude RP, Kalraiya RD. Regulation of melanoma metastasis to lungs by cell surface Lysosome Associated Membrane Protein-1 (LAMP1) via galectin-3. Biochem Biophys Res Commun. 2014;449(3):332-7.
142. Dany M, Gencer S, Nganga R, Thomas RJ, Oleinik N, Baron KD, et al. Targeting FLT3-ITD signaling mediates ceramide-dependent mitophagy and attenuates drug resistance in AML. Blood. 2016;128(15):1944-58.
143. Chou HL, Lin YH, Liu W, Wu CY, Li RN, Huang HW, et al. Combination Therapy of Chloroquine and C(2)-Ceramide Enhances Cytotoxicity in Lung Cancer H460 and H1299 Cells. Cancers (Basel). 2019;11(3).
144. Strelow A, Bernardo K, Adam-Klages S, Linke T, Sandhoff K, Kronke M, et al. Overexpression of acid ceramidase protects from tumor necrosis factor-induced cell death. J Exp Med. 2000;192(5):601-12.
145. Elojeimy S, Liu X, McKillop JC, El-Zawahry AM, Holman DH, Cheng JY, et al. Role of acid ceramidase in resistance to FasL: therapeutic approaches based on acid ceramidase inhibitors and FasL gene therapy. Mol Ther. 2007;15(7):1259-63.
146. Liu X, Elojeimy S, El-Zawahry AM, Holman DH, Bielawska A, Bielawski J, et al. Modulation of ceramide metabolism enhances viral protein apoptin's cytotoxicity in prostate cancer. Mol Ther. 2006;14(5):637-46.
147. Flowers M, Fabrias G, Delgado A, Casas J, Abad JL, Cabot MC. C6-ceramide and targeted inhibition of acid ceramidase induce synergistic decreases in breast cancer cell growth. Breast Cancer Res Treat. 2012;133(2):447-58.
148. Liu X, Elojeimy S, Turner LS, Mahdy AE, Zeidan YH, Bielawska A, et al. Acid ceramidase inhibition: a novel target for cancer therapy. Front Biosci. 2008;13:2293-8.
149. Holman DH, Turner LS, El-Zawahry A, Elojeimy S, Liu X, Bielawski J, et al. Lysosomotropic acid ceramidase inhibitor induces apoptosis in prostate cancer cells. Cancer Chemother Pharmacol. 2008;61(2):231-42.
150. Hernandez-Corbacho MJ, Salama MF, Canals D, Senkal CE, Obeid LM. Sphingolipids in mitochondria. Biochim Biophys Acta Mol Cell Biol Lipids. 2017;1862(1):56-68.
151. Dany M, Ogretmen B. Ceramide induced mitophagy and tumor suppression. Biochim Biophys Acta. 2015;1853(10 Pt B):2834-45.
152. Bellot G, Garcia-Medina R, Gounon P, Chiche J, Roux D, Pouyssegur J, et al. Hypoxia-induced autophagy is mediated through hypoxia-inducible factor induction of BNIP3 and BNIP3L via their BH3 domains. Mol Cell Biol. 2009;29(10):2570-81.
153. Chourasia AH, Macleod KF. Tumor suppressor functions of BNIP3 and mitophagy. Autophagy. 2015;11(10):1937-8.
154. Ney PA. Mitochondrial autophagy: Origins, significance, and role of BNIP3 and NIX. Biochim Biophys Acta. 2015;1853(10 Pt B):2775-83.
155. Wong YC, Ysselstein D, Krainc D. Mitochondria-lysosome contacts regulate mitochondrial fission via RAB7 GTP hydrolysis. Nature. 2018;554(7692):382-6.
156. Bingol B, Sheng M. Mechanisms of mitophagy: PINK1, Parkin, USP30 and beyond. Free Radic Biol Med. 2016;100:210-22.
157. Ma S, Attarwala IY, Xie XQ. SQSTM1/p62: A Potential Target for Neurodegenerative Disease. ACS Chem Neurosci. 2019;10(5):2094-114.
158. Tagashira H, Shinoda Y, Shioda N, Fukunaga K. Methyl pyruvate rescues mitochondrial damage caused by SIGMAR1 mutation related to amyotrophic lateral sclerosis. Biochim Biophys Acta. 2014;1840(12):3320-34.
159. Oleinik N, Kim J, Roth BM, Selvam SP, Gooz M, Johnson RH, et al. Mitochondrial protein import is regulated by p17/PERMIT to mediate lipid metabolism and cellular stress. Sci Adv. 2019;5(9):eaax1978.
160. Zhao XG, Sun RJ, Yang XY, Liu DY, Lei DP, Jin T, et al. Chloroquine-enhanced efficacy

of cisplatin in the treatment of hypopharyngeal carcinoma in xenograft mice. PLoS One. 2015;10(4):e0126147.
161. Chude CI, Amaravadi RK. Targeting Autophagy in Cancer: Update on Clinical Trials and Novel Inhibitors. Int J Mol Sci. 2017;18(6).
162. Walker NI, Harmon BV, Gobe GC, Kerr JF. Patterns of cell death. Methods Achiev Exp Pathol. 1988;13:18-54.
163. Laster SM, Wood JG, Gooding LR. Tumor necrosis factor can induce both apoptic and necrotic forms of cell lysis. J Immunol. 1988;141(8):2629-34.
164. Liu X, Yang W, Guan Z, Yu W, Fan B, Xu N, et al. There are only four basic modes of cell death, although there are many ad-hoc variants adapted to different situations. Cell Biosci. 2018;8:6.
165. Galluzzi L, Vitale I, Aaronson SA, Abrams JM, Adam D, Agostinis P, et al. Molecular mechanisms of cell death: recommendations of the Nomenclature Committee on Cell Death 2018. Cell Death Differ. 2018;25(3):486-541.
166. Porter AG, Janicke RU. Emerging roles of caspase-3 in apoptosis. Cell Death Differ. 1999;6(2):99-104.
167. Julien O, Wells JA. Caspases and their substrates. Cell Death Differ. 2017;24(8):1380-9.
168. Dixon SJ, Lemberg KM, Lamprecht MR, Skouta R, Zaitsev EM, Gleason CE, et al. Ferroptosis: an iron-dependent form of nonapoptotic cell death. Cell. 2012;149(5):1060-72.
169. Seiler A, Schneider M, Forster H, Roth S, Wirth EK, Culmsee C, et al. Glutathione peroxidase 4 senses and translates oxidative stress into 12/15-lipoxygenase dependent- and AIF-mediated cell death. Cell Metab. 2008;8(3):237-48.
170. Xie Y, Hou W, Song X, Yu Y, Huang J, Sun X, et al. Ferroptosis: process and function. Cell Death Differ. 2016;23(3):369-79.
171. Wang H, Sun L, Su L, Rizo J, Liu L, Wang LF, et al. Mixed lineage kinase domain-like protein MLKL causes necrotic membrane disruption upon phosphorylation by RIP3. Mol Cell. 2014;54(1):133-46.
172. Murphy JM, Czabotar PE, Hildebrand JM, Lucet IS, Zhang JG, Alvarez-Diaz S, et al. The pseudokinase MLKL mediates necroptosis via a molecular switch mechanism. Immunity. 2013;39(3):443-53.
173. Cookson BT, Brennan MA. Pro-inflammatory programmed cell death. Trends Microbiol. 2001;9(3):113-4.
174. Gong W, Shi Y, Ren J. Research progresses of molecular mechanism of pyroptosis and its related diseases. Immunobiology. 2020;225(2):151884.
175. Zhang X, Matsuda M, Yaegashi N, Nabe T, Kitatani K. Regulation of Necroptosis by Phospholipids and Sphingolipids. Cells. 2020;9(3).
176. Kroemer G, Martin SJ. Caspase-independent cell death. Nat Med. 2005;11(7):725-30.
177. Lock EA, Reed CJ, Kinsey GR, Schnellmann RG. Caspase-dependent and -independent induction of phosphatidylserine externalization during apoptosis in human renal carcinoma Cak(1)-1 and A-498 cells. Toxicology. 2007;229(1-2):79-90.
178. Shlomovitz I, Speir M, Gerlic M. Flipping the dogma - phosphatidylserine in non-apoptotic cell death. Cell Commun Signal. 2019;17(1):139.
179. Thon L, Mohlig H, Mathieu S, Lange A, Bulanova E, Winoto-Morbach S, et al. Ceramide mediates caspase-independent programmed cell death. FASEB J. 2005;19(14):1945-56.
180. Pacheco FJ, Almaguel FG, Evans W, Rios-Colon L, Filippov V, Leoh LS, et al. Docosahexanoic acid antagonizes TNF-alpha-induced necroptosis by attenuating oxidative stress, ceramide production, lysosomal dysfunction, and autophagic features. Inflamm Res. 2014;63(10):859-71.
181. Gong YN, Guy C, Crawford JC, Green DR. Biological events and molecular signaling following MLKL activation during necroptosis. Cell Cycle. 2017;16(19):1748-60.
182. Tonnus W, Meyer C, Paliege A, Belavgeni A, von Massenhausen A, Bornstein SR, et al.

The pathological features of regulated necrosis. J Pathol. 2019;247(5):697-707.
183. Jorgensen I, Miao EA. Pyroptotic cell death defends against intracellular pathogens. Immunol Rev. 2015;265(1):130-42.
184. Wee P, Wang Z. Epidermal Growth Factor Receptor Cell Proliferation Signaling Pathways. Cancers (Basel). 2017;9(5).
185. Rubin Grandis J, Melhem MF, Gooding WE, Day R, Holst VA, Wagener MM, et al. Levels of TGF-alpha and EGFR protein in head and neck squamous cell carcinoma and patient survival. J Natl Cancer Inst. 1998;90(11):824-32.
186. Chung CH, Ely K, McGavran L, Varella-Garcia M, Parker J, Parker N, et al. Increased epidermal growth factor receptor gene copy number is associated with poor prognosis in head and neck squamous cell carcinomas. J Clin Oncol. 2006;24(25):4170-6.
187. Santini J, Formento JL, Francoual M, Milano G, Schneider M, Dassonville O, et al. Characterization, quantification, and potential clinical value of the epidermal growth factor receptor in head and neck squamous cell carcinomas. Head Neck. 1991;13(2):132-9.
188. Sheu JJ, Hua CH, Wan L, Lin YJ, Lai MT, Tseng HC, et al. Functional genomic analysis identified epidermal growth factor receptor activation as the most common genetic event in oral squamous cell carcinoma. Cancer Res. 2009;69(6):2568-76.
189. O'Neil BH, Allen R, Spigel DR, Stinchcombe TE, Moore DT, Berlin JD, et al. High incidence of cetuximab-related infusion reactions in Tennessee and North Carolina and the association with atopic history. J Clin Oncol. 2007;25(24):3644-8.
190. Wheeler DL, Huang S, Kruser TJ, Nechrebecki MM, Armstrong EA, Benavente S, et al. Mechanisms of acquired resistance to cetuximab: role of HER (ErbB) family members. Oncogene. 2008;27(28):3944-56.
191. Rosa R, Marciano R, Malapelle U, Formisano L, Nappi L, D'Amato C, et al. Sphingosine kinase 1 overexpression contributes to cetuximab resistance in human colorectal cancer models. Clin Cancer Res. 2013;19(1):138-47.
192. Li S, Schmitz KR, Jeffrey PD, Wiltzius JJ, Kussie P, Ferguson KM. Structural basis for inhibition of the epidermal growth factor receptor by cetuximab. Cancer Cell. 2005;7(4):301-11.
193. Akita RW, Sliwkowski MX. Preclinical studies with Erlotinib (Tarceva). Semin Oncol. 2003;30(3 Suppl 7):15-24.
194. Nishimura Y, Bereczky B, Ono M. The EGFR inhibitor gefitinib suppresses ligand-stimulated endocytosis of EGFR via the early/late endocytic pathway in non-small cell lung cancer cell lines. Histochem Cell Biol. 2007;127(5):541-53.
195. Shepherd FA, Rodrigues Pereira J, Ciuleanu T, Tan EH, Hirsh V, Thongprasert S, et al. Erlotinib in previously treated non-small-cell lung cancer. N Engl J Med. 2005;353(2):123-32.
196. Haringhuizen A, van Tinteren H, Vaessen HF, Baas P, van Zandwijk N. Gefitinib as a last treatment option for non-small-cell lung cancer: durable disease control in a subset of patients. Ann Oncol. 2004;15(5):786-92.
197. Gregoire V, Hamoir M, Chen C, Kane M, Kawecki A, Julka PK, et al. Gefitinib plus cisplatin and radiotherapy in previously untreated head and neck squamous cell carcinoma: a phase II, randomized, double-blind, placebo-controlled study. Radiother Oncol. 2011;100(1):62-9.
198. Tang X, He J, Li B, Zheng Y, Li K, Zou S, et al. Efficacy and Safety of Gefitinib in Patients with Advanced Head and Neck Squamous Cell Carcinoma: A Meta-Analysis of Randomized Controlled Trials. J Oncol. 2019;2019:6273438.
199. Soulieres D, Senzer NN, Vokes EE, Hidalgo M, Agarwala SS, Siu LL. Multicenter phase II study of erlotinib, an oral epidermal growth factor receptor tyrosine kinase inhibitor, in patients with recurrent or metastatic squamous cell cancer of the head and neck. J Clin Oncol. 2004;22(1):77-85.
200. Myrick D, Blackinton D, Klostergaard J, Kouttab N, Maizel A, Wanebo H, et al. Paclitaxel-induced apoptosis in Jurkat, a leukemic T cell line, is enhanced by ceramide. Leuk Res. 1999;23(6):569-78.

201. Ahsan A. Mechanisms of Resistance to EGFR Tyrosine Kinase Inhibitors and Therapeutic Approaches: An Update. Adv Exp Med Biol. 2016;893:137-53.
202. Trusolino L, Bertotti A. Compensatory pathways in oncogenic kinase signaling and resistance to targeted therapies: six degrees of separation. Cancer Discov. 2012;2(10):876-80.
203. Kaufmann K, Bach K, Thiel G. The extracellular signal-regulated protein kinases Erk1/Erk2 stimulate expression and biological activity of the transcriptional regulator Egr-1. Biol Chem. 2001;382(7):1077-81.
204. Bourbon NA, Yun J, Kester M. Ceramide directly activates protein kinase C zeta to regulate a stress-activated protein kinase signaling complex. J Biol Chem. 2000;275(45):35617-23.
205. Liu DX, Qian D, Wang B, Yang JM, Lu Z. p300-Dependent ATF5 acetylation is essential for Egr-1 gene activation and cell proliferation and survival. Mol Cell Biol. 2011;31(18):3906-16.
206. de Belle I, Huang RP, Fan Y, Liu C, Mercola D, Adamson ED. p53 and Egr-1 additively suppress transformed growth in HT1080 cells but Egr-1 counteracts p53-dependent apoptosis. Oncogene. 1999;18(24):3633-42.
207. Virolle T, Adamson ED, Baron V, Birle D, Mercola D, Mustelin T, et al. The Egr-1 transcription factor directly activates PTEN during irradiation-induced signalling. Nat Cell Biol. 2001;3(12):1124-8.
208. Nair P, Muthukkumar S, Sells SF, Han SS, Sukhatme VP, Rangnekar VM. Early growth response-1-dependent apoptosis is mediated by p53. J Biol Chem. 1997;272(32):20131-8.
209. Wen W, Wu J, Liu L, Tian Y, Buettner R, Hsieh MY, et al. Synergistic anti-tumor effect of combined inhibition of EGFR and JAK/STAT3 pathways in human ovarian cancer. Mol Cancer. 2015;14:100.
210. Wu K, Chang Q, Lu Y, Qiu P, Chen B, Thakur C, et al. Gefitinib resistance resulted from STAT3-mediated Akt activation in lung cancer cells. Oncotarget. 2013;4(12):2430-8.
211. Zhou H, Summers SA, Birnbaum MJ, Pittman RN. Inhibition of Akt kinase by cell-permeable ceramide and its implications for ceramide-induced apoptosis. J Biol Chem. 1998;273(26):16568-75.
212. Bourbon NA, Sandirasegarane L, Kester M. Ceramide-induced inhibition of Akt is mediated through protein kinase Czeta: implications for growth arrest. J Biol Chem. 2002;277(5):3286-92.
213. Kolter T, Sandhoff K. Sphingolipid metabolism diseases. Biochim Biophys Acta. 2006;1758(12):2057-79.
214. Jin J, Mullen TD, Hou Q, Bielawski J, Bielawska A, Zhang X, et al. AMPK inhibitor Compound C stimulates ceramide production and promotes Bax redistribution and apoptosis in MCF7 breast carcinoma cells. J Lipid Res. 2009;50(12):2389-97.
215. Schiffmann S, Ziebell S, Sandner J, Birod K, Deckmann K, Hartmann D, et al. Activation of ceramide synthase 6 by celecoxib leads to a selective induction of C16:0-ceramide. Biochem Pharmacol. 2010;80(11):1632-40.
216. Separovic D, Breen P, Boppana NB, Van Buren E, Joseph N, Kraveka JM, et al. Increased killing of SCCVII squamous cell carcinoma cells after the combination of Pc 4 photodynamic therapy and dasatinib is associated with enhanced caspase-3 activity and ceramide synthase 1 upregulation. Int J Oncol. 2013;43(6):2064-72.
217. Zhang Y, Li X, Becker KA, Gulbins E. Ceramide-enriched membrane domains--structure and function. Biochim Biophys Acta. 2009;1788(1):178-83.
218. Irwin ME, Mueller KL, Bohin N, Ge Y, Boerner JL. Lipid raft localization of EGFR alters the response of cancer cells to the EGFR tyrosine kinase inhibitor gefitinib. J Cell Physiol. 2011;226(9):2316-28.
219. Bronte G, Rolfo C, Giovannetti E, Cicero G, Pauwels P, Passiglia F, et al. Are erlotinib and gefitinib interchangeable, opposite or complementary for non-small cell lung cancer treatment? Biological, pharmacological and clinical aspects. Crit Rev Oncol Hematol. 2014;89(2):300-13.
220. Karaman MW, Herrgard S, Treiber DK, Gallant P, Atteridge CE, Campbell BT, et al. A

quantitative analysis of kinase inhibitor selectivity. Nat Biotechnol. 2008;26(1):127-32.
221. Xu MJ, Johnson DE, Grandis JR. EGFR-targeted therapies in the post-genomic era. Cancer Metastasis Rev. 2017;36(3):463-73.
222. Hartmann S, Neckel N, Seher A, Mutzbauer G, Brands RC, Linz C, et al. Erlotinib and gefitinib responsiveness in head and neck cancer cell lines--a comparing analysis with cetuximab. Clin Oral Investig. 2016;20(4):759-69.
223. Hannun YA, Obeid LM. Sphingolipids and their metabolism in physiology and disease. Nat Rev Mol Cell Biol. 2018;19(3):175-91.
224. Ryland LK, Fox TE, Liu X, Loughran TP, Kester M. Dysregulation of sphingolipid metabolism in cancer. Cancer Biol Ther. 2011;11(2):138-49.
225. Spinedi A, Bartolomeo SD, Piacentini M. Apoptosis induced by N-hexanoylsphingosine in CHP-100 cells associates with accumulation of endogenous ceramide and is potentiated by inhibition of glucocerebroside synthesis. Cell Death Differ. 1998;5(9):785-91.
226. Itoh M, Kitano T, Watanabe M, Kondo T, Yabu T, Taguchi Y, et al. Possible role of ceramide as an indicator of chemoresistance: decrease of the ceramide content via activation of glucosylceramide synthase and sphingomyelin synthase in chemoresistant leukemia. Clin Cancer Res. 2003;9(1):415-23.
227. Liu YY, Patwardhan GA, Bhinge K, Gupta V, Gu X, Jazwinski SM. Suppression of glucosylceramide synthase restores p53-dependent apoptosis in mutant p53 cancer cells. Cancer Res. 2011;71(6):2276-85.
228. Prinetti A, Basso L, Appierto V, Villani MG, Valsecchi M, Loberto N, et al. Altered sphingolipid metabolism in N-(4-hydroxyphenyl)-retinamide-resistant A2780 human ovarian carcinoma cells. J Biol Chem. 2003;278(8):5574-83.
229. Uemura S, Kabayama K, Noguchi M, Igarashi Y, Inokuchi J. Sialylation and sulfation of lactosylceramide distinctly regulate anchorage-independent growth, apoptosis, and gene expression in 3LL Lewis lung carcinoma cells. Glycobiology. 2003;13(3):207-16.
230. Liu YY, Gupta V, Patwardhan GA, Bhinge K, Zhao Y, Bao J, et al. Glucosylceramide synthase upregulates MDR1 expression in the regulation of cancer drug resistance through cSrc and beta-catenin signaling. Mol Cancer. 2010;9:145.
231. Zeng G, Gao L, Birkle S, Yu RK. Suppression of ganglioside GD3 expression in a rat F-11 tumor cell line reduces tumor growth, angiogenesis, and vascular endothelial growth factor production. Cancer Res. 2000;60(23):6670-6.
232. Lang Z, Guerrera M, Li R, Ladisch S. Ganglioside GD1a enhances VEGF-induced endothelial cell proliferation and migration. Biochem Biophys Res Commun. 2001;282(4):1031-7.
233. Mukherjee P, Faber AC, Shelton LM, Baek RC, Chiles TC, Seyfried TN. Thematic review series: sphingolipids. Ganglioside GM3 suppresses the proangiogenic effects of vascular endothelial growth factor and ganglioside GD1a. J Lipid Res. 2008;49(5):929-38.
234. Chung TW, Kim SJ, Choi HJ, Kim KJ, Kim MJ, Kim SH, et al. Ganglioside GM3 inhibits VEGF/VEGFR-2-mediated angiogenesis: direct interaction of GM3 with VEGFR-2. Glycobiology. 2009;19(3):229-39.
235. Rippo MR, Malisan F, Ravagnan L, Tomassini B, Condo I, Costantini P, et al. GD3 ganglioside directly targets mitochondria in a bcl-2-controlled fashion. FASEB J. 2000;14(13):2047-54.
236. Malisan F, Testi R. GD3 ganglioside and apoptosis. Biochim Biophys Acta. 2002;1585(2-3):179-87.
237. Hankins JL, Fox TE, Barth BM, Unrath KA, Kester M. Exogenous ceramide-1-phosphate reduces lipopolysaccharide (LPS)-mediated cytokine expression. J Biol Chem. 2011;286(52):44357-66.
238. Zappa F, Failli M, De Matteis MA. The Golgi complex in disease and therapy. Curr Opin Cell Biol. 2018;50:102-16.
239. Yang YP, Hu LF, Zheng HF, Mao CJ, Hu WD, Xiong KP, et al. Application and

interpretation of current autophagy inhibitors and activators. Acta Pharmacol Sin. 2013;34(5):625-35.
240. Mizumura K, Cloonan SM, Nakahira K, Bhashyam AR, Cervo M, Kitada T, et al. Mitophagy-dependent necroptosis contributes to the pathogenesis of COPD. J Clin Invest. 2014;124(9):3987-4003.
241. Xianyong Ma DD, and Weidong Chen. Inhibitors and Activators of SOD, GSH-Px, and CAT2017.
242. Ikonomov OC, Altankov G, Sbrissa D, Shisheva A. PIKfyve inhibitor cytotoxicity requires AKT suppression and excessive cytoplasmic vacuolation. Toxicol Appl Pharmacol. 2018;356:151-8.
243. Kimura TE, Duggirala A, Hindmarch CC, Hewer RC, Cui MZ, Newby AC, et al. Inhibition of Egr1 expression underlies the anti-mitogenic effects of cAMP in vascular smooth muscle cells. J Mol Cell Cardiol. 2014;72:9-19.
244. Platt FM. Sphingolipid lysosomal storage disorders. Nature. 2014;510(7503):68-75.
245. Neufeld EF. Lysosomal storage diseases. Annu Rev Biochem. 1991;60:257-80.
246. Lin CF, Tsai CC, Huang WC, Wang YC, Tseng PC, Tsai TT, et al. Glycogen Synthase Kinase-3beta and Caspase-2 Mediate Ceramide- and Etoposide-Induced Apoptosis by Regulating the Lysosomal-Mitochondrial Axis. PLoS One. 2016;11(1):e0145460.
247. Kaushik S, Bandyopadhyay U, Sridhar S, Kiffin R, Martinez-Vicente M, Kon M, et al. Chaperone-mediated autophagy at a glance. J Cell Sci. 2011;124(Pt 4):495-9.
248. Aits S, Jaattela M. Lysosomal cell death at a glance. J Cell Sci. 2013;126(Pt 9):1905-12.
249. Yang L, Ying S, Hu S, Zhao X, Li M, Chen M, et al. EGFR TKIs impair lysosome-dependent degradation of SQSTM1 to compromise the effectiveness in lung cancer. Signal Transduct Target Ther. 2019;4:25.
250. Bartz RR, Piantadosi CA. Clinical review: oxygen as a signaling molecule. Crit Care. 2010;14(5):234.
251. Li JZ, Gao W, Chan JY, Ho WK, Wong TS. Hypoxia in head and neck squamous cell carcinoma. ISRN Otolaryngol. 2012;2012:708974.
252. Krijnen PA, Nijmeijer R, Meijer CJ, Visser CA, Hack CE, Niessen HW. Apoptosis in myocardial ischaemia and infarction. J Clin Pathol. 2002;55(11):801-11.
253. Broughton BR, Reutens DC, Sobey CG. Apoptotic mechanisms after cerebral ischemia. Stroke. 2009;40(5):e331-9.
254. Liu W, Shen SM, Zhao XY, Chen GQ. Targeted genes and interacting proteins of hypoxia inducible factor-1. Int J Biochem Mol Biol. 2012;3(2):165-78.
255. Benita Y, Kikuchi H, Smith AD, Zhang MQ, Chung DC, Xavier RJ. An integrative genomics approach identifies Hypoxia Inducible Factor-1 (HIF-1)-target genes that form the core response to hypoxia. Nucleic Acids Res. 2009;37(14):4587-602.
256. Kumar H, Choi DK. Hypoxia Inducible Factor Pathway and Physiological Adaptation: A Cell Survival Pathway? Mediators Inflamm. 2015;2015:584758.
257. Manalo DJ, Rowan A, Lavoie T, Natarajan L, Kelly BD, Ye SQ, et al. Transcriptional regulation of vascular endothelial cell responses to hypoxia by HIF-1. Blood. 2005;105(2):659-69.
258. Elvidge GP, Glenny L, Appelhoff RJ, Ratcliffe PJ, Ragoussis J, Gleadle JM. Concordant regulation of gene expression by hypoxia and 2-oxoglutarate-dependent dioxygenase inhibition: the role of HIF-1alpha, HIF-2alpha, and other pathways. J Biol Chem. 2006;281(22):15215-26.
259. Denko NC, Fontana LA, Hudson KM, Sutphin PD, Raychaudhuri S, Altman R, et al. Investigating hypoxic tumor physiology through gene expression patterns. Oncogene. 2003;22(37):5907-14.
260. Chi JT, Wang Z, Nuyten DS, Rodriguez EH, Schaner ME, Salim A, et al. Gene expression programs in response to hypoxia: cell type specificity and prognostic significance in human cancers. PLoS Med. 2006;3(3):e47.
261. Wood SM, Gleadle JM, Pugh CW, Hankinson O, Ratcliffe PJ. The role of the aryl

hydrocarbon receptor nuclear translocator (ARNT) in hypoxic induction of gene expression. Studies in ARNT-deficient cells. J Biol Chem. 1996;271(25):15117-23.
262. Greijer AE, van der Groep P, Kemming D, Shvarts A, Semenza GL, Meijer GA, et al. Up-regulation of gene expression by hypoxia is mediated predominantly by hypoxia-inducible factor 1 (HIF-1). J Pathol. 2005;206(3):291-304.
263. Bilton RL, Booker GW. The subtle side to hypoxia inducible factor (HIFalpha) regulation. Eur J Biochem. 2003;270(5):791-8.
264. Agani F, Jiang BH. Oxygen-independent regulation of HIF-1: novel involvement of PI3K/AKT/mTOR pathway in cancer. Curr Cancer Drug Targets. 2013;13(3):245-51.
265. Warfel NA, Dolloff NG, Dicker DT, Malysz J, El-Deiry WS. CDK1 stabilizes HIF-1alpha via direct phosphorylation of Ser668 to promote tumor growth. Cell Cycle. 2013;12(23):3689-701.
266. Hubbi ME, Gilkes DM, Hu H, Kshitiz, Ahmed I, Semenza GL. Cyclin-dependent kinases regulate lysosomal degradation of hypoxia-inducible factor 1alpha to promote cell-cycle progression. Proc Natl Acad Sci U S A. 2014;111(32):E3325-34.
267. Ravi R, Mookerjee B, Bhujwalla ZM, Sutter CH, Artemov D, Zeng Q, et al. Regulation of tumor angiogenesis by p53-induced degradation of hypoxia-inducible factor 1alpha. Genes Dev. 2000;14(1):34-44.
268. Gradin K, McGuire J, Wenger RH, Kvietikova I, fhitelaw ML, Toftgard R, et al. Functional interference between hypoxia and dioxin signal transduction pathways: competition for recruitment of the Arnt transcription factor. Mol Cell Biol. 1996;16(10):5221-31.
269. Uniacke J, Perera JK, Lachance G, Francisco CB, Lee S. Cancer cells exploit eIF4E2-directed synthesis of hypoxia response proteins to drive tumor progression. Cancer Res. 2014;74(5):1379-89.
270. Chee NT, Lohse I, Brothers SP. mRNA-to-protein translation in hypoxia. Mol Cancer. 2019;18(1):49.
271. Young MM, Kester M, Wang HG. Sphingolipids: regulators of crosstalk between apoptosis and autophagy. J Lipid Res. 2013;54(1):5-19.
272. Mammucari C, Milan G, Romanello V, Masiero E, Rudolf R, Del Piccolo P, et al. FoxO3 controls autophagy in skeletal muscle in vivo. Cell Metab. 2007;6(6):458-71.
273. Jin Z, Zheng L, Xin X, Li Y, Hua T, Wu T, et al. Upregulation of forkhead box O3 transcription is involved in C2-ceramide induced apoptosis and autophagy in ovarian cancer cells in vitro. Mol Med Rep. 2014;10(6):3099-105.
274. Tracy K, Dibling BC, Spike BT, Knabb JR, Schumacker P, Macleod KF. BNIP3 is an RB/E2F target gene required for hypoxia-induced autophagy. Mol Cell Biol. 2007;27(17):6229-42.
275. Baetz D, Regula KM, Ens K, Shaw J, Kothari S, Yurkova N, et al. Nuclear factor-kappaB-mediated cell survival involves transcriptional silencing of the mitochondrial death gene BNIP3 in ventricular myocytes. Circulation. 2005;112(24):3777-85.
276. Ikeda R, Tajitsu Y, Iwashita K, Che XF, Yoshida K, Ushiyama M, et al. Thymidine phosphorylase inhibits the expression of proapoptotic protein BNIP3. Biochem Biophys Res Commun. 2008;370(2):220-4.
277. Mahon PC, Baril P, Bhakta V, Chelala C, Caulee K, Harada T, et al. S100A4 contributes to the suppression of BNIP3 expression, chemoresistance, and inhibition of apoptosis in pancreatic cancer. Cancer Res. 2007;67(14):6786-95.
278. Liu X, Zhang W, Wu Z, Yang Y, Kang YJ. Copper levels affect targeting of hypoxia-inducible factor 1alpha to the promoters of hypoxia-regulated genes. J Biol Chem. 2018;293(38):14669-77.
279. Bruick RK. Expression of the gene encoding the proapoptotic Nip3 protein is induced by hypoxia. Proc Natl Acad Sci U S A. 2000;97(16):9082-7.
280. Sowter HM, Ratcliffe PJ, Watson P, Greenberg AH, Harris AL. HIF-1-dependent regulation of hypoxic induction of the cell death factors BNIP3 and NIX in human tumors. Cancer Res. 2001;61(18):6669-73.

281. Zhang Y, Liu D, Hu H, Zhang P, Xie R, Cui W. HIF-1alpha/BNIP3 signaling pathway-induced-autophagy plays protective role during myocardial ischemia-reperfusion injury. Biomed Pharmacother. 2019;120:109464.
282. Guzy RD, Hoyos B, Robin E, Chen H, Liu L, Mansfield KD, et al. Mitochondrial complex III is required for hypoxia-induced ROS production and cellular oxygen sensing. Cell Metab. 2005;1(6):401-8.
283. Zhang H, Bosch-Marce M, Shimoda LA, Tan YS, Baek JH, Wesley JB, et al. Mitochondrial autophagy is an HIF-1-dependent adaptive metabolic response to hypoxia. J Biol Chem. 2008;283(16):10892-903.
284. Selwan EM, Finicle BT, Kim SM, Edinger AL. Attacking the supply wagons to starve cancer cells to death. FEBS Lett. 2016;590(7):885-907.
285. Chakrama FZ, Seguin-Py S, Le Grand JN, Fraichard A, Delage-Mourroux R, Despouy G, et al. GABARAPL1 (GEC1) associates with autophagic vesicles. Autophagy. 2010;6(4):495-505.
286. Lee K, Zhang H, Qian DZ, Rey S, Liu JO, Semenza GL. Acriflavine inhibits HIF-1 dimerization, tumor growth, and vascularization. Proc Natl Acad Sci U S A. 2009;106(42):17910-5.
287. Kung AL, Zabludoff SD, France DS, Freedman SJ, Tanner EA, Vieira A, et al. Small molecule blockade of transcriptional coactivation of the hypoxia-inducible factor pathway. Cancer Cell. 2004;6(1):33-43.
288. Kong D, Park EJ, Stephen AG, Calvani M, Cardellina JH, Monks A, et al. Echinomycin, a small-molecule inhibitor of hypoxia-inducible factor-1 DNA-binding activity. Cancer Res. 2005;65(19):9047-55.
289. Jing X, Yang F, Shao C, Wei K, Xie M, Shen H, et al. Role of hypoxia in cancer therapy by regulating the tumor microenvironment. Mol Cancer. 2019;18(1):157.
290. Lin CF, Chen CL, Chiang CW, Jan MS, Huang WC, Lin YS. GSK-3beta acts downstream of PP2A and the PI 3-kinase-Akt pathway, and upstream of caspase-2 in ceramide-induced mitochondrial apoptosis. J Cell Sci. 2007;120(Pt 16):2935-43.
291. Flugel D, Gorlach A, Michiels C, Kietzmann T. Glycogen synthase kinase 3 phosphorylates hypoxia-inducible factor 1alpha and mediates its destabilization in a VHL-independent manner. Mol Cell Biol. 2007;27(9):3253-65.
292. Semenza GL. Hypoxia-inducible factor 1 (HIF-1) pathway. Sci STKE. 2007;2007(407):cm8.
293. Hammond EM, Dorie MJ, Giaccia AJ. ATR/ATM targets are phosphorylated by ATR in response to hypoxia and ATM in response to reoxygenation. J Biol Chem. 2003;278(14):12207-13.
294. Fan J, Yang X, Bi Z. Acriflavine suppresses the growth of human osteosarcoma cells through apoptosis and autophagy. Tumour Biol. 2014;35(10):9571-6.
295. Zhang L, Li L, Liu H, Prabhakaran K, Zhang X, Borowitz JL, et al. HIF-1alpha activation by a redox-sensitive pathway mediates cyanide-induced BNIP3 upregulation and mitochondrial-dependent cell death. Free Radic Biol Med. 2007;43(1):117-27.
296. Zhu L, Qi B, Hou D. Roles of HIF1alpha- and HIF2alpha-regulated BNIP3 in hypoxia-induced injury of neurons. Pathol Res Pract. 2019;215(4):822-7.
297. Ma Z, Chen C, Tang P, Zhang H, Yue J, Yu Z. BNIP3 induces apoptosis and protective autophagy under hypoxia in esophageal squamous cell carcinoma cell lines: BNIP3 regulates cell death. Dis Esophagus. 2017;30(9):1-8.
298. Westerlind H, Ramanujam R, Uvehag D, Kuja-Halkola R, Boman M, Bottai M, et al. Modest familial risks for multiple sclerosis: a registry-based study of the population of Sweden. Brain. 2014;137(Pt 3):770-8.
299. Ebers GC. Environmental factors and multiple sclerosis. Lancet Neurol. 2008;7(3):268-77.
300. Trapp BD, Nave KA. Multiple sclerosis: an immune or neurodegenerative disorder? Annu Rev Neurosci. 2008;31:247-69.

301. Dutta R, Trapp BD. Mechanisms of neuronal dysfunction and degeneration in multiple sclerosis. Prog Neurobiol. 2011;93(1):1-12.
302. International Multiple Sclerosis Genetics C, Wellcome Trust Case Control C, Sawcer S, Hellenthal G, Pirinen M, Spencer CC, et al. Genetic risk and a primary role for cell-mediated immune mechanisms in multiple sclerosis. Nature. 2011;476(7359):214-9.
303. International Multiple Sclerosis Genetics C, Beecham AH, Patsopoulos NA, Xifara DK, Davis MF, Kemppinen A, et al. Analysis of immune-related loci identifies 48 new susceptibility variants for multiple sclerosis. Nat Genet. 2013;45(11):1353-60.
304. Gianfrancesco MA, Stridh P, Shao X, Rhead B, Graves JS, Chitnis T, et al. Genetic risk factors for pediatric-onset multiple sclerosis. Mult Scler. 2018;24(14):1825-34.
305. Stys PK. Pathoetiology of multiple sclerosis: are we barking up the wrong tree? F1000Prime Rep. 2013;5:20.
306. Stoffel W, Bosio A. Myelin glycolipids and their functions. Curr Opin Neurobiol. 1997;7(5):654-61.
307. Saher G, Brugger B, Lappe-Siefke C, Mobius W, Tozawa R, Wehr MC, et al. High cholesterol level is essential for myelin membrane growth. Nat Neurosci. 2005;8(4):468-75.
308. Marcus J, Popko B. Galactolipids are molecular determinants of myelin development and axo-glial organization. Biochim Biophys Acta. 2002;1573(3):406-13.
309. Suzuki K, Suzuki Y. Globoid cell leucodystrophy (Krabbe's disease): deficiency of galactocerebroside beta-galactosidase. Proc Natl Acad Sci U S A. 1970;66(2):302-9.
310. Itoh M, Hayashi M, Fujioka Y, Nagashima K, Morimatsu Y, Matsuyama H. Immunohistological study of globoid cell leukodystrophy. Brain Dev. 2002;24(5):284-90.
311. Sugama S, Kim SU, Ida H, Eto Y. Psychosine cytotoxicity in rat neural cell cultures and protection by phorbol ester and dimethyl sulfoxide. Pediatr Res. 1990;28(5):473-6.
312. Voccoli V, Tonazzini I, Signore G, Caleo M, Cecchini M. Role of extracellular calcium and mitochondrial oxygen species in psychosine-induced oligodendrocyte cell death. Cell Death Dis. 2014;5:e1529.
313. O'Sullivan C, Dev KK. Galactosylsphingosine (psychosine)-induced demyelination is attenuated by sphingosine 1-phosphate signalling. J Cell Sci. 2015;128(21):3878-87.
314. Ho PP, Kanter JL, Johnson AM, Srinagesh HK, Chang EJ, Purdy TM, et al. Identification of naturally occurring fatty acids of the myelin sheath that resolve neuroinflammation. Sci Transl Med. 2012;4(137):137ra73.
315. Wang CY, Deneen B, Tzeng SF. BRCA1/BRCA2-containing complex subunit 3 controls oligodendrocyte differentiation by dynamically regulating lysine 63-linked ubiquitination. Glia. 2019;67(9):1775-92.
316. Menon KK, Piddlesden SJ, Bernard CC. Demyelinating antibodies to myelin oligodendrocyte glycoprotein and galactocerebroside induce degradation of myelin basic protein in isolated human myelin. J Neurochem. 1997;69(1):214-22.
317. Hennes EM, Baumann M, Lechner C, Rostasy K. MOG Spectrum Disorders and Role of MOG-Antibodies in Clinical Practice. Neuropediatrics. 2018;49(1):3-11.
318. Ketelslegers IA, Van Pelt DE, Bryde S, Neuteboom RF, Catsman-Berrevoets CE, Hamann D, et al. Anti-MOG antibodies plead against MS diagnosis in an Acquired Demyelinating Syndromes cohort. Mult Scler. 2015;21(12):1513-20.
319. Sarfaraz S, Adhami VM, Syed DN, Afaq F, Mukhtar H. Cannabinoids for cancer treatment: progress and promise. Cancer Res. 2008;68(2):339-42.
320. Javid FA, Phillips RM, Afshinjavid S, Verde R, Ligresti A. Cannabinoid pharmacology in cancer research: A new hope for cancer patients? Eur J Pharmacol. 2016;775:1-14.
321. Sanchez C, Galve-Roperh I, Canova C, Brachet P, Guzman M. Delta9-tetrahydrocannabinol induces apoptosis in C6 glioma cells. FEBS Lett. 1998;436(1):6-10.
322. Sanchez C, Galve-Roperh I, Rueda D, Guzman M. Involvement of sphingomyelin hydrolysis and the mitogen-activated protein kinase cascade in the Delta9-tetrahydrocannabinol-

induced stimulation of glucose metabolism in primary astrocytes. Mol Pharmacol. 1998;54(5):834-43.
323. Galve-Roperh I, Sanchez C, Cortes ML, Gomez del Pulgar T, Izquierdo M, Guzman M. Anti-tumoral action of cannabinoids: involvement of sustained ceramide accumulation and extracellular signal-regulated kinase activation. Nat Med. 2000;6(3):313-9.
324. Gomez del Pulgar T, Velasco G, Sanchez C, Haro A, Guzman M. De novo-synthesized ceramide is involved in cannabinoid-induced apoptosis. Biochem J. 2002;363(Pt 1):183-8.
325. Guzman M. Cannabinoids: potential anticancer agents. Nat Rev Cancer. 2003;3(10):745-55.
326. Blazquez C, Sanchez C, Daza A, Galve-Roperh I, Guzman M. The stimulation of ketogenesis by cannabinoids in cultured astrocytes defines carnitine palmitoyltransferase I as a new ceramide-activated enzyme. J Neurochem. 1999;72(4):1759-68.
327. Carracedo A, Lorente M, Egia A, Blazquez C, Garcia S, Giroux V, et al. The stress-regulated protein p8 mediates cannabinoid-induced apoptosis of tumor cells. Cancer Cell. 2006;9(4):301-12.
328. Mimeault M, Pommery N, Wattez N, Bailly C, Henichart JP. Anti-proliferative and apoptotic effects of anandamide in human prostatic cancer cell lines: implication of epidermal growth factor receptor down-regulation and ceramide production. Prostate. 2003;56(1):1-12.
329. Cianchi F, Papucci L, Schiavone N, Lulli M, Magnelli L, Vinci MC, et al. Cannabinoid receptor activation induces apoptosis through tumor necrosis factor alpha-mediated ceramide de novo synthesis in colon cancer cells. Clin Cancer Res. 2008;14(23):7691-700.
330. Gustafsson K, Christensson B, Sander B, Flygare J. Cannabinoid receptor-mediated apoptosis induced by R(+)-methanandamide and Win55,212-2 is associated with ceramide accumulation and p38 activation in mantle cell lymphoma. Mol Pharmacol. 2006;70(5):1612-20.
331. Gustafsson K, Sander B, Bielawski J, Hannun YA, Flygare J. Potentiation of cannabinoid-induced cytotoxicity in mantle cell lymphoma through modulation of ceramide metabolism. Mol Cancer Res. 2009;7(7):1086-98.
332. Barbado MV, Medrano M, Caballero-Velazquez T, Alvarez-Laderas I, Sanchez-Abarca LI, Garcia-Guerrero E, et al. Cannabinoid derivatives exert a potent anti-myeloma activity both in vitro and in vivo. Int J Cancer. 2017;140(3):674-85.